

Incorporation of metal-organic frameworks (MOFs) in polymeric membranes for gas separation applications

Aylin Kertik

Supervisors:

Prof. dr. ir. I.F.J. Vankelecom
Prof. dr. ir. R.G.H. Lammertink
(University of Twente)
Dr. ir. L.H. Wee

Dissertation presented in partial fulfilment of the requirements for the degree of Doctor of Bioscience Engineering (PhD)

September 2018

INCORPORATION OF METAL-ORGANIC FRAMEWORKS (MOFS) IN POLYMERIC MEMBRANES FOR GAS SEPARATION APPLICATIONS

Aylin KERTIK

Supervisor:

Prof. dr. ir. I.F.J. Vankelecom
Prof. dr. ir. R.G.H. Lammertink (University of Twente)
Dr. ir. L.H. Wee

Members of the Examination Committee:

Prof. dr. ir. Bruno Cammue (Chairman)
Prof. dr. ir. Bart Goderis
Prof. dr. ir. Christine Kirschhock
Prof. dr. Paolo Pescarmona
Prof. dr. ir. Yujiro Itami (FujiFilm Nederland)

Dissertation presented in
partial fulfilment of the
requirements for the
degree of Doctor of
Bioscience Engineering
(PhD)

September 2018

© 2018 KU Leuven – Faculty of Bioscience Engineering
Uitgegeven in eigen beheer, Aylin KERTIK, Leuven

Alle rechten voorbehouden. Niets uit deze uitgave mag worden vermenigvuldigd en/of openbaar gemaakt worden door middel van druk, fotokopie, microfilm, elektronisch of op welke andere wijze ook zonder voorafgaandelijke schriftelijke toestemming van de uitgever.

All rights reserved. No part of the publication may be reproduced in any form by print, photoprint, microfilm, electronic or any other means without written permission from the publisher.

Acknowledgements

Primum prima, I am deeply indebted to my promotor, Prof. Dr. Ivo Vankelecom, for his never-ending support, and for believing in me. Without him, this dissertation would simply not come into existence. Dr. Lik Hong Wee has been irreplaceable for this work: thanks to his dedicated focus, insight and help, this work could reach its full potential. I would also like to thank Prof. Dr. Rob Lammertink for agreeing to be my promotor at the University of Twente. And of course, it's been a great honour to be a part of the Erasmus-Mundus Doctorate in Membrane Engineering (EUDIME) family. I am grateful to the programme for funding this PhD.

I am much obliged to the jury members and the chairman for sparing the time and effort for the completion of this PhD. Kitty Nijmeijer and Damien Quemener have helped and inspired me throughout this project. It may not be customary, but I would also like to thank Wannes Meert for the Arenberg Doctoral School (ADS) dissertation template for L^AT_EX, which was used in the writing of this dissertation.

This PhD took me many places from Leuven to Montpellier, and to Enschede. Where ever I roamed, I was lucky to find people very dear to me: Marleny Caceres, Mette Birch Kristensen, Timon Rijnaarts, Rik Kuenen, Namik Akkilic, Violeta Martin, Charu Basu, Antoine Kemperman, Sinem Tas, Jeroen Didden (een dikke merci voor de vertaling), Clement Achille, João Marreiros, Maarten Bastin, Maxime Corvilain, Parimal Naik, Elke Dom, Stefaan Reyniers, Rhea Verbeke, and Maxime Deforche (in no specific order).

The feathers of a bird flock together, after all. I owe a humongous “Tesekkurler” to Veysi Altun, M. Burak Baran, Ayse Karagoz, Serkan Yildiz, Tuba Ayhan, Serdar Okcu, Sarp Kerman, Oguzhan Okudur, Fulya Ulu, Enis and Pelin (and Defne) Leblebici, Deniz Kocaay, Bensu Tunca, Cagatay Altintas, and many many more. Speaking of flocks, here's one to all the concerts and festivals with (among others) Ivo Goeyens, Kristof Lodewijks, Fahri Kucukali, and Mihir

Gupta.

Since I started working at Materialise in 2016, I stepped into a new world. Thanks to my wonderful colleagues, Karel Reynders, Amaury Joly, Paula Magalhaes, Babette Claessens, Anick Favier, Isabelle Liesenborghs, Olivier Diegerick, Victoria Pantelakis, Lisa Morosini, Lieve Boeykens, Ante Rimac, Koen Bas and many more, that step felt as soft as a cat's. I have learned a lot from them, and I hope to continue to do so.

They say that best friends are those that you rely on, even though you are miles apart. Pelin Ozluk and Zafer Eren have (as always) been my most subjective confidants and defenders throughout this period in my life. I cherish the times we got to spend together, and I regret the times that we can't. The latter, though, I got to spend with Sam Smet, Pieter Verlooy, and Paolo Forte. May our bond remain stronger than a cockroach surviving a nuclear fallout.

Surely, I forgot to add some people here: you know yourselves, and you know me. So, here's a big "Thank you", and an even bigger "Sorry!" from the bottom of my heart.

It's funny that the people closest to oneself is mentioned last in such pieces of text. I am forever grateful to Antoine Selim Bilgin for being there for me every step of the way. Words are not always enough to express the deepest feelings, so all I can say is "I am rubber, you are glue". My family, with their unconditional love, has been my compass to turn to in the face of it all.

The last but not the least, I would like to thank music. When all else failed, music was there to lift me up and help me fight my demons.

Doch wenn wir aufgeben enden wir

Abstract

The concept of mixed-matrix membranes (MMM) has been highly attractive for gas separation research since the 1970s, when it was discovered that the addition of zeolite 5A in a polymer results in an increase in the gas diffusion time-lag compared to the neat polymer. MMMs are, in essence, composite materials consisting of filler particles homogeneously dispersed in a polymeric matrix. They are designed for the purpose of exploiting the desirable properties of their counterparts. Over the last few decades, numerous types of fillers ranging from carbon molecular sieves, carbon nanotubes, ordered mesoporous silica and zeolites have been used to prepare highly productive MMMs. Non-porous fillers have been utilised to manipulate polymer chain packing and modify the free volume of the polymer, while porous fillers achieved molecular sieving to separate gases according to their size and shape. Fillers that possess well-defined pore sizes, such as zeolites, showed great potential but their distribution in the polymer matrix and adhesion therein has proven to be problematic. Distribution problems are largely caused by the necessity of post-synthesis calcination for removing leftover templates, which also causes the particles to form strong aggregates. Breaking down these aggregates is possible by strong mixing methods such as ultrasonication, which makes the membrane fabrication method more complicated and inefficient in terms of time and energy. On the other hand, the intrinsic lack of affinity between the inorganic zeolite and the organic polymer phase causes the formation of non-selective defects across the membrane cross-section, resulting in significant losses in selectivity. The solutions suggested for promoting adhesion, such as compatibilisers, silylation etc. have also proven to be material-intensive.

An alternative filler material, metal organic frameworks (MOF) have stirred up excitement in MMM research, as well as many of their fields of application. MOFs are a new class of hybrid materials that consist of metal ions bound together with organic linkers that form a porous framework. In terms of gas separation, MOFs are very attractive materials owing to their tailorable chemistry, tunable composition, well-defined pore size, pore flexibility, and

breathing effects. They essentially consist of metal ions bridged with organic linkers that form a porous framework. Contrary to inorganic fillers such as zeolites, the organic linkers in MOFs offer better adhesion to the polymer, providing an advantage in preventing membrane defects. Unfortunately, MOFs are not completely free of problems of aggregation and aggregate detachment. Recent research has shown that breaking down aggregates by ultrasonication triggers drastic distortion in the morphology and particle size distribution of MOF particles. This work aimed at preventing the formation of aggregates to prepare membranes with high loading, so that the selective behaviour of MOFs can be exploited to the fullest.

As the first step of this research, a novel method was devised to use non-dried MOFs to prepare MMMs. Attempts at synthesising MOFs inside a polymer solution did not yield the desired MOF loading. Moreover, the unreacted MOF precursors plasticised the membrane, resulting in gel-like forms. Higher MOF loading was achieved by using separately synthesised MOFs without drying. A comparison with MMMs comprising dried MOFs showed that, MMMs with non-dried MOFs did not suffer from MOF aggregation or MOF-polymer detachment, and showed better gas separation performance. This trend was consistent for MMMs with ZIF-8, ZIF-7 and $\text{NH}_2\text{-MIL-53(Al)}$, proving that this principle is generic.

These MOF-loaded membranes were further subjected to high thermal treatment conditions to achieve very high mixed-gas selectivities. Two well-known MOFs for gas separation, ZIF-8 and ZIF-7 were used. The controlled thermal treatment resulted in a synergy of MOF amorphisation and cross-linking. Amorphisation refers to the disruption of long-range ordering of MOF building units, followed by densification and loss of crystallinity. The Zn-N bonds in ZIF-8 is broken during amorphisation, creating unsaturated Zn^{2+} sites, which in turn can act as an additional cross-linker for the polymer chains. Combined with the heat-induced polymer-polymer cross-linking, polymer-MOF cross-linking creates a strong interwoven structure that increases the CO_2/CH_4 selectivity, and stabilises the MMMs against CO_2 -induced plasticisation. Mixed-gas separation analyses have revealed the outstanding separation performance of these membranes, which surpassed the Robeson upper-bound of 1991, and reached that of 2008. This work is the first reported concept of this synergy between MOF amorphisation and cross-linking in membranes.

Finally, the same method was applied to the incorporation of $\text{NH}_2\text{-MIL-53(Al)}$, a MOF that shows breathing behaviour, in MMMs. Following the thermal treatment as described in the previous part, even higher gas separation performances were achieved. XRD analysis revealed that the polymer chains penetrated the MOF pores, partially blocking the pore entrances. Owing to this partial blockage, the MOF pores were not completely sealed upon transition to

the narrow-pore form of the MOF. Moreover, these MOF particles are thought to provide a cross-linked network at the mouth of the pore, which resulted in improved selectivities. The polymer chains acting like foundation piles provided a network that was able to maintain its separation properties at pressures as high as 40 bar.

Beknopte samenvatting

Het concept van zogenaamde mixed-matrix membranes (MMMs) is bijzonder aantrekkelijk voor onderzoek naar gasscheidingen sinds in 1970 werd ontdekt dat de toevoeging van zeoliet A aan een polymeer de gasdiffusie beïnvloedt ten opzichte van de onge vulde polymeer. MMMs zijn composietmaterialen bestaande uit vullers homogeen verspreid in een polymeermatrix waarbij de voordelen van beide materiaaltypes worden gecombineerd. In de afgelopen decennia werden verschillende types van vullers, variërend van koolstof moleculaire zeven, koolstof nanobuisjes, geordende mesoporeuze silica en zeolieten toegepast in de bereiding van MMMs. Niet-poreuze vullers werden gebruikt om de stapeling van polymeerketens en het vrije volume te beïnvloeden, terwijl poreuze vullers worden ingezet omwille van hun moleculaire zeefeigenschappen. Ondanks hun potentieel ondervinden vullers met goed gedefinieerde poriegrootte, zoals zeolieten, problemen met de dispersie in een polymeermatrix. Enerzijds kunnen dergelijke dispersieproblemen worden veroorzaakt door de noodzaak van post-synthese calcinatie om de overgebleven templates te verwijderen met risico op sterke aggregatie van de vullers. Het breken van deze aggregaten kan door sterke methoden zoals ultrasone trillingen gebeuren, waarbij het synthesemethodes weliswaar ingewikkelder en inefficiënt in termen van tijd en energie worden. Anderzijds kan de vorming van niet-selectieve defecten, met aanzienlijk verlies aan selectiviteit, worden verklaard door lage affiniteit tussen de anorganische zeoliet en organische polymeerfase. Mogelijke oplossingen voor het bevorderen van de hechting, zoals bijvoorbeeld silylering, blijken ook materiaalintensief te zijn. Een ander type vuller, metaal-organische roosters (MOFs), werden vaak toegepast in MMM onderzoek. MOFs zijn zeer aantrekkelijke materialen voor gasscheidingen vanwege hun veelzijdige chemie, goed gedefinieerde poriegrootte, porieflexibiliteit en ademhalings-effecten. Zij bestaan uit metaalionen verbonden door organische linkers die een poreuze structuur vormen. In vergelijking met anorganische vullers zoals zeolieten, bieden MOFs een betere hechting aan het polymeer dankzij deze organische linkers ondanks eveneens problemen met aggregatie. Recent onderzoek heeft aangetoond dat drastische vervorming

van de morfologie en variatie in deeltjesgrootte worden veroorzaakt door het afbreken van aggregaten door ultrasone trillingen. Dit werk is gericht op het voorkomen van de vorming van aggregaten om membranen met hoge vullerlading te bereiden, zodat het selectieve gasscheidingsgedrag van MOFs ten volle benut kan worden.

Als eerste stap werd een nieuwe methode ontwikkeld om ongedroogde MOFs te gebruiken ter bereiding van MMMs. Pogingen om MOFs te synthetiseren binnen een polymeeroplossing leverden niet de gewenste MOF lading op. Bovendien trad plasticizatie van het membraan op door niet-gereageerde MOF-precursoren, resulterend in gel-achtige vormen. Hogere MOF ladingen werden bereikt met ongedroogde MOFs die apart gesynthetiseerd waren. Vergeleken met MMMs met gedroogde MOFs bleek dat incorporatie van niet-gedroogde MOFs minder onderhevig was aan MOF aggregatie of defectvorming tussen vuller polymeer, resulterend in betere gasscheiding. Deze trend werd bevestigd voor MMMs met ZIF-8, ZIF-7 en $\text{NH}_2\text{-MIL-53(Al)}$, en toont de algemene toepasbaarheid van de methode aan.

Daarna werden deze hoogbeladen membranen onderworpen aan intense thermische behandelingsomstandigheden om zeer hoge selectiviteiten te bereiken. Twee gekende MOFs voor gasscheiding, ZIF-8 en ZIF-7 werden gebruikt. De gecontroleerde thermische behandeling resulteerde in een synergetisch effect van MOF amorfisatie en cross-linking. Amorfisatie verwijst naar de verstoring van de ordening van het MOF materiaal, resulterend in verhoogde dichtheid en gaselectiviteit. De Zn-N bindingen in ZIF-8 zijn verbroken door de amorfisatie, waardoor onverzadigde Zn^{2+} regio's worden gevormd. Deze regio's functioneren als extra cross-linker voor de polymeerketens. Een combinatie van polymeer-polymeer en polymeer-MOF cross-linking resulteerde in een sterk vervlochten structuur dat de CO_2/CH_4 selectiviteit verhoogde, en stabiliseerde de MMMs tegen CO_2 -geïnduceerde plasticificatie. Het uitstekende scheidingsgedrag bleek de Robeson upper-bound van 1991 en 2008 te overtreffen. Dit werk toonde als eerste dit synergetische effect tussen MOF amorfisatie, cross-linking in membranen en het gasscheidingsgedrag aan.

Het laatste deel van dit onderzoek betreft de inbouw in MMMs van $\text{NH}_2\text{-MIL-53(Al)}$, een MOF die ademhalingseffecten vertoont. Na de thermische behandeling zoals beschreven in het vorige deel, toonden deze membranen zelfs hogere gasscheidingsprestaties. Uit XRD analyse bleek dat de polymeerketens de poriën doordrongen, waardoor de porie-ingangen gedeeltelijk werden geblokkeerd. Door deze gedeeltelijke blokkering werden de MOF-poriën niet volledig afgesloten bij amorfisatie van de MOF. Bovendien resulteerde een vervlochten netwerk aan de poriemond in verhoogde selectiviteiten waarbij de scheidingseigenschappen werden behouden bij drukken tot 40 bar.

Abbreviations

2-mim	2-methyl imidazole
6FDA	2,2'-bis(3,4-dicarboxyphenyl)hexafluoropropane dianhydride
ABS	Acrylonitrile butadiene styrene
APTES	3-aminopropyltriethoxysilane
ATR-FTIR	Attenuated total reflectance Fourier transform infrared spectroscopy
BDC	1,4-benzodicarboxylic acid
BTC	1,3,5-benzenetricarboxylic acid
CA	Cellulose acetate
CFC	Chlorofluorocarbon
CMS	Carbon molecular sieve
CNT	Carbon nanotube
CVD	Chemical vapour deposition
DABA	3,5-diaminobenzoic acid
dabco	1,4-diazabicyclo(2.2.2)octane
DAM	Diaminomesitylene
DEA	Diethanol amine
DDR	Deca-dodecasil 3R
DMF	Dimethyl formamide
dobc	2,5-dioxido-1,4-benzenedicarboxylate
dodbc	2,5-dioxibenzene-1,4-dicarboxylate
DSC	Differential scanning calorimetry
DWCNT	Double-walled carbon nanotube
EDX	Energy dispersive X-ray spectroscopy
EELS	Electron energy loss spectroscopy
ELNES	Electronic near-edge structure
FEI	Field Electron and Ion Company
FFT	Fast Fourier transform
GC	Gas chromatography
GS	Gas separation
HAADF	High-angle annular dark field

HKUST	Hong Kong University of Science and Technology
HRTEM	High-resolution transmission electron microscope
HTGS	High-throughput gas separation
IMS	Innovative Membrane Systems
LMWA	Low molecular weight additive
MCM	Mobil Composition of Matter
MEA	Monoethanol amine
MFI	Mordenite framework inverted
MIL	Materials of Institut Lavoisier
MMM	Mixed-matrix membrane
MOF	Metal-organic framework
MTR	Membrane Technology & Research
MWCNT	Multiple-wall carbon nanotube
ndc	1,4-naphthalene dicarboxylate
ODA	Oxydianiline
ODPA	4,4'-oxydiphthalic anhydride
PC	Polycarbonate
PCP	Porous coordination polymer
PDMS	Polydimethylsiloxane
PEEK	Polyether ether ketone
PEI	Polyetherimide
PI	Polyimide
PIM	Polymer with intrinsic microporosity
PMP	Poly(4-methyl-1-pentyne)
pNA	p-nitroaniline
POEM	Poly((oxyethylene) ₉ methacrylate
PPEES	Poly(phenylene ether ether sulfone)
PPO	Poly(p-phenylene oxide)
PS	Polystyrene
PSf	Polysulfone
PTMSP	Poly[1-(trimethylsilyl)-1-propyne]
PVC	Polyvinyl chloride
PVDF	Polyvinylidene fluoride
SAED	Selected area electron diffraction
SAPO	Silicoaluminophosphate
SEM	Scanning electron microscope
SI	Spectral imaging
STP	Standard temperature and pressure
STEM	Scanning transmission electron microscope
SWCNT	Single-walled carbon nanotube
TAP	2,4,6-triaminopyrimidine
TEA	Triethylamine

TEM	Transmission electron microscope
TGA	Thermogravimetric analysis
TMDA	2,3,5,6-tetramethylbenzene-1,4-diamine
UiO	Universitetet i Oslo
UOP	Universal Oil Products
UST	Universal Testsystem
XPS	X-ray photoelectron spectroscopy
XRD	X-ray diffraction
ZIF	Zeolitic imidazolate framework
ZSM	Zeolite socony mobil

Contents

Abstract	iii
Abbreviations	ix
Contents	xiii
List of Figures	xvii
List of Tables	xxi
1 Introduction	1
1.1 Gas separation	1
1.2 Membranes for gas separation	2
1.2.1 The current technology for natural gas purification	6
1.3 Organic membranes	9
1.3.1 Polymeric membranes	9
1.3.2 Carbon membranes	14
1.4 Inorganic membranes	17
1.4.1 Metallic membranes	17
1.4.2 Zeolite membranes	17
1.4.3 Silica membranes	19

1.5	Metal-organic framework (MOF)-based membranes	20
1.6	Mixed-matrix membranes	22
1.6.1	Prediction of mixed-matrix membrane performance	24
1.6.2	Problems encountered in fabricating MMMs	25
1.6.3	MOF-based MMMs	26
1.7	Motivation for this work	28
1.8	Dissertation overview	29
2	Mixed-matrix membranes prepared from non-dried MOFs for CO₂/CH₄ separations.	43
2.1	Abstract	43
2.2	Introduction	44
2.3	Experimental procedure	46
2.3.1	Materials	46
2.3.2	<i>In-situ</i> synthesis of MOF particles	46
2.3.3	Preparation of MMMs with wet MOFs	47
2.3.4	Preparation of conventional MMMs	48
2.3.5	Characterisation	48
2.4	Results and discussion	49
2.4.1	Synthesis of ZIF-8 particles in a PI-solution	49
2.4.2	Non-dried vs. dried MOFs	51
2.4.3	Gas separation performance	52
2.4.4	Comparison with the Maxwell model	56
2.5	Conclusions	57
2.6	Acknowledgements	60
3	Highly selective gas separation membrane using <i>in-situ</i> amorphised metal-organic frameworks	69

3.1	Abstract	69
3.2	Introduction	70
3.3	Experimental procedure	73
3.3.1	Synthesis of MOF particles	73
3.3.2	Preparation of MMMs	73
3.3.3	The annealing process	74
3.3.4	Membrane characterisation	74
3.3.5	Analysis of gas separation properties	75
3.4	Results and discussion	76
3.4.1	Thermo-oxidative cross-linking of MMMs	76
3.4.2	The microstructure of the MMMs	86
3.4.3	The gas separation properties of MMMs	91
3.4.4	TEM analysis of MMMs with ZIF-7	99
3.5	Conclusions	100
3.6	Acknowledgements	101
4	Controlling the topological pore channels of NH₂-MIL-53(Al) via cross-linking with polymer chains for selective natural gas purification	117
4.1	Abstract	118
4.2	Introduction	118
4.3	Experimental procedure	121
4.3.1	Materials	121
4.3.2	Synthesis of NH ₂ -MIL-53(Al) nanoparticles	122
4.3.3	Fabrication of PI-NH ₂ -MIL-53(Al)- MMMs	122
4.3.4	Characterisation of membranes	123
4.4	Results and discussion	124
4.5	Conclusions	137
4.6	Acknowledgements	137

5	General conclusions	151
6	Future prospects	153
6.1	Future prospects	153
6.1.1	Improvement of membrane fluxes	153
6.1.2	Investigation of other polymer-MOF pairs	154
6.1.3	Investigation of other applications	154
	Curriculum vitae	157
	List of publications	159

List of Figures

1.1	A schematic representation of a membrane	3
1.2	The historical development of membrane technology for gas separation	4
1.3	Possible mechanisms for gas separation with membranes	6
1.4	The distribution of free volume.	10
1.5	Schematic representation of dual mode sorption	11
1.6	The permeability-selectivity trade-off maps for various gases	14
1.7	The 2008 trade-off map for CO ₂ /CH ₄	15
1.8	The structures of MOF-5, HKUST-1, ZIF-22, ZIF-8 and ZIF-7.	22
1.9	The schematic depiction and the SEM picture of an MMM	23
1.10	Schematic representation of gas transport in MMMs at lower and higher loadings	24
1.11	The four possible interphase morphologies in MMMs	25
2.1	The structures of ZIF-8, ZIF-7, NH ₂ -MIL-53(Al).	46
2.2	Matrimid® films with Zn(NO ₃) ₂ and 2-mim.	47
2.3	SEM images of Matrimid® and ZIF-8@Matrimid® MMMs.	50
2.4	XRD diffractogram of ZIF-8@Matrimid® MMMs, and membranes with controlled loading of dried ZIF-8.	51

2.5	XRD diffractogram of MMMs with increased precursor concentration to achieve theoretical loadings of 13, 33 and 53 wt.%. . .	52
2.6	Cross-sectional SEM images of MMMs with increased precursor concentration to achieve a theoretical loadings of 13, 33 and 53 wt.%.	52
2.7	SEM images of MMMs with ZIF-8, ZIF-7 and NH ₂ -MIL-53(Al).	53
2.8	XRD patterns of MMMs with non-dried and dried MOFs.	54
2.9	The gas separation performance of MMMs with non-dried (filled symbols) and dried ZIF-8, ZIF-7 and NH ₂ -MIL-53(Al).	55
2.10	Enhancement in selectivity with non-dried and dried MOFs.	56
2.11	A comparison of membrane performances with Maxwell predictions for ZIF-8, ZIF-7 and NH ₂ -MIL-53(Al).	58
3.1	The structures of ZIF-8 and ZIF-7.	71
3.2	CO ₂ adsorption isotherm of ZIF-8 at 35 °C.	72
3.3	The solubility of pure Matrimid® membranes after annealing at 250 °C and 350 °C.	77
3.4	Visual, thermal and solubility tests of the thermally treated membranes.	77
3.5	Thermo-oxidative cross-linking of the membranes.	79
3.6	The ATR-FTIR patterns of the Matrimid® and MMMs with 40 wt.% ZIF-8 loading as a function of temperature.	80
3.7	The proposed thermo-oxidative cross-linking mechanism for Matrimid®.	81
3.8	The proposed cross-linking mechanism of the MOF in the MMM.	82
3.9	The TGA plot and derivatives of the Matrimid® membranes.	83
3.10	The TGA plot and derivatives for MMMs with 40 wt.% ZIF-8 loading.	83
3.11	The dependency of the membrane tensile strength on the heat treatment temperature.	84
3.12	The XPS patterns of MMMs with ZIF-8.	86

3.13	The XRD diffractograms of Matrimid® and MMMs with 20 wt.% and 30 wt.% ZIF-8.	87
3.14	TEM imaging of MMMs with 40 wt.% loading.	88
3.15	XRD diffractograms of pre-amorphised ZIF-8 obtained by ball-milling and as-synthesised ZIF-8.	89
3.16	The XRD diffractogram of ZIF-8 powder subjected to thermal treatment at 350 °C.	89
3.17	Effect of MOF loading and annealing temperature on the membrane morphology as observed by SEM.	90
3.18	The evolution of the gas selectivity of the thermally treated membranes.	93
3.19	SEM images of as-synthesised ZIF-8 and pre-amorphised ZIF-8 obtained by ball-milling.	94
3.20	N ₂ adsorption-desorption isotherms of as-synthesised ZIF-8 and pre-amorphised ZIF-8 prepared by ball-milling.	95
3.21	ATR-FTIR spectrum of MMM prepared from pre-amorphised ZIF-8 prepared via ball-milling.	95
3.22	Top and cross-sectional SEM images of MMM filled with pre-amorphised ZIF-8 prepared by ball-milling.	96
3.23	The SEM images of the MMMs with 20, 30 and 40 wt.% ZIF-7 loading.	97
3.24	The solubility tests of MMMs with ZIF-7.	98
3.25	The gas separation performance of MMMs with ZIF-7.	98
3.26	TEM characterisation of MMMs with 40 wt.% ZIF 7 loading.	102
3.27	HAADF-STEM images and EEL spectra from the 40% ZIF-7 loaded MMM.	103
3.28	The map of n^* and σ^* bonding states	104
4.1	The chemical structure of Matrimid® and NH ₂ -MIL-53(Al).	120
4.2	The change in colour of the pure PI membranes and MMMs, as a function of MOF loading and treatment temperature.	125

4.3	The TGA plots of Matrimid® powder and bulk NH ₂ -MIL-53(Al), Matrimid® membranes, and MMMs with NH ₂ -MIL-53(Al).	126
4.4	The solubility tests of MMMs treated at 160 °C, 250 °C, 350 °C.	127
4.5	FTIR spectra of Matrimid® and MMMs with 20 wt.%, 30 wt.% and 40 wt.% NH ₂ -MIL-53(Al) loading.	128
4.6	The proposed mechanism for cross-linking between the polymer and the NH ₂ -MIL-53(Al).	128
4.7	The evolution of the tensile strength of unfilled Matrimid® and MMMs with 40 wt.% NH ₂ -MIL-53(Al).	129
4.8	XRD diffractogram of MMMs with 40 wt.% NH ₂ -MIL-53(Al) loading.	130
4.9	XRD diffractogram of Matrimid® membranes.	131
4.10	XRD diffractogram of MMMs with 20 wt.% NH ₂ -MIL-53(Al) loading.	131
4.11	XRD diffractogram of MMMs with 30 wt.% NH ₂ -MIL-53(Al) loading.	132
4.12	SEM images of unfilled PI, and MMMs with 20 wt.%, 30 wt.% and 40 wt.% NH ₂ -MIL-53(Al).	133
4.13	TEM characterisation of MMMs with 40 wt.% NH ₂ -MIL-53(Al) loading.	134
4.14	The evolution of the gas selectivity of the thermally treated membranes.	136

List of Tables

1.1	Classification of membranes according to the size range of penetrants and driving forces involved	3
1.2	Commercial gas separation applications, membrane producers and systems	5
1.3	The typical composition of natural gas prior to purification and sales specifications	7
1.4	The typical composition of biogas	8
1.5	The emission levels for fossil fuels	8
1.6	The gas permeation and separation properties of some polymeric membranes	15
1.7	The gas permeation and separation properties of some zeolite membranes	19
1.8	The gas permeation and separation properties of some MOF membranes	22
1.9	The gas permeation and separation properties of mixed-matrix membranes	27
2.1	The gas separation measurements from this work.	59
2.2	Maxwell predictions for Matrimid®/ZIF-8 MMMs.	59
2.3	Maxwell predictions for Matrimid®/ZIF-7 MMMs.	60
2.4	Maxwell predictions for Matrimid®/NH ₂ -MIL-53(Al) MMMs.	60

3.1	The tensile strength of Matrimid® and MMMs with 40% ZIF-8.	84
3.2	Physicochemical properties of as-synthesised ZIF-8 and pre-amorphised ZIF-8 prepared by ball-milling.	92
3.3	The gas separation data of MMMs and polymeric membranes from this work and literature.	105
4.1	The tensile strength of unfilled Matrimid® and MMMs with 40 wt.% NH ₂ -MIL-53(Al).	129
4.2	Comparison of GS performance from this work with literature data from MMMs comprising commercial polymers.	138

Chapter 1

Introduction

Using membranes for gas separation is an important field of industry. Membranes are attractive owing to their low capital and operating costs, low energy requirements, and ease of operation. Gas-selective membranes are used for separations such as O₂ and N₂ enrichment from air, H₂ recovery, and natural gas purification.^[1]

In this chapter, an overview of the concept of gas separation and of gas separation methods is provided. The overview is succeeded by a description of the types of membranes for gas separation and transport mechanisms, followed by a discussion of the materials science aspects in membrane research. The chapter is concluded with the outline of the organisation of this dissertation.

1.1 Gas separation

Gas separation is the general term for processes involving the removal of gaseous impurities from gas streams. As of today, various processes from once-through wash operations to complex multi-step recycle systems have been developed for gas separation. Gas separation processes usually involve one of the five mechanisms listed below:

- Absorption into a liquid, which refers to transferring a gaseous component into a liquid phase in which it is soluble.
- Adsorption on a solid, which refers to the selective concentration of one or more component(s) of a gas mixture on the surface of a microporous

solid.

- Permeation through a membrane, which refers to the selective permeation of one or more component(s) of a gas mixture from one side of the membrane to the other.
- Chemical conversion to another compound, which refers to catalytic and non-catalytic gas phase reactions, and reaction of gaseous components with solids.
- Condensation, which refers to cooling the gas stream to a temperature where certain organic compounds have low vapour pressure, and collecting the condensate.^[2]

Commercial gas separation applications are: (1) hydrogen recovery from nitrogen-bearing gases (e.g. ammonia synthesis purge gas), (2) hydrogen removal and recovery from hydrocarbons (e.g. methane) and other slower permeating gases (e.g. carbon monoxide), (3) removal of carbon dioxide, hydrogen sulfide, and water vapour from methane and other hydrocarbon gases (e.g. upgrading natural gas to meet pipeline specifications), (4) oxygen or nitrogen separation from air (e.g. nitrogen production for inert blanketing), (5) helium removal and recovery from natural gas, (6) solvent vapour removal from exhaust gases.^[2]

In the past two decades, the gas separation equipment market has evolved into a US\$ 150 million/year business^[3]; and like each growing market, gas separation requires new technologies to be developed. Development of gas-selective membranes is a dynamic and rapidly growing field^[1], which will be further discussed in the following section.

1.2 Membranes for gas separation

A membrane is defined as a thin barrier between two phases, through which differential transport occurs under a variety of cross-sectional driving forces. The driving force can be pressure, temperature, or concentration difference.^[4] A schematic representation of a membrane is shown in Figure 1.1. There is a wide variety of materials used for fabricating membranes such as polymers, carbon molecular sieves (CMS), zeolites and metal-organic frameworks (MOF). Membrane modules for GS may be packaged as flat sheets (plate and spiral wound), or hollow fibers.^[5]

There are four developed (microfiltration, ultrafiltration, reverse osmosis, and electro dialysis), two developing (gas separation and pervaporation), and two to-be-developed (carrier facilitated transport and membrane contactors) industrial

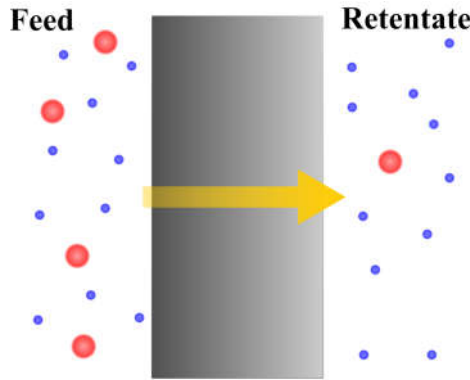


Figure 1.1: A schematic representation of a membrane.

membrane technologies. Table 1.1 classifies membranes according to the driving forces involved, and the particle size range for penetrants rejected by different membrane types.

Although the potential of membranes in gas purification was known by the late 1960s, the lack of technology for fabricating high-performance membranes hindered the advancement in the field.^[3] The first application of membranes for gas purification was for the Manhattan Project (a codename for a World War II project conducted to develop the first atomic bomb), where microporous metal membranes were used to separate uranium-235 from uranium-238. The plant constructed in Tennessee, USA, is the first large-scale use of gas purification membranes. Unfortunately, the uniqueness and secrecy of the project prevented its potential impact on the long-term development of membrane-based gas purification.^[6] Figure 1.2 shows the chronological development of membrane-based gas separation.

Table 1.1: Classification of membranes according to the size range of penetrants and driving forces involved.^[5-8]

Membrane Type	Size Range	Driving Force
Microfiltration	200-10000 Å	Pressure difference
Ultrafiltration	10-200 Å	Pressure difference
Nanofiltration	5-20 Å	Pressure difference
Reverse osmosis	<2 Å	Pressure difference
Electrodialysis	–	Electrical potential difference
Solution-diffusion	3-5 Å	Pressure difference

The technological breakthrough in the utilisation of polymeric membranes in

natural gas purification came with the development of asymmetric membranes.^[9] Later, the first large industrial application of gas separation membranes was achieved by Permea in 1980, launching Prism®, which is a H₂ separation membrane.^[2,3] The principal gas separation markets, producer companies and membrane systems are listed in Table 1.2.

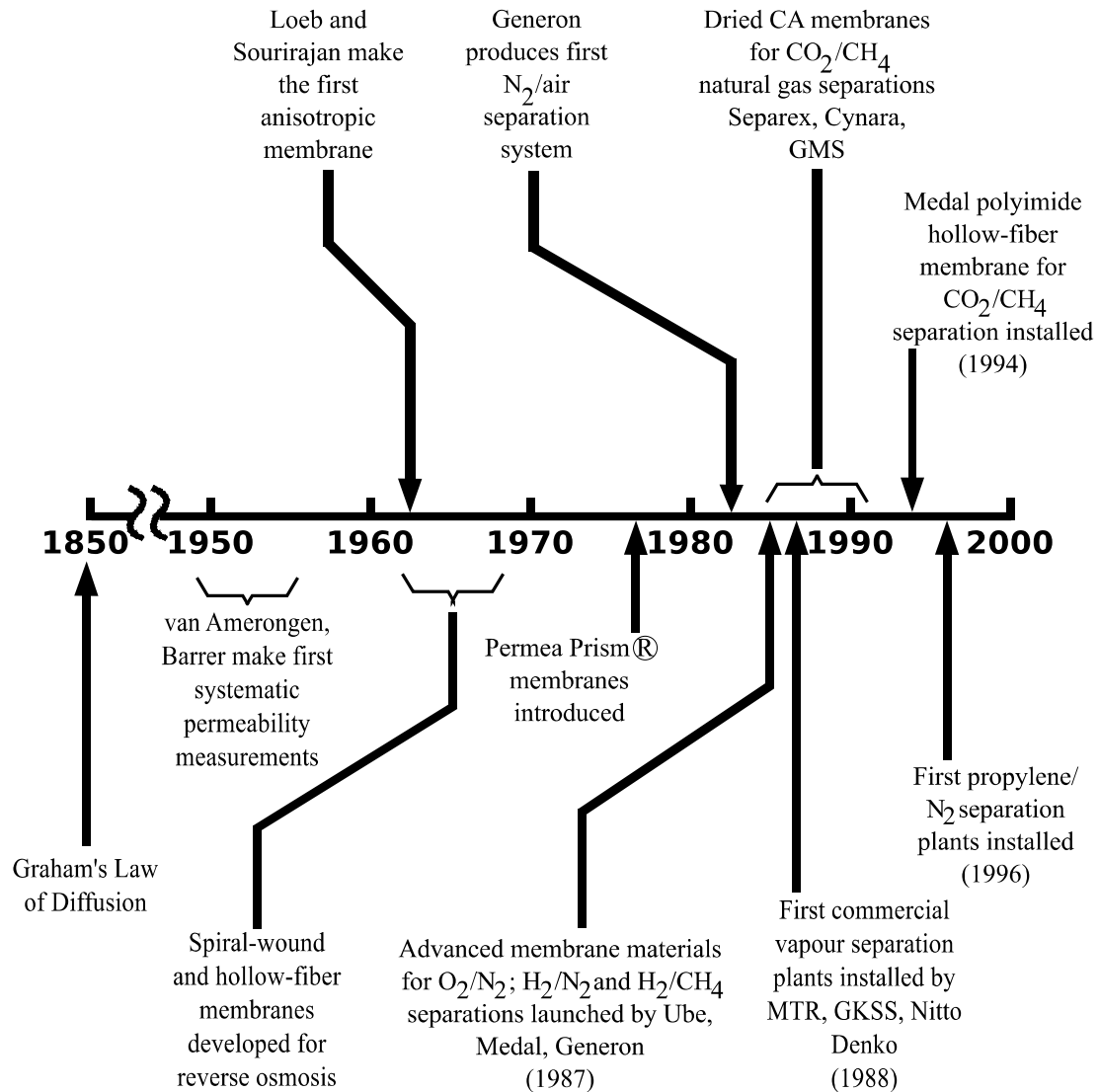


Figure 1.2: The historical development of membrane technology for gas purification, adapted from ref.^[3].

There are five mechanisms for transport of gaseous species with membranes:

- *Knudsen diffusion* occurs when gas molecules move through pores that are small enough to prevent bulk diffusion.

- *Surface diffusion* occurs by the migration of gas molecules along the pore walls of a porous membrane. The intensity of interaction between the pore walls and the adsorbed gas molecules determines the rate of surface diffusion, and the efficiency of separation.
- *Capillary condensation* occurs when adsorbed gas molecules undergo partial condensation at low vapour pressure. Condensed gas molecules diffuse faster through pores than the un-condensed, resulting in separation.
- *Molecular sieving* occurs when gas molecules are separated by size exclusion. For a material with a pore size relative to the kinetic diameter of a gas molecule, the diffusion of smaller gas molecules will be accelerated, while that of larger gas molecules will be hindered. A gas separation membrane must have a pore diameter between the kinetic diameters of the two penetrants for effective molecular sieving.
- *Solution-diffusion* separation relies on the solubility of gases within the membrane, and their diffusion through the membrane matrix.^[11] It manifests itself in three steps: a gas molecule from the upstream first sorbs into the membrane, diffuses across the cross-section, and finally desorbs into the downstream.^[4]

Table 1.2: Commercial gas separation applications, membrane producers and systems.^[10]

Gas separation	Application	Commercial suppliers (Product ^a)
O ₂ -N ₂	Nitrogen generation, oxygen enrichment	Air Products (PRISM), Generon, Praxair, Air Liquid (Floal), Parker Gas Separation, Ube
H ₂ -hydrocarbons	Refinery hydrogen recovery	Air Products, Air Liquid, Praxair, Ube
CO ₂ -CH ₄ , H ₂ S-CH ₄	Natural gas sweetening, biogas upgrading	NATCO (Cynara), Kvaerner, Air Products (PRISM), Air Liquid (MEDAL), Ube, UOP (Separex), FujiFilm (Apura), Evonik (SEPURAN)
H ₂ O-hydrocarbons H ₂ O-air	Natural gas dehydration Air dehydration	Kvaerner, Air Products Air Products (PRISM), Parker Balston, Praxair
Hydrocarbons-air	Pollution control, hydrocarbon recovery	Borsig-GMT, MTR

^aWhere applicable

Figure 1.3 shows a scheme of three common mechanisms for gas separation: Knudsen diffusion, molecular sieving, and solution-diffusion. Transport through dense polymeric membranes occurs by the solution-diffusion mechanism.

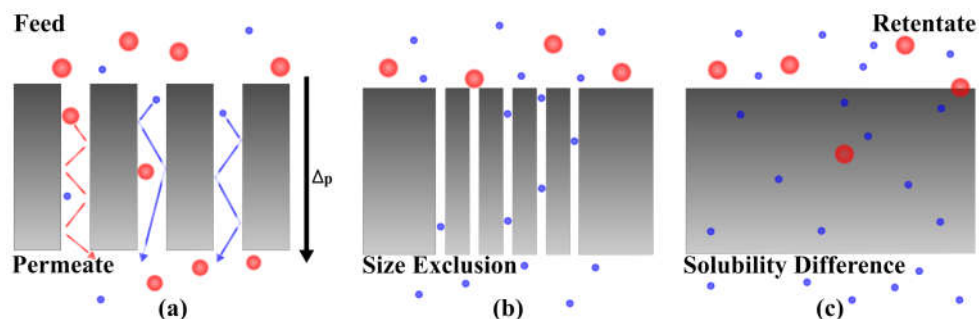


Figure 1.3: The three most common mechanisms for gas separation with membranes: (a) Knudsen diffusion (b) molecular sieving (c) solution-diffusion, adapted from^[11].

There are numerous advantages to utilising membranes for gas separation, such as low capital investment and environmental impact, ease of operation, installation, scale-up and incorporation of new membrane developments, good weight and space efficiency, minimal associated hardware and utility requirements, no moving parts, flexibility, and reliability.^[2]

1.2.1 The current technology for natural gas purification

Natural gas is a colourless and odourless mixture of combustible gases, consisting primarily of CH_4 .^[12,13] Purification of natural gas is the largest industrial separation that involves the removal of contaminants such as hydrocarbons, H_2O , N_2 , H_2S and CO_2 from CH_4 .^[14,15] Also known as natural gas enrichment or sweetening, this operation has been active since the 1980's.^[15,16] The composition of natural gas varies according to the source and extraction method. Many natural gas wells are majorly contaminated by CO_2 , which has to be removed prior to delivery to pipelines to minimise corrosion. In the US, roughly 28% of the natural gas has a CO_2 content above pipeline specifications ($<2\%$).^[14] Alternatively, biogas can be upgraded to natural gas.^[17] The typical compositions for natural gas and biogas are given in Table 1.3 and Table 1.4.

Although it has been utilised as a fuel for more than 150 years, the demand for natural gas has risen rather recently. As seen in Table 1.5, the emission levels for natural gas are very low compared to other fossil fuels. The development of large-diameter, high-pressure pipelines and compressors, and gas storage reservoirs consequently encouraged an increase in the demand and transport

Table 1.3: The typical composition of natural gas prior to purification and sales specifications.^[18]

Gas	Chemical Formula	Amount (%)	Sales Specifications
Methane	CH ₄	70–90	90%
Ethane	C ₂ H ₆		<3–4%
Propane	C ₃ H ₈	0–20 ^a	
Butane	C ₄ H ₁₀		~3% ^b
Carbon dioxide	CO ₂	0–8	<2%
Oxygen	O ₂	0–0.2	–
Nitrogen	N ₂	0–5	<4%
Hydrogen sulphide	H ₂ S	0–5	<4 ppm
Water	H ₂ O	saturated	<100 ppm
Rare gases	Ar, He, Ne, Xe	trace	–

^aTotal amount of C₂–C₄

^bTotal amount of C₃–C₅

of natural gas.^[19] As of 2015, natural gas accounts for 23.8% of global energy consumption (95 trillion standard cubic feet natural gas^[14]) with a 10-year average production and consumption growth of 2.4% and 2.3%, respectively.^[20] This demand has directed attention to efficient purification methods, because large amounts of CO₂ in natural gas not only reduces the energy content of the mixture, but it is also acidic and therefore corrosive to pipelines.^[21,22] The annual world market for natural gas roughly amounts to \$22 billion, and it will continue to grow considerably.^[23,24] Therefore, efficient next-generation CO₂/CH₄ separations are becoming increasingly important for clean gaseous fuel production.^[25]

The majority of natural gas purification operations involve amine adsorption processes which are operated by passing natural gas through an amine solvent that dissolves or captures impurities by chemical reactions. The most common adsorption systems are monoethanolamine (MEA) and diethanolamine (DEA). Amine adsorption systems present certain disadvantages due to their large size, energy-intensive operation, loss of feasibility at high CO₂ content in the feed, and environmental concerns caused by amine losses.^[18]

CO₂-selective membranes of polymers such as cellulose acetate or polyimide have been used since the 1980's. The current largest membrane facility is capable of processing 700 million scfd (standart cubic feet per day).^[26] Membrane modules are advantageous due to the lower total emission of greenhouse gases and solvent-free operation.^[18]

Table 1.4: The typical composition of biogas based on source.^[17]

Gas	Chemical Formula	Amount (%)		
		Agricultural ^a	Landfill	Industrial
Methane	CH ₄	50–80	50–80	50–70
Carbon dioxide	CO ₂	30–50	20–50	30–50
Hydrogen sulphide	H ₂ S	0.70	0.10	0.80
Hydrogen	H ₂	0–2	0–5	0–2
Nitrogen	N ₂	0–1	0–3	0–1
Oxygen	O ₂	0–1	0–1	0–1
Carbon monoxide	CO	0–1	0–1	0–1
Ammonia	NH ₃	trace	trace	trace
Siloxanes	-	trace	trace	trace
Water	H ₂ O	saturation	saturation	saturation

^aAs waste source

The membrane market is expected to grow solidly over the following years, mostly driven by:

- General economic expansion,
- Environmental pressures,
- General demand for greater purity in separation fields,
- Decreasing membrane prices.^[27]

Table 1.5: The emission levels for fossil fuels.^[13]

Pollutant ^a	Natural Gas	Oil	Coal
Carbon dioxide	117000	164000	208000
Carbon monoxide	40	33	208
Nitrogen oxides	92	448	457
Sulfur oxides	1	1122	2591
Particulates	7	84	2744
Mercury	0.000	0.007	0.016

^aExpressed as lb/10⁹ BTU energy

Coupled with the increasing demand for natural gas, development of membranes for effective purification of natural gas has become, and will remain, an attractive research area.

1.3 Organic membranes

1.3.1 Polymeric membranes

Polymers can be classified as crystalline, semi-crystalline, and amorphous. In polymers, crystallinity refers to chains packed in an orderly fashion to form stacks that resemble the arrangement of crystals. Amorphousness, on the other hand, is defined by the polymer chains that cannot pack together regularly enough to form crystalline arrangements. At low temperatures, the molecular motion of the polymer chains in an amorphous region is restricted, which is known as the glassy state. At high temperatures, the polymer chains are more flexible, and able to move more freely, which is known as the rubbery state. The transition between these two states is observed at a so-called *glass transition temperature*, T_g . Below T_g , polymer chains have lower mobility (they are only able to perform limited segmental motions), thus unrelaxed volumes are present within the bulk material. Above T_g , polymer chains are more mobile and the polymer consists of relaxed volumes.^[28]

The permeability of gases in polymers is largely attributed to the chain mobility and inter-chain packing properties of polymers, i.e. when the thermal motions of polymer chain segments generate temporary gaps larger than the gas molecules, the gas molecules perform diffusive jumps through the matrix. The total volume of these temporary gaps is called the *free volume*, the increase of which usually encourages the passage of larger molecules.^[29] Free volume is typically defined as the difference between the specific volume of the polymer and the volume occupied by the molecules constituting the polymer, as shown in Equation 1.1.

$$v_f = v - v_o \quad (1.1)$$

Where v_f is the free volume, v is the specific volume of the polymer i.e. the reciprocal of the polymer density, and v_o is the volume occupied by the molecules themselves.^[6] Figure 1.4 shows the distribution of free volume. Interstitial free volume is the free volume that's unavailable to permeants, because too much energy is required for the permeant molecules to move about freely. The hole free volume is the volume available to penetrants.^[30]

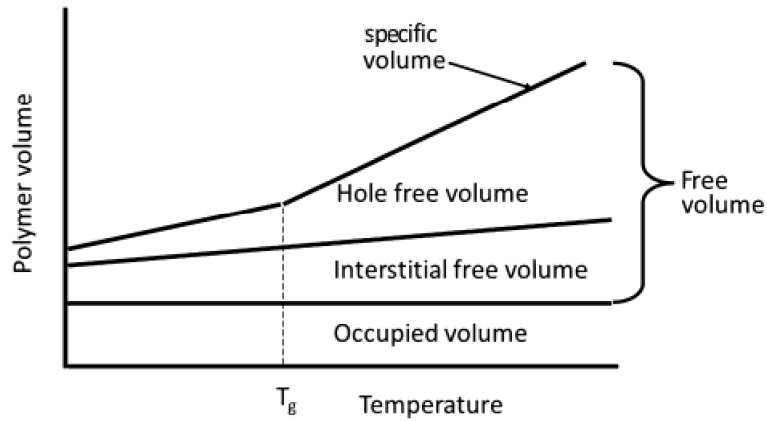


Figure 1.4: The distribution of free volume.^[30]

It was suggested that a diffusing molecule can move from one position to another only when a free volume in its neighbourhood exceeds a certain critical value;^[31] so it can be said that the transport of gases in polymers is dependent on the free volume.^[32] Although this model is fully applicable for amorphous polymers, polymers with crystalline regions require a different explanation.^[31] For amorphous polymers, gas solubility obeys Henry's Law,^[33] whereas for crystalline or semi-crystalline polymers, the sorption of gas molecules occurs both on sites that obey Henry's Law, and sites that obey Langmuir-type sorption, namely the unrelaxed sites in the polymer. This behaviour is described by a so-called dual-mode sorption model, as shown in Equation 1.2, and depicted in Figure 1.5.

$$C = C_D + C_H = k_D p + \frac{C'_H b p}{1 + b p} \quad (1.2)$$

where C is the total gas concentration in a glassy polymer, C_D is the gas concentration based on Henry's Law sorption, C_H is the gas concentration based on Langmuir sorption, k_D is Henry's Law coefficient (the penetrant dissolved in the polymer matrix at equilibrium, $cm^3 STP/cm^3 polymer atm$), b is Langmuir's hole affinity constant (the sorption affinity for a particular gas-polymer system, atm^{-1}), C'_H is the Langmuir sorption capacity (amount of non-equilibrium excess free volume in glassy state, $cm^3 STP/cm^3 polymer$).^[33]

The transport of gases in a membrane occurs mainly via solution-diffusion, which assumes that the gas permeation rate is dependent on the solubility coefficient (S), a thermodynamic parameter, and the diffusion coefficient (D), a kinetic parameter.^[29] The product of D_i and S_i is known as *permeability*, P ,

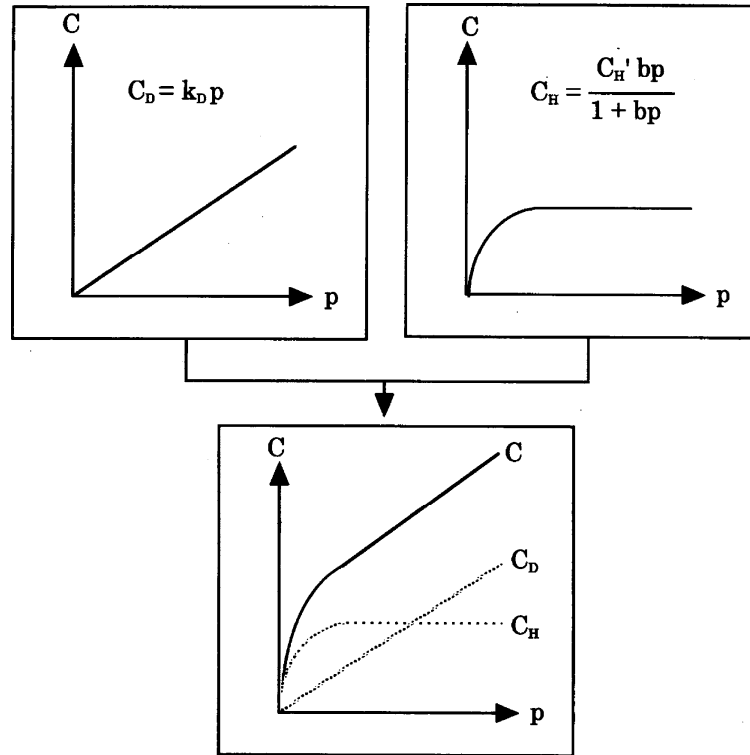


Figure 1.5: Schematic representation of (left) Henry sorption (right) Langmuir sorption and (bottom) dual mode sorption.^[34]

and it measures a membrane's ability to permeate gas.^[35] The permeability of a gas can be written as given in Equation 1.3:

$$P = DS \quad (1.3)$$

More specifically, the gas transport properties of polymeric membranes is calculated as given in Equation 1.4:

$$j_i = \frac{D_i S_i (p_{i0} - p_{il})}{l} \quad (1.4)$$

where j_i is the molar flux ($cm^3 STP$ of i), l is thickness of the membrane, p_{i0} is the partial pressure of i on the feed side, p_{il} is the partial pressure of i on the permeate side, D_i is the diffusion coefficient of i , thus the mobility of individual molecules in the membrane material, S_i is the sorption coefficient of i ($cm^3 STP$ of i/cm^3 of polymer), thus the number of molecules dissolved in the membrane material.^[35]

Permeability equals the flux of a gas diffusing through the membrane normalised by the difference in cross-membrane partial pressure multiplied by the thickness

of the membrane. The most widely used unit for permeability is Barrer, which corresponds to $10^{-10} \text{cm}^3 \text{STP} \cdot \text{cm} / \text{cm}^2 \cdot \text{s} \cdot \text{cmHg}$. Equation 1.5 shows the formula for the calculation of permeability:

$$P_A = \frac{\text{flux}_A l}{\Delta p_A} \quad (1.5)$$

where P_A is the permeability of the membrane, l is the thickness of the membrane, Δp_A is the partial pressure difference across the membrane.^[36]

The second key parameter, *ideal selectivity*, or briefly *selectivity*, describes a membrane's ability to separate two gases, i and j . In mathematical terms, selectivity is the ratio of the permeability of i , (P_i) to the permeability of j , (P_j), as shown in Equation 1.6.

$$\alpha = \frac{P_i}{P_j} \quad (1.6)$$

The ratio of the diffusion coefficients of two gases, D_i/D_j , is known as the *mobility selectivity* which favours the permeation of smaller molecules over the larger ones. For polymeric materials, the mobility of a gas decreases with increasing molecule size, due to the relatively higher interaction of larger molecules with more polymer segments slowing down the gas molecules.

The ratio of sorption coefficients, K_i/K_j , is known as *sorption selectivity*. It reflects the ratio of the energies required for the gases to be sorbed by the polymer (condensation), which usually increases with molecular size. Sorption selectivity favours the permeation of larger and more condensable molecules. These two competing phenomena produce the different selectivity properties between rubbery and glassy polymers.

The ideal selectivity is not a very accurate estimation of membrane performance, especially when highly soluble or plasticising gases (such as CO_2) are concerned. The plasticisation dilates the membrane, allowing larger gas molecules to permeate, as well. In this case, mixed-gas selectivity, Equation 1.7, reflects a more realistic approach,^[37] as it is measured in a single experiment with a mixed feed. Mixed gas selectivity is calculated with the formula:

$$\alpha_{ij} = \frac{y_i/y_j}{x_i/x_j} \quad (1.7)$$

where y_i , y_j are the mole fractions of i and j in the permeate, and x_i and x_j are the mole fractions of i and j in the feed.

Limitations of polymeric membranes

Polymers have been preferred for gas separation owing to their robustness, mechanical integrity, ease of processing, and manufacturing costs. Ideally, a perfect gas separation membrane must have both high permeability and high selectivity. However, there is a trade-off relationship between permeability and selectivity (i.e. increased permeability of a gas brings along a decrease in selectivity).^[38] The fundamental basis for this trade-off can be explained by the intrinsic backbone flexibility of polymers, which determines their size and shape selectivity abilities:

- Decreased chain mobility decreases the permeability and increases the selectivity. However, only the additive structures that can reduce the mobile linkage concentration without changing the intersegmental packing can increase the selectivity without permeability loss.
- Structures such as pendant groups inhibit the inter-chain packing and torsional motion of flexible linkages on the backbone, and they can potentially increase the permeability and maintain the selectivity.^[28]

In 1991, Robeson introduced a so-called *upper-bound*, which identifies the upper limit for polymeric membrane performance for gas separation. Figure 1.6 shows the upper-bound for various gas pairs: the selectivity is on the ordinate, and the permeability of the faster-permeating gas is on the abscissa.^[1,4] Driven by the improvements in membrane literature, the upper-bound curve was updated in 2008,^[39] as shown in Figure 1.7.

Moreover, poor stability at high temperature and pressure is another limiting factor for the use of polymeric membranes for CO_2/CH_4 .^[41]

The types of polymers used for fabricating gas separation membranes are mostly synthetic amorphous polymers such as polysulfone and polyimide (Matrimid®)^[28,42] and glassy polymers such as cellulose acetate. Table 1.6 shows a modest list of some studies carried out by utilising different polymers from literature. A more detailed list can be found in Chapter 3 and 4.

With the introduction of the upper-bound, the interest for alternative materials shifted towards carbon and inorganic materials,^[4] which will be covered in the following sections.

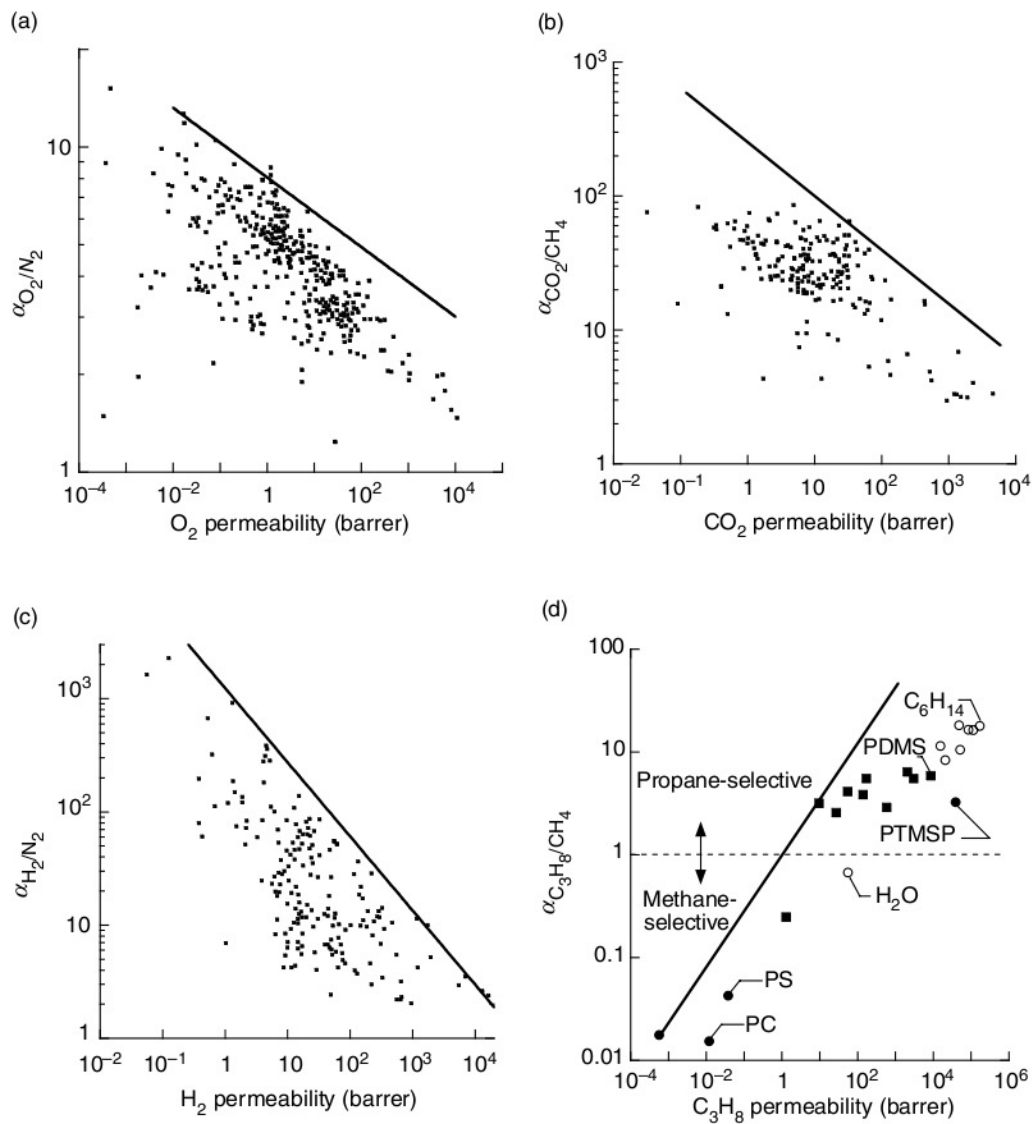


Figure 1.6: The permeability-selectivity trade-off maps for (a) O_2/N_2 , (b) CO_2/CH_4 , (c) H_2/N_2 , (d) C_3H_8/CH_4 .^[40]

1.3.2 Carbon membranes

Carbon-based membranes are attractive for their thermal, mechanical, and chemical stability as well as excellent gas separation performance. These membranes are usually prepared by the carbonisation of polymeric membranes, where the choice of the polymer precursor is of great importance for the properties of the final membrane.^[49]

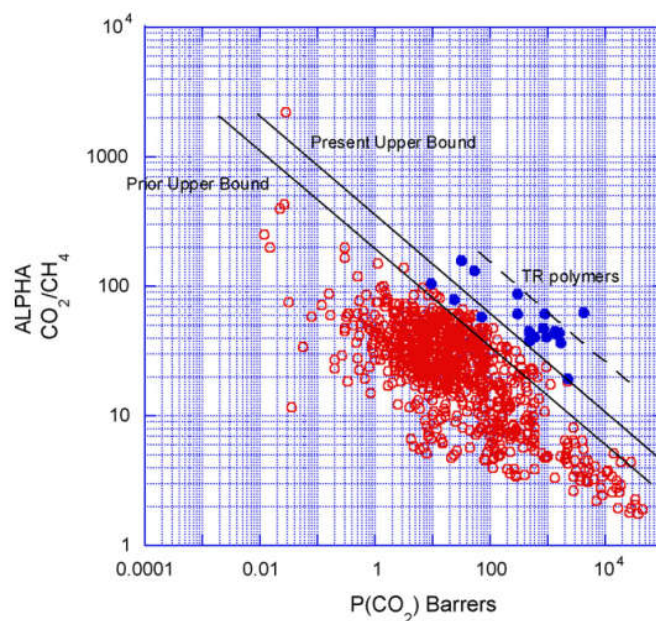


Figure 1.7: The 2008 permeability/selectivity trade-off map for CO₂/CH₄.

Carbon molecular sieve (CMS) membranes

CMS membranes are prepared by carbonising polymeric precursors in an inert atmosphere or under vacuum. The type of polymeric precursor (polyimides, polyfurfuryl alcohol, phenolic resins, polyacrylonitrile, cellulose derivatives, polyetherimide etc.), the carbonisation conditions (heating rate, atmosphere and final temperature) and modifications (pre- or post-treatments, e.g. activation and oxidation) determine the final properties of the CMS membranes. Owing to their small pore size, CMS membranes possess high selectivity for the

Table 1.6: The gas permeation and separation properties of some polymeric membranes.

Polymer	Permeability (Barrer) ^a				Selectivity		Ref.
	CH ₄	N ₂	O ₂	CO ₂	O ₂ /N ₂	CO ₂ /CH ₄	
Matrimid®5218	0.19	0.25	1.7	6.5	6.6	34	[43,44]
6FDA-DAM:DABA 2:1	4.58	–	–	133	–	29	[45]
ABS	–	0.103	0.7	–	6.8	–	[46]
PC	0.374	0.267	1.81	15.3	6.8	23.6	[47]
Ultem®1000	0.037	0.052	0.38	1.45	7.3	38.8	[48]

^a1 Barrer=10⁻¹⁰cm³STP.cm/cm².s.cmHg

separation of gas mixtures.^[50] CMS membranes can be prepared as unsupported or supported modules in the form of flat sheets, capillary tubes or hollow fibers, but they are usually brittle when unsupported. The supported membranes are formed on a macroporous support layer made from e.g. aluminum oxide. While supported membranes are preferable due to their improved mechanical strength, their preparation is difficult; largely due to the necessity of repeated polymer deposition (usually by spin-coating) and carbonisation cycles to obtain defect-free layers.^[51-53]

Typically, CMS membranes are able to perform in non-oxidising environments between 773-1173 K. However, they are vulnerable to organic traces such as H₂S, NH₃, or chlorofluorocarbons (CFC) in the feed. Compared to polymeric membranes, carbon-based membranes are more expensive by 1-3 orders of magnitude per unit area^[54,55], which implies that a CMS membrane must exhibit an exceptional separation performance to become economically feasible. In addition, the high temperature treatment that is intrinsic to the preparation of these materials will always remain an important cost aspect.

Carbon nanotube (CNT) membranes

CNTs are graphite sheets wrapped into a tubular shape, and capped with a fullerene (C₆₀) sphere on each end, which has to be removed to allow sorption. The structure of the tubes can vary from zigzag to armchair shapes, depending on the extent of the twists along the tube length. CNTs can be composed of a single wall (SWCNT), or of multiple walls (MWCNT) made up of layers of single-walled tubes that are aligned approximately 3.4 Å apart. Due to their unusual mechanical and electronic properties, CNTs have attracted great interest since their discovery in 1991. CNTs are quite unique in their structure, and thermal and chemical stability. Typical methods for CNT synthesis are laser ablation, chemical vapor deposition, and electric arc discharge.^[56]

The superior adsorption capacities of CNTs for various organic and inorganic pollutants in air or aqueous streams have been linked to the smooth surfaces of the tube walls, which is thought to enhance the permeation. For example, double-walled nanotubes (DWNT) and MWNT membranes synthesised for separation of gases were reported to have gas transport rates 1-2 orders of magnitude greater than the Knudsen diffusion model predictions.^[56] CNTs can also be tailored for particular purposes by modifying their pore structure or by grafting functional groups on the surface by chemical or thermal treatment. However, the literature on CNTs for CO₂-related separations is still very limited.

1.4 Inorganic membranes

Inorganic membranes are usually of microporous nature, with pore diameters smaller than 2 nm. They can be classified as crystalline (such as zeolites and MOFs), metallic (such as palladium or palladium alloys) and amorphous (such as silica). The separation of gases through these membranes usually occurs by molecular sieving or selective surface diffusion on the pores, or a combination of both.^[50,57] The development of inorganic membranes dates back to the 1940s,^[4,54] with the production of a homogenous porous (20-40 Å pores) glass Vycor in 1945 by Corning Glass.^[1,4] The first large-scale membrane-based separation process was using inorganic membranes for enrichment of uranium in the Manhattan Project.^[4]

1.4.1 Metallic membranes

Metallic membranes related to CO₂ processes are dense films through which H₂ permeates in its atomic form. Since they only allow the permeation of hydrogen, they are used when extremely high purities of hydrogen is required. The separation of H₂ follows a highly specific transport mechanism, where (i) molecular hydrogen diffuses to the membrane surface, (ii) reversible dissociative adsorption occurs on the surface (iii) atomic hydrogen dissolves into and (iv) diffuses through the bulk metal, followed by (v) hydrogen atoms re-associating on the membrane surface at the permeate side and (vi) molecular hydrogen diffusing away from the surface. The selectivity of these membranes is very high owing to the dense structure and the highly specific mode for H₂ passage. This dense structure also prevents the passage of the relatively large CO₂ molecules.^[50,55] However, due to their dense nature, they exhibit low fluxes.

Metal membranes present advantages in terms of operability at high temperatures and high H₂ solubilities. The gas permeability is a function of the metal lattice structure and structural defects, as well as the reactivity to gases present in the feed. However, metallic membranes are susceptible to flux loss due to increased formation of hydrides (which also increases the risks of H₂ embrittlement, especially for pure metals).^[55]

1.4.2 Zeolite membranes

Zeolites are, in the original definition, microporous crystalline aluminosilicates composed of TO₄ tetrahedra (T= Si, Al) with O atoms connecting the neighbouring tetrahedra. A structure with Si as T will form an uncharged solid.

A structure that also comprises Al makes the framework negatively charged, and extra-framework cations are needed to keep the charge of the overall framework neutral. Nowadays, many other chemical compositions also exist for zeolites containing elements other than Si and Al. The framework structure contains interconnected voids that are occupied by the cations and water molecules. The cations can undergo ion exchange, and water may be removed reversibly, usually by the application of heat. The resulting structure is a crystalline host with micropores and voids available for permeation by hosts.^[58,59] As physical adsorbents, zeolites are the most widely studied and patented materials for CO₂ capture.^[57,60]

Zeolite membranes exhibit shape selectivity, and are known for their inherent thermal and chemical stability leading to a long-term stable separation performance. An ideal zeolite membrane must be formed of well-connected crystals to produce a polycrystalline thin film. Unfortunately, the difficulty of obtaining such defect-free structures is the main reason for the variations in literature data and the differences between experimental and modeling studies.^[57] Also, other non-ideal effects, such as random orientation of crystals, intercrystalline interfacial resistance, intracrystalline grain boundary resistance and intrusion of the crystals into the ceramic supports influence the permeation properties of the final membranes.^[57] The economical feasibility of zeolite membrane production is another burden on their industrial attractiveness: while the estimated cost for a polymeric membrane is around US\$ 20/m², a zeolite membrane costs around US\$ 3000/m².^[61]

Various types of zeolites, such as zeolite A, Y, P, DDR, chabazite, MFI-type zeolite (the Al-containing ZSM-5 and the silicalite-1), SAPO-34 and mordenite have been used in membrane-based gas separation^[50,62] and aqueous organic pervaporation, which is their only commercially successful application.^[63] Suzuki got the first patent on zeolite membranes in 1987,^[26] and the first industrial-scale plant based on NaA zeolite membranes for pervaporation dehydration of organic/water mixtures has been built by Mitsui Engineering and Shipbuilding Co. Ltd. since 2000.^[64]

Moreover, zeolites with terminal hydroxyl groups are generally susceptible to moisture, which makes it necessary to dehydrate the gas feed before contacting the membrane. Competitive sorption of water is a well-known reason for drastic reductions in CO₂ adsorption capacity. The membrane can be regenerated at elevated temperatures (typically >300°C, depending on the sorption enthalpy of the water on the zeolite), but this results in a significant increase in the operation costs.^[60]

A brief overview of the gas separation performance of some zeolite membranes is given in Table 1.7.

1.4.3 Silica membranes

Amorphous silica is an attractive material owing to its thermal stability and high gas separation performance.^[69] Membranes of this material are commonly produced by sol-gel synthesis or *chemical vapour deposition* (CVD). A typical silica membrane consists of at least three layers: a separating layer, one or more intermediate layers, and a support. A popular configuration for these systems is an asymmetric structure with an α -alumina-based substrate and a γ -alumina-based intermediate. The intermediate layer has a lower surface roughness and smaller pores in order to better support the final selective silica microporous layer coated on top.^[55]

Silica-based microporous membranes have certain desirable properties, such as the low precursor cost compared to zeolites. However, they are generally less selective than dense zeolite membranes. They are also sensitive to SO_2 and H_2S poisoning and pore blockage by water. Moreover, silica membranes are unstable at high temperatures and in the presence of steam, which results in decreased permeability due to pore collapse. A method for stabilising silica membranes is to add Ti, Zr, Fe, or Al into the network.^[50,57]

The transformation of silica materials to silica membranes opens a new window of opportunity for the effective separation of CO_2 on which only few studies have focused to date. The fabrication of thin and defect free silica membranes containing CO_2 -philic functional groups is a potential research field worth being studied.

Limitations of inorganic membranes

The permeation of gases through inorganic membranes is controlled by two key factors: they permeate either through the channels of the material (in

Table 1.7: The gas permeation and separation properties of some zeolite membranes.

Zeolite	Pore Size (Å)	Permeance ($10^{-8}/\text{mol.m}^2.\text{s.Pa}$)				Selectivity		Ref.
		CH_4	N_2	O_2	CO_2	O_2/N_2	CO_2/CH_4	
NaA	4.1	–	1.2	3.13	–	2.61	–	[64]
Y-type	7.4	0.5-0.7	1-3	–	10-30	–	20-43	[65]
SAPO-34	3.8	0.46	–	–	46	–	142	[66]
DDR-type	3.6x4.4	0.12	–	–	42	–	340	[67]
NaY	7-8	–	15	–	55	–	–	[68]

accordance with the molecular sieving properties of the material), or-because defect-free synthesis of inorganic membranes is very difficult-through the large defects in the membrane.^[64] The latter has tremendous negative effects on the selectivity of the resultant membrane. The additional fabrication-related issues are inadequate sealing of the modules and the unavoidable utilization of inorganic supports which are thick, brittle, less scalable, less compact, and more expensive.^[50,57] Many inorganic membranes are not tolerant for water vapor in the gas mixture. Most also require several steps in processing, some of which at very high temperatures; rendering a continuous synthesis process hard to realise and thus increasing production costs further.^[70]

1.5 Metal-organic framework (MOF)-based membranes

MOFs, also known as porous coordination polymers (PCP), are a relatively new class of hybrid materials that consist of metal ions bound together with organic linkers that form a porous framework. The resulting membranes can thus, strictly speaking, not be considered as inorganic, but rather a transition between inorganic and organic membranes. MOFs have attracted much attention due to their enormous structural and chemical diversity, as well as highly tunable nature.^[71-73] MOF synthesis is realised through the formation of coordination bonds, and is less energy-intensive and easier in comparison to zeolites. In general, MOFs have a relatively low thermal and chemical stability with some significant exceptions, like the members of the zeolitic imidazolate framework (ZIF) family.^[74] Since their introduction about two decades ago, MOFs have been studied extensively for gas separation applications, owing to properties such as high surface area, well-defined pore size, pore flexibility, presence of active metal centers (that can interact with guest molecules), tunable sorption and composition, as well as gate-opening and breathing effects.^[72,73] Pore flexibility can act as a negative trait when bigger guest molecules can also penetrate the pores. Therefore, controlling the gate opening and breathing effects is a challenging aspect in the utilization of MOFs in separation of gases.^[72]

Similar to zeolite membranes, MOF membranes can be synthesised by *In-situ* growth or secondary (seeded) growth.^[72] Zeolite membranes require 550-600 °C to remove templates entrapped in their pores, whereas MOF membranes require a mild 100-200 °C to remove entrapped solvent from their pores. The general concerns for MOF membranes are heterogeneous nucleation, crystallite intergrowth, poor bonding with support, poor stability, and formation of cracks during membrane formation or activation.^[72] *in-situ* growth of MOF membranes is complicated by the lack of interfacial bonding between the MOF

and the substrate.^[72] Support modification facilitates MOF film preparation. Membranes of ZIF-7,^[75] ZIF-8,^[75] ZIF-22,^[75] and ZIF-90^[76] were successfully deposited on alumina support modified with 3-aminopropyltriethoxysilane (APTES) and the resulting membranes showed a clear cut off between H₂ and CO₂ permeance. Alternatively, thermal modification of the support by rapid evaporation of a linker solution achieved covalent attachment of linker to the support.^[77] Although high-temperature calcination can achieve covalent bonding between zeolite seeds, MOFs prepared this way need additional polymer binder to attach the seeds to the support.^[72] Secondary growth is easier to perform, but controlling the microstructure has proven to be difficult.

The first examples of MOF membranes were HKUST-1 (Cu₃(BTC)₂) and MOF-5 membranes. Dense coatings of HKUST-1 were deposited on α -alumina, combining the seeding method with using mother synthesis liquors of low concentration. Depending on the synthesis conditions, the thickness of the MOF layer varied between 2-5 microns with no preferred orientation.^[78] MOF-5 membranes on α -alumina support were prepared by *in-situ*^[79] and microwave-induced seeding^[80] followed by solvothermal secondary growth. They showed Knudsen behaviour in the selective permeation of gases. Unlike the *in-situ* method, the seeded membranes had preferential orientation of the MOF crystals, opening great possibilities for controllable microstructures in MOF membranes. The structures of HKUST-1 and MOF-5 are given in Figure 1.8.

The ZIF family of MOFs is noteworthy owing to their relatively small pores (usually smaller than 5 Å) as well as chemical and thermal stabilities. MOFs such as ZIF-8 are particularly interesting for CO₂ separation in industrial settings, since they have been reported to maintain their crystal structure in harsh environments such as boiling water, and organic solvents.^[81] ZIF-8 membranes^[77] with microstructures controllable by the pH of the growth solution showed selectivities of 3.9 for H₂/CO₂ and 4.5 for CO₂/N₂. Using PEI to enhance the adhesion of the ZIF-7 seed layer to the support yielded membranes with an ideal selectivity of 6.7 for H₂/CO₂.^[82] ZIF-22 membranes on modified supports had a H₂/CO₂ separation performance of 7.2 for mixed-gas conditions that exceeded the Knudsen constants. Although the selectivity at 423 K suffered slightly, it still remained above the Knudsen predictions.^[76] The structures of ZIF-7, ZIF-8 and ZIF-22 are given in Figure 1.8.

A list of the gas separation performance of some well-known MOFs can be found in Table 1.8.

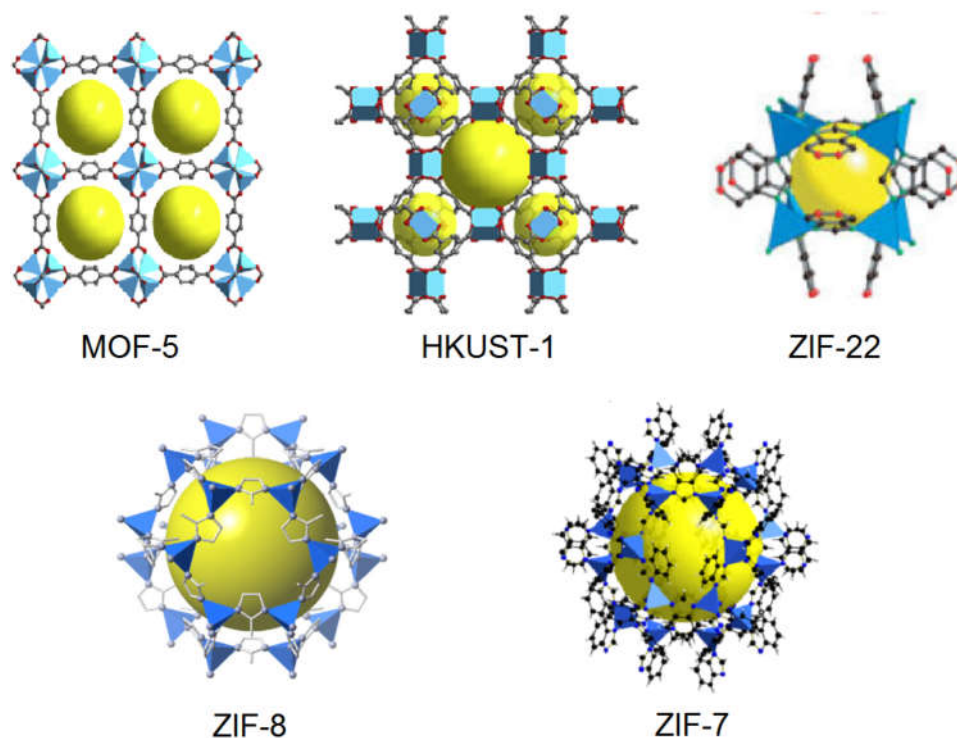


Figure 1.8: The structures of MOF-5^[83], HKUST-1^[83], ZIF-22^[84], ZIF-8^[85] and ZIF-7^[86]. The blue regions represent the metal nodes, which are bound by organic linkers. The empty space in the pores is represented by the yellow spheres.

Table 1.8: The gas permeation and separation properties of some MOF membranes.

MOF	Pore Size (Å)	Permeance (1/mol.m ² .s.Pa)				Selectivity		Ref.
		CH ₄	N ₂	O ₂	CO ₂	O ₂ /N ₂	CO ₂ /CH ₄	
ZIF-8	3.4	2.42x10 ⁻⁶	-	-	1.69x10 ⁻⁵	-	7.2	[87]
ZIF-69	7.8	22.4x10 ⁻⁹	-	-	102.3x10 ⁻⁹	-	4.6	[88]
Co ₃ (HCOO) ₆	5.5	1.56x10 ⁻⁷	-	-	1.97x10 ⁻⁶	-	12.63	[89]
Cu ₂ (ndc) ₂ (dabco)	3.5-4	0.66x10 ⁻⁸	-	-	3x10 ⁻⁸	-	4.5	[90]
MOF-5	15.6	170x10 ⁻⁸	125x10 ⁻⁸	-	100x10 ⁻⁸	-	0.6	[79]
ZIF-8	3.4	0.1x10 ⁻⁷	0.15x10 ⁻⁷	0.55x10 ⁻⁷	0.45x10 ⁻⁷	3.7	4.5	[77]
HKUST-1	9	0.65x10 ⁻⁶	0.49x10 ⁻⁶	0.5x10 ⁻⁶	0.4x10 ⁻⁶	1.02	0.6	[91]

1.6 Mixed-matrix membranes

Although polymers are easy to process into large surface-area membranes, a trade-off exists between selectivity and permeability for these materials.

Inorganic materials such as zeolites are outstanding candidates for gas separation as a result of their “molecular-size” pore sizes, but fabricating them into defect-free membranes is highly costly. A new approach was first offered in the 1970s by Paul and Kemp, who found that the addition of zeolite 5A particles into a polymeric matrix causes a significant increase on the diffusion time lag compared to the neat polymer. Further in 1988, researchers at Universal Oil Products (UOP) reported the first composite membranes capable of suppressing the Robeson upper-bound.^[92–94]

These composite membranes, conventionally called *mixed-matrix membranes* (MMM), aim to surpass the so-called upper-bound by combining the ease of processibility of polymers with the superior molecular sieving properties of filler particles.^[94] An MMM is ideally a composite material that consists of filler particles homogenously dispersed in a polymeric matrix. Figure 1.9 shows the depiction and the SEM image of a mixed-matrix membrane with a polymeric matrix and dispersed filler particles.

Over the last few decades, numerous types of porous and non-porous fillers ranging from carbon molecular sieves, carbon nanotubes, ordered mesoporous silica to zeolites have been used to prepare MMMs. Non-porous fillers have been used to manipulate the polymer chain packing and modify the free volume of the polymer, while porous fillers provided molecular sieving to separate gases according to their size and shape.^[1]

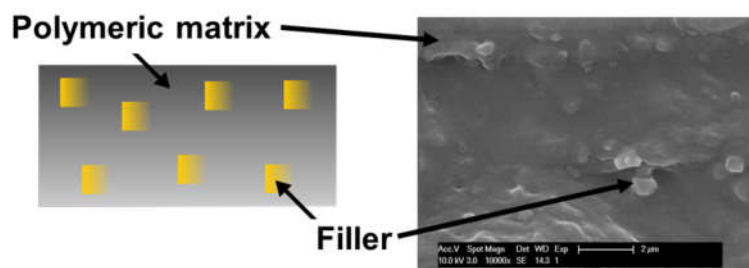


Figure 1.9: The schematic depiction and the SEM picture of an MMM.

The permeation of gases in a mixed-matrix membrane occurs both through the free volume in the polymer matrix and the pores of the filler particles. The extent of molecular sieving achieved is dependent on the filler pore size and loading, which defines a gas molecule’s probability of passing through a filler in its diffusion path. As seen on Figure 1.10, when the loading is relatively low, the gases permeate through a combination of the filler pores and the polymer matrix or directly along the polymer matrix. In this case, the molecular sieving effect will be relatively weaker. When the loading is increased to an optimal level, the gas molecules will follow a permeation path that consists of connected filler pores, which will achieve highly effective molecular sieving. For this reason,

increasing the loading as high as physically possible is necessary for obtaining highly selective MMMs.

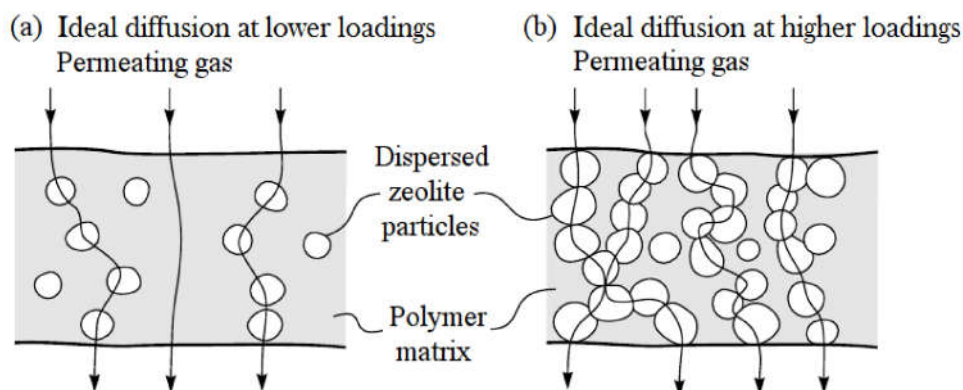


Figure 1.10: Schematic representation of gas transport in MMMs at (a) lower loadings (b) higher loadings.^[6] The gas permeation in the polymeric part of the membrane occurs via solution-diffusion.

With the introduction of fillers in a polymer, a tertiary phase called the *interphase* is formed at the interfacial region between the polymer and the filler. Although the ratio of the interphasic region to the bulk membrane is small, the type of interphase morphology strongly affects the overall properties. There are four possible interphase morphologies as shown in Figure 1.11. Case I corresponds to the ideal morphology, where the polymer surrounding the filler has the same properties as the bulk polymer, and there are no interphasic defects. Case II is the defective morphology caused by the detachment of polymer chains from the filler. Case III stands for the phenomena known as *chain rigidification*, where the polymer chains in direct contact with the filler are more rigid in comparison with the bulk polymer and exhibit different properties. Case IV represents a situation called *pore blockage*, where the surface pores of the filler are partially sealed by the relatively rigid polymer chains.^[1]

1.6.1 Prediction of mixed-matrix membrane performance

There are various theoretical expressions for predicting the separation performance of MMMs, such as the models suggested by Maxwell (1873), Bruggemann (1935), Higuchi and Higuchi (1960), Bottcher (1945), and Davis (1977).^[95] The Maxwell model adapted for spherical particles, as seen in Equation 1.8, is the most popular method for estimating the permeability and selectivity of an MMM comprised of a polymer matrix and dispersed filler particles of known permeabilities. The Maxwell model was originally developed for calculating the electrical conductivity of composites.

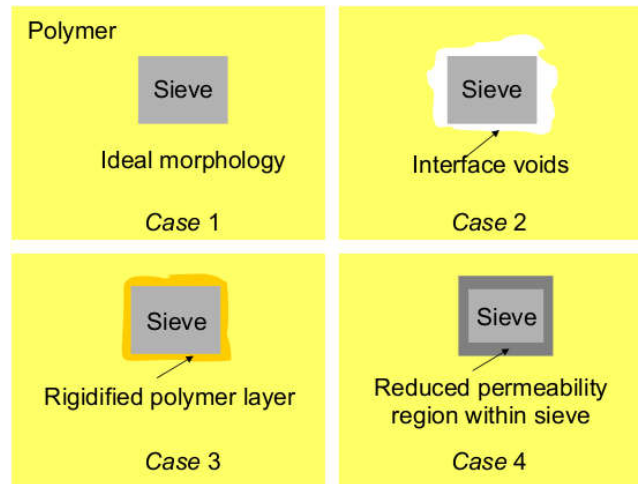


Figure 1.11: The four possible interphase morphologies in MMMs.^[1]

$$P = P_m \left[\frac{2(1 - \phi) + (1 + 2\phi)\lambda_{dm}}{(2 + \phi) + (1 - \phi)\lambda_{dm}} \right] \quad (1.8)$$

P is the effective permeability of permeant in MMM, P_m is the effective permeability of the permeant in the matrix (continuous phase), ϕ is the volume fraction of filler particles, λ_{dm} is the ratio of the permeability of dispersed filler particles (P_d) to the permeability of the matrix (P_m).^[96] However, it should be noted that the Maxwell model assumes an ideal case with no membrane defects and that all the membrane components show the same properties.^[1] Thus, generally, there is a discrepancy between these predictions and the actual membrane performance, especially with higher filler loadings.^[95]

1.6.2 Problems encountered in fabricating MMMs

For fabrication of highly selective MMMs, various glassy and rubbery polymers have been used as the matrix, and zeolites, carbon molecular sieves, activated carbons, non-porous silica, C_{60} , and graphite have been used as fillers.^[1,47,61,97] The separation properties were seen to vary immensely with the MMM composition. For example, membranes prepared with rubbery polymers have shown significant permeability increase at high zeolite loading; however, the lack of mechanical stability and desirable selectivities compared to glassy polymers rendered their application practically unattractive.^[94] Glassy polymers with separation performances that lie suitably closer to the upper-bound, on the other hand, presented another obstacle: poor compatibility between the polymer

and the filler, which results in non-selective voids in the membrane.^[94,98–100] These voids, in return, result in huge decreases in selectivity.

In order to overcome this challenge, numerous methods have been developed by researchers, some of which can be listed as:

- Maintaining the polymer chain flexibility by annealing above- T_g during membrane formation,^[94,97,99,101,102]
- Modification of the external surface of a zeolite by silane-coupling agents to promote adhesion between the filler and the polymer,^[97,98,103,104]
- Addition of a low molecular weight additive (LMWA) as compatibiliser to create a link between the polymer chains and the filler,^[47,105]
- Preparing membranes by melt processing,^[106,107]
- Addition of plasticisers that decrease the overall T_g and increase polymer chain mobility during membrane formation,^[51]
- Annealing vitrified membranes above T_g ,^[51]
- Coating of filler particles with a thin layer of polymer, prior to their incorporation into the bulk polymer (priming).^[61,103,104,108]

A review of literature on the CO_2/CH_4 separation properties of MMMs is summarised in Table 1.9.

1.6.3 MOF-based MMMs

Inorganic fillers that possess well-defined pore sizes, such as zeolites, showed great potential but their distribution in the polymer matrix and adhesion to the polymer chains has proven to be problematic. Distribution problems are largely caused by the necessity of post-synthesis calcination for removing leftover templates, which also causes the particles to form strong aggregates. Breaking down these aggregates is possible by strong mixing methods such as ultrasonication, which makes the membrane fabrication method more complicated and inefficient in terms of time and energy. On the other hand, the intrinsic lack of affinity between the inorganic zeolite and the organic polymer phase causes the formation of non-selective defects across the membrane cross-section, resulting in significant losses in selectivity. The solutions suggested for promoting adhesion, such as compatibilisers, silylation etc. have also proven to be material-intensive. As alternative fillers, MOFs have stirred up excitement in MMM research, as well as many of their fields of application. In terms of

Table 1.9: The gas permeation and separation properties of mixed-matrix membranes

Polymer	Additive/Loading (%)	Method	Permeability (Barrer) ¹		Selectivity	Ref.
			CH ₄	CO ₂		
Matrimid®5218	-	-	0.21	7.29	34.71	[109]
	Meso-ZSM-5/20 wt. %	Mixing	0.13	8.65	66.07	
Matrimid®5218	-	-	6.86	8.34	1.22	[105]
	Zeolite 13X/43 wt. %	Compatibiliser (TAP)	0.0048 ¹	0.64	1.22	
	Zeolite 4A/43 wt. %	Compatibiliser (TAP)	0.0003	0.185	1.22	[103]
PS	-	-	0.17	4.5	26.5	
	MCM41/20 wt. %	Priming	0.34	7.8	23	[47]
PC	-	-	0.374	8.80	23.5	
	Zeolite 4A/20 wt. %	Compatibiliser (pNA)	0.078	0.144	51	[110]
Matrimid®	ZIF-8/50 ^a	Priming	- ^b	n/a ^c	89.15	[111]
Matrimid®	CuBDC (nanosheet)/8.2	Mixing	-	2.78	88.2	[24]
Matrimid®	Ni ₂ (dodbc)/23	Mixing/sonication	-	14.7	32.5	[112]
Matrimid®	MIL-53/15	Priming	-	12.43	51.8	[113]
Matrimid®	Cu-BTC/30	Priming	-	176	23	[114]
Matrimid®	MOF-5/10	Mixing/sonication	-	11.10	51	[115]
Matrimid®	NH ₂ -MIL-53(Al)/25	Mixing/sonication	-	107	3.9	[116]
Ultem®	Cu-BTC/35	Mixing/sonication/priming	-	4.1	34	[117]
PEI	Cubic-MOF-5/25	Mixing/sonication/priming	-	5.39	23.43	

^aLoading calculated as (wt. MOF)/(wt. polymer)^bMixed gas measurements^cNot reported^{c1} 1 Barrer=10⁻¹⁰ cm³ STP.cm/cm².s.cmHg

gas separation, MOFs are very attractive materials owing to their tailorable chemistry, tunable composition, well-defined pore size, pore flexibility, and breathing effects. They essentially consist of metal ions bridged with organic linkers that form a porous framework. Contrary to inorganic fillers such as zeolites, the organic linkers in MOFs offer better adhesion to the polymer, providing an advantage in preventing membrane defects. Unfortunately, MOFs are not completely free of problems of aggregation and aggregate detachment. Recent research has shown that breaking down aggregates by ultrasonication triggers drastic distortion in the morphology and particle size distribution of MOF particles.^[118] On the other hand, polymeric membranes are prone to plasticisation effects with e.g. at high CO₂ pressures; whereas MOF additives are not. Provided that the MOF particles have good interaction with the polymer matrix, the overall plasticisation resistance of the membranes can be improved with the addition of MOFs.^[119]

The first example of the incorporation of MOFs into a polymer for gas separation has been reported for copper(II)biphenyl-dicarboxylate-triethylenediamine in poly-(3-acetoxyethylthiophene) to give improved CH₄ selectivity compared to the pure polymer.^[120] In the following decade, MMMs with various MOFs e.g. ZIF-8,^[110,121-123] ZIF-7,^[124] ZIF-90,^[125] MOF-5,^[114,117] CuBTC,^[113,116,126] CuBDC,^[111] Ni₂(dodbc),^[24] MIL-53,^[112] NH₂-MIL-53(Al),^[115,126-128] MIL-68(Al),^[129] and UiO66^[130,131] have been reported in various commercial and non-commercial polymer combinations, loadings, and post-treatment methods. A concise table is given in Table 1.9, detailed tables can be found in Chapters 3 and 4. The MOF particles were not only incorporated in their powder form. Hwang et al.^[122] embedded hollow ZIF-8 shells into a graft polymer. Good polymer-filler contact, and good dispersion was achieved between the polymer and the hollow MOF shells. Up to 10x improvement in pure CO₂ permeability was reached without drastic sacrifices to the permeability. Rodenas et al.^[111] reported MMMs comprising CuBDC nanosheets embedded in PI matrix. The membranes showed impressive selectivities of 88 for CO₂/CH₄ mixtures at 298 K.

1.7 Motivation for this work

Amine sorption technologies can produce high-purity products, but they are not economically feasible for the separation of mixtures with high CO₂ concentrations (>20%). Membranes currently available on the market, on the other hand, do not offer sufficient selectivities, which lead to increased hydrocarbon losses during separation. Moreover, polymers are usually prone to plasticisation upon CO₂ permeation, which further decreases the selectivities,

and increases the hydrocarbon losses. The main motivation of this work is to combine the molecular sieving effect of MOFs with the processibility of polymers to fabricate highly stable and productive MMMs with high MOF loading. Ideally, high productivity can be achieved by a combination of high selectivity and high permeability. High selectivity is needed to obtain a high-purity product, while high permeability is preferable for minimising the membrane area and therefore capital costs.^[132] CH₄ losses during gas separation can be reduced by using membranes with high selectivity and high stability against plasticisation. Moreover, as the industry will start resorting to highly contaminated natural gas wells (CO₂ content up to >90%), highly selective membranes will gain increased importance.

1.8 Dissertation overview

This work focused on the preparation of MOF-containing MMMs for gas separation applications. The first step was to investigate MMM preparation methods alternative to the conventional recipes, thereby aiming to bypass the drying of MOF particles and overcoming the particle aggregation, even at high MOF loadings. The rest of the research has been based on the findings of this investigation, with the addition of thermal post-synthesis steps that allowed to alter the chemical structure of the polymer and the MOF synergetically. As a result, outstanding membrane performances have been obtained.

This dissertation consists of six chapters, including this introduction chapter.

Chapter 2 is based on the preparation of MMMs comprising MOFs. The first approach has been to synthesise MOF particles directly inside a polymeric solution. The aim was to overcome the issues with particle aggregation before they occurred. The major problem was to achieve a high MOF synthesis yield, which was solved by synthesising and washing the MOF particles separately. This method not only produced sturdy membranes with excellent MOF dispersion, it also allowed to have absolute control over the MOF loading.

Chapter 3 includes details on the preparation and testing of MMMs comprising *in-situ* amorphised ZIF-8. Membrane preparation was based on the work in Chapter 1, with the addition of thermal post-processing steps to increase the adhesion between the MOF and the polymer. As the temperature was increased, it was observed that the structure of the membranes changed significantly: the polymer phase was cross-linked, and the MOF phase was amorphised. This synergy of effects produced MMMs with impressive gas separation properties that surpass the Robeson upper-bound. The successful

production and characterisation results of MMMs with ZIF-7 showed that this method is generic.

Chapter 4 is based on the study in Chapter 3. In order to assess the behaviour of breathing MOFs in this application, a typical breathing MOF, NH₂-MIL-53(Al), was selected. The synergetic effects have been consistent with these MMMs, moreover the polymer chains were able to penetrate the MOF pores undergoing configurational transition. As a result, the polymer chains were able to cross-link to the amine groups; forming MMMs that exhibit the highest gas separation performances ever reported for MOF-based MMMs.

Chapter 5 describes the conclusions derived from this research, and **Chapter 6** points to prospects for future research.

References

- [1] T.-S. Chung, L. Y. Jiang, Y. Li and S. Kulprathipanja. “Mixed Matrix Membranes (MMMs) comprising organic polymers with dispersed inorganic fillers for gas separation”. *Prog. Poly. Sci.* 32 (2007), pp. 483–507.
- [2] A. L. Kohl and R. B. Nielsen. *Gas Purification 5th Edition*. Gulf Publishing, 1997.
- [3] R. W. Baker. “Future Directions of Membrane Gas Separation Technology”. *Ind. Eng. Chem. Res.* 41 (2002), pp. 1393–1411.
- [4] P. Pandey and R. Chauhan. “Membranes for gas separation”. *Prog. Polym. Sci.* 26 (2001), pp. 853–893.
- [5] D. W. Wallace. “Crosslinked Hollow Fiber Membranes for Natural Gas Purification and Their Manufacture from Novel Polymers”. PhD thesis. The University of Texas at Austin, 2004.
- [6] R. W. Baker. *Membrane Technology and Applications*. John Wiley & Sons, 2004.
- [7] J. Wagner. *Membrane Filtration Handbook: Practical Hints and Tips*. Osmonics Inc., 2001.
- [8] T. Matsuura. *Synthetic Membranes and Membrane Separation Processes*. CRC Press, 1994.
- [9] S. Sridhar, B. Smitha and T. M. Aminabhavi. “Separation of Carbon Dioxide from Natural Gas Mixtures through Polymeric Membranes-A Review”. *Separation & Purification Reviews* 36 (2007), pp. 113–174.
- [10] A. F. Ismail, K. C. Khulbe, T. Matsuura et al. *Gas separation membranes*. Vol. 7. Springer, 2015.
- [11] C. A. Scholes, S. E. Kentish and G. W. Stevens. “Carbon Dioxide Separation through Polymeric Membrane Systems for Flue Gas Applications”. *Recent Patents on Chemical Engineering* 1 (2008), pp. 52–66.
- [12] R. D. Treloar. *Gas Installation Technology*. Wiley-Blackwell, 2009.
- [13] <http://naturalgas.org/overview/background/>. accessed on July 21st, 2017. URL: <http://naturalgas.org/overview/background/>.
- [14] R. W. Baker and K. Lokhandwala. “Natural gas processing with membranes: An overview”. *Industrial & Engineering Chemistry Research* 47.7 (2008), pp. 2109–2121.
- [15] R. W. Baker. *Membrane Technology and Applications*. Chichester, UK: John Wiley & Sons, Ltd, 2012.

- [16] Y. Yampolskii, I. Pinnau and B. Freeman, eds. *Materials Science of Membranes for Gas and Vapor Separation*. Chichester, UK: John Wiley & Sons, Ltd, 2006.
- [17] X. Y. Chen, H. Vinh-Thang, A. A. Ramirez, D. Rodrigue and S. Kaliaguine. “Membrane gas separation technologies for biogas upgrading”. *RSC Advances* 5 (31 2015), pp. 24399–24448.
- [18] A. M. W. Hillock. “Crosslinkable Polyimide Mixed Matrix Membranes for Natural Gas Purification”. PhD thesis. Georgia Institute of Technology, 2005.
- [19] H. D. Beggs. *Gas Production Operations*. Oil & Gas Consultants International Inc., 1984.
- [20] B. Global. *Natural gas - 2015 in review*. 2016.
- [21] S. Li, J. L. Falconer and R. D. Noble. “SAPO-34 membranes for CO₂/CH₄ separation”. *Journal of Membrane Science* 241 (2004), pp. 121–135.
- [22] S. J. Miller, W. J. Koros and D. Q. Vu. “Mixed matrix membrane technology: enhancing gas separations with polymer/molecular sieve composites”. *From Zeolites to Porous MOF Materials-the 40th Anniversary of International Zeolite Conference*. Elsevier B. V., 2007, pp. 1590–1596.
- [23] W. J. Koros and R. Mahajan. “Pushing the limits on possibilities for large scale gas separation: which strategies?” *Journal of Membrane Science* 175.2 (2000), pp. 181–196.
- [24] J. E. Bachman and J. R. Long. “Plasticization-resistant Ni₂(dobdc)/polyimide composite membranes for the removal of CO₂ from natural gas”. *Energy Environ. Sci.* 9.6 (2016), pp. 2031–2036.
- [25] A. W. Thornton, D. Dubbeldam, M. S. Liu, B. P. Ladewig, A. J. Hill and M. R. Hill. “Feasibility of zeolitic imidazolate framework membranes for clean energy applications”. *Energy & Environmental Science* 5.6 (2012), p. 7637.
- [26] S. Li, R. D. Noble and J. L. Falconer. “SAPO-34 membranes for CO₂/CH₄ separations: Effect of Si/Al ratio”. *Microporous and Mesoporous Materials* 110 (2007), pp. 310–317.
- [27] K. Sutherland. *Profile of the International Membrane Industry: Market Prospects to 2008*. Third. Elsevier Ltd., 2004.
- [28] R. Mahajan. “Formation, Characterization and Modelling of Mixed Matrix Membrane Materials”. PhD thesis. Georgia Institute of Technology, 2000.

- [29] C.-C. Hu, C.-S. Chang, R.-C. Ruaan and J.-Y. Lai. "Effect of free volume and sorption on membrane gas transport". *Journal of Membrane Science* 226 (2003), pp. 51–61.
- [30] R. P. Danner. "Measuring and correlating diffusivity in polymer-solvent systems using free-volume theory". *Fluid Phase Equilibria* 362 (2014), pp. 19–27.
- [31] M. H. Kloppfer and B. Flaconneche. "Transport Properties of Gases in Polymers: Bibliographic Review". *Oil & Gas Science Technology* 56 (2001), pp. 223–244.
- [32] A. Bos, I. G. M. Punt, M. Wessling and H. Strathmann. " CO_2 -induced plasticization phenomena in glassy polymers". *Journal of Membrane Science* 155 (1999), pp. 67–78.
- [33] S. Kanehashi and K. Nagai. "Analysis of dual-mode model parameters for gas sorption in glassy polymers". *Journal of Membrane Science* 253 (2005), pp. 117–138.
- [34] Y. Tsujita. "Gas sorption and permeation of glassy polymers with microvoids". *Progress in Polymer Science* 28 (2003), pp. 1377–1401.
- [35] N. N. Li, A. G. Fane, W. S. W. Ho and T. Matsuura. *Advanced Membrane Technology and Applications*. John Wiley & Sons, 2008.
- [36] A. M. W. Hillock and W. J. Koros. "Cross-Linkable Polyimide Membrane for Natural Gas Purification and Carbon Dioxide Plasticization Reduction". *Macromolecules* 40 (2007), pp. 583–587.
- [37] Y. Yampolskii. "Polymeric Gas Separation Membranes". *Macromolecules* 45.8 (2012), pp. 3298–3311.
- [38] S. Husain. "Mixed Matrix Dual Layer Hollow Fiber Membranes for Natural Gas Separation". PhD thesis. Georgia Institute of Technology, 2006.
- [39] L. M. Robeson. "The upper bound revisited". *Journal of Membrane Science* 320.1-2 (2008), pp. 390–400.
- [40] Y. Yampolskii, I. Pinnau and B. Freeman. *Materials Science of Membranes for Gas and Vapor Separation*. John Wiley & Sons, 2006.
- [41] S. Li, G. Alvarado, R. D. Noble and J. L. Falconer. "Effects of impurities on CO_2/CH_4 separations through SAPO-34 membranes". *Journal of Membrane Science* 251 (2004), pp. 59–66.
- [42] J. D. Perry. "Formation and Characterization of Hybrid Membranes Utilizing High-Performance Polyimides and Carbon Molecular Sieves". PhD thesis. Georgia Institute of Technology, 2007.

- [43] T.-S. Chung, S. S. Chan, R. Wang, Z. Lu and C. He. "Characterization of permeability and sorption in Matrimid/C60 mixed matrix membranes". *Journal of Membrane Science* 211 (2003), pp. 91–99.
- [44] P. S. Tin, T. S. Chung, Y. Liu, R. Wanc, S. L. Liu and K. P. Pramoda. "Effects of cross-linking modification on gas separation performance of Matrimid membranes". *Journal of Membrane Science* 225 (2003), pp. 77–90.
- [45] J. D. Wind, D. R. Paul and W. J. Koros. "Natural Gas Permeation in Polyimide Membranes". *Journal of Membrane Science* 228 (2004), pp. 227–236.
- [46] J. Marchese, E. Garis, M. Anson, N. A. Ochoa and C. Pagliero. "Gas sorption, permeation and separation of ABS copolymer membrane". *Journal of Membrane Science* 221 (2003), pp. 185–197.
- [47] D. Şen, H. Kalipçilar and L. Yilmaz. "Development of polycarbonate based zeolite 4A filled mixed matrix gas separation membranes". *Journal of Membrane Science* 303 (2007), pp. 194–203.
- [48] D. Q. Vu, W. J. Koros and S. J. Miller. "Mixed matrix membranes using carbon molecular sieves II. Modeling permeation behavior". *Journal of Membrane Science* 211 (2003), pp. 335–348.
- [49] X. He and M.-B. Hägg. "Optimization of Carbonization Process for Preparation of High Performance Hollow Fiber Carbon Membranes". *Industrial & Engineering Chemistry Research* 50.13 (2011), pp. 8065–8072.
- [50] F. Gallucci, E. Fernandez, P. Corengia and M. van Sint Annaland. "Recent advances on membranes and membrane reactors for hydrogen production". *Chemical Engineering Science* 92.0 (2013), pp. 40–66.
- [51] L.-J. Wang and F. C.-N. Hong. "Effects of surface treatments and annealing on carbon-based molecular sieve membranes for gas separation". *Applied Surface Science* 240.1–4 (2005), pp. 161–174.
- [52] A. K. Itta, H.-H. Tseng and M.-Y. Wey. "Fabrication and characterization of PPO/PVP blend carbon molecular sieve membranes for H₂/N₂ and H₂/CH₄ separation". *Journal of Membrane Science* 372.1–2 (2011), pp. 387–395.
- [53] H.-H. Tseng and A. K. Itta. "Modification of carbon molecular sieve membrane structure by self-assisted deposition carbon segment for gas separation". *Journal of Membrane Science* 389.0 (2012), pp. 223–233.
- [54] A. Ismail and L. David. "A review on the latest development of carbon membranes for gas separation". *Journal of Membrane Science* 193.1 (2001), pp. 1–18.

- [55] N. W. Ockwig and T. M. Nenoff. "Membranes for Hydrogen Separation". *Chemical Reviews* 110.4 (2010), pp. 2573–2574.
- [56] J. K. Holt, H. G. Park, Y. Wang, M. Stadermann, A. B. Artyukhin, C. P. Grigoropoulos, A. Noy and O. Bakajin. "Fast Mass Transport Through Sub-2-Nanometer Carbon Nanotubes". *Science* 312.5776 (2006), pp. 1034–1037.
- [57] K. Ramasubramanian, Y. Zhao and W. Winston Ho. "CO₂ capture and H₂ purification: Prospects for CO₂-selective membrane processes". *AIChE Journal* 59.4 (2013), pp. 1033–1045.
- [58] H. Bekkum. *Introduction to zeolite science and practice*. Amsterdam New York: Elsevier, 2001.
- [59] S. Auerbach. *Handbook of zeolite science and technology*. New York: M. Dekker, 2003.
- [60] D. M. D'Alessandro, B. Smit and J. R. Long. "Carbon Dioxide Capture: Prospects for New Materials". *Angewandte Chemie International Edition* 49.35 (2010), pp. 6058–6082.
- [61] D. Q. Vu, W. J. Koros and S. J. Miller. "Mixed matrix membranes using carbon molecular sieves I. Preparation and experimental results". *Journal of Membrane Science* 211 (2003), pp. 311–334.
- [62] H. Yang, Z. Xu, M. Fan, R. Gupta, R. B. Slimane, A. E. Bland and I. Wright. "Progress in carbon dioxide separation and capture: A review". *Journal of Environmental Sciences* 20.1 (2008), pp. 14–27.
- [63] Y. Lin and M. C. Duke. "Recent progress in polycrystalline zeolite membrane research". *Current Opinion in Chemical Engineering* 2.2 (2013). Nanotechnology / Separation engineering, pp. 209–216.
- [64] X. Xu, Y. Bao, C. Song, W. Yang, J. Liu and L. Lin. "Synthesis, characterization and single gas permeation properties of NaA zeolite membrane". *Journal of Membrane Science* 249 (2004), pp. 51–64.
- [65] K. Kusakabe, T. Kuroda, A. Murata and S. Morooka. "Formation of a Y-Type Zeolite Membrane on a Porous α -Alumina Tube for Gas Separation". *Ind. Eng. Chem. Res.* 36 (1997), pp. 649–655.
- [66] S. Li, M. A. Carreon, Y. Zhang, H. H. Funke, R. D. Noble and J. L. Falconer. "Scale-up of SAPO-34 membranes for CO₂/CH₄ separation". *Journal of Membrane Science* 352 (2010), pp. 7–13.
- [67] S. Himeno, T. Tomita, K. Suzuki, K. Nakayama, K. Yajima and S. Yoshida. "Synthesis and Permeation Properties of a DDR-Type Zeolite Membrane for Separation of CO₂/CH₄ Gaseous Mixtures". *Ind. Eng. Chem. Res.* 46 (2007), pp. 6989–6997.

- [68] K. Kusakabe, T. Kuroda and S. Morooka. "Separation of carbon dioxide from nitrogen using ion-exchanged faujasite-type zeolite membranes formed on porous support tubes". *Journal of Membrane Science* 148 (1998), pp. 13–23.
- [69] H. L. Castricum, H. F. Qureshi, A. Nijmeijer and L. Winnubst. "Hybrid silica membranes with enhanced hydrogen and CO₂ separation properties". *Journal of Membrane Science* 488.0 (2015), pp. 121–128.
- [70] C. M. Zimmerman, A. Singh and W. J. Koros. "Tailoring mixed matrix composite membranes for gas separations". *Journal of Membrane Science* 137.1–2 (1997), pp. 145–154.
- [71] P. Goh, A. Ismail, S. Sanip, B. Ng and M. Aziz. "Recent advances of inorganic fillers in mixed matrix membrane for gas separation". *Separation and Purification Technology* 81.3 (2011), pp. 243–264.
- [72] M. Shah, M. C. McCarthy, S. Sachdeva, A. K. Lee and H.-k. Jeong. "Current Status of Metal-Organic Framework Membranes for Gas Separations : Promises and Challenges". *Industrial & Engineering Chemistry Research* 51 (2012), pp. 2179–2199.
- [73] J.-R. Li, R. J. Kuppler and H.-C. Zhou. "Selective gas adsorption and separation in metal-organic frameworks." *Chemical Society reviews* 38.5 (2009), pp. 1477–504.
- [74] J.-R. Li, Y. Ma, M. C. McCarthy, J. Sculley, J. Yu, H.-K. Jeong, P. B. Balbuena and H.-C. Zhou. "Carbon dioxide capture-related gas adsorption and separation in metal-organic frameworks". *Coordination Chemistry Reviews* 255.15–16 (2011), pp. 1791–1823.
- [75] A. Huang, H. Bux, F. Steinbach and J. Caro. "Molecular-sieve membrane with hydrogen permselectivity: ZIF-22 in LTA topology prepared with 3-aminopropyltriethoxysilane as covalent linker". *Angewandte Chemie* 122.29 (2010), pp. 5078–5081.
- [76] A. Huang, W. Dou and J. Caro. "Steam-stable zeolitic imidazolate framework ZIF-90 membrane with hydrogen selectivity through covalent functionalization". *Journal of the American Chemical Society* 132.44 (2010), pp. 15562–15564.
- [77] M. C. McCarthy, V. Varela-Guerrero, G. V. Barnett and H.-K. Jeong. "Synthesis of zeolitic imidazolate framework films and membranes with controlled microstructures". *Langmuir* 26.18 (2010), pp. 14636–14641.
- [78] J. Gascon, S. Aguado and F. Kapteijn. "Manufacture of dense coatings of Cu₃(BTC)₂ (HKUST-1) on α -alumina". *Microporous and Mesoporous Materials* 113.1 (2008), pp. 132–138.

- [79] Y. Liu, Z. Ng, E. A. Khan, H.-K. Jeong, C.-b. Ching and Z. Lai. "Synthesis of continuous MOF-5 membranes on porous α -alumina substrates". *Microporous and Mesoporous Materials* 118.1 (2009), pp. 296–301.
- [80] Y. Yoo, Z. Lai and H.-K. Jeong. "Fabrication of MOF-5 membranes using microwave-induced rapid seeding and solvothermal secondary growth". *Microporous and Mesoporous Materials* 123.1 (2009), pp. 100–106.
- [81] K. S. Park, Z. Ni, A. P. Coté, J. Y. Choi, R. Huang, F. J. Uribe-Romo, H. K. Chae, M. O'Keeffe and O. M. Yaghi. "Exceptional chemical and thermal stability of zeolitic imidazolate frameworks". *Proceedings of the National Academy of Sciences* 103.27 (2006), pp. 10186–10191.
- [82] Y.-S. Li, F.-Y. Liang, H. Bux, A. Feldhoff, W.-S. Yang and J. Caro. "Molecular sieve membrane: supported metal-organic framework with high hydrogen selectivity". *Angewandte Chemie* 122.3 (2010), pp. 558–561.
- [83] H. Wang, Q.-L. Zhu, R. Zou and Q. Xu. "Metal-Organic Frameworks for Energy Applications". *Chem* 2.1 (2017), pp. 52–80.
- [84] H. Hayashi, A. P. Cote, H. Furukawa, M. O'Keeffe and O. M. Yaghi. "Zeolite A imidazolate frameworks". *Nature materials* 6.7 (2007), p. 501.
- [85] Y.-R. Lee, M.-S. Jang, H.-Y. Cho, H.-J. Kwon, S. Kim and W.-S. Ahn. "ZIF-8: A comparison of synthesis methods". *Chemical Engineering Journal* 271 (2015), pp. 276–280.
- [86] E. Perez, C. Karunaweera, I. Musselman, K. Balkus and J. Ferraris. "Origins and Evolution of Inorganic-Based and MOF-Based Mixed-Matrix Membranes for Gas Separations". *Processes* 4.3 (2016), p. 32.
- [87] S. R. Venna and M. A. Carreon. "Highly permeable zeolite imidazolate framework-8 membranes for CO₂/CH₄ separation". *Journal of the American Chemical Society* 132.1 (2009), pp. 76–78.
- [88] Y. Liu, G. Zeng, Y. Pan and Z. Lai. "Synthesis of highly c-oriented ZIF-69 membranes by secondary growth and their gas permeation properties". *Journal of membrane science* 379.1 (2011), pp. 46–51.
- [89] X. Zou, F. Zhang, S. Thomas, G. Zhu, V. Valtchev and S. Mintova. "Co₃(HCOO)₆ microporous metal-organic framework membrane for separation of CO₂/CH₄ mixtures". *Chemistry-A European Journal* 17.43 (2011), pp. 12076–12083.
- [90] A. Bétard, H. Bux, S. Henke, D. Zacher, J. Caro and R. A. Fischer. "Fabrication of a CO₂-selective membrane by stepwise liquid-phase deposition of an alkylether functionalized pillared-layered metal-organic framework [Cu₂ L₂P]_n on a macroporous support". *Microporous and Mesoporous Materials* 150 (2012), pp. 76–82.

- [91] Y. Mao, H. Huang, W. Cao, J. Li, L. Sun, X. Jin, X. Peng et al. "Room temperature synthesis of free-standing HKUST-1 membranes from copper hydroxide nanostrands for gas separation". *Chemical Communications* 49.50 (2013), pp. 5666–5668.
- [92] S. Kulprathipanja, R. W. Neuzil and N. N. Li. "Separation of Fluids by Means of Mixed Matrix Membranes". English. 4740219. 1988.
- [93] Y. Li, T.-S. Chung, Z. Huang and S. Kulprathipanja. "Dual-layer polyethersulfone (PES)/BTDA-TDI/MDI co-polyimide (P84) hollow fiber membranes with a submicron PES-zeolite beta mixed matrix dense-selective layer for gas separation". *Journal of Membrane Science* 277 (2006), pp. 28–37.
- [94] Y. Li, T.-S. Chung, C. Chao and S. Kulprathipanja. "The effects of polymer chain rigidification, zeolite pore size and pore blockage on polyethersulfone (PES)-zeolite A mixed matrix membranes". *Journal of Membrane Science* 260 (2005), pp. 45–55.
- [95] T. T. Moore, R. Mahajan, D. Q. Vu and W. J. Koros. "Hybrid membrane materials comprising organic polymers with rigid dispersed phases". *AIChE journal* 50.2 (2004), pp. 311–321.
- [96] R. Pal. "Permeation models for mixed matrix membranes". *Journal of Colloid and Interface Science* 317 (2007), pp. 191–198.
- [97] R. Mahajan and W. J. Koros. "Mixed Matrix Membrane Materials With Glassy Polymers, Part 2". *Polymer Engineering and Science* 42 (2002), pp. 1432–1441.
- [98] T. W. Pechar, S. Kim, B. Vaughan, E. Marand, M. Tsapatsis, H. K. Jeong and C. J. Cornelius. "Fabrication and characterization of polyimide-zeolite L mixed matrix membranes for gas separations". *Journal of Membrane Science* 277 (2006), pp. 195–202.
- [99] Y. Li, H.-M. Guan, T.-S. Chung and S. Kulprathipanja. "Effects of novel silane modification of zeolite surface on polymer chain rigidification and partial pore blockage in polyethersulfone (PES)-zeolite A mixed matrix membranes". *Journal of Membrane Science* 275 (2006), pp. 17–28.
- [100] S. Shu, S. Husain and W. J. Koros. "A general strategy for adhesion enhancement in polymeric composites by formation of nanostructured particle surfaces". *Journal of Physical Chemistry C* 111 (2007), pp. 652–657.
- [101] Y. Li, T. Chung, Z. Huang and S. Kulprathipanja. "Dual-layer polyethersulfone (PES)/BTDA-TDI/MDI co-polyimide (P84) hollow fiber membranes with a submicron PES-zeolite beta mixed matrix dense-selective layer for gas separation". *Journal of Membrane Science* 277.1-2 (June 2006), pp. 28–37.

- [102] R. Mahajan, R. Burns, M. Schaeffer and W. J. Koros. “Challenges in forming successful mixed matrix membranes with rigid polymeric materials”. *Journal of Applied Polymer Science* 86.4 (2002), pp. 881–890.
- [103] S. Kim and E. Marand. “High permeability nano-composite membranes based on mesoporous MCM-41 nanoparticles in a polysulfone matrix”. *Microporous and Mesoporous Materials* 114 (2008), pp. 129–136.
- [104] A. M. Hillock, S. J. Miller and W. J. Koros. “Crosslinked mixed matrix membranes for the purification of natural gas: Effects of sieve surface modification”. *Journal of Membrane Science* 314.1-2 (2008), pp. 193–199.
- [105] H. H. Yong, H. C. Park, Y. S. Kang, J. Won and W. N. Kim. “Zeolite-filled polyimide membrane containing 2,4,6-triaminopyrimidine”. *Journal of Membrane Science* 188 (2001), pp. 151–163.
- [106] T. T. Moore and W. J. Koros. “Non-ideal effects in organic-inorganic materials for gas separation membranes”. *Journal of Molecular Structure* 739.1-3 (2005), pp. 87–98.
- [107] T. M. Gur. “Permselectivity of zeolite filled polysulfone gas separation membranes”. *Journal of Membrane Science* 93.3 (1994), pp. 283–289.
- [108] R. Mahajan and W. J. Koros. “Factors Controlling Successful Formation of Mixed-Matrix Membranes”. *Ind. Eng. Chem. Res.* 39 (2000), pp. 2692–2696.
- [109] Y. Zhang, K. J. B. Jr., I. H. Musselman and J. P. Ferraris. “Mixed-matrix membranes composed of Matrimid® and mesoporous ZSM-5 nanoparticles”. *Journal of Membrane Science* 325 (2008), pp. 28–39.
- [110] M. J. C. Ordoñez, K. J. Balkus Jr., J. P. Ferraris and I. H. Musselman. “Molecular sieving realized with ZIF-8/Matrimid® mixed-matrix membranes”. *Journal of Membrane Science* 361.1-2 (2010), pp. 28–37.
- [111] T. Rodenas, I. Luz, G. Prieto, B. Seoane, H. Miro, A. Corma, F. Kapteijn, F. X. Llabres i Xamena and J. Gascon. “Metal-organic framework nanosheets in polymer composite materials for gas separation.” *Nature materials* 14.1 (2015), pp. 48–55.
- [112] F. Dorosti, M. Omidkhah and R. Abedini. “Fabrication and characterization of Matrimid/MIL-53 mixed matrix membrane for CO₂/CH₄ separation”. *Chemical Engineering Research and Design* 92.11 (2014), pp. 2439–2448.
- [113] S. Basu, A. Cano-Odena and I. F. Vankelecom. “Asymmetric Matrimid®/[Cu₃(BTC)₂] mixed-matrix membranes for gas separations”. *Journal of membrane science* 362.1 (2010), pp. 478–487.

- [114] E. V. Perez, K. J. Balkus Jr., J. P. Ferraris and I. H. Musselman. “Mixed-matrix membranes containing MOF-5 for gas separations”. *Journal of Membrane Science* 328.1-2 (2009), pp. 165–173.
- [115] T. Rodenas, M. Van Dalen, P. Serra-Crespo, F. Kapteijn and J. Gascon. “Mixed matrix membranes based on NH₂-functionalized MIL-type MOFs: Influence of structural and operational parameters on the CO₂/CH₄ separation performance”. *Microporous and Mesoporous Materials* 192 (2013), pp. 35–42.
- [116] C. Duan, X. Jie, D. Liu, Y. Cao and Q. Yuan. “Post-treatment effect on gas separation property of mixed matrix membranes containing metal organic frameworks”. *Journal of Membrane Science* 466 (2014), pp. 92–102.
- [117] M. Arjmandi and M. Pakizeh. “Mixed matrix membranes incorporated with cubic-MOF-5 for improved polyetherimide gas separation membranes: Theory and experiment”. *Journal of Industrial and Engineering Chemistry* 20.5 (2014), pp. 3857–3868.
- [118] J. A. Thompson, K. W. Chapman, W. J. Koros, C. W. Jones and S. Nair. “Sonication-induced Ostwald ripening of ZIF-8 nanoparticles and formation of ZIF-8/polymer composite membranes”. *Microporous and Mesoporous Materials* 158.0 (2012), pp. 292–299.
- [119] H. B. T. Jeazet, C. Staudt and C. Janiak. “Metal-organic frameworks in mixed-matrix membranes for gas separation”. *Dalton Transactions* 41.46 (2012), pp. 14003–14027.
- [120] H. Yehia, T. Pisklak, J. Ferraris, K. Balkus and I. Musselman. “Methane facilitated transport using copper (II) biphenyl dicarboxylate-triethylenediamine/poly (3-acetoxyethylthiophene) mixed matrix membranes”. *Abstracts of Papers of the American Chemical Society*. Vol. 227. AMER CHEMICAL SOC 1155 16TH ST, NW, WASHINGTON, DC 20036 USA. 2004, U351–U351.
- [121] Q. Song, S. K. Nataraj, M. V. Roussanova, J. C. Tan, D. J. Hughes, W. Li, P. Bourgoin, M. A. Alam, A. K. Cheetham, S. a. Al-Muhtaseb and E. Sivaniah. “Zeolitic imidazolate framework (ZIF-8) based polymer nanocomposite membranes for gas separation”. *Energy & Environmental Science* 5.8 (2012), pp. 8359–8369.
- [122] S. Hwang, W. S. Chi, S. J. Lee, S. H. Im, J. H. Kim and J. Kim. “Hollow ZIF-8 nanoparticles improve the permeability of mixed matrix membranes for CO₂/CH₄ gas separation”. *Journal of Membrane Science* 480 (2015), pp. 11–19.

- [123] Y. Dai, J. Johnson, O. Karvan, D. S. Sholl and W. Koros. “Ultem®/ZIF-8 mixed matrix hollow fiber membranes for CO₂/N₂ separations”. *Journal of Membrane Science* 401 (2012), pp. 76–82.
- [124] T. Li, Y. Pan, K.-V. Peinemann and Z. Lai. “Carbon dioxide selective mixed matrix composite membrane containing ZIF-7 nano-fillers”. *Journal of Membrane Science* 425-426 (2013), pp. 235–242.
- [125] T. Yang and T.-S. Chung. “Room-temperature synthesis of ZIF-90 nanocrystals and the derived nano-composite membranes for hydrogen separation”. *Journal of Materials Chemistry A* 1.19 (2013), pp. 6081–6090.
- [126] E. A. Feijani, H. Mahdavi and A. Tavasoli. “Poly(vinylidene fluoride) based mixed matrix membranes comprising metal organic frameworks for gas separation applications”. *Chemical Engineering Research and Design* 96 (2015), pp. 87–102.
- [127] R. Abedini, M. Omidkhah and F. Dorosti. “Highly permeable poly(4-methyl-1-pentyne)/NH₂-MIL-53(Al) mixed matrix membrane for CO₂/CH₄ separation”. en. *RSC Advances* 4.69 (2014), p. 36522.
- [128] B. Zornoza, A. Martinez-Joaristi, P. Serra-Crespo, C. Téllez, J. Coronas, J. Gascon and F. Kapteijn. “Functionalized flexible MOF as filler in mixed matrix membranes for highly selective separation of CO₂ from CH₄ at elevated pressures”. *Chemical communications (Cambridge, England)* 47.33 (2011), pp. 9522–9524.
- [129] B. Seoane, V. Sebastian, C. Téllez and J. Coronas. “Crystallization in THF: the possibility of one-pot synthesis of mixed matrix membranes containing MOF MIL-68(Al)”. *CrystEngComm* 68.Table 1 (2013), pp. 1–5.
- [130] O. G. Nik, X. Y. Chen and S. Kaliaguine. “Functionalized metal organic framework-polyimide mixed matrix membranes for CO₂/CH₄ separation”. *Journal of Membrane Science* 414 (2012), pp. 48–61.
- [131] M. W. Anjum, F. Vermoortele, A. L. Khan, B. Bueken, D. E. De Vos and I. F. Vankelecom. “Modulated UiO-66-based mixed-matrix membranes for CO₂ separation”. *ACS applied materials & interfaces* 7.45 (2015), pp. 25193–25201.
- [132] P. M. Budd, K. J. Msayib, C. E. Tattershall, B. S. Ghanem, K. J. Reynolds, N. B. McKeown and D. Fritsch. “Gas separation membranes from polymers of intrinsic microporosity”. *Journal of Membrane Science* 251.1 (2005), pp. 263–269.

Chapter 2

Mixed-matrix membranes prepared from non-dried MOFs for CO₂/CH₄ separations.

Adapted and largely based on:

A. Kertik et al. “Mixed matrix membranes prepared from non-dried MOFs for CO₂/CH₄ separations”. *RSC Adv.* 6.115 (2016), pp. 114505–114512

A.K. contributed by the design and conduction of experiments, data analysis, and writing. *A.L.K.* helped with the experiment design. *I.F.J.V.* helped with the data interpretation, and revised the paper.

2.1 Abstract

Mixed-matrix membranes (MMMs) aim at combining the processibility of polymers with the molecular-sieving of fillers to improve the gas separation performance. Metal-organic frameworks (MOFs) are a new family of materials with promising potential as filler. The first part of this work reports on exploiting the versatility of MOF synthesis routes by forming ZIF-8 particles in polymer solutions to subsequently cast membranes directly from the solution. Although MOFs can be synthesised in a polymer medium, the decline in the synthesis

yield does not allow for high loading in the MMMs. The second part describes a method for preparing MMMs with the commercial polyimide (PI) Matrimid® and ZIF-8, ZIF-7 and NH₂-MIL-53(Al) as non-dried filler with 30 wt.% and 50 wt.% loading. A comparison of this method with the conventional approach of drying MOFs prior to incorporation exhibits the flexibility MOFs provide in membrane synthesis. In contrast, zeolites require calcination before they can be used. The membranes with non-dried MOFs show some improvement in performance as compared to the unfilled polymer-only membranes, while those with dried MOFs even lose the inherent selectivity of the polymer.

2.2 Introduction

Membranes are energy-efficient and environmentally-friendly alternatives to existing gas separation technologies, such as cryogenic distillation and adsorption.^[2,3] The current membrane market is dominated by polymers due to their low cost, flexibility and processibility. These desirable properties are countered by their lower thermal and chemical stabilities, as well as lower selectivities.^[4] The Robeson upper-bound illustrates the performance trade-off between permeability and selectivity for polymers.^[5,6] Membranes made of carbon,^[7] metals,^[8] and zeolites^[9] have been investigated as alternatives. Despite high thermal and chemical stabilities, well-defined pore sizes and the subsequent superior selectivities, their application on a larger scale has been impeded by the high cost of production, the challenges in fabricating defect-free membranes, and the inherent brittleness.^[10]

Mixed-matrix membranes (MMM) are composites consisting of filler particles homogeneously dispersed in a polymeric matrix.^[11,12] They aim at exploiting the desirable properties of their counterparts. The permeation of gases in polymers occurs via a solution-diffusion mechanism. This mechanism manifests itself in three steps: a gas molecule in the upstream sorbs into the membrane, diffuses across the cross-section, and finally desorbs into the downstream.^[2,13,14] For fillers with a pore size relative to the kinetic diameter of the penetrating gases, the diffusion of smaller gases is accelerated whereas larger gases cannot enter the pores. This size exclusion mechanism is known as molecular sieving.^[13-15] Over the last decades, porous fillers ranging from carbon molecular sieves^[16,17] and carbon nanotubes^[18-20] to ordered mesoporous silica^[21,22] and zeolites^[23-26] have been used in MMMs to provide molecular sieving to separate gases according to size and shape.^[27] In addition, non-porous fillers manipulated the polymer chain packing and modified the free volume.^[28,29] Conventionally, an MMM is fabricated by dispersing the filler particles in a solvent, followed by adding polymer and mixing further to obtain a homogeneous solution. This

solution is then cast to be dried or annealed. The dispersion of filler and the polymer-zeolite adhesion are notorious problems in membrane preparation.^[11] Poor dispersion is often created by post-synthesis calcination of fillers for the removal of templates, which leads to the irreversible formation of strong particle agglomerates.^[30,31] It is possible to break down these agglomerates to some extent by strong mixing methods,^[32,33] but these methods make the fabrication complicated and inefficient in terms of time and energy. The intrinsic lack of affinity between the inorganic and organic phases causes the formation of non-selective voids that lead to significant losses in selectivity.^[34] Many solutions suggested to promote adhesion, such as using compatibilisers,^[35,36] silylation,^[37] priming^[38,39] etc., have proven to be material- and time-intensive, and sometimes fail to enhance dispersion.

Recently, metal organic frameworks (MOFs) have stirred up excitement for MMMs, as well as for catalysis,^[40] sensing,^[41] magnetism,^[42] semiconductors,^[43] and drug delivery.^[44] For gas separation, MOFs are very attractive owing to their tailorable chemistry, tunable composition, well-defined pore size, pore flexibility, and breathing effects.^[45] They consist of metal ions bridged with organic linkers that form a porous framework.^[45] Contrary to inorganic fillers, the organic linkers in MOFs offer better adhesion to the polymer.^[15] Unfortunately, MOFs are not completely free of aggregation. ZIF-8 nanocrystals can stay in stable colloidal dispersion before drying, but are not re-dispersible after drying.^[46] Ultrasonication can distort the shape, size distribution, and structure of the MOF particles.^[47] Recent reports^[48–50] suggest storing MOFs in colloidal state to prevent the formation of strong covalent bonds between the particles. In another study, a one-pot approach for preparing MMMs by adding the polymer directly into the MOF synthesis liquor after MOF crystallisation, was reported.^[51]

For this work, Matrimid®, a well-known commercial polyimide with properties that fall close to the Robeson upper-bound^[52,53] was chosen as polymer. As filler, three different MOFs, namely ZIF-8, ZIF-7 and NH₂-MIL-53(Al), were selected. The MOF structures are given in Figure 2.1. ZIF-8 is composed of Zn(II) ion clusters linked by imidazolate ligands, with pores of 3.4 Å in diameter. The pores are easily accessible to smaller gases such as CO₂ and H₂.^[52] ZIF-7 belongs to the same family as ZIF-8, and exhibits a hexagonal distorted sodalite topology formed by connecting zinc clusters with benzimidazole.^[48,54] ZIF-7 has an estimated pore size of 3 Å.^[55] MIL-53(Al) consists of AlO₄(OH)₂ octahedra and 1,4-benzenedicarboxylate (terephthalate) linkers,^[56] which can be amino-functionalised to form NH₂-MIL-53(Al) with amine moieties on the surface.^[57] This MOF exhibits a so-called breathing behaviour by changing from a narrow pore (*np*) structure to a large pore (*lp*) structure at high partial pressures of CO₂.^[58,59]

Two novel preparation methods are designed in this work to prepare high-loading

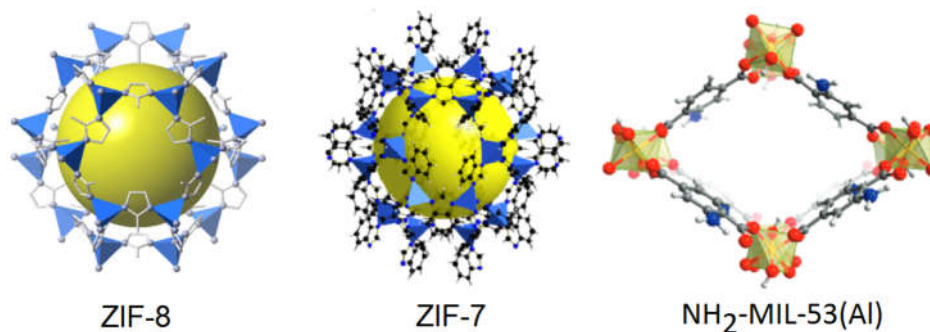


Figure 2.1: The structures of ZIF-8^[60], ZIF-7^[61] and NH₂-MIL-53(Al)^[59].

MMMs, as well as to simplify and optimize earlier approaches. The first part focuses on the synthesis of MOF particles inside a polymeric solution. This solution with perfectly dispersed MOFs will then be used directly as membrane casting solution. A second part investigates the difference between MMMs prepared with the conventional method and the so-called “wet-MOF method”.

2.3 Experimental procedure

2.3.1 Materials

Polyimide (Matrimid®5218) was kindly provided by Huntsman (Switzerland) and used after drying at 110 °C overnight. For ZIF-8 synthesis, zinc nitrate hexahydrate (Zn(NO₃)₂·6H₂O) and 2-methylimidazole (C₄H₆N₂) were obtained from Acros Organics (Belgium). Triethylamine (C₆H₁₅N) was purchased from Merck (Germany). For ZIF-7 synthesis, benzimidazole (C₇H₆N₂) was obtained from Acros Organics (Belgium). For NH₂-MIL-53(Al) synthesis, 2-aminoterephthalic acid (H₂NC₆H_{3-1,4}-(CO₂H)₂) and aluminum nitrate nonahydrate (Al(NO₃)₃·9H₂O) were obtained from ChemLab and Acros Organics, respectively. Dimethylformamide ((CH₃)₂NCOH, DMF), chloroform (CHCl₃), and methanol (CH₃OH) were purchased from Acros Organics (Belgium) and VWR (Belgium) and used for solvent exchange and membrane preparation. All solvents were dried overnight using activated zeolite 4A beads prior to use.

2.3.2 *In-situ* synthesis of MOF particles

ZIF-8@Matrimid® membranes were prepared *in-situ* by adding MOF precursors inside a dilute solution (5 wt.%) of Matrimid® in DMF at 20, 40, 60 or 80

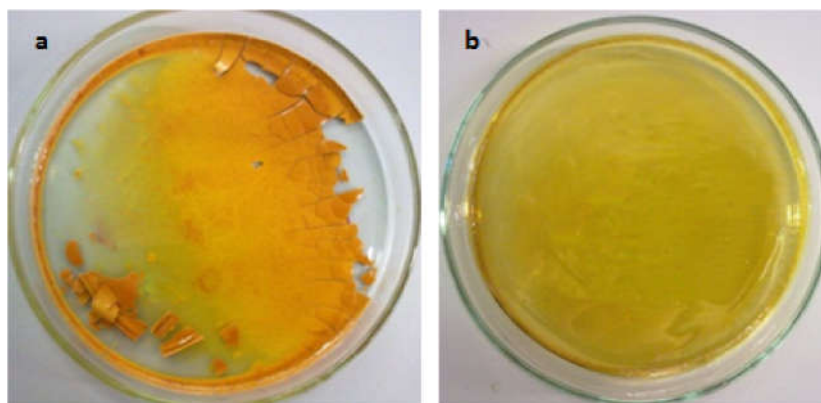


Figure 2.2: Matrimid® with 20 wt.% (a) $\text{Zn}(\text{NO}_3)_2$ and (b) 2-mim.

°C. In contrast to a previous report on a one-pot synthesis method^[51], this approach refers to crystallising MOF particles in a polymeric solution. The ZIF-8 synthesis recipe was adapted from ref.^[52] with a 2-methylimidazole (2-mim) to $\text{Zn}(\text{NO}_3)_2$ ratio of 8:1. This modification was applied in order to overcome the brittleness caused by the unreacted $\text{Zn}(\text{NO}_3)_2$ that remains in the membrane. Figure 2.2a and b show membranes prepared by adding 20 wt.% of $\text{Zn}(\text{NO}_3)_2$ and 2-mim to Matrimid®, respectively. While Matrimid® with 2-mim formed a homogeneous, standalone membrane, the membrane with $\text{Zn}(\text{NO}_3)_2$ was brittle and broken. The recipe was downscaled to match the amount of DMF in the polymer solution (10 mL). Unlike the original procedure, the synthesis compounds were added directly into the Matrimid® solution. The mixture was stirred for 4 days to give enough time for ZIF-8 synthesis, which was then poured into a petri dish to dry at 100 °C until the membrane solidified.

In order to increase the amount of ZIF-8 particles in the Matrimid® solution, the concentration of the synthesis components was increased to give 13, 33 and 53 wt.% loading, as calculated based on the yield reported in ref.^[52].

2.3.3 Preparation of MMMs with wet MOFs

ZIF-8 was synthesised as described in ref.^[52]. Upon cooling, the particles were washed with DMF, methanol, and CHCl_3 , respectively. ZIF-7 was synthesised by dissolving zinc nitrate hexahydrate (0.302 g) and benzimidazole (0.769 g) in DMF (400 mL), and magnetically stirring the mixture for 48 h at room temperature. The particles were washed with DMF, methanol, and CHCl_3 , respectively. $\text{NH}_2\text{-MIL-53}(\text{Al})$ was synthesised by dissolving 2-aminoterephthalic acid (2g) and $\text{Al}(\text{NO}_3)_3 \cdot 9\text{H}_2\text{O}$ (2g) in distilled water (400 mL). The solution was heated to 100 °C for 6 h. Upon cooling, the particles

were centrifuged and washed with DMF, methanol and CHCl₃, respectively. At the end of the synthesis procedure, the MOF particles were washed as detailed below, and the remaining sludge was separated into two equal parts, one part was dried in the oven overnight (240 °C for ZIF-8, 100 °C for ZIF-7 and NH₂-MIL-53(Al)), and the other part was kept in CHCl₃ to be directly used for membrane fabrication. In order to prepare a membrane solution, the MOF dispersion and Matrimid® were mixed in certain amounts to achieve the desired membrane loading, as shown in Equation 2.1, and stirred magnetically overnight. When a homogenous mixture was obtained, it was poured into a petri dish and dried at room temperature under N₂ until the membrane solidified. The solidified membranes were gradually heated to 100 °C and dried for two days, allowing to cool down gradually prior to their removal from the oven.

$$Loading(wt.\%) = \frac{wt.MOF}{(wt.MOF + wt.polymer)} \quad (2.1)$$

2.3.4 Preparation of conventional MMMs

The membranes with MOF loadings of 1, 3, 6, 10 and 13 wt.% were prepared by dispersing the particles in DMF followed by the addition of Matrimid® and casting the solution into a petri dish. Membranes with 30 and 50 wt.% dried MOF loading were prepared by dispersing the particles in CHCl₃. All membranes were dried at 100 °C for two days, allowing to cool down gradually prior to their removal from the oven.

2.3.5 Characterisation

The morphology of membrane cross-sections was observed using a JEOL JSM-1060LV. The SEM samples were prepared by freeze-fracturing in liquid N₂. In order to prevent charge build-up, the samples were sputtered with Au/Pd for three cycles of 20 s. X-ray diffraction patterns were obtained using a Stoe-HT X-ray diffractometer with CuKα radiation ($\lambda=1.54 \text{ \AA}$) at room temperature. The gas separation performance of a membrane is determined by the permeability of penetrants, and the separation factor. The rate at which gas molecules permeate through a membrane is the permeability coefficient, defined as the product of the diffusion and solubility coefficients, as shown in Equation 2.2, where P_i , D_i and S_i are the permeability, diffusion and solubility coefficients of species i , respectively.

$$P_i = D_i S_i \quad (2.2)$$

The selectivity of a membrane for pure gases (ideal selectivity) is the ratio of the permeation coefficient of component i to that of component j , as given in Equation 2.3, where $\alpha_{i/j}$ is the ideal selectivity for i over j , and P_i and P_j are the permeabilities of i and j , respectively.

$$\alpha_{i/j} = P_i/P_j \quad (2.3)$$

Pure-gas selectivity fails to provide a real-life estimation of membrane performance, especially when highly soluble gases (such as CO₂) are concerned. The mixed-gas selectivity, obtained by mixed-gas permeation measurements, is more realistic, as it is obtained with a mixed feed and competitive sorption is also taking place during permeation. Mixed-gas selectivity is calculated as given in 2.4, where y_i , y_j are the mole fractions of i and j in the permeate, and x_i and x_j are the mole fractions of i and j in the feed, respectively.

$$\alpha_{i/j} = \frac{y_i/y_j}{x_i/x_j} \quad (2.4)$$

The gas separation performance for binary gas mixtures was tested using a custom-built, high-throughput gas separation system (HTGS), described in detail in ref.^[62]. A mixed-gas feed of 50-50% vol. CO₂-CH₄ at 35 °C and 10 bar cross-membrane pressure difference was used. The composition of the permeate side was analysed by gas chromatography (GC) until three consecutive measurements gave the same result, which indicates steady-state. The reported selectivities are the average of these three measurements. Permeabilities were measured using the constant-volume variable-pressure method after steady-state was ensured.

2.4 Results and discussion

2.4.1 Synthesis of ZIF-8 particles in a PI-solution

ZIF-8 particles were synthesised in a dilute solution of Matrimid® by directly adding Zn(NO₃)₂·6H₂O and 2-methylimidazole to it, and stirring the mixture at 20, 40, 60 or 80 °C for 4 days. As seen in Figure 2.3, no ZIF-8 particles could be observed in the cross-sections of the membranes prepared at 20 or 40 °C, but some particles could be observed for samples prepared at 60 and 80 °C. As a result of the *in-situ* synthesis approach, these particles are perfectly distributed in the polymer matrix.

The XRD diffractogram of the MMMs (Figure 2.4a) did not exhibit the characteristic peaks of ZIF-8. Due to the presence of unreacted Zn-source

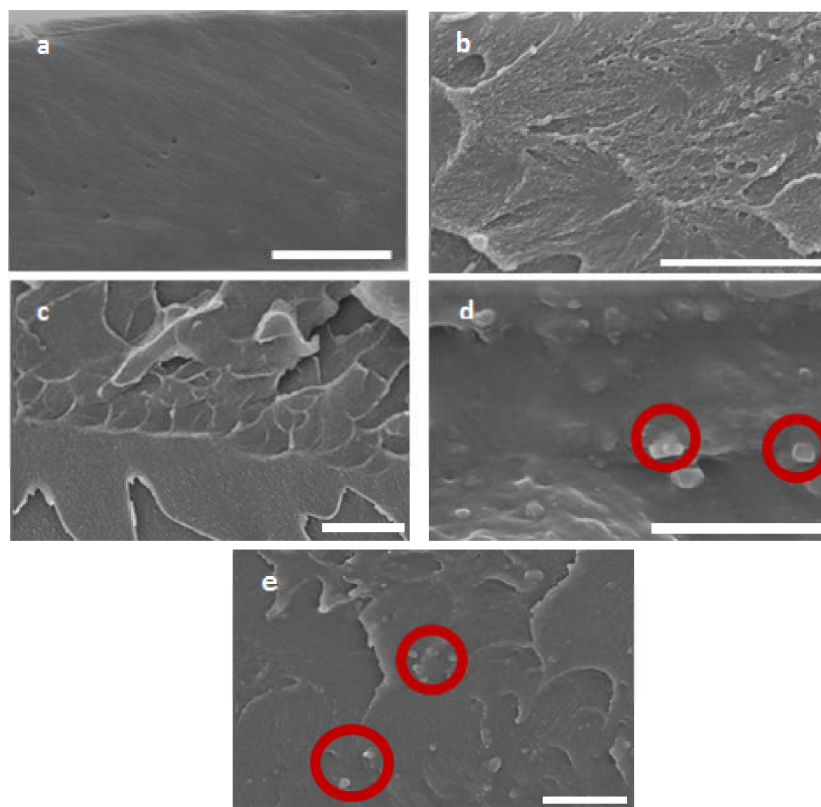


Figure 2.3: SEM images of (a) Matrimid, and ZIF-8@Matrimid[®] MMMs prepared at (b) 20 °C , (c) 40 °C , (d) 60 °C and (e) 80 °C. The bars represent 5 μm . The red circles show ZIF-8 particles.

in the membranes, TGA could not be used to determine the ZIF-8 loading based on the Zn content.^[63] Instead, the XRD diffractogram of conventional MMMs with pre-synthesised MOFs at loadings of 1, 3, 6, 10 and 13 wt.% were used for comparison, (Figure 2.4b and Figure 2.6). These membranes were prepared by dispersing pre-synthesised and dried MOF particles in a solvent, and adding the polymer to this mixture. As the characteristic peaks of ZIF-8 started to appear only from 6 wt.% loading onward for these samples, the ZIF-8 loading in the *in-situ* prepared MMMs was thus assumed to be below 6 wt.%, and hence much below the limits of application. In an attempt to increase the ZIF-8 loading, the concentration of MOF precursors in the polymer solution was increased to achieve up to a theoretical 53 wt.% of MOF loading, based on a 48% conversion of the precursors. In addition to the gelation of this mixture, and the failure to form standalone layers; these membranes also did not show any indication of significant loading, as shown in Figure 2.4 and Figure 2.5; with the exception of a Zn(OH)₂ peak around 27-28° that signifies low crystallinity.^[64] (Fig. 2.5b). Therefore, it was clear that changing the synthesis

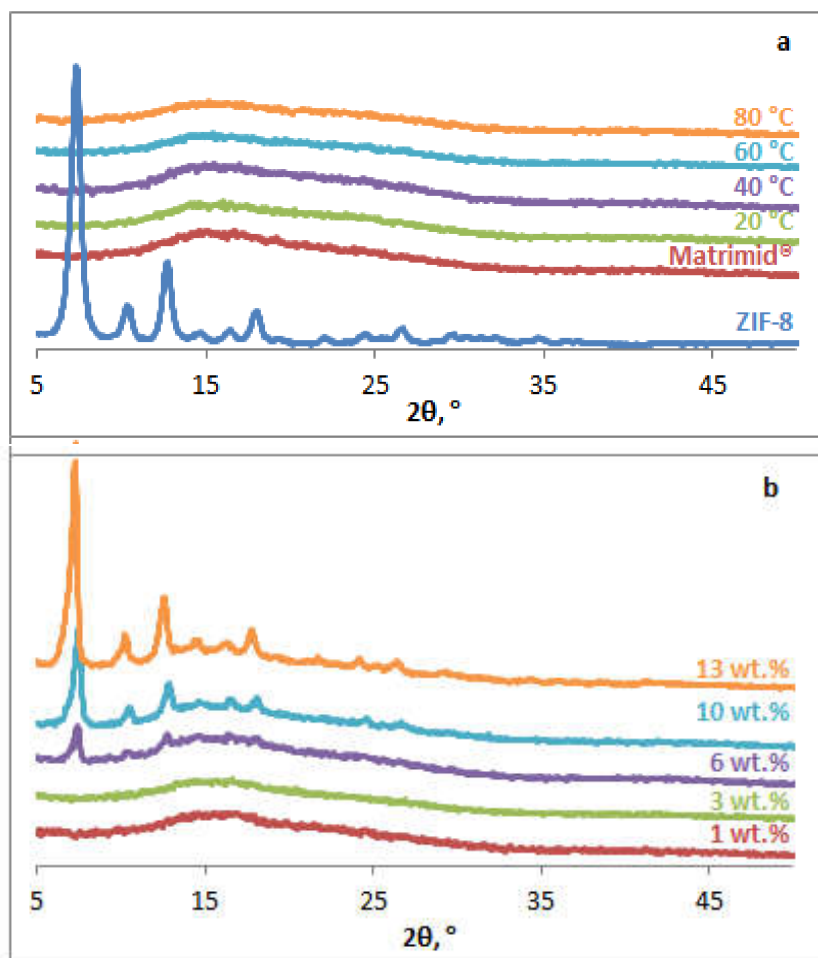


Figure 2.4: XRD diffractogram of (a) ZIF-8@Matrimid® prepared at 20, 40, 60 and 80 °C, and (b) membranes with controlled loading of dried ZIF-8.

medium from a solvent to a polymer solution was detrimental to the synthesis yield, regardless of the concentration of the precursors.

2.4.2 Non-dried vs. dried MOFs

The membrane preparation method was changed to omitting post-synthesis drying, similar to ref.^[65]. In order to demonstrate the effectiveness of this method, membranes with dried MOFs were also prepared for comparison. Comparability was assured by preparing the MMMs with dried MOFs (MOF^{dr} from now on) by using the exact method as for non-dried MOFs (MOF^{n-dr} from now on), i.e. only magnetic stirring was applied to distribute the MOF^{dr} particles. The cross-sectional SEM images (Figure 2.7) exhibit the clear difference between

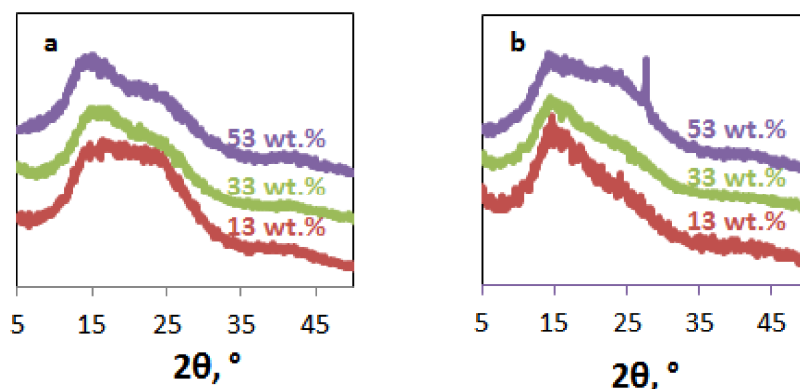


Figure 2.5: XRD diffractogram of MMMs with increased precursor concentration to achieve theoretical loadings of 13, 33 and 53 wt.%, synthesised at (a) 20 °C and (b) 60 °C.

MMMs with dried and non-dried MOFs. MOFs^{dr} formed big agglomerates that were completely detached from the polymer, especially at high loadings. On the contrary, the MOFs^{n-dr} were perfectly distributed and embedded in the polymer, despite the very high loadings (30 and 50 wt.%).

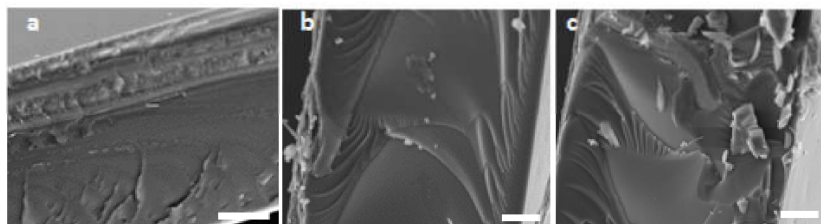


Figure 2.6: Cross-sectional SEM images of MMMs with increased precursor concentration to achieve a theoretical loading of (a) 13 (b) 33 (c) 53 wt.%.

As shown in Figure 2.8, the XRD diffractogram of the MMMs were in agreement with their respective MOFs for both the wet and dry synthesis method. The diffractogram show that the MOF particles remained intact during membrane preparation (thanks to the mild mixing conditions); as opposed to the work in ref.^[47], where high-intensity ultrasonication of MOF particles resulted in changes in the structure of ZIF-8 particles.

2.4.3 Gas separation performance

Gas separation performance is a direct indicator of the presence or absence of microdefects,^[66] and the good dispersion of MOFs in MMMs. There was an

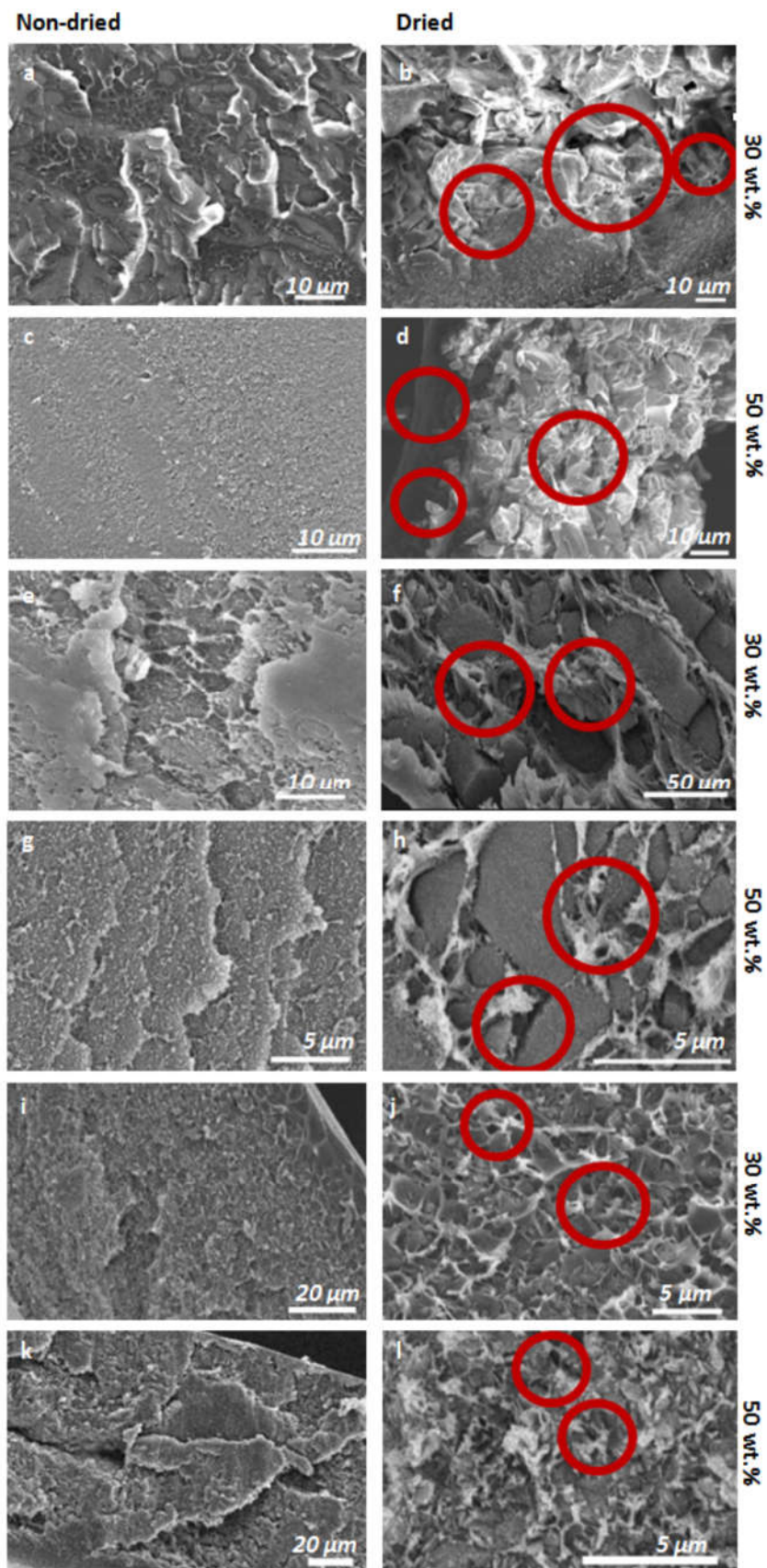


Figure 2.7: SEM images of MMMs with (a-d) ZIF-8, (e-h) ZIF-7 and (i-l) NH₂-MIL-53(Al). The red circles mark the defective interface between the Matrimid® matrix and the agglomerated MOF particles.

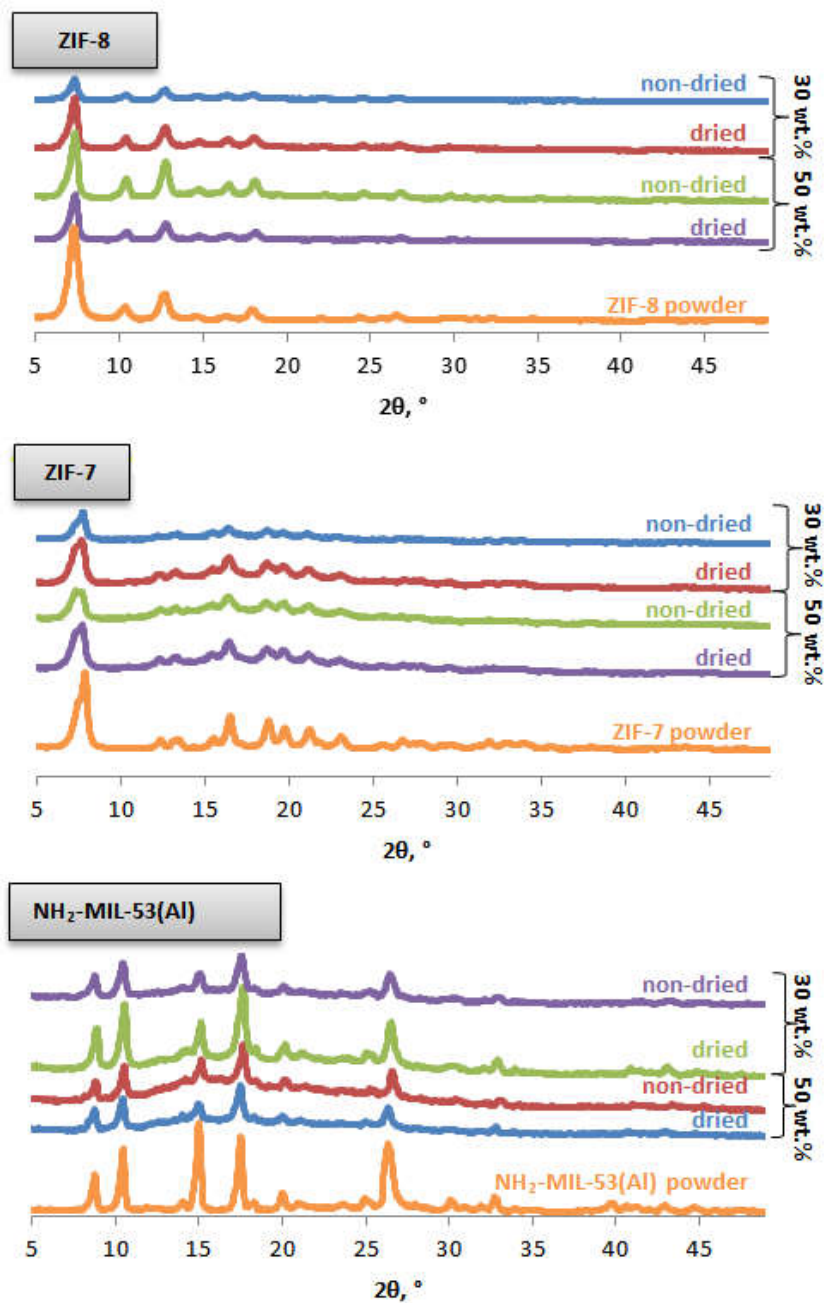


Figure 2.8: XRD patterns of MMMs with non-dried and dried MOFs.

obvious difference between the gas separation performances of the MMMs with non-dried and dried MOFs, as given in Figure 2.9.

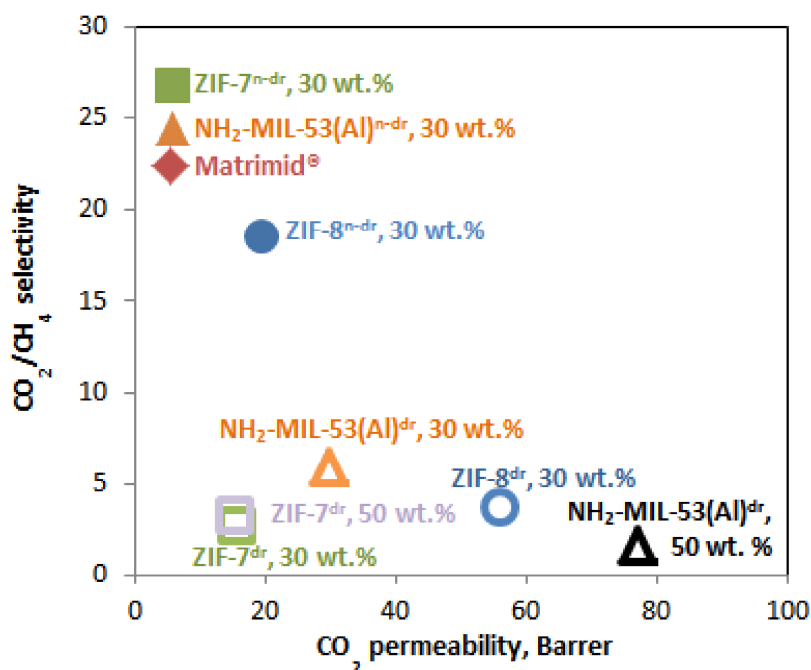


Figure 2.9: The gas separation performance of MMMs with non-dried and dried ZIF-8, ZIF-7 and NH₂-MIL-53(Al).

The MMM with 30 wt.% ZIF-8^{n-dr} exhibited a tripled CO₂ permeability compared to the unfilled polymer along with a slight decrease in selectivity from 22.3 to 18.6. The higher increase in the permeation of CO₂ compared to CH₄ can be attributed to the intrinsic framework flexibility of ZIF-8,^[67–69] which allows for the faster diffusion of both gases. Although it belongs to the same family as ZIF-8, ZIF-7^{n-dr} exhibited a selectivity increase over unfilled Matrimid® and a small increase in permeability. Both MOFs undergo similar guest-induced “gate opening”^[70,71] but their intrinsic pore apertures are different: ZIF-8 has a larger pore aperture of 3.4 Å versus 3.0 Å for ZIF-7. In addition, it has been reported that ZIF-8 is much more susceptible to the enlargement of the pore aperture via the “gate opening” phenomenon.^[72] Therefore, the ZIF-8^{n-dr} and ZIF-7^{n-dr} showed opposite improvement in membrane performance as MMM fillers. Just like ZIF-7^{n-dr}, the MMMs with NH₂-MIL-53(Al)^{n-dr} showed no change in permeability and a small increase in selectivity. In contrast to its unfunctionalised parent, the *np* form of NH₂-MIL-53(Al) is preferred at low CO₂ pressures (below 10 bar^[58]). Therefore, it is sensible that there is no significant increase in permeability for the measurement conditions of this work

(5 bar). All in all, these MMMs show improved selective behaviour without sacrificing the intrinsic permeability of the polymer.

In agreement with the SEM results, the defects formed by the dried MOFs caused complete deterioration of the inherent selectivity of the polymer. The agglomerates (that were formed as a result of drying) created non-selective voids that made the selectivity drop substantially. The permeabilities were increased up to 13 times. For a better comparison of the extent of change in selectivity, the enhancement ratio was calculated as the ratio of the selectivity of the MMM to that of the polymer (Figure 2.10). The improvement in membrane performance followed the order ZIF-7^{n-dr} > NH₂-MIL-53(Al)^{n-dr} > ZIF-8^{n-dr} for MOFs^{n-dr} whereas the selectivity decay did not follow a certain order, but it clearly could not exceed 0.3 for MOFs^{dr}.

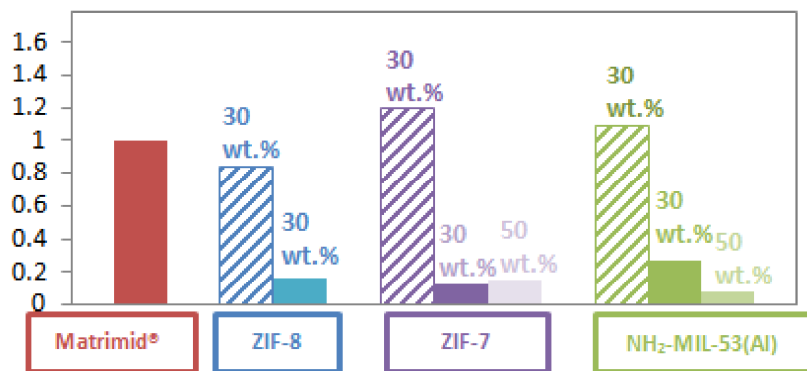


Figure 2.10: Enhancement in selectivity with non-dried (striped bars) and dried (filled bars) MOFs.

2.4.4 Comparison with the Maxwell model

There are various theoretical expressions for predicting the gas separation performance of MMMs. An adaptation of the Maxwell model, which was originally developed for calculating the electrical conductivity of composites, is conventionally used to estimate the permeability and selectivity of an MMM comprised of counterparts of known permeabilities. The Maxwell model assumes a dispersed phase within a continuous matrix in the absence of defects i.e. no interfacial voids, and no distortion in the separation properties of the counterparts.^[10] The effective permeability of a composite material can be calculated as given in Equation 2.5.

$$P = P_m \left[\frac{n.P_d + (1 - n)P_m + (1 - n)\phi(P_d - P_m)}{n.P_d + (1 - n)P_m - n\phi(P_d - P_m)} \right] \quad (2.5)$$

P is the effective permeability of the penetrant in the MMM, and Φ is the volume fraction of the dispersed phase in the continuous matrix phase. P_m and P_d are the penetrant permeabilities in the matrix and the dispersed phase, respectively, and n is the shape factor for the dispersed phase. When $n=0$ and $n=1$, the equation corresponds to transport through a laminate in parallel and in series, respectively.^[73] For a dilute suspension of spherical particles ($n=1/3$), the Maxwell equation will be as given in Equation 2.6.

$$P = P_m \left[\frac{P_d + 2P_m - 2\phi(P_m - P_d)}{P_d + 2P_m + \phi(P_m - P_d)} \right] = P_m \left[\frac{2(1 - \phi) + (1 + 2\phi)\lambda_{dm}}{(2 + \phi) + (1 - \phi)\lambda_{dm}} \right] \quad (2.6)$$

λ_{dm} is the ratio of the permeability of the dispersed filler particles (P_d) to the permeability of the matrix P_m .^[74] The Maxwell model generally predicts the permeability well when Φ is less than about 0.2. Moreover, the Maxwell model cannot predict the correct behaviour when Φ is close to the maximum packing volume fraction of filler particles. The model does not account for particle size distribution, particle shape, and aggregation of particles.^[74]

Figure 2.11 shows the comparison of the experimental results from this work and the Maxwell predictions based on different literature reports for MOF performances. Detailed information on the Maxwell predictions is given in Table 2.2, 2.3 and 2.4. ZIF-8^{*n-dr*} matches the permeability but cannot reach the selectivity predicted, whereas ZIF-7^{*n-dr*} matches the predicted selectivity much better, but falls short on permeability. NH₂-MIL-53(Al)^{*n-dr*} cannot reach the permeability and selectivity predicted, which may be related to the interaction between the amino groups of the MOF with the amide groups of the polymer chains.^[75,76]

2.5 Conclusions

Two different approaches were applied to prepare MOF-containing MMMs. First, ZIF-8 particles were synthesised by adding the MOF precursors directly into a dilute solution of Matrimid®. Although individual particles could be observed in the SEM images, XRD analysis revealed that the loading was too low for practical use. Increasing the concentration of the precursors did not achieve higher filler content. Moreover, the membranes were gelled by the unreacted

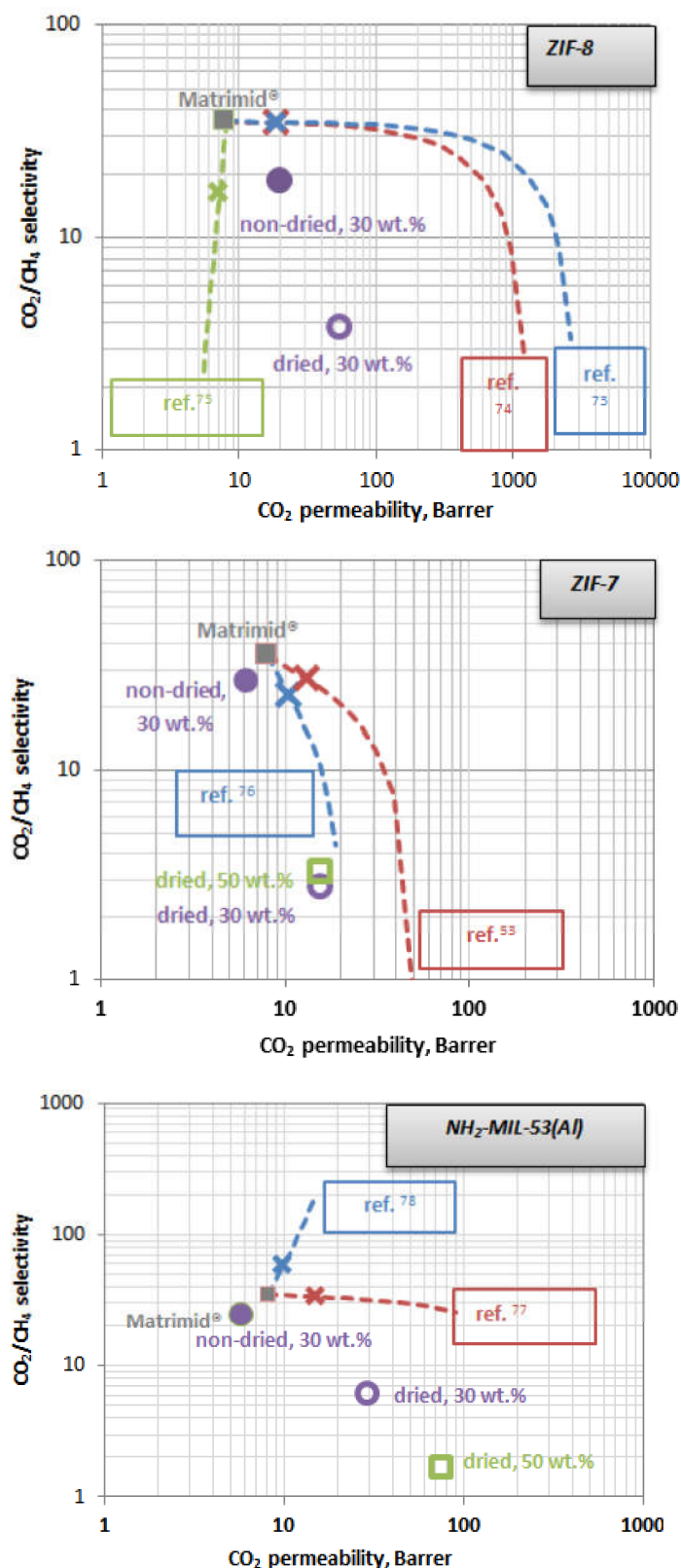


Figure 2.11: A comparison of membrane performances with Maxwell predictions for (a) ZIF-8, (b) ZIF-7 and (c) NH₂-MIL-53(Al). The filled and empty symbols represent the data from this work, with non-dried and dried MOFs, respectively. The dashed lines show the Maxwell predictions from 0 to 100 wt.% loading with the reference used for the 100 wt.% MOF performance mentioned in frames. The predictions for 30 wt.% loading are marked with X's on the dashed lines.

Table 2.1: The gas separation measurements from this work.

Membrane	MOF loading, wt.%	CO ₂ permeability, Barrer	CO ₂ /CH ₄ selectivity
Unfilled Matrimid®	0	5.6 ± 0.7	22.3 ± 0.2
ZIF-8 ^{n-dr}	30	19.6 ± 0.3	18.6 ± 0.2
ZIF-8 ^{dr}	30	55.7 ± 1.4	3.7 ± 0.2
ZIF-7 ^{n-dr}	30	5.7 ± 0.6	26.8 ± 1.3
ZIF-7 ^{dr}	30	15.9 ± 1	2.7 ± 0.1
	50	15.3 ± 1.4	3.23 ± 0.1
NH ₂ -MIL-53(Al) ^{n-dr}	30	5.7 ± 0.2	24.5 ± 0.6
NH ₂ -MIL-53(Al) ^{dr}	30	29.9 ± 2.4	5.9 ± 0.1
	50	77.2 ± 5.7	1.6 ± 0.1

Table 2.2: Maxwell predictions for Matrimid®/ZIF-8 MMMs.

Loading, wt.%	CO ₂ permeability, Barrer			CO ₂ /CH ₄ selectivity		
	Ref.1 ¹	Ref.2 ²	Ref.3 ³	Ref.1 ¹	Ref.2 ²	Ref.3 ³
10	7.8	10.8	10.9	26.8	34.9	35.0
20	7.5	14.3	14.4	20.7	34.7	34.9
30	7.2	18.7	18.8	16.2	34.6	34.8
40	6.9	24.5	24.8	12.6	34.4	34.8
50	6.7	32.5	33.1	9.9	34.1	34.6
60	6.4	44.4	45.4	7.7	33.8	34.5
70	6.2	63.6	65.7	5.9	33.2	34.2
80	6.0	100.1	105.3	4.4	32.2	33.8
90	5.7	196.8	217.2	3.2	29.6	32.4
100	5.5	1192.0	2658.0	2.2	2.8	3.3

^aZIF-8 membrane at 2 atm feed pressure and 308 K, pure gas measurements.

^bZIF-8 membrane at 1.1-2 bar feed pressure and 298 K, pure gas measurements.

^cZIF-8 membrane at 1 bar feed pressure and 298 K, pure gas measurements.

precursors. Secondly, in order to increase and control MOF loading, MOFs were synthesised separately and embedded into the membrane in their non-dried form to prevent the formation of agglomerates during drying. The different properties of the MOFs resulted in different outcomes in terms of gas separation performance. ZIF-8^{n-dr} showed an impressive increase in permeability along with a slight loss of selectivity, whereas ZIF-7^{n-dr} and NH₂-MIL-53(Al)^{n-dr} exhibited increased selectivities and very small increases in permeability. Dried MOFs prepared using the same method were severely agglomerated and detached from the polymer to the extent that the inherent selectivity of Matrimid® was lost. Maxwell predictions overestimated the performances, probably due to the flexible nature of the MOFs.

Table 2.3: Maxwell predictions for Matrimid®/ZIF-7 MMMs.

Loading, wt.%	CO ₂ permeability, Barrer		CO ₂ /CH ₄ selectivity	
	Ref.4 ¹	Ref.5 ²	Ref.4 ¹	Ref.5 ²
10	8.8	9.5	30.1	32.1
20	9.7	11.1	25.9	29.5
30	10.6	13.0	22.4	27.1
40	11.6	15.3	19.2	24.7
50	12.7	18.0	16.2	22.2
60	14.0	21.4	13.3	19.5
70	15.4	25.6	10.4	16.3
80	17.0	31.1	7.5	12.5
90	18.9	38.5	4.4	7.6
100	21.0	49.0	1.1	0.9

^aZIF-7 membrane at 1 bar feed pressure and 473 K, pure gas measurements.

^bZIF-7 membrane at 1 bar feed pressure and 493 K, pure gas measurements.

Table 2.4: Maxwell predictions for Matrimid®/NH₂-MIL-53(Al) MMMs.

Loading, wt.%	CO ₂ permeability, Barrer		CO ₂ /CH ₄ selectivity	
	Ref.6 ¹	Ref.7 ²	Ref.6 ¹	Ref.7 ²
10	8.6	9.9	41.2	34.6
20	9.2	12.2	48.6	34.1
30	9.9	14.9	57.7	33.7
40	10.6	18.2	68.9	33.2
50	11.3	22.3	83.0	32.7
60	12.1	27.7	101.1	32.0
70	13.0	35.1	124.7	31.2
80	13.9	45.5	156.5	30.1
90	14.9	61.7	201.1	28.5
100	16.0	90.0	266.7	25.7

^aBack-calculated from MMM data at 5 bar and 298 K, pure gas measurements.

^bBack-calculated from MMM data at 10.3 bar and 308 K, pure gas measurements.

2.6 Acknowledgements

A. K. is thankful to the Erasmus-Mundus Doctorate in Membrane Engineering Programme. We also would like to thank IAP funding of the Belgian Federal government and Huntsman (Switzerland) for kindly providing the Matrimid®.

References

- [1] A. Kertik, A. L. Khan and I. F. J. Vankelecom. "Mixed matrix membranes prepared from non-dried MOFs for CO₂/CH₄ separations". *RSC Adv.* 6.115 (2016), pp. 114505–114512.
- [2] P. Pandey and R. Chauhan. "Membranes for gas separation". *Prog. Polym. Sci.* 26 (2001), pp. 853–893.
- [3] S. Sridhar, B. Smitha and T. M. Aminabhavi. "Separation of Carbon Dioxide from Natural Gas Mixtures through Polymeric Membranes-A Review". *Separation & Purification Reviews* 36 (2007), pp. 113–174.
- [4] M. Shah, M. C. McCarthy, S. Sachdeva, A. K. Lee and H.-k. Jeong. "Current Status of Metal-Organic Framework Membranes for Gas Separations : Promises and Challenges". *Industrial & Engineering Chemistry Research* 51 (2012), pp. 2179–2199.
- [5] L. M. Robeson. "Correlation of separation factor versus permeability for polymeric membranes". *Journal of Membrane Science* 62.2 (1991), pp. 165–185.
- [6] L. M. Robeson. "The upper bound revisited". *Journal of Membrane Science* 320.1-2 (2008), pp. 390–400.
- [7] S. Lagorsse. "Carbon molecular sieve membranes: Sorption, kinetic and structural characterization". *Journal of Membrane Science* 241.2 (2004), pp. 275–287.
- [8] F. Gallucci, E. Fernandez, P. Corengia and M. van Sint Annaland. "Recent advances on membranes and membrane reactors for hydrogen production". *Chemical Engineering Science* 92 (2013), pp. 40–66.
- [9] N. Kosinov, J. Gascon, F. Kapteijn and E. J. Hensen. "Recent developments in zeolite membranes for gas separation". *Journal of Membrane Science* 499 (2016), pp. 65–79.
- [10] T.-S. Chung, L. Y. Jiang, Y. Li and S. Kulprathipanja. "Mixed Matrix Membranes (MMMs) comprising organic polymers with dispersed inorganic fillers for gas separation". *Prog. Poly. Sci.* 32 (2007), pp. 483–507.
- [11] R. Mahajan, R. Burns, M. Schaeffer and W. J. Koros. "Challenges in forming successful mixed matrix membranes with rigid polymeric materials". *Journal of Applied Polymer Science* 86.4 (2002), pp. 881–890.
- [12] T. T. Moore and W. J. Koros. "Non-ideal effects in organic-inorganic materials for gas separation membranes". *Journal of Molecular Structure* 739.1–3 (2005), pp. 87–98.

- [13] C. A. Scholes, S. E. Kentish and G. W. Stevens. “Carbon Dioxide Separation through Polymeric Membrane Systems for Flue Gas Applications”. *Recent Patents on Chemical Engineering* 1 (2008), pp. 52–66.
- [14] P. Goh, A. Ismail, S. Sanip, B. Ng and M. Aziz. “Recent advances of inorganic fillers in mixed matrix membrane for gas separation”. *Separation and Purification Technology* 81.3 (2011), pp. 243–264.
- [15] H. B. T. Jeazet, C. Staudt and C. Janiak. “Metal-organic frameworks in mixed-matrix membranes for gas separation”. *Dalton Transactions* 41.46 (2012), pp. 14003–14027.
- [16] W. Rafizah and A. Ismail. “Effect of carbon molecular sieve sizing with poly(vinyl pyrrolidone) K-15 on carbon molecular sieve–polysulfone mixed matrix membrane”. *Journal of Membrane Science* 307.1 (2008), pp. 53–61.
- [17] D. Q. Vu, W. J. Koros and S. J. Miller. “Mixed matrix membranes using carbon molecular sieves I. Preparation and experimental results”. *Journal of Membrane Science* 211 (2003), pp. 311–334.
- [18] S. Kim, L. Chen, J. K. Johnson and E. Marand. “Polysulfone and functionalized carbon nanotube mixed matrix membranes for gas separation: Theory and experiment”. *Journal of Membrane Science* 294.1-2 (2007), pp. 147–158.
- [19] S. Kim, J. R. Jinschek, H. Chen, D. S. Sholl and E. Marand. “Scalable fabrication of carbon nanotube/polymer nanocomposite membranes for high flux gas transport”. *Nano Letters* 7.9 (2007), pp. 2806–2811.
- [20] S. Kim, T. W. Pechar and E. Marand. “Poly(imide siloxane) and carbon nanotube mixed matrix membranes for gas separation”. *Desalination* 192.1 (2006), pp. 330–339.
- [21] S. Kim and E. Marand. “High permeability nano-composite membranes based on mesoporous MCM-41 nanoparticles in a polysulfone matrix”. *Microporous and Mesoporous Materials* 114.1-3 (2008), pp. 129–136.
- [22] B. D. Reid, F. A. Ruiz-Trevino, I. H. Musselman, K. J. Balkus, J. P. Ferraris et al. “Gas permeability properties of polysulfone membranes containing the mesoporous molecular sieve MCM-41”. *Chemistry of materials* 13.7 (2001), pp. 2366–2373.
- [23] S. Husain and W. J. Koros. “Mixed matrix hollow fiber membranes made with modified HSSZ-13 zeolite in polyetherimide polymer matrix for gas separation”. *Journal of Membrane Science* 288.1 (2007), pp. 195–207.

- [24] T. W. Pechar, S. Kim, B. Vaughan, E. Marand, M. Tsapatsis, H. K. Jeong and C. J. Cornelius. "Fabrication and characterization of polyimide-zeolite L mixed matrix membranes for gas separations". *Journal of Membrane Science* 277.1 (2006), pp. 195–202.
- [25] D. Şen, H. Kalipçılar and L. Yilmaz. "Development of polycarbonate based zeolite 4A filled mixed matrix gas separation membranes". *Journal of Membrane Science* 303.1 (2007), pp. 194–203.
- [26] Ş. B. Tantekin-Ersolmaz, Ç. Atalay-Oral, M. Tatlier, A. Erdem-Şenatalar, B. Schoeman and J. Sterte. "Effect of zeolite particle size on the performance of polymer-zeolite mixed matrix membranes". *Journal of Membrane Science* 175.2 (2000), pp. 285–288.
- [27] C. E. Powell and G. G. Qiao. "Polymeric CO₂/N₂ gas separation membranes for the capture of carbon dioxide from power plant flue gases". *Journal of Membrane Science* 279.1 (2006), pp. 1–49.
- [28] T. Merkel, B. Freeman, R. Spontak, Z. He, I. Pinnau, P. Meakin and A. Hill. "Ultrapervious, reverse-selective nanocomposite membranes". *Science* 296.5567 (2002), pp. 519–522.
- [29] T. Merkel, B. Freeman, R. Spontak, Z. He, I. Pinnau, P. Meakin and A. Hill. "Sorption, transport, and structural evidence for enhanced free volume in poly (4-methyl-2-pentyne)/fumed silica nanocomposite membranes". *Chemistry of Materials* 15.1 (2003), pp. 109–123.
- [30] L. Huang, Z. Wang, J. Sun, L. Miao, Q. Li, Y. Yan and D. Zhao. "Fabrication of ordered porous structures by self-assembly of zeolite nanocrystals". *Journal of the American Chemical Society* 122.14 (2000), pp. 3530–3531.
- [31] M. Smaïhi, E. Gavilan, J.-O. Durand and V. P. Valtchev. "Colloidal functionalized calcined zeolite nanocrystals". *Journal of Materials Chemistry* 14.8 (2004), pp. 1347–1351.
- [32] Y. Dai, J. Johnson, O. Karvan, D. S. Sholl and W. Koros. "Ultem®/ZIF-8 mixed matrix hollow fiber membranes for CO₂/N₂ separations". *Journal of Membrane Science* 401 (2012), pp. 76–82.
- [33] L. M. Vane, V. V. Namboodiri and T. C. Bowen. "Hydrophobic zeolite-silicone rubber mixed matrix membranes for ethanol-water separation: effect of zeolite and silicone component selection on pervaporation performance". *Journal of Membrane Science* 308.1 (2008), pp. 230–241.
- [34] R. Mahajan and W. J. Koros. "Mixed Matrix Membrane Materials With Glassy Polymers, Part 2". *Polymer Engineering and Science* 42 (2002), pp. 1432–1441.

- [35] E. Karatay, H. Kalipçilar and L. Yilmaz. "Preparation and performance assessment of binary and ternary PES-SAPO 34-HMA based gas separation membranes". *Journal of Membrane Science* 364.1 (2010), pp. 75–81.
- [36] H. H. Yong, H. C. Park, Y. S. Kang, J. Won and W. N. Kim. "Zeolite-filled polyimide membrane containing 2, 4, 6-triaminopyrimidine". *Journal of Membrane Science* 188.2 (2001), pp. 151–163.
- [37] I. F. Vankelecom, S. Van den broeck, E. Merckx, H. Geerts, P. Grobet and J. B. Uytterhoeven. "Silylation to improve incorporation of zeolites in polyimide films". *The Journal of Physical Chemistry* 100.9 (1996), pp. 3753–3758.
- [38] S. A. Hashemifard, A. F. Ismail and T. Matsuura. "Mixed matrix membrane incorporated with large pore size halloysite nanotubes (HNT) as filler for gas separation: experimental". *Journal of colloid and interface science* 359.2 (2011), pp. 359–370.
- [39] R. Mahajan and W. J. Koros. "Factors Controlling Successful Formation of Mixed-Matrix Membranes". *Ind. Eng. Chem. Res.* 39 (2000), pp. 2692–2696.
- [40] J. Lee, O. K. Farha, J. Roberts, K. A. Scheidt, S. T. Nguyen and J. T. Hupp. "Metal-organic framework materials as catalysts". *Chemical Society Reviews* 38.5 (2009), pp. 1450–1459.
- [41] L. E. Kreno, K. Leong, O. K. Farha, M. Allendorf, R. P. Van Duyne and J. T. Hupp. "Metal-organic framework materials as chemical sensors". *Chemical reviews* 112.2 (2011), pp. 1105–1125.
- [42] O. Kahn. "Chemistry and physics of supramolecular magnetic materials". *Accounts of chemical research* 33.10 (2000), pp. 647–657.
- [43] C. G. Silva, A. Corma and H. Garcia. "Metal-organic frameworks as semiconductors". *Journal of Materials Chemistry* 20.16 (2010), pp. 3141–3156.
- [44] P. Horcajada, C. Serre, G. Maurin, N. A. Ramsahye, F. Balas, M. Vallet-Regi, M. Sebban, F. Taulelle and G. Férey. "Flexible porous metal-organic frameworks for a controlled drug delivery". *Journal of the American Chemical Society* 130.21 (2008), pp. 6774–6780.
- [45] J.-R. Li, R. J. Kuppler and H.-C. Zhou. "Selective gas adsorption and separation in metal-organic frameworks". *Chemical Society Reviews* 38.5 (2009), pp. 1477–1504.
- [46] J. Cravillon, S. Munzer, S.-J. Lohmeier, A. Feldhoff, K. Huber and M. Wiebcke. "Rapid room-temperature synthesis and characterization of nanocrystals of a prototypical zeolitic imidazolate framework". *Chemistry of Materials* 21.8 (2009), pp. 1410–1412.

- [47] J. A. Thompson, K. W. Chapman, W. J. Koros, C. W. Jones and S. Nair. "Sonication-induced Ostwald ripening of ZIF-8 nanoparticles and formation of ZIF-8/polymer composite membranes". *Microporous and Mesoporous Materials* 158.0 (2012), pp. 292–299.
- [48] T. Li, Y. Pan, K.-V. Peinemann and Z. Lai. "Carbon dioxide selective mixed matrix composite membrane containing ZIF-7 nano-fillers". *Journal of Membrane Science* 425-426 (2013), pp. 235–242.
- [49] Q. Song, S. K. Nataraj, M. V. Roussenova, J. C. Tan, D. J. Hughes, W. Li, P. Bourgoïn, M. A. Alam, A. K. Cheetham, S. a. Al-Muhtaseb and E. Sivaniah. "Zeolitic imidazolate framework (ZIF-8) based polymer nanocomposite membranes for gas separation". *Energy & Environmental Science* 5.8 (2012), pp. 8359–8369.
- [50] T. Yang, Y. Xiao and T.-S. Chung. "Poly-/metal-benzimidazole nano-composite membranes for hydrogen purification". *Energy & Environmental Science* 4.10 (2011), pp. 4171–4180.
- [51] B. Seoane, V. Sebastian, C. Téllez and J. Coronas. "Crystallization in THF: the possibility of one-pot synthesis of mixed matrix membranes containing MOF MIL-68(Al)". *CrystEngComm* 68.Table 1 (2013), pp. 1–5.
- [52] M. J. C. Ordoñez, K. J. Balkus Jr., J. P. Ferraris and I. H. Musselman. "Molecular sieving realized with ZIF-8/Matrimid® mixed-matrix membranes". *Journal of Membrane Science* 361.1-2 (2010), pp. 28–37.
- [53] S. Sridhar, R. Veerapur, M. Patil, K. Gudasi and T. Aminabhavi. "Matrimid polyimide membranes for the separation of carbon dioxide from methane". *Journal of applied polymer science* 106.3 (2007), pp. 1585–1594.
- [54] J. Caro. "Hierarchy in inorganic membranes." *Chemical Society reviews* 45 12 (2016), pp. 3468–78.
- [55] Y.-S. Li, F.-Y. Liang, H. Bux, A. Feldhoff, W.-S. Yang and J. Caro. "Molecular sieve membrane: supported metal-organic framework with high hydrogen selectivity". *Angewandte Chemie* 122.3 (2010), pp. 558–561.
- [56] B. Zornoza, C. Téllez, J. Coronas, J. Gascon and F. Kapteijn. "Metal organic framework based mixed matrix membranes: An increasingly important field of research with a large application potential". *Microporous and Mesoporous Materials* 166 (2013), pp. 67–78.

- [57] B. Zornoza, A. Martinez-Joaristi, P. Serra-Crespo, C. Téllez, J. Coronas, J. Gascon and F. Kapteijn. "Functionalized flexible MOF as filler in mixed matrix membranes for highly selective separation of CO₂ from CH₄ at elevated pressures". *Chemical communications (Cambridge, England)* 47.33 (2011), pp. 9522–9524.
- [58] S. Couck, J. F. M. Denayer, G. V. Baron, T. Remy, J. Gascon and F. Kapteijn. "An Amine-Functionalized MIL-53 Metal-Organic Framework with Large Separation Power for CO₂ and CH₄". *Journal of the American Chemical Society* 131.18 (2009), pp. 6326–6327.
- [59] E. Stavitski, E. A. Pidko, S. Couck, T. Remy, E. J. M. Hensen, B. M. Weckhuysen, J. Denayer, J. Gascon and F. Kapteijn. "Complexity behind CO₂ capture on NH₂-MIL-53(Al)". *Langmuir* 27.7 (2011), pp. 3970–3976.
- [60] Y.-R. Lee, M.-S. Jang, H.-Y. Cho, H.-J. Kwon, S. Kim and W.-S. Ahn. "ZIF-8: A comparison of synthesis methods". *Chemical Engineering Journal* 271 (2015), pp. 276–280.
- [61] E. Perez, C. Karunaweera, I. Musselman, K. Balkus and J. Ferraris. "Origins and Evolution of Inorganic-Based and MOF-Based Mixed-Matrix Membranes for Gas Separations". *Processes* 4.3 (2016), p. 32.
- [62] A. L. Khan, S. Basu, A. Cano-Odena and I. F. Vankelecom. "Novel high throughput equipment for membrane-based gas separations". *Journal of Membrane Science* 354.1-2 (2010), pp. 32–39.
- [63] C. Zhang, Y. Dai, J. R. Johnson, O. Karvan and W. J. Koros. "High performance ZIF-8/6FDA-DAM mixed matrix membrane for propylene/propane separations". *Journal of Membrane Science* 389 (2012), pp. 34–42.
- [64] K. Kida, M. Okita, K. Fujita, S. Tanaka and Y. Miyake. "Formation of high crystalline ZIF-8 in an aqueous solution". *CrystEngComm* 15.9 (2013), pp. 1794–1801.
- [65] J. Cravillon, S. Muunzer, S.-J. Lohmeier, A. Feldhoff, K. Huber and M. Wiebcke. "Rapid room-temperature synthesis and characterization of nanocrystals of a prototypical zeolitic imidazolate framework". *Chemistry of Materials* 21.8 (2009), pp. 1410–1412.
- [66] B. Zornoza, C. Casado and A. Navajas. *Advances in hydrogen separation and purification with membrane technology*. Elsevier: Amsterdam, The Netherlands, 2013.

- [67] D. Fairen-Jimenez, R. Galvelis, A. Torrissi, A. D. Gellan, M. T. Wharmby, P. A. Wright, C. Mellot-Draznieks and T. Dueren. "Flexibility and swing effect on the adsorption of energy-related gases on ZIF-8: combined experimental and simulation study". *Dalton Transactions* 41.35 (2012), pp. 10752–10762.
- [68] L. Hertag, H. Bux, J. Caro, C. Chmelik, T. Remsungnen, M. Knauth and S. Fritzsche. "Diffusion of CH₄ and H₂ in ZIF-8". *Journal of Membrane Science* 377.1 (2011), pp. 36–41.
- [69] E. Haldoupis, T. Watanabe, S. Nair and D. S. Sholl. "Quantifying Large Effects of Framework Flexibility on Diffusion in MOFs: CH₄ and CO₂ in ZIF-8". *ChemPhysChem* 13.15 (2012), pp. 3449–3452.
- [70] D. Fairen-Jimenez, S. Moggach, M. Wharmby, P. Wright, S. Parsons and T. Duren. "Opening the gate: framework flexibility in ZIF-8 explored by experiments and simulations". *Journal of the American Chemical Society* 133.23 (2011), pp. 8900–8902.
- [71] S. Aguado, G. Bergeret, M. P. Titus, V. Moizan, C. Nieto-Draghi, N. Bats and D. Farrusseng. "Guest-induced gate-opening of a zeolite imidazolate framework". *New Journal of Chemistry* 35.3 (2011), pp. 546–550.
- [72] M. R. Ryder, B. Civalleri, T. D. Bennett, S. Henke, S. Rudic, G. Cinque, F. Fernandez-Alonso and J.-C. Tan. "Identifying the role of terahertz vibrations in metal-organic frameworks: from gate-opening phenomenon to shear-driven structural destabilization". *Physical review letters* 113.21 (2014), p. 215502.
- [73] T. T. Moore, R. Mahajan, D. Q. Vu and W. J. Koros. "Hybrid membrane materials comprising organic polymers with rigid dispersed phases". *AIChE journal* 50.2 (2004), pp. 311–321.
- [74] R. Pal. "Permeation models for mixed matrix membranes". *Journal of Colloid and Interface Science* 317 (2007), pp. 191–198.
- [75] T. Rodenas, M. van Dalen, E. Garcia-Perez, P. Serra-Crespo, B. Zornoza, F. Kapteijn and J. Gascon. "Visualizing MOF Mixed Matrix Membranes at the Nanoscale: Towards Structure-Performance Relationships in CO₂/CH₄ Separation Over NH₂-MIL-53 (Al)@ PI". *Advanced Functional Materials* 24.2 (2014), pp. 249–256.
- [76] R. F. Boyer and R. L. Miller. "Polymer chain stiffness parameter, σ , and cross-sectional area per chain". *Macromolecules* 10.5 (1977), pp. 1167–1169.

Chapter 3

Highly selective gas separation membrane using *in-situ* amorphised metal-organic frameworks

Adapted and largely based on:

A. Kertik et al. “Highly selective gas separation membrane using in-situ amorphised metal-organic frameworks”. *Energy Environ. Sci.* 10 (11 2017), pp. 2342–2351

A.K. contributed by the design and conduction of experiments, data analysis, and writing. *L.H.W.* helped with data interpretation and writing, revised the paper, and prepared the ball-milled amorphous MOFs. *K.S.* and *S.B.* conducted the TEM experiments and analysed the results. *J.A.M.* revised the paper. *I.F.J.V.* helped with the data interpretation, and revised the paper.

3.1 Abstract

Conventional carbon dioxide (CO₂) separation in the petrochemical industry via e.g. cryogenic distillation is energy-intensive and environmentally unfriendly. Alternatively, separations based on polymeric membranes are of significant interest, owing to their low production cost, low energy consumption, and ease

of upscaling. However, the implementation of commercial polymeric membranes is limited by their permeability and selectivity trade-off, and the insufficient thermal and chemical stability. Herein, a novel type of amorphous mixed-matrix membrane (MMM) able to separate CO₂/CH₄ mixtures with the highest selectivities ever reported for MOF-based MMMs is presented. The MMM preparation method was based on the findings of the previous chapter, with the addition of a thermal treatment to improve the separation performance. The resulting MMM consists of an amorphised metal-organic framework (MOF) dispersed in an oxidatively cross-linked matrix achieved by fine tuning of the thermal treatment temperature in air up to 350°C, which drastically boosts the separation properties of the MMM. In addition, the treatment also improves the filler-polymer adhesion and induces an oxidative cross-linking of the polyimide matrix, resulting in MMMs with increased stability or plasticisation resistance at high pressure up to 40 bar, marking a new milestone as new molecular sieve MOF MMMs for challenging natural gas purification applications. A new field for the use of amorphised MOFs and a variety of separation opportunities for such MMMs are thus opened.

3.2 Introduction

Nanoporous materials with well-defined and size-selective channels are essential elements for gas sorption, storage, separation and catalysis.^[2] Metal-organic frameworks (MOFs) with their large surface area, tunable pore size and chemical tailorability, emerged as excellent alternatives to more conventional porous materials.^[3] MOFs are formed by the supramolecular coordination of metal ions/clusters and organic bridging ligands.^[3,4] These repeating building units exhibit three-dimensional frameworks with long-range ordering and variable pore architectures. Combined with their chemical versatility, MOFs endow via selective adsorption and molecular sieving for numerous potential applications ranging from separation to catalysis, sensing, magnetism, photoluminescence and drug delivery.^[2,3,5] Self-supporting membranes prepared from such nanostructured porous materials have been prepared for gas separation,^[6] but making defect-free and mechanically robust membranes has proven to be very challenging. In contrast, polymers are easily processible into large membrane modules, and are already widely used in industrial gas separations for e.g. CO₂ removal. However, they often suffer from a permeability/selectivity trade-off, as depicted by the Robeson upper-bound.^[7,8] Commercial polymers can rarely surpass this upper-bound. Despite various attempts to improve the performance of commercial polymers, a reliable approach has not been accomplished to date.^[9] Designing special macromolecular

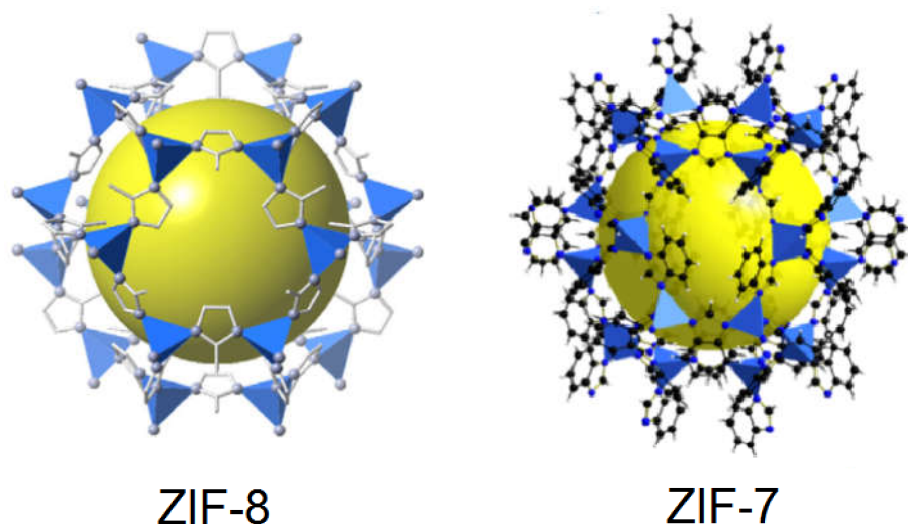


Figure 3.1: The structures of ZIF-8^[25] and ZIF-7^[26]. The blue regions represent the metal nodes, which are bound by organic linkers. The empty space in the pores is represented by the yellow spheres.

structures lacks up-scaling potential, and membranes tend to suffer from long-term instability.

An alternative approach is mixed-matrix membranes (MMMs) that consist of fillers dispersed in a polymer. While the polymer offers mechanical stability and processibility,^[3] a filler with well-defined sorption properties provides more selective permeation.^[10] As filler, zeolitic imidazolate frameworks (ZIFs) as a sub-family of MOFs analogous to inorganic zeolites, are particularly interesting (the CO₂ absorption isotherm of ZIF-8 is given in Figure 3.2).^[11] ZIF-8 is an archetypal ZIF, consisting of Zn(II)-linkers and 2-methyl-imidazole anions coordinated in a cubic sodalite topology having interconnected pore cavities and a pore aperture of 11.6 Å and 3.4 Å, respectively, rendering it capable of separating various gas mixtures.^[12–15] ZIF-7 belongs to the same family as ZIF-8, and exhibits a hexagonal distorted sodalite topology formed by connecting zinc clusters with benzimidazole, with an estimated pore size of 3 Å.^[16–18] The structures of ZIF-8 and ZIF-7 are given in Figure 3.1. Poor compatibility between filler and polymer is a notorious problem in preparing MMMs.^[19,20] Methods such as above-Tg annealing,^[21] filler surface modification,^[19] melt-processing,^[22] priming^[10] and using low-molecular-weight additives,^[23] or plasticisers^[24] have been applied to overcome this problem.

Some MOFs, and specifically ZIFs exhibit a solid-solid phase transformation known as amorphisation. Amorphous MOFs (*a*MOFs) are networks that retain their basic building blocks but exhibit no long-range ordering.^[5] *a*MOFs are

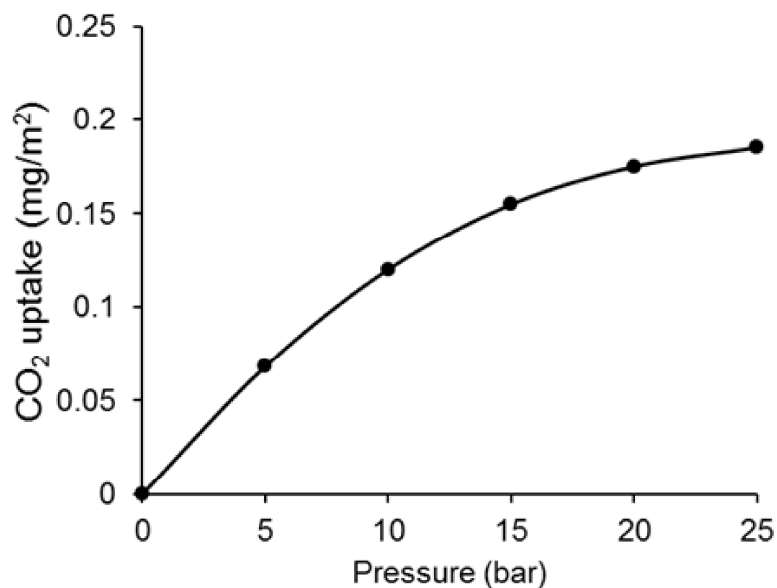


Figure 3.2: CO₂ adsorption isotherm of ZIF-8 at 35 °C. Experimental data is taken from ref.^[27].

obtained by introducing disorder into their parent crystalline frameworks through heating, pressure or mechanical ball-milling.^[5] Amorphisation is a well-known concept for inorganic materials, but the application of *a*MOFs is largely unexplored.^[5,28,29] The current potential application is limited to drug-release^[30,31] and entrapping harmful substances.^[32,33] In the previous chapter, a very effective method to prepare highly loaded MMMs was suggested. In order to improve the separation performance of these membranes, the membrane preparation method was extended by a detailed thermal treatment step. In this chapter, we show that amorphised MOFs can be created *in-situ* in a ZIF-containing polyimide membrane by a controlled thermal treatment in air. Combined with the remarkable changes in polymer properties, this MOF transformation generates MMMs with the highest CO₂/CH₄ mixed-gas selectivities reported so far for membranes based on commercial polymers, marking a new milestone in the latest Robeson's upper-bound plot, and offering new opportunities to highly selective separations in a variety of related applications.

3.3 Experimental procedure

3.3.1 Synthesis of MOF particles

ZIF-8 particles were prepared by a modified version of the recipe from Ordoñez et al.,^[34] using a molar excess of 2-methyl imidazole to $\text{Zn}(\text{NO}_3)_2 \cdot 6\text{H}_2\text{O}$. Post-synthesis, the solution was centrifuged and washed with DMF, methanol, and CHCl_3 , respectively. The MOF sludge collected after the final centrifuge step was re-distributed in CHCl_3 and stored as such. ZIF-7 was synthesised by dissolving zinc nitrate hexahydrate (0.302 g) and benzimidazole (0.769 g) in DMF (400 mL), and magnetically stirring the mixture for 48 hours at room temperature. The synthesis solution was centrifuged and washed with DMF, methanol, and finally CHCl_3 . The MOF sludge collected after the final centrifugation step was re-distributed in CHCl_3 and stored as such. Pre-amorphised ZIF-8 powder was prepared according to the method reported by Cheetham and co-workers.^[35] 150 mg of ZIF-8 powder was placed inside a 10 mL stainless steel jar alongside a 10 mm stainless steel milling ball at room temperature. The sealed reactor was subjected to 30 Hz milling in a Retsch MM400 grinder mill for 30 min. After milling, the solid product was recovered and characterised by XRD, SEM and N_2 physisorption.

3.3.2 Preparation of MMMs

MMMs of 20, 30 and 40 wt.% loading were prepared for this work. An amount of the MOF mixture with known MOF content was weighed, and the Matrimid® (dried overnight at 110°C) was dissolved in this mixture. The polymer concentration was adjusted around 7 wt.% to obtain a reasonably viscous solution that can still be cast and will not suffer from MOF precipitation upon casting. The final mixture was given enough time for the polymer to fully dissolve. As proof of the effectiveness of our membrane fabrication method, an additional step of ultrasonication was not needed for obtaining a mixture with a perfect MOF distribution. The MOF loading was calculated as follows:

$$\text{Loading}(\text{wt.}\%) = 100 \frac{wt_{MOF}}{wt_{MOF} + wt_{polymer}} \quad (3.1)$$

The membrane solution was cast into specifically designed petri dishes that consist of glass rings attached to the flat glass surfaces to ensure uniform membrane thickness was obtained. The cast solution was allowed to vitrify overnight at room temperature in a N_2 atmosphere to prevent contact with the

air humidity. Upon vitrification, the membrane was carefully removed from the petri dish, and placed in an oven for annealing.

3.3.3 The annealing process

The dried membranes were placed between glass supports to prevent curving, and placed in an oven. The oven was heated to 100°C (above the boiling point of CHCl₃), 160°C (slightly above the boiling point of DMF), 250°C (above the boiling points of CHCl₃ and DMF and below the T_g of Matrimid) or 350 °C (above the T_g of Matrimid), and the process was carried out in air. The heating process was designed as heating at 1 °C/min from room temperature to the final annealing temperature with 50 °C increments. At each increment, the oven was kept isothermally for 2 hours. The membranes remained at the final temperature for 24 hours, and were removed after the oven cooled down to room temperature naturally. Immediate quenching is known to cause the formation of voids between the polymer and the filler due to the difference in the thermal expansion coefficients of the two materials. By allowing the MMMs to cool down naturally, the attachment between the polymer chains and the MOFs was protected.

3.3.4 Membrane characterisation

Attenuated total reflectance Fourier transform infrared spectroscopy (ATR-FTIR) was conducted in air using a Varian 620 FT-IR imaging microscope with a Germanium crystal. The samples were analysed over a wavelength range from 400 to 4000 cm⁻¹ with a spectral resolution of 4 cm⁻¹ and 64 scans. The morphology of the membrane cross-sections was observed with a JEOL JSM-1060LV scanning electron spectroscopy (SEM). The membranes that were flexible were freeze-fractured, and the samples that were already too brittle were made to break as evenly as possible in liquid N₂. In order to prevent charge build-up due to the non-conductive nature of the polymers, the samples were sputtered with Au/Pd for three cycles of 20 seconds. X-ray diffraction (XRD) diffractograms of MOF particles and membranes were obtained by using a Stoe-HT X-ray diffractometer, with CuKα radiation, λ=1.54 Å at room temperature. The thermogravimetric behaviour of the MOFs and membranes were analysed with TA Instruments TGA-Q500. The samples were heated from room temperature with a heating rate of 5 °C/min up to 100 °C, kept isothermally for 10 minutes, then with 2 °C/min up to 160 °C, and remained at 160 °C for 10 minutes, and finally with 10 °C/min to 500 °C under N₂. Differential scanning calorimetry (DSC) measurements were carried out using a TA Instruments DSC

Q2000 using Al hermetic closed pans and in N₂ atmosphere. The samples were first kept isothermally at 20 °C for 10 minutes, then heated to 370 °C with a heating rate of 10 °C/minute. After 5 minutes, the samples were cooled down to 20 °C at 10 °C/minute, and re-heated to 370 °C using the previously described method. The mechanical strength tests were conducted at room temperature using a Universal Testsystem (UTS) with 0.0001 mm position resolution and load cells up to 200 N. Scanning transmission electron microscopy (STEM) and spectral imaging (SI) were carried out with an aberration-corrected Titan 60-300 microscope (FEI) operated at 120 kV acceleration voltage, equipped with an Enfinium spectrometer (Gatan) and a high-efficiency energy dispersive X-ray (EDX) detector (Super-X). Images of the membrane cross-section were captured with high-angle annular dark field scanning transmission electron microscopy (HAADF-STEM). Two samples were prepared with a UC7 ultramicrotome (Leica) with a thickness of 90 nm for imaging and EDX, and 40 nm for diffraction and electron energy-loss spectral imaging. For SI convergence and collection, angles of 10 mrad and 15 mrad were applied, respectively. TEM diffraction was performed to test for crystallinity using a Philips CM 20 microscope operated at 200 kV. The diffraction pattern was recorded for a previously unexposed area at relatively low magnification comprising several ZIF particles to prevent beam damage. For analysis and quantification of energy-loss spectra HyperSpy (an open source Python library.^[36]) was used. Quantification includes removal of plural scattering contributions in the core-loss spectra using low energy-loss spectra. The resulting C/N ratio map was processed by a small Gaussian smoothing filter (size 3x3).

3.3.5 Analysis of gas separation properties

The gas separation performance of membranes for binary gas mixtures was tested using a custom-built, high-throughput gas separation system (HTGS). The membranes were tested with a 50-50% vol. CO₂/CH₄ mixture at 35 °C and 10 bar cross-membrane pressure difference. High-pressure measurements were carried out under the same conditions, with the exception of 40 bar cross-membrane pressure difference. The composition of the permeate side was measured by gas chromatography (GC). The membranes were first allowed to reach steady-state overnight. Steady-state was confirmed when consecutive GC measurements gave the same result. Then three more measurements were taken, and their average was reported. Each final data point reported is an average of two membranes, and two coupons from each membrane. The permeabilities were measured at steady-state using a constant-volume variable-pressure permeation system. The overall permeability (P_o) and the relative permeability of CO₂ (P_{CO_2}) was calculated by Equation 3.2:

$$P_o = \frac{\alpha V l}{A R T \Delta P} \quad (3.2)$$

where α is the rate of pressure increase in the downstream with respect to time, V is the downstream volume, l is the membrane thickness, A is the membrane surface area, R is the ideal gas constant, T is the permeation temperature, and ΔP is the cross-membrane pressure difference.

$$P_{CO_2} = P_o \frac{y_{CO_2}}{x_{CO_2}} \quad (3.3)$$

where P_o is the overall permeability, y_{CO_2} and x_{CO_2} denote the CO_2 content at the permeate and the feed side, respectively.

3.4 Results and discussion

3.4.1 Thermo-oxidative cross-linking of MMMs

Choice of the right material pair, coupled with the optimisation of the membrane fabrication process is the key to designing a high-performance MMM. For this work, a commercially available polyimide (PI), Matrimid®, was chosen as the matrix polymer. Matrimid® is a commercial polyimide with properties that fall close to the Robeson upper-bound.^[34,37] ZIF-8, a promising candidate for CO_2 capture, was chosen as the filler. ZIF-8 has also been reported to undergo amorphisation.^[5,27] MMMs with different ZIF-8 loadings (20, 30 and 40 wt.%) were prepared and thermally treated at 100, 160, 250 or 350°C in air for periods up to 24h. After a prolonged treatment at 350°C for 24 h, a significant change in membrane colour was noted as shown in Figure 3.4a to d. The membranes changed from light yellow to dark brown when the temperature was increased. Interestingly, the onset of darkening for the MMMs was 250°C, whereas it was 350°C for the unfilled polymer, suggesting that the embedded ZIF-8 has significant influence on the thermal behaviour of the MMMs. According to the TG analysis (Figure 3.4e,f), the Matrimid® membrane annealed at 100°C shows a significant weight loss (10.3 wt.%) from 170-470°C, whereas the unfilled Matrimid® membrane treated at 350°C only shows a negligible weight loss (1.2 wt.%). A similar trend is observed for the thermally treated MMM (18.2 wt.% for 100°C and 4.2 wt.% for 350°C). More importantly, the embedded ZIF-8 is not degraded upon heating to 340°C, in contrast to the bulk ZIF-8 powder under similar conditions. The significant enhancement of thermal stability and the change in the visual properties of the membranes suggests thermo-oxidative

cross-linking of the polymer. To confirm this hypothesis, solubility tests were performed and are presented in the Figure 3.3 for the unfilled Matrimid®, and in Figure 3.4 g-i for the MMMs. All membranes treated above 160°C became largely insoluble in a good solvent for the polymer such as chloroform after 2 days (Figure 3.4h,i).

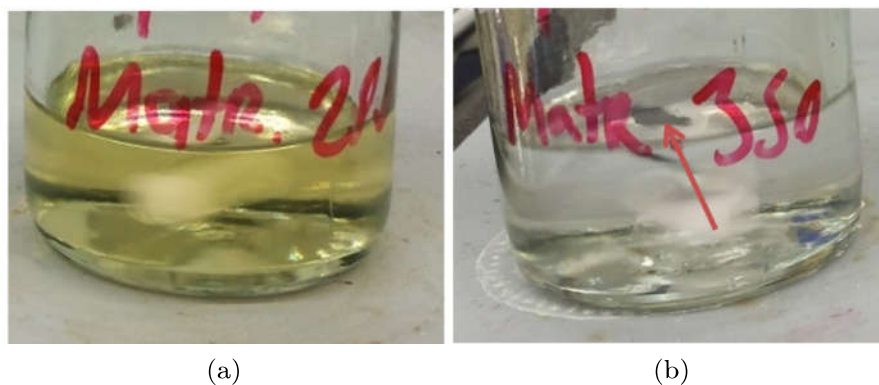


Figure 3.3: The solubility of pure Matrimid® membranes after annealing at (a) 250 °C and (b) 350 °C. In (b), the membrane is indicated by the red arrow.

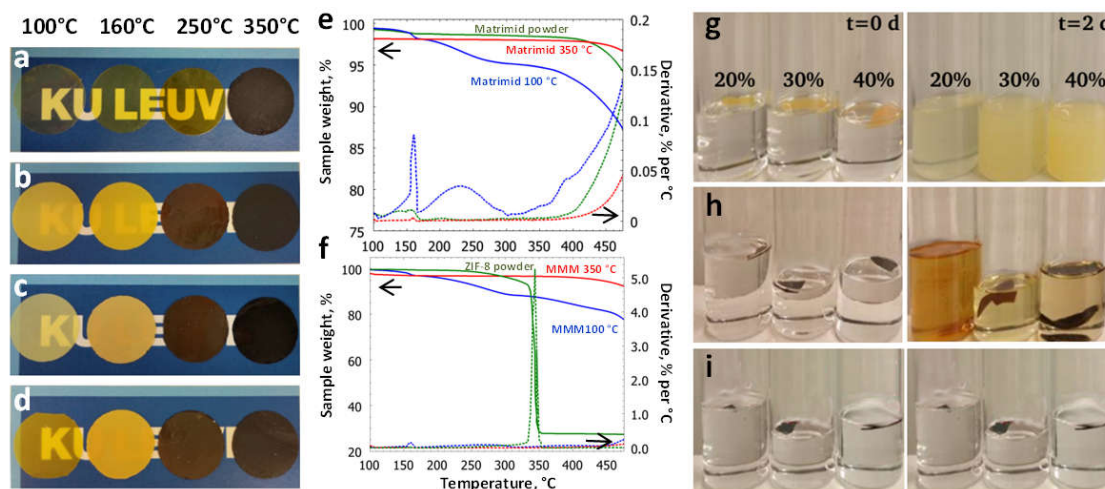


Figure 3.4: Visual, thermal and solubility tests of the thermally treated membranes. The annealing influences the visual properties of the (a) Matrimid® and MMMs with (b) 20, (c) 30, and (d) 40% ZIF-8 loading. (e,f) The TGA curves and the derivative weight loss curves for Matrimid® and the MMM with 40 wt.% ZIF-8 loading. The solubility tests for MMMs thermally treated at (g) 160, (h) 250 and (i) 350 °C.

In order to elucidate the underlying chemistry of the thermo-oxidative cross-linking of Matrimid®, the membranes were characterised by ATR-FTIR (Figure

3.5a). The adsorption bands at 2960, 2927, and 2864 cm^{-1} assigned to the aliphatic C–H stretching vibration decreased in intensity with increasing temperature in line with the observed darker colour of Matrimid®. It has been previously reported that oxidative cross-linking occurs at the methylene bridges of the polymer, which is associated with the ketone and aromatic C=O stretching vibrations at 1600 and 930 cm^{-1} , respectively.^[38] A decrease at 823 cm^{-1} and increase at 1604 cm^{-1} was observed here, which could be assigned to methyl and C=O oxidation, respectively, with increasing thermal treatment temperature. In general, thermal oxidation of polymers involves free-radical chain reactions. In the present study, a prolonged thermal treatment at 350 °C in the presence of oxygen induces oxidation and cross-linking. The methyl groups in the polyimide are oxidised to provide readily available cross-linking sites via the formation of -CH₂ radicals. These free radicals react with O₂ to form peroxy radicals (ROO·), which can further abstract a hydrogen from adjacent polymer chains to generate hydroperoxide (ROOH) moieties. These hydroperoxides then undergo sequential termination steps to induce inter-chain cross-linking.^[39] The concise mechanism for thermo-oxidative cross-linking is shown in Figure 3.5c. A complete chain reaction mechanism including the initiation, propagation and termination steps is illustrated in Figure 3.7 and 3.8. The excess water content found in the cross-linked MMMs (2.6 wt.%) versus 0.7 wt.% in the MMMs annealed at 100 °C according to TGA (Figure 3.5d, Figure 3.9 and 3.10) is mainly due to the water formation as a result of the chain termination reaction. Glass transition temperatures (T_g) increased as the thermo-oxidative cross-linking of methylene bridging groups became more prominent.^[40,41] While the T_g of the unfilled polymer increased to 340 °C, it reached 350 °C for the MMM treated at the same temperature. The tensile strength of the membranes evolved in line with this cross-linking, as shown in Table 3.1 and Figure 3.11. Due to the MOF loading, the tensile strength of the MMMs was overall below that of Matrimid®. However, it still exhibited an exponential increase with thermal treatment temperature, i.e. with increasing cross-linking.

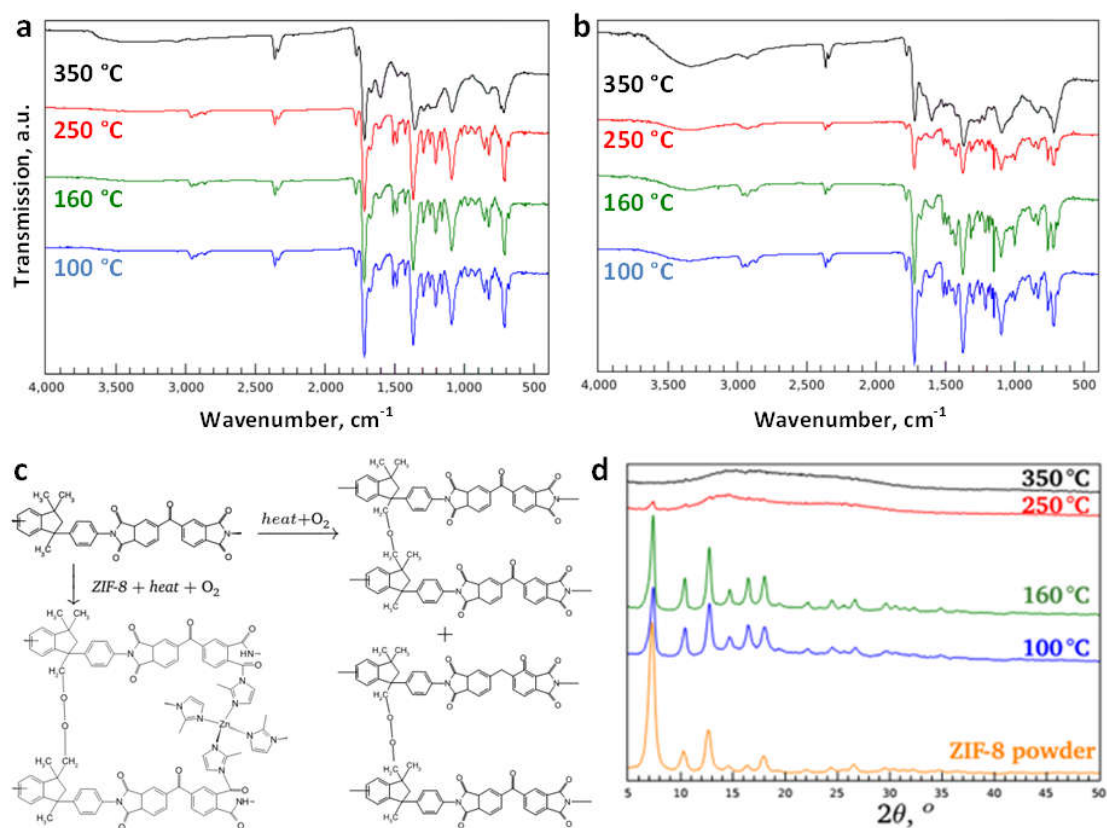


Figure 3.5: Thermo-oxidative cross-linking of the membranes. The FTIR patterns of the (a) Matrimid® and (b) MMMs with 40 wt.% ZIF-8 loading as a function of temperature. (c) The suggested cross-linking mechanism for the PI and the MMM based on the FTIR results. (d) The characteristic XRD diffractogram of ZIF-8-containing MMMs. Enlarged versions of ATR-FTIR spectra of (a) Matrimid® and (b) the MMMs with assigned peaks are provided in Figure 3.6.

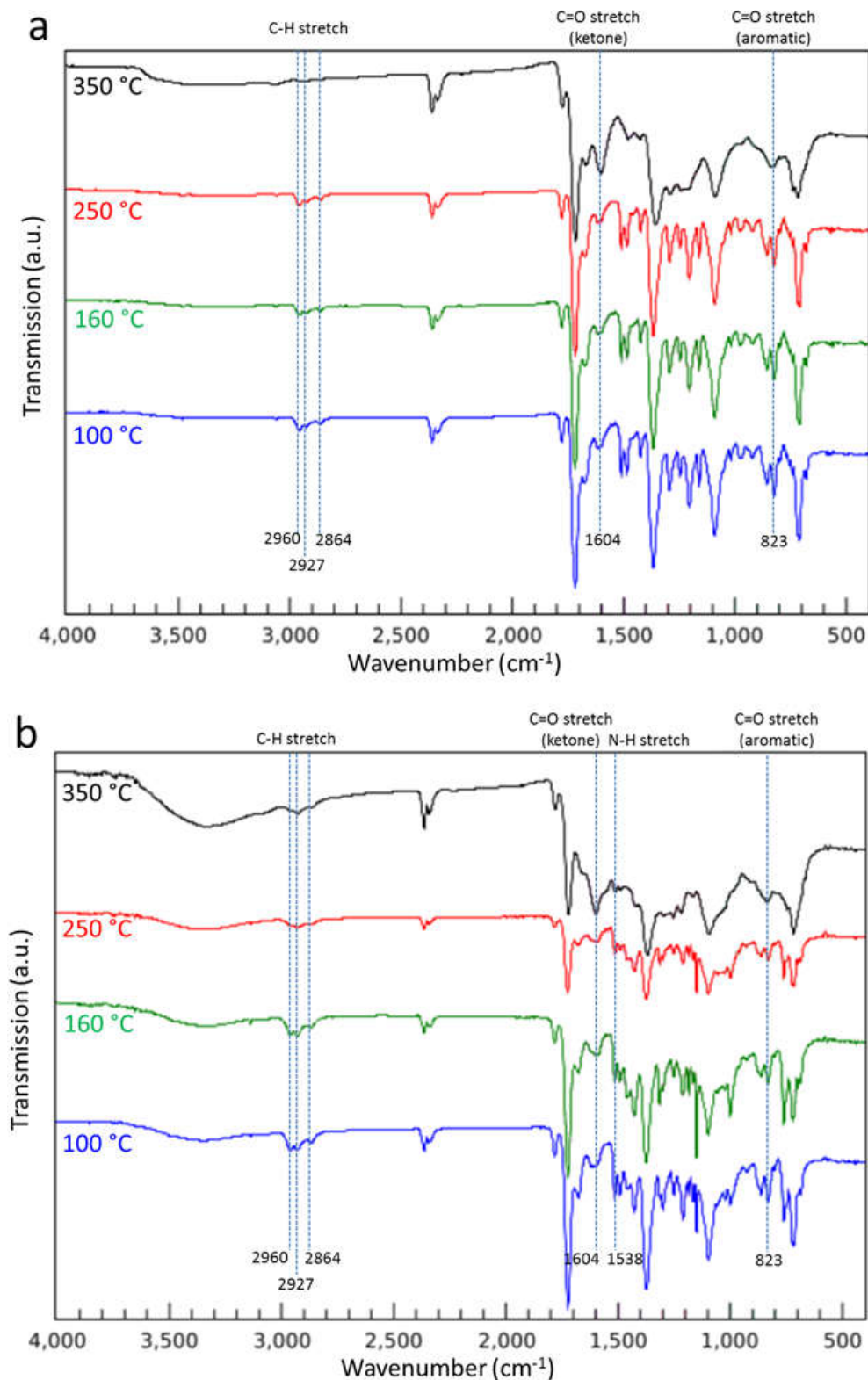


Figure 3.6: The ATR-FTIR patterns of the (a) Matrimid® and (b) MMMs with 40 wt.% ZIF-8 loading as a function of temperature.

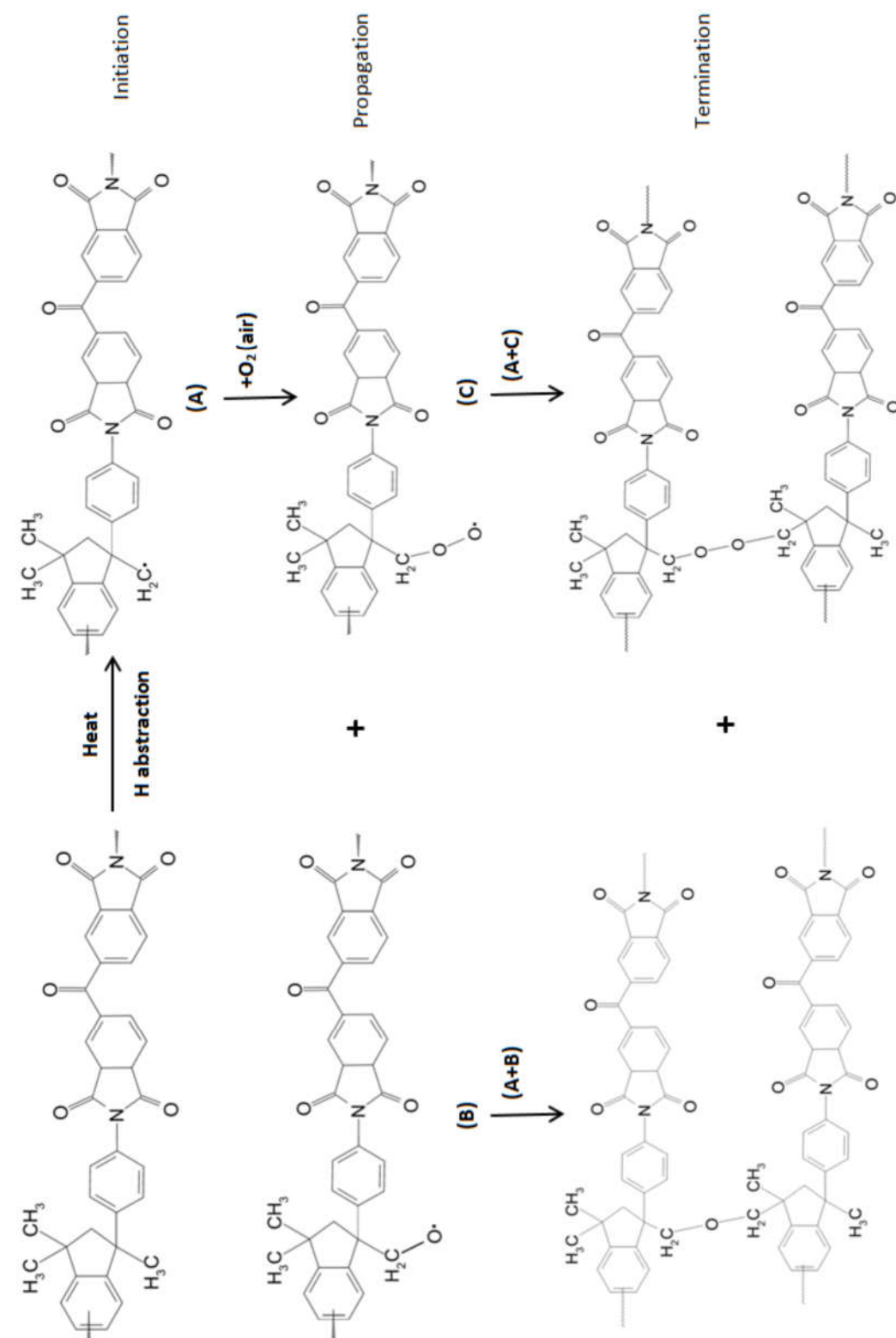


Figure 3.7: The proposed thermo-oxidative cross-linking mechanism for Matrimid®.

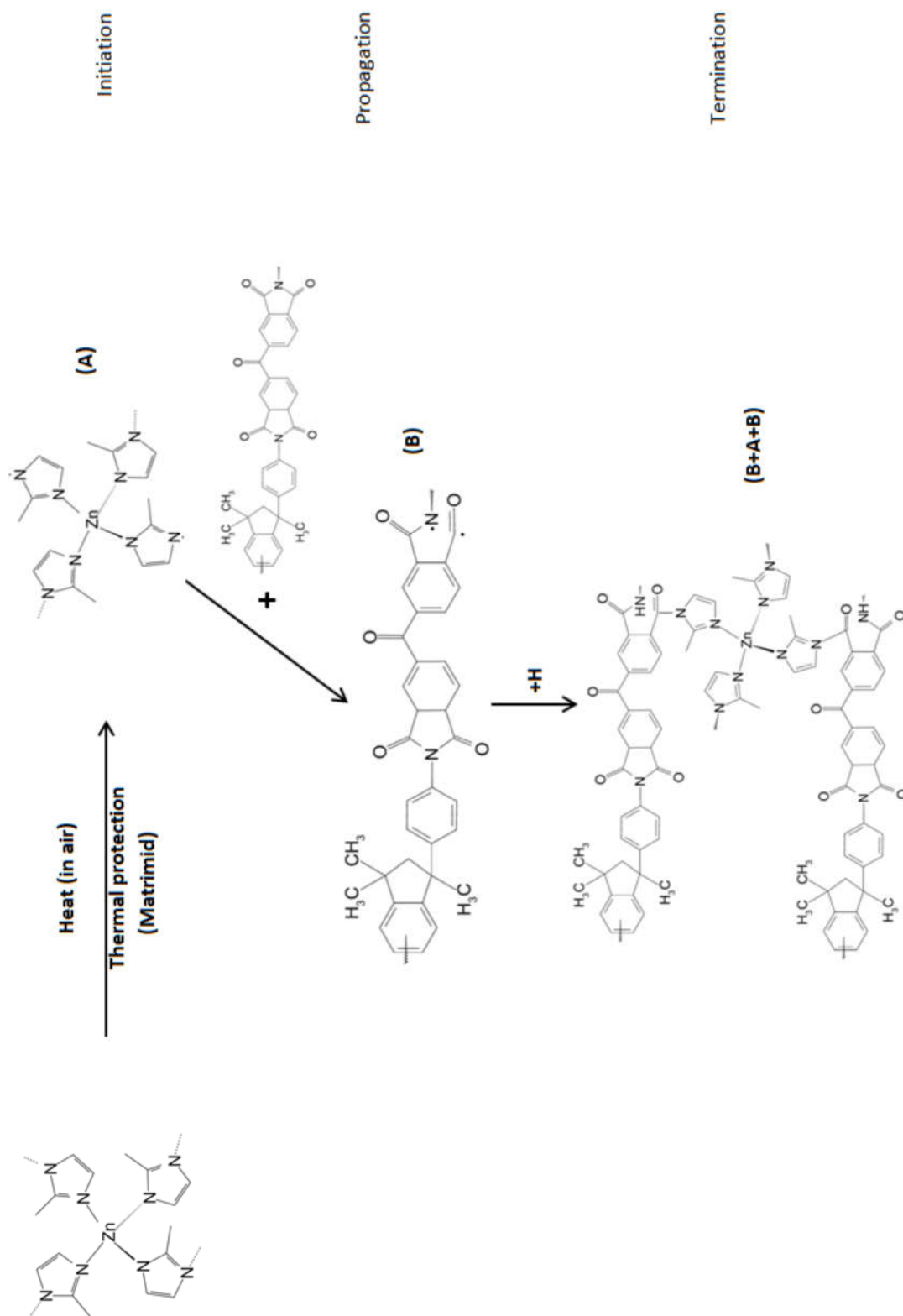


Figure 3.8: The proposed cross-linking mechanism of the MOF in the MMM. It should be noted that this mechanism is shown separately for clarity. In the MMMs, this mechanism and the polymer cross-linking proposed in Figure 3.7 occur simultaneously.

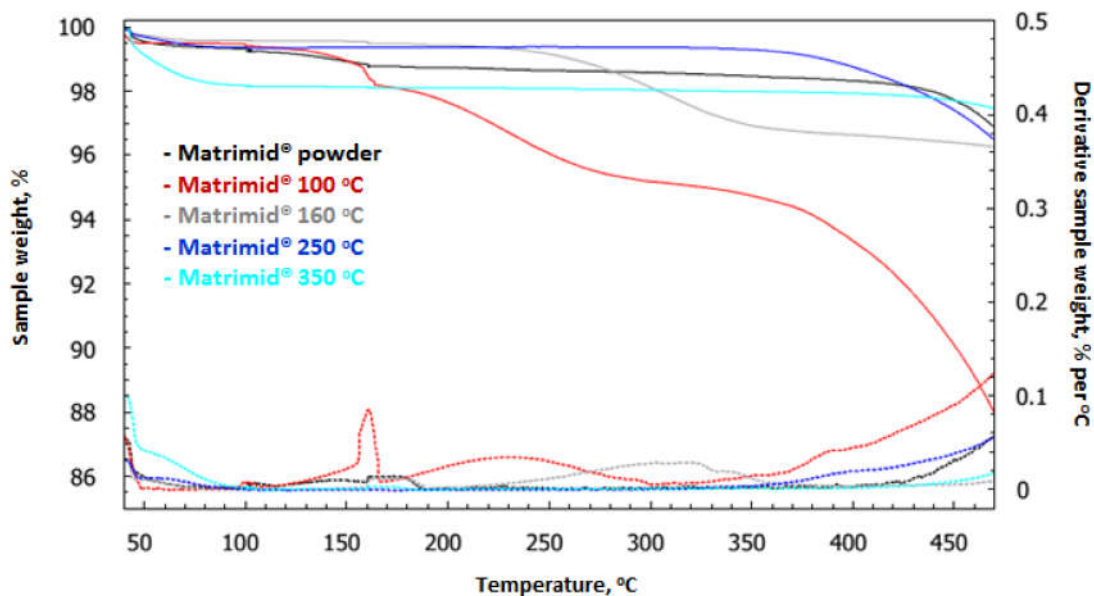


Figure 3.9: The TGA plot (solid lines) and derivatives (dotted lines) of the Matrimid® membranes.

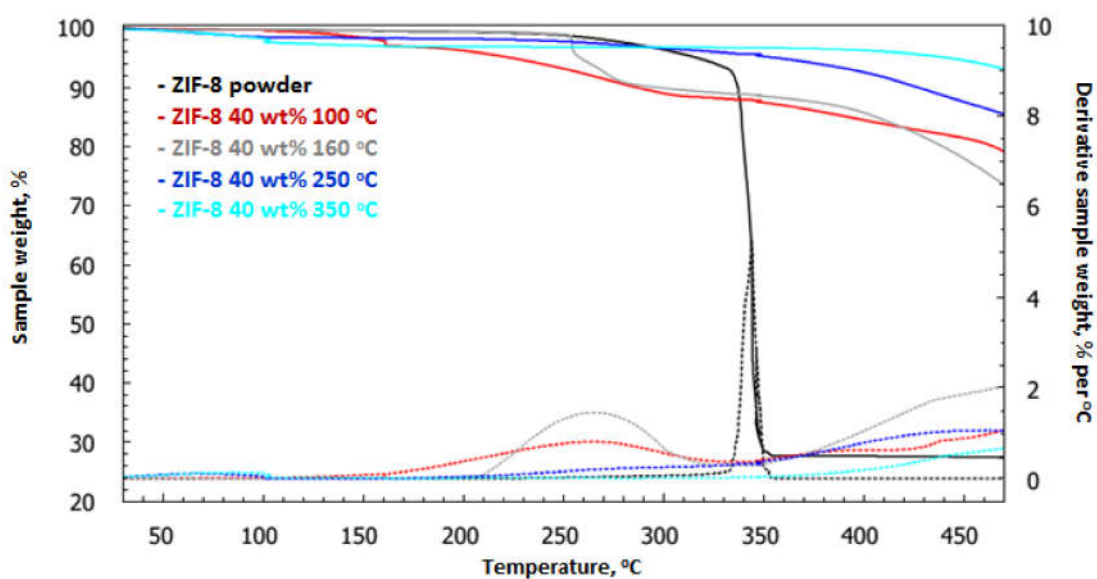


Figure 3.10: The TGA plot (solid lines) and derivatives (dotted lines) for MMMs with 40 wt.% ZIF-8 loading.

The Matrimid® membranes thermally treated at 250 °C were completely dissolved after 2 days whereas the MMMs treated at the same temperature were more resistant to solvation, especially at high ZIF-8 loadings. The observation suggests that the embedded ZIF-8 actually acts as an additional chemical cross-linker upon heating. Chemical cross-linking is known to realise the

Table 3.1: The tensile strength of Matrimid® and MMMs with 40% ZIF-8.

Membrane	Tensile strength (MPa)
Matrimid® treated at 100 °C (M100)	85.3
Matrimid® treated at 160 °C (M160)	101.8
Matrimid® treated at 250 °C (M250)	118.6
Matrimid® treated at 350 °C (M350)	22.1
MMM with 40% ZIF-8, treated at 100 °C (Z8-40-100)	6.3
MMM with 40% ZIF-8, treated at 160 °C (Z8-40-160)	5.2
MMM with 40% ZIF-8, treated at 250 °C (Z8-40-250)	12.0
MMM with 40% ZIF-8, treated at 350 °C (Z8-40-350)	33.8

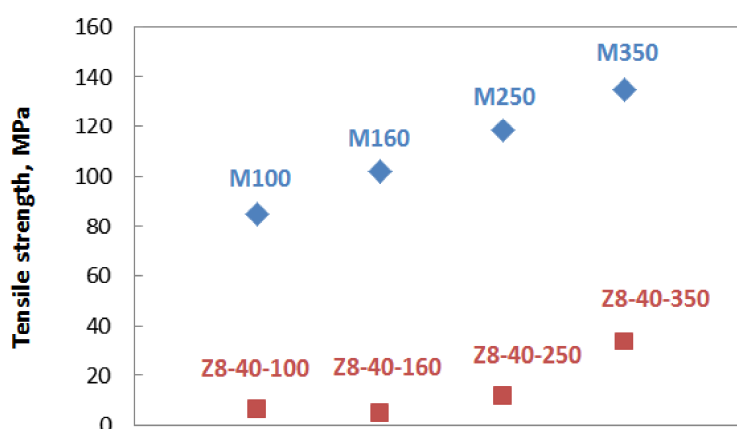


Figure 3.11: The dependency of the membrane tensile strength on the heat treatment temperature.

reduction of the plasticisation tendency of Matrimid® membranes,^[42] which is critical for their application in CO₂ separations. There have been reports of plasticisation-resistant MMMs exhibiting direct cross-linking between MOF and polyimide.^[43,44] According to the ATR-FTIR spectra (Figure 3.5b), apart from the previously observed enhanced absorption bands for C=O and the decline in C–H stretching vibration, an additional band largely masked by Matrimid® at 1538 cm⁻¹ was noted. This band can be tentatively assigned to the aromatic N–H stretching band of the amide group, confirming the cross-linking of Matrimid® with the imidazolate in ZIF-8. The cross-linking of imidazole from *a*ZIF-8 with Matrimid®, as based on the ATR-FTIR studies, is tentatively shown in Figure 3.5c.

XPS analysis clearly illustrated the presence of the peaks assigned to Zn²⁺, Zn2p₃ and Zn2p₁ (Figure 3.12). As ZIF-8 is amorphised, the Zn–N bonds are the first to break and create unsaturated Zn²⁺ sites, as reflected in the

increased intensity of the XPS peaks for the MMM treated at 350 °C. Recently, cross-linking of the organic ligand in MOF with polymer gel has been reported via acidification with concentrated HCl for breaking the coordinative bonding between the Zn(II) ion and the carboxylate anion.^[45] However, for our system, the cross-linking of Matrimid® with the molecular building units of ZIF-8 hints at a phase transition upon thermal treatment. Although the structural transformation of ZIF-8 has been extensively studied by Cheetham^[28] and Friščić,^[46,47] amorphisation of ZIF-8 by thermal treatment has not been realised to date, mainly due to the direct oxidation of ZIF-8 to ZnO in air. In order to evaluate the crystallinity of the thermally treated membranes, XRD was performed (Figure 3.5d and Figure 3.13a-c). For the MMMs thermally treated at 100 °C and 160 °C, the crystalline structures of the ZIF-8 nanoparticles remained intact, but when treated at higher temperatures (250 and 350 °C), the typical XRD diffractions were no longer observed (Figure 3.5d). The disappearance of the crystalline peaks suggest the amorphisation of the embedded ZIF-8. The amorphous state of the ZIF-8 embedded in the Matrimid® matrix was further confirmed by TEM electron diffraction (Figure 3.14a). No diffraction spots at high camera length that could indicate the presence of ZIF-8 crystals were observed. Electron diffraction only reveals rings representative of amorphous phases at low camera length. Nevertheless, the absorption bands at 1365 and 1091 cm⁻¹ are assigned to the stretching modes of the C–N–C of the imide 5-membered ring are preserved, indicating that the imidazole is thus not oxidised during this amorphisation process. The combined XRD, ATR-FTIR and electron diffraction results confirm that the basic building blocks and the connectivity of the amorphised ZIF-8 counterparts is retained, but the loss of crystalline XRD reflections suggests that long-range periodic ordering is lacking. From previous studies by Lee et al.,^[48] direct thermal treatment of ZIF-8 at 350 °C induces ZnO formation at high temperatures. In our MMMs, no ZnO was formed as evidenced from the XRD diffractograms (Figure 3.5d) by the absence of the characteristic diffraction peaks in the region between 30-40° (2 Θ , Figure 3.15). In addition, the ZnO band at 500 cm⁻¹ is not observed from the FTIR spectra, which further excludes its formation at high temperature.^[48] Although ZIF-8 has been reported to undergo amorphisation via ball-milling or compression,^[5] amorphisation through thermal treatment has not been documented to date yet, since bulk ZIF-8 powder is more likely to undergo a direct chemical conversion to ZnO upon thermal treatment (Figure 3.16).^[48] We assume that the Matrimid® might provide thermochemical protection for the embedded ZIF-8 under a relatively slow heating rate and a prolonged 24 h thermal treatment, which is in full agreement with the TGA results.

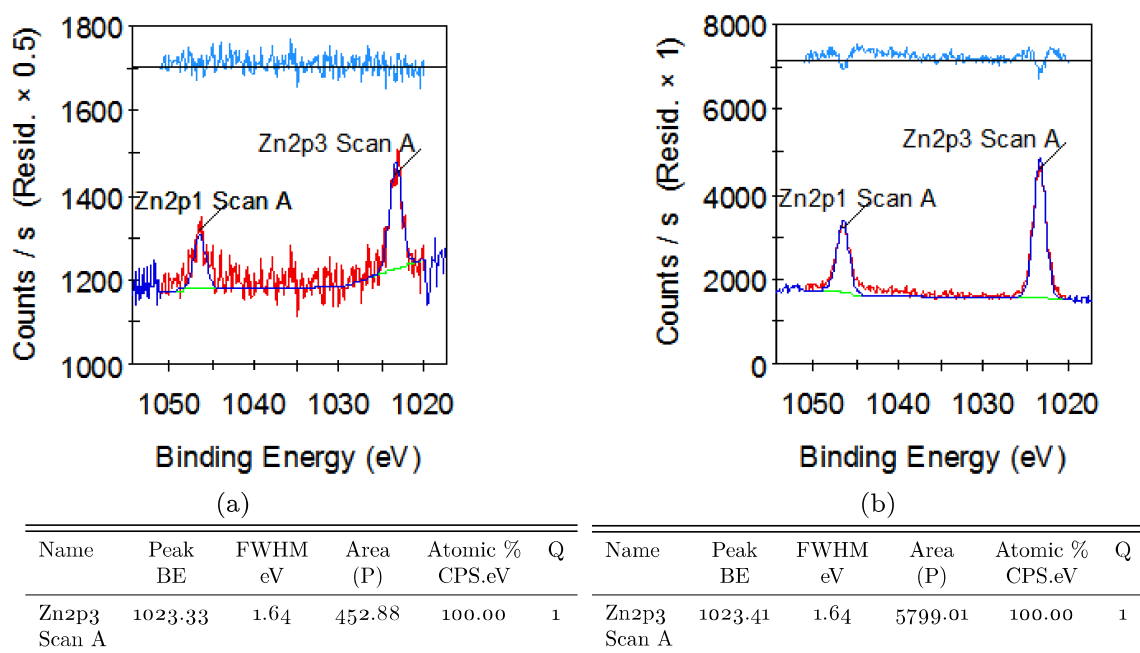


Figure 3.12: The XPS patterns of MMMs with ZIF-8 (40 wt.%) treated at (a) 100 °C and (b) 350 °C.

3.4.2 The microstructure of the MMMs

The influence of thermal treatment on the structural morphology of the membranes was studied by SEM (Figure 3.17), revealing that the ZIF-8 particles are well-dispersed with excellent filler-polymer adhesion even at high ZIF-8 loadings. No large clusters nor aggregates of ZIF-8 particles were observed. Intriguingly, by increasing the annealing temperature, high quality membranes with a smooth cross-section of homogeneous microstructure were successfully fabricated. In order to gain insights into the internal structural morphology and grain distribution within MMMs, and amorphous ZIF-8-polyimide interaction, advanced STEM analyses were performed on ultrathin cross-sections as shown in Figure 3.14. A cross-section of an MMM with 40 wt.% ZIF-8 loading was prepared by ultramicrotomy with a thickness of 90 nm for HAADF-STEM and EDX measurements. Overviews at low and high magnification using HAADF-STEM are shown in Figure 3.14b and c, respectively. A clear contrast between ZIF-8 (light regions) and polymer (dark regions) allows direct identification of different nanostructure phases. According to the HAADF-STEM images, the ZIF-8 nanoparticles are well distributed. EDX mapping was applied across the area in Figure 3.14c to investigate the distribution of certain elements. The

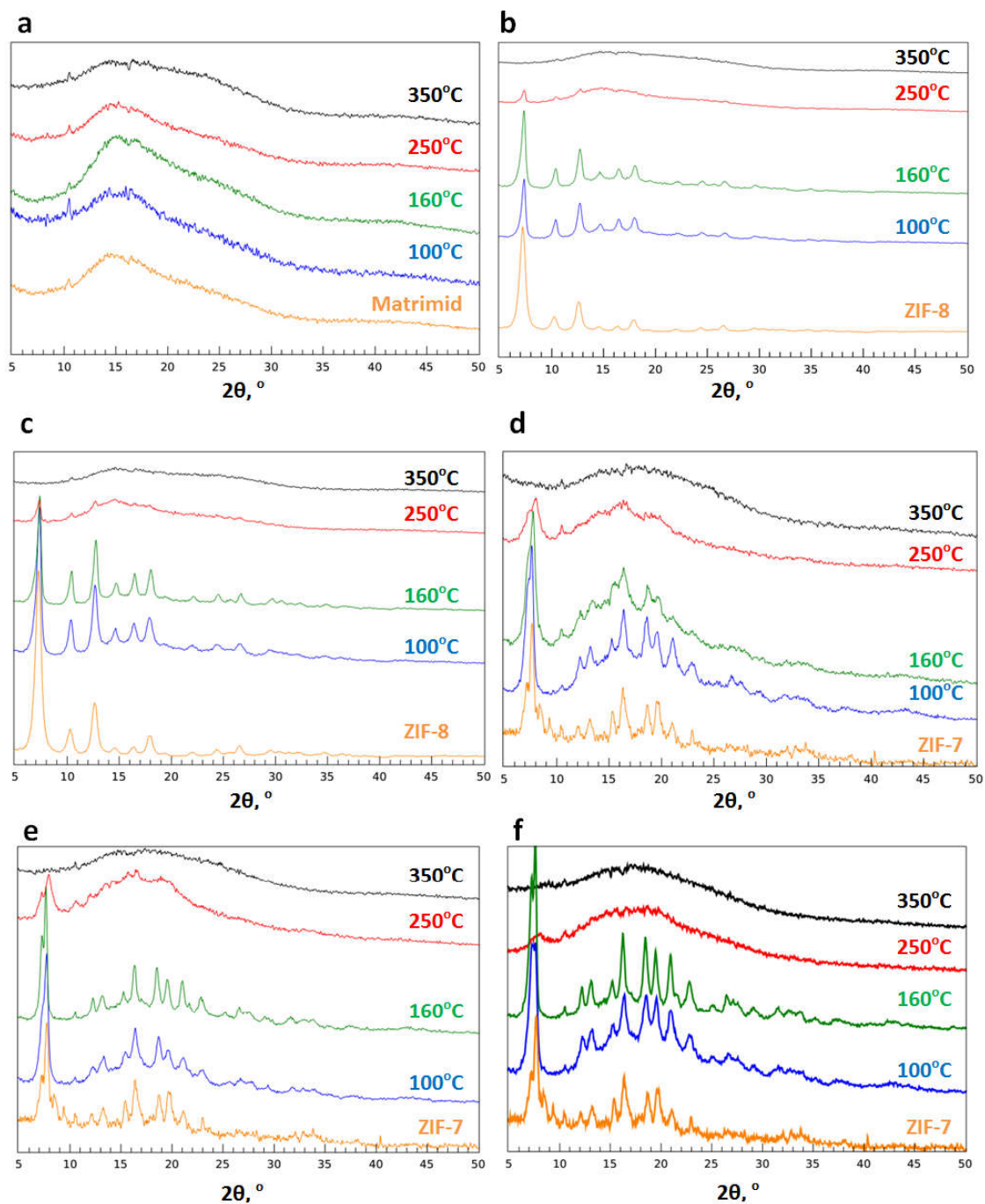


Figure 3.13: The XRD diffractograms of (a) Matrimid® and MMMs with (b) 20 wt.% and (c) 30 wt.% ZIF-8. MMMs with (d) 20 wt.%, (e) 30 wt.%, (f) 40 wt.% ZIF-7 loading are also given.

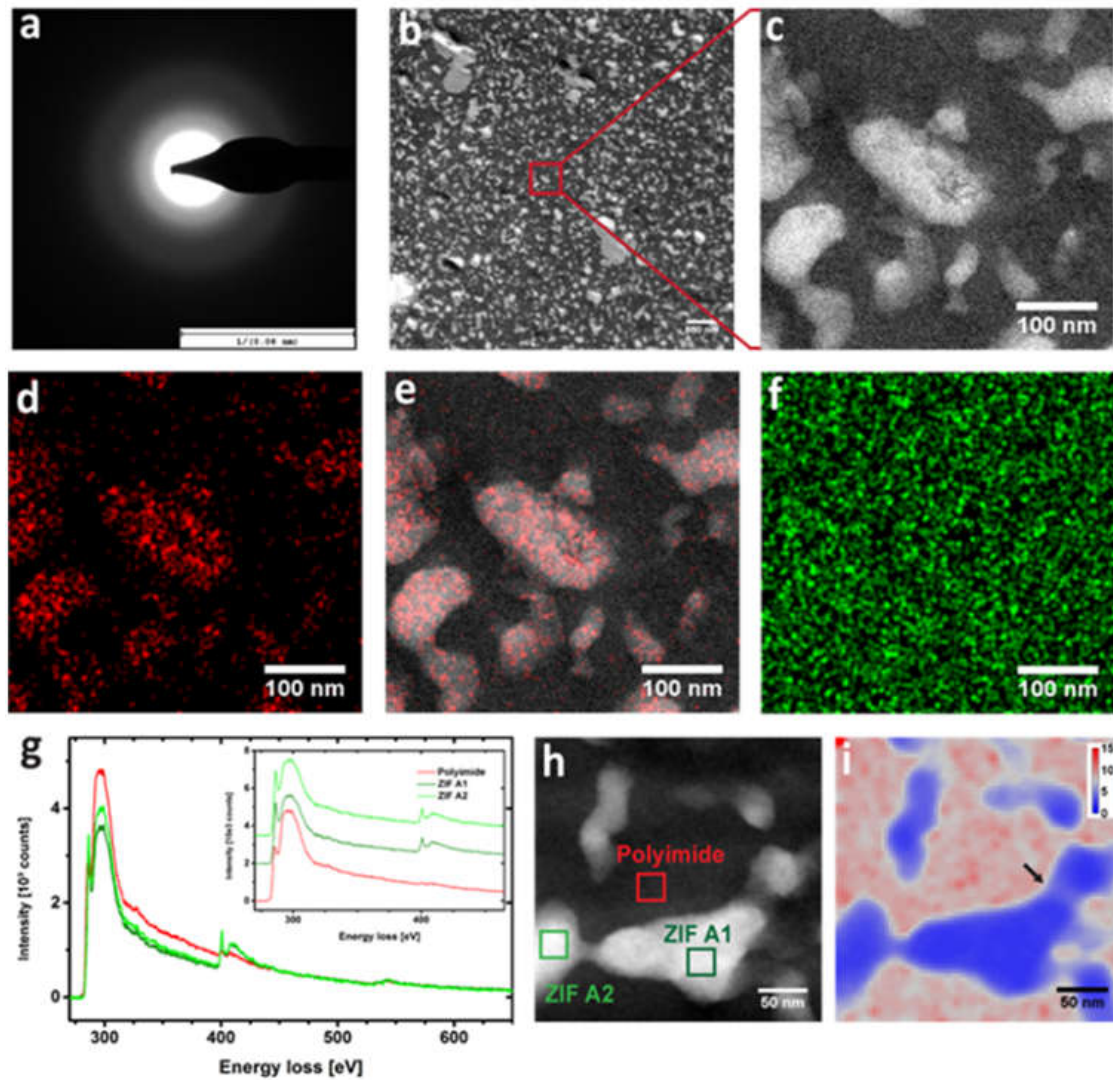


Figure 3.14: TEM imaging of MMMs with 40 wt.% loading. (a) Electron diffraction. (b) HAADF-STEM image of MMMs with 40% ZIF-8. (c) High magnification view with HAADF-STEM. (d) Zn map from EDX measurement corresponding to the area shown in c. (e) Overlay between HAADF image and Zn map. (f) EDX map showing the O distribution. (g) Average core energy-loss spectra for a polymer region and ZIF-8 regions. (h) HAADF-STEM overview image for STEM-SI map. Boxes indicate regions of averaging for spectra in g. (i) Map depicting the ratio between C and N contents calculated from spatially resolved core energy-loss spectra of the region outlined by HAADF-STEM in h.

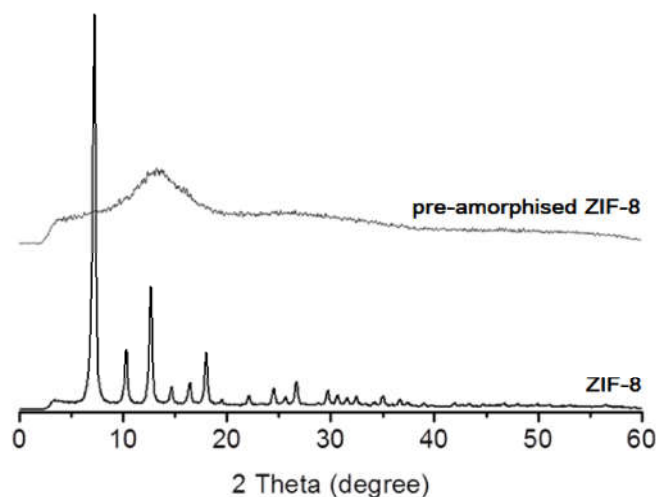


Figure 3.15: XRD diffractograms of pre-amorphised ZIF-8 obtained by ball-milling and as-synthesised ZIF-8.

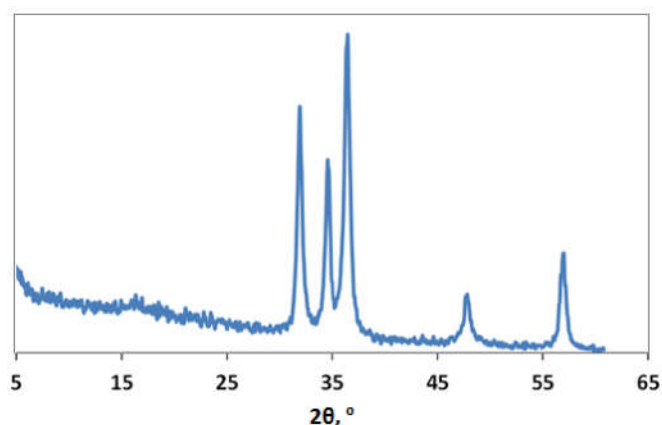


Figure 3.16: The XRD diffractogram of ZIF-8 powder subjected to thermal treatment at 350 °C.

resulting map for Zn (Figure 3.14d) and its overlay with the HAADF image (Figure 3.14e) demonstrates that Zn is only localised in the ZIF-8 areas and not dispersed into the polymer. Mapping of O (Figure 3.14f) reveals a homogeneous distribution; no specific enrichment within the particles is observed, which confirms the observation from XRD and ATR-FTIR that the embedded ZIF-8 is not converted to ZnO upon heating at 350 °C.

Figure 3.14g shows core-loss energy-loss spectra taken for a polyimide area and two ZIF-8 areas as indicated in the HAADF image in Figure 3.14h. Spectra are averages from STEM-SI data. A cross-section of 40 nm thickness was used to reduce effects from multiple scattering. To obtain an STEM-SI data

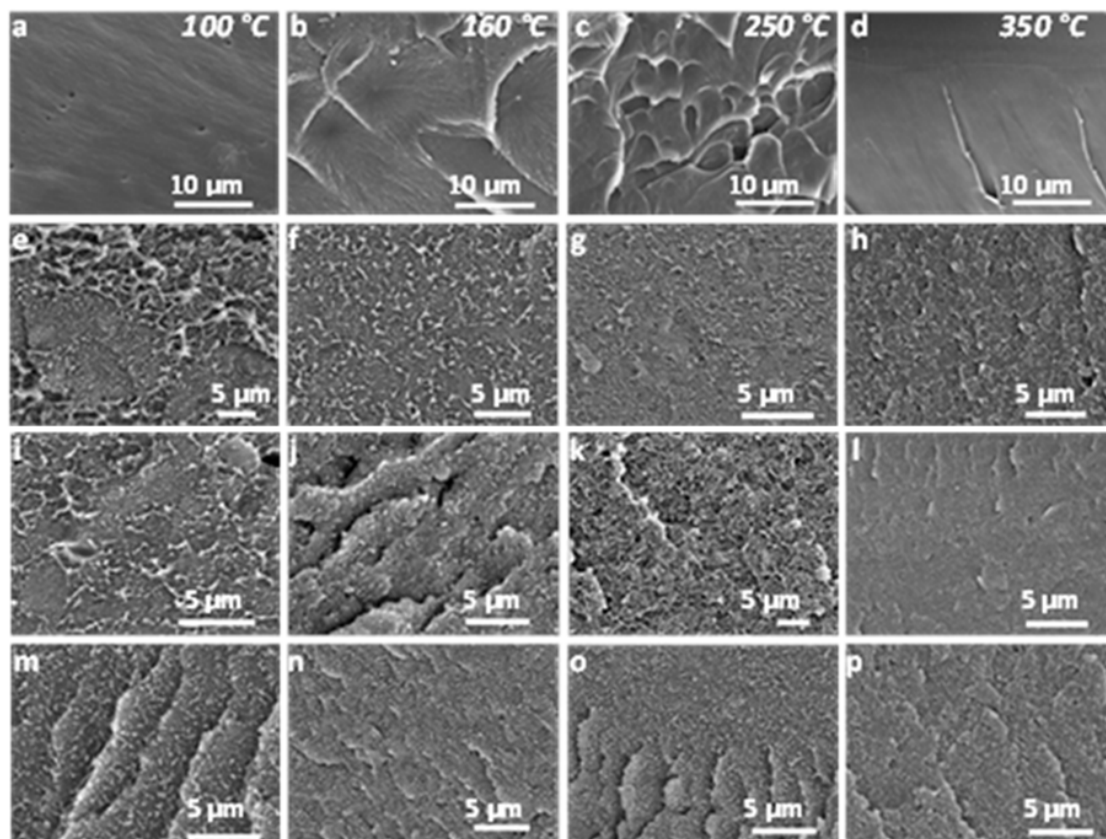


Figure 3.17: Effect of MOF loading and annealing temperature on the membrane morphology as observed by SEM. The cross-sectional images of (a-d) Matrimid® and MMMs with (e-h) 20, (i-l) 30, (m-p) 40 wt.% ZIF-8 loading, respectively. The annealing temperature is given at the top of each column.

set, the focused beam was scanned across the region outlined in Figure 3.14h while recording an energy-loss spectrum for each scan position. The energy range is 275-650 eV so that core-loss signals contain information about the C-K edge (ca. 285 eV), N-K edge (ca. 397 eV), and O-K edge (ca. 532 eV). Spectra were corrected for multiple scattering (see Methods section) and the background signal was fitted by a power law function and subtracted. This allows quantitative comparison of the different element edges. It can be clearly seen that ZIF particles show much stronger signals for N and an elevated signal for π^* in relation to σ^* excitations compared to polyimide. The total integrated peak intensities remain the same. However, sharper peaks for the N-edge and the π^* excitation for ZIF-8 nanoparticles indicate a better ordering of amorphous ZIF-8 building units than the amorphous polymer matrix. The O concentration is very low over the entire investigated region. Therefore, the spatially resolved spectra were used to quantify the local C and N compositions yielding a map of

C/N ratios as shown in Figure 3.14i. The map shows that the amorphous ZIF-8 regions in blue with high N concentrations exhibit a sharp boundary towards the polymer regions of high relative C content (red). Around the boundaries between the polymer and the ZIF-8 particles, there is a small interfacial layer with intermediate C/N ratios (the grey layer around the ZIF-8 regions, Figure 3.14i). Since the signals result from integration over the thickness of 40 nm, the interfacial profiles can be induced by the varying C/N ratios along the path of the electrons through the cross-section. However, as indicated by the black arrow in Figure 3.14i, such a layer is also visible in a region where only a thin part of ZIF-8 is found. The constant occurrence of the same interfacial C/N ratio provides evidence of a cross-linking between the imidazole in amorphised ZIF-8 and polymer.

3.4.3 The gas separation properties of MMMs

The possibilities of these MMMs exhibiting intrinsic homogeneity achieved via thermally sealed interfacial defects alongside the incorporated interspersed amorphous ZIF-8 having interesting and unique structural and physicochemical properties for the separation of CO₂ from CO₂/CH₄ (50/50% vol.) mixtures were subsequently investigated. The membranes were tested using a custom-built, high-throughput gas separation system (HTGS). Figure 3.18 shows the separation performance with respect to temperature and ZIF-8 loading. The Matrimid® membranes (Figure 3.18a) showed a significant increase in selectivity from 22 to 40 upon treatment at 250 °C. Astonishingly, the cross-linked pure Matrimid® membranes at 350 °C already achieved a selectivity value of 76, almost 4 times the standard pure Matrimid® membranes (selectivity of CO₂/CH₄ = 20). It should be mentioned that the Matrimid® membranes thermally treated at 350 °C with plasticisation resistance have been previously reported.^[49] However, the lower selectivities of 44 in comparison to our results are probably due to the shorter treatment times (15-30 minutes) applied. In a control experiment, the separation performance of an MMM prepared from pre-amorphised ZIF-8 filler was investigated for CO₂/CH₄ under similar operating conditions. The amorphised ZIF-8 sample was prepared via ball-milling, as reported by Cheetham and co-workers.^[35] The characterisation (XRD, SEM and N₂ physisorption) of the pre-amorphised ZIF-8 prepared by ball-milling is presented in Figure 3.19, 3.15, 3.20 and Table 3.2. The reported method for ZIF-8 amorphisation by ball-milling proved to be highly reproducible. The evidence of polymer-polymer and polymer-amorphous ZIF-8 cross-linking is confirmed by ATR-FTIR, as presented in Figure 3.21. However, the separation results revealed that this MMM with 30 wt.% loading failed to achieve high CO₂/CH₄ selectivity in comparison to the cross-linked MMMs prepared via *in-situ* thermo-oxidative

Table 3.2: Physicochemical properties of as-synthesised ZIF-8 and pre-amorphised ZIF-8 prepared by ball-milling.

Sample	BET surface area (cm ² /g)	Micropore volume obtained from <i>t</i> -plot (cm ³ /g)	Total pore volume (cm ² /g)
ZIF-8	1877	0.66	1.33
Pre-amorphised ZIF-8	16	-	0.09

treatment (Table 3.3). According to SEM imaging, significant agglomerations and large particles were observed in the pre-amorphised ZIF-8 sample compared to the as-synthesised ZIF-8 (Figure 3.22). Top view and cross-sectional SEM images show that large particle agglomerations and interfacial voids were clearly visible throughout the MMM (Figure 3.22). The results explicitly explain the poor separation performance of the MMM prepared from pre-amorphised ZIF-8 filler. The results reveal that thermally induced *in-situ* amorphisation of ZIF-8 in the polymer matrix has distinct advantages over the use of pre-amorphised ZIF-8 for the preparation of defect-free MMMs.

Figure 3.18b-d shows the MMM selectivity with regard to ZIF-8 loadings (20, 30 and 40 wt.%) and thermal treatment temperatures (100-350 °C). The thermally treated MMMs (20 wt.%) at 100-160 °C exhibit permeabilities up to 20 Barrer which is more than double the permeabilities of the unfilled Matrimid® membranes (8 Barrer). The enhanced permeability is most probably due to the introduction of porosity by the MOF, leading to faster diffusion of the gas molecules by providing easy pathways for the penetrant gases. This phenomenon is more obvious at a higher ZIF-8 loading (30-40 wt.%), achieving permeabilities up to 57 Barrer. Similar to the unfilled Matrimid® membranes, MMMs treated at low temperatures (100-160 °C) do not show an improved selectivity, instead an increase in CO₂ permeabilities are observed (Figure 3.18b), possibly due to the interfacial defects between ZIF-8 nanoparticles and the polymer, as well as the residual DMF trapped in ZIF-8. However, with the increase in thermal treatment temperature to 250 °C and 350 °C, a significant jump in selectivities is still achieved. The cross-linked MMMs loaded with 30 wt.% of amorphous ZIF-8 achieved the highest selectivity of 162 without sacrificing too much permeability. The superior CO₂/CH₄ selectivities achieved can be explained by several reasons. (1) cross-linked polymer networks were achieved via thermo-oxidative cross-linking reactions at 350 °C which serve as a molecular sieve network for CO₂ separation over CH₄ in a mixed-gas condition. (2) The polymer is also cross-linked with the imidazolate linker at the edges of the amorphous ZIF-8 particles, hence eliminating defects at the polymer–filler interface. The cross-linking at the interface of amorphous ZIF-8 with the polymer perfectly sealed the grain boundary at the interface, which gave a defect-free MMM, as evidenced by the HAADF-STEM imaging. (3) The

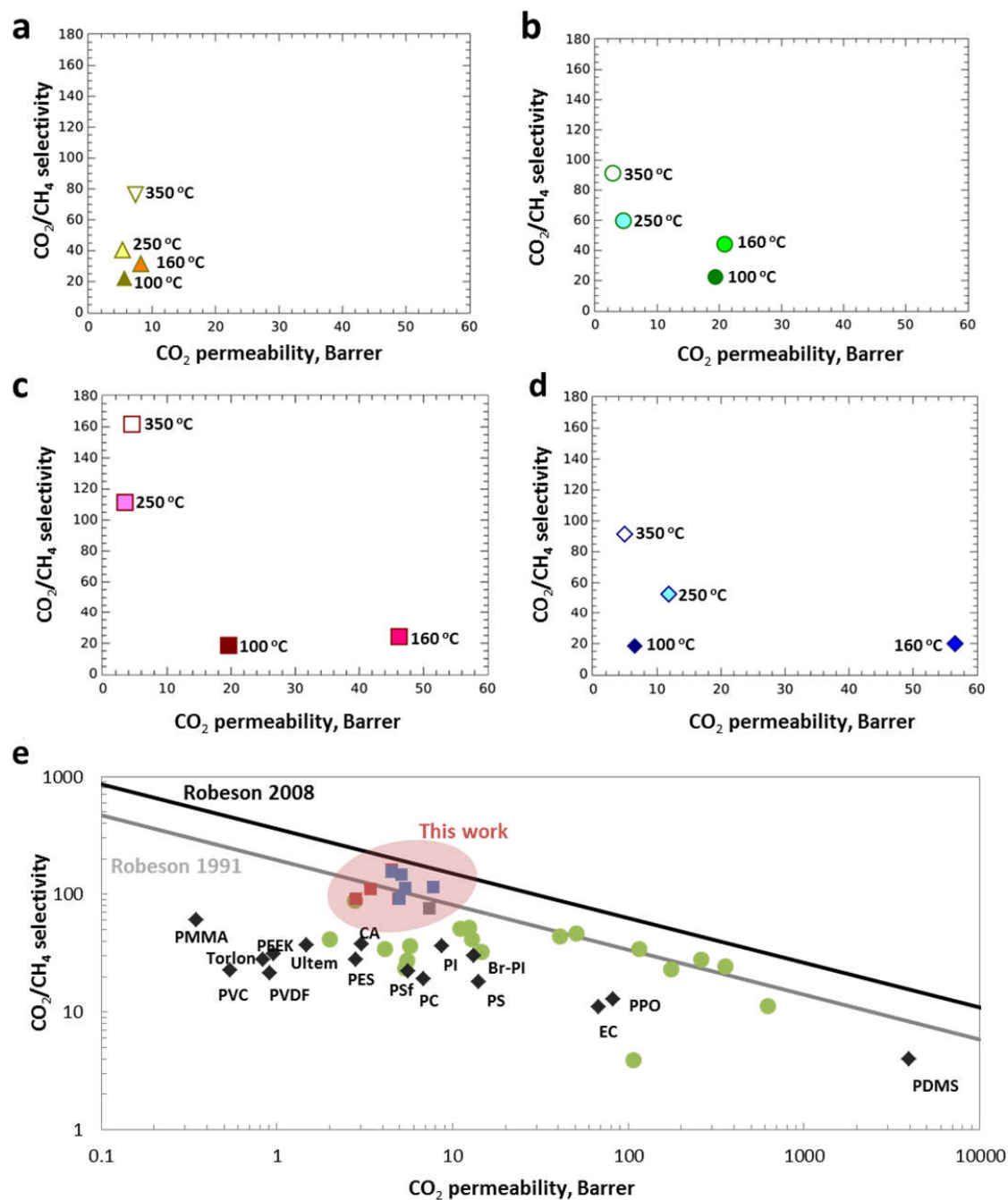


Figure 3.18: The evolution of the gas selectivity of the thermally treated membranes. (a) Matrimid® and (b-d) MMMs with 20, 30 and 40% ZIF-8 loading with increasing annealing temperature. (e) The gas separation performance of the membranes prepared for this work, primary commercial polymers (black diamonds) and various MOF-based MMMs from literature (green dots) plotted against the Robeson plot of 1991 and 2008. The red and blue squares represent data from MMMs with ZIF-8 and ZIF-7, respectively. A fully detailed comparison of the data in this plot together with the measurements conditions can be found in the Table 3.3.

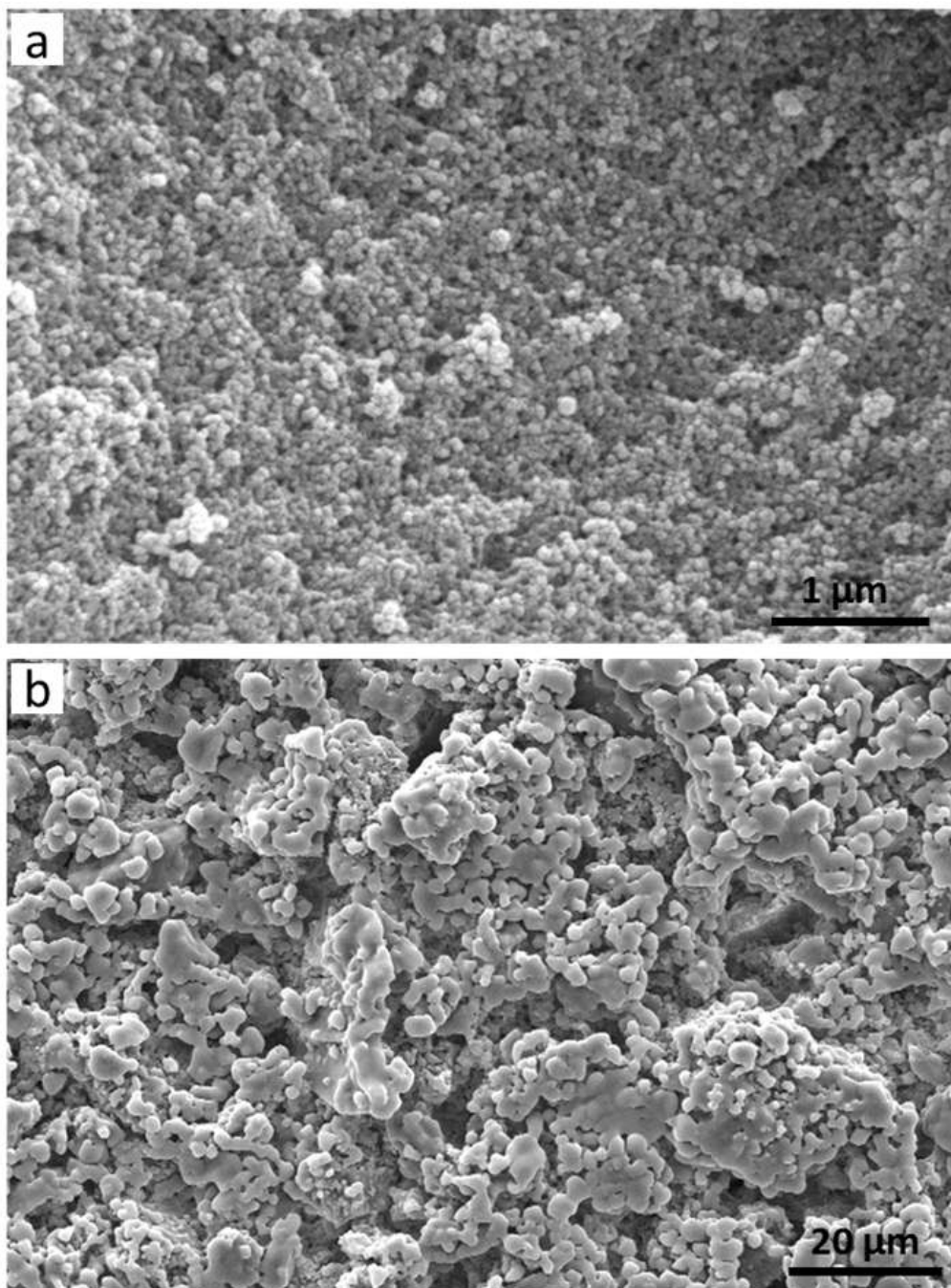


Figure 3.19: SEM images of (a) as-synthesised ZIF-8 and (b) pre-amorphised ZIF-8 obtained by ball-milling.

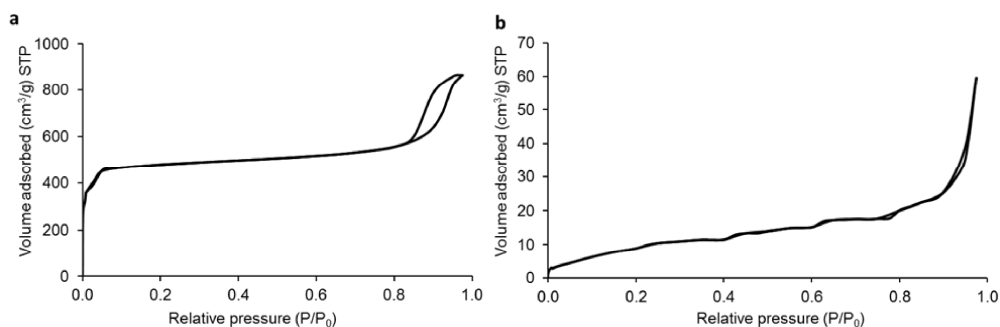


Figure 3.20: N₂ adsorption-desorption isotherms of (a) as-synthesised ZIF-8 and (b) pre-amorphised ZIF-8 prepared by ball-milling.

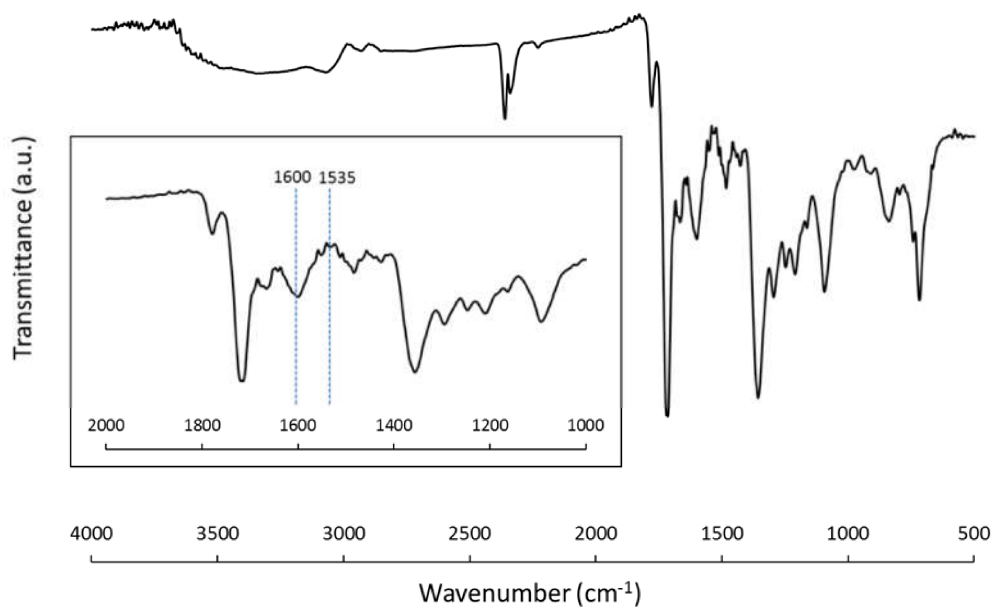


Figure 3.21: ATR-FTIR spectrum of MMM prepared from pre-amorphised ZIF-8 prepared via ball-milling. The inset shows the enlarged region from range 2000-1000 cm⁻¹ indicating the peaks at 1600 cm⁻¹ and 1535 cm⁻¹ which are assigned to C=O and N-H stretching vibrations attributed from polymer-polymer and polymer-*a*ZIF-8 cross-linking, respectively.

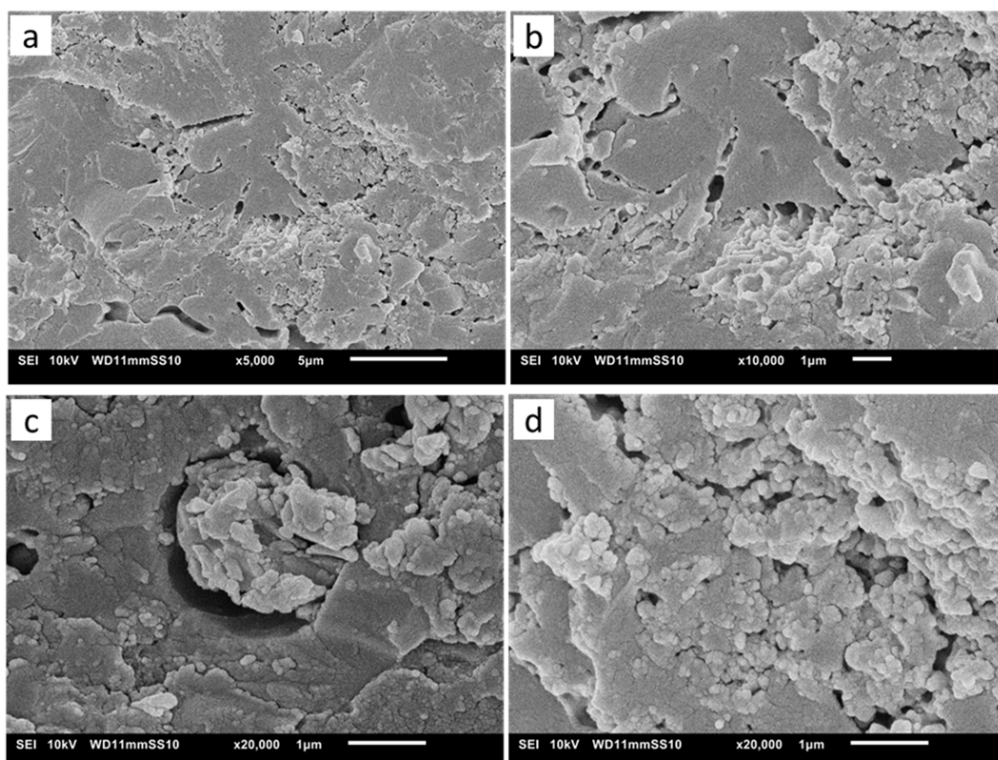


Figure 3.22: (a,b) Top and (c,d) cross-sectional SEM images of MMM filled with pre-amorphised ZIF-8 prepared by ball-milling (30 wt.%) viewed at different magnifications.

improved selectivity may also be attributed to the significant rigidification of the polymer around the filler. The densification of the polymer matrix after cross-linking decreases the CH_4 permeability more than the CO_2 permeability, which results overall in an improved CO_2/CH_4 selectivity. Similar phenomena have been reported for cross-linked polymers of intrinsic microporosity (PIMs) with improved selectivity for CO_2/CH_4 separation.^[50] Increasing T_g also suggests better interactions between the amorphous ZIF-8 nanoparticles with the polymer chains; restricting the motions of the polymer chains, which also adds to the benefit of plasticisation resistance at high pressure (40 bar) (*vide infra*). (4) The abundance of unsaturated Zn^{2+} and imidazolate linkers, originating from the building blocks of the amorphous ZIF-8 fillers, could also further promote stronger quadrupolar interactions with CO_2 .^[51] (5) Last but not least, the embedded crystalline ZIF-8 fillers in the polymer matrix were amorphised as a result of the thermal treatment. According to the EELS imaging, amorphisation of ZIF-8 also leads to a better ordering of the MOF structure in the cross-linked polymer matrix. The amorphous ZIF-8 possessing an interpenetrated, densely packed network structure can serve as an efficient molecular sieve for

CH₄ molecules.^[52] An earlier demonstration of the capability of ZIF-8 to trap molecules in the absence of long-range structural periodicity was reported by Chapman et al.,^[33] with structural evidence for the retention of I₂ within the pore network of amorphised ZIF-8.

ZIF-7 loaded MMMs show a similar trend in the separation of CO₂/CH₄ confirming that the demonstrated method is generic (see Figure 3.23, 3.24, 3.25, 3.26, 3.27, 3.28 and Table 3.3). Based on the separation performance of the MMMs for CO₂/CH₄ separation, the results suggest that the different chemical structures of ZIF-8 and ZIF-7 have an impact on the separation properties of the MMMs. ZIF-8 is composed of tetrahedral zinc(II) and 2-methylimidazolate, whereas ZIF-7 is composed of tetrahedral zinc(II) and benzimidazolate. The freely available methyl functional groups on the ZIF-8 linkers could enhance polymer-filler cross-linking. As a result, the amorphous MMMs prepared from ZIF-8 filler gave a slightly higher selectivity than ZIF-7 loaded MMMs. Fine-tuning of the surface properties of ZIF for further improvement in CO₂/CH₄ gas separation performance via e.g. incorporation of accessible amine functionality has been reported.^[53,54] The incorporation of those mixed-linker ZIFs into the polymer membranes proved to be effective for improving the ideal selectivity for CO₂/CH₄ separations.^[54]

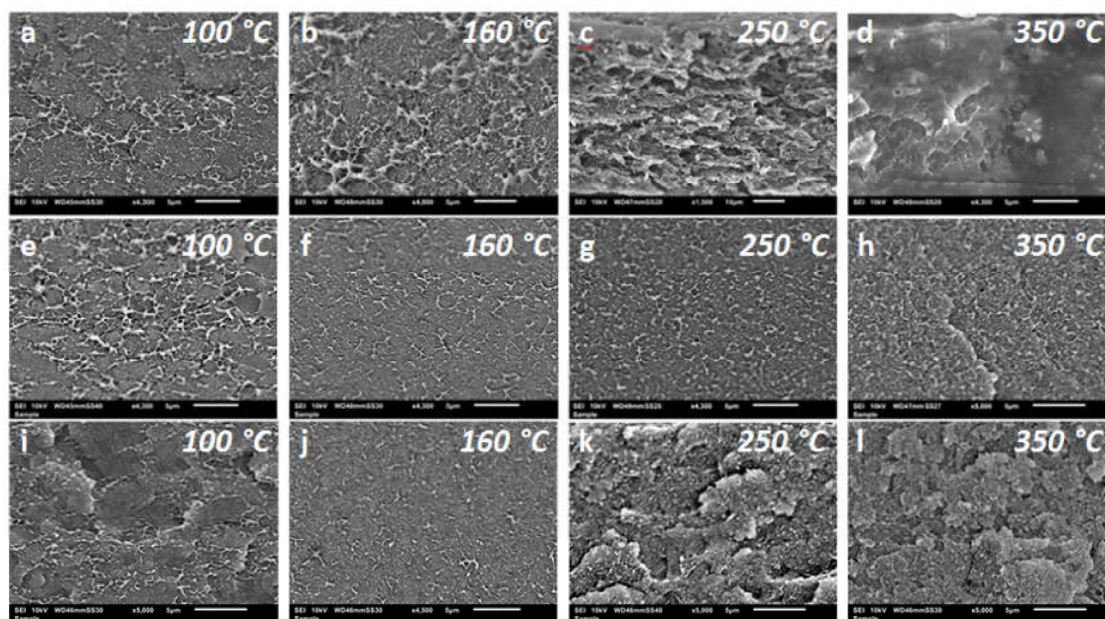


Figure 3.23: The SEM images of the MMMs with (a-d) 20, (e-h) 30, (i-l) 40 wt.% ZIF-7 loading. The improvement in the MMM morphology with increasing temperature followed trend similar to the MMMs with ZIF-8.

Over the years, extensive research on improving the performance of commercially

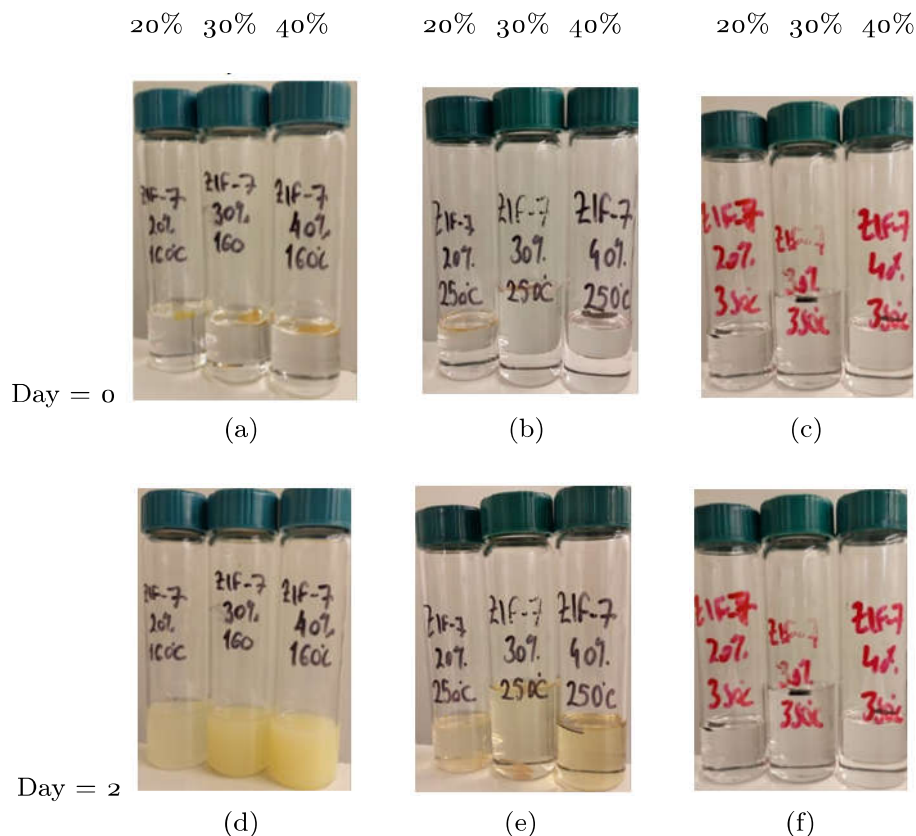


Figure 3.24: The solubility tests of MMMs with ZIF-7, treated at (a,d) 160 °C, (b,e) 250 °C, (c,f) 350 °C.

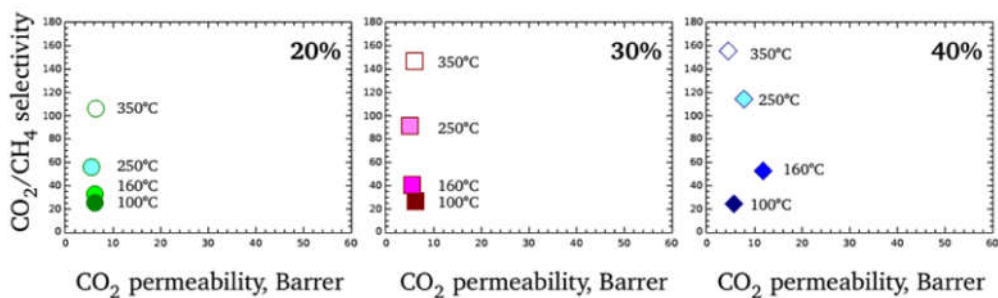


Figure 3.25: The gas separation performance of MMMs with ZIF-7.

available polymer membranes for CO₂/CH₄ separation via impregnation with MOFs aiming to exceed the Robeson upper-bound has taken place. Commercial polymers, such as PSF, Ultem®, PPEES or Matrimid® often lead to MMMs with separation properties well below the Robeson upper-bound.^[34,55] A typical Robeson plot of CO₂/CH₄ selectivity versus CO₂ permeability is presented in Figure 3.18e, revealing that the reported cross-linked MMMs containing

amorphous ZIF-8 have a separation performance that reaches the state-of-the-art upper-bound of 2008, showing the highest selectivities reported so far for MOF-based MMMs for CO₂/CH₄ separations. More importantly, gas separation measurements conducted at 40 bar feed pressure confirmed that the implemented post-synthesis treatment induced resistance to plasticisation, with selectivities of 90.8 ± 4.2 , 134 ± 7.6 and 140 ± 11.5 for the Matrimid®, ZIF-8 and ZIF-7 membranes with 40 wt.% loading, respectively (Table 3.3), as a logical consequence of the strong polymer cross-linking.

3.4.4 TEM analysis of MMMs with ZIF-7

Techniques such as selected area electron diffraction (SAED), HAADF-STEM imaging, EDX mapping and EELS were used to investigate the structure, morphology and chemical distribution of ZIF-7 loaded MMMs. Similar to the ZIF-8-based MMMs, the TEM sample for ZIF-7-based MMMs was prepared using an ultramicrotome (Leica), to obtain a lamella with a thickness of ~ 50 nm. The diffraction and EDX analyses were carried out with an FEI Osiris microscope operated at kV. The EEL spectral images were recorded using an aberration corrected FEI Titan 60-300 microscope, operated at 120 kV.

From an SAED analysis (Figure 3.26a), no diffraction spots were observed for ZIF-7 loaded membranes, indicating an unordered structure. Figure 3.26b (HAADF-STEM) shows a homogenous distribution of nanoparticles embedded inside the MMM. The high intensity regions correspond to the ZIF-7 nanoparticles and the darker regions correspond to the membrane. The chemical distribution of the individual elements was visualised by EDX mapping (Figure 3.26c-f). The Zn and N content were mainly observed on the ZIF-7 particle; whereas elements such as C, O were detected in the polymer.

EELS analysis was used to investigate the cross-linking between membrane and ZIF-7 nanoparticles. First, the local C to N maps were revealed after quantification of the spectral map. The different bonding states of C-K edge were also visualised using the same dataset. Figure 3.27b displays the averaged spectra acquired from the MMM (spectrum plotted in red) and from a ZIF-7 particle (spectrum plotted in black). Both spectra show the C-K and N-K ionisation edge (c.a 284 and 401 eV, respectively). The electronic near-edge structure (ELNES) of the C-K edge starting at 284 eV clearly displays the n^* and σ^* bond excitations in both spectra. The ZIF-7 particles show stronger N-K intensity and n^* bond excitation in comparison to the rest of the membrane. To obtain the quantified compositional comparison of N and C; the background intensity of EEL spectra was fitted by a power law function and subtracted. Afterwards, the spectra were corrected for multiple scattering. This allows a

quantitative comparison of different element edges and results in a spatial map of the N-to-C composition ratio. Figure 3.27c and d depict the individual C and N intensity maps. The C intensity is rather homogeneous throughout the selected region. N was detected both on the membrane and ZIF-7, however the intensity increases abruptly at the ZIF-7.

Using these two maps, the C content to N ratio map was obtained, as shown in Figure 3.27e. The C strength is ~ 10 times of N strength on the polymer. This ratio is reduced to ~ 3 in the center of the ZIF-7 particles.

The same multiple scattered corrected spectrum image was also used to visualise the strength map of n^* and σ^* bonding states in a qualitative manner. First, the C-K edge was separated into the components such as the n^* and $n^* + \sigma^*$ using a blind source separation (a PCA method) implemented in Hyperspy^[36], see Figure 3.28a. Then, the two components were fit to the spectral dataset to obtain the bonding state map. The fitting was performed using the EELSMODEL^[56] program. The results from the analysis are presented in Figure 3.28b and c. In Figure 3.28b, it can be clearly observed that the n^* bond intensity gets stronger on the ZIF-7 nanoparticle (highlighted with the red arrow). In Figure 3.28c, the distribution of the $n^* + \sigma^*$ bonds are depicted. The intensity of $n^* + \sigma^*$ bonds are homogeneously distributed through the MMM. At the interface (depicted with a blue arrow), the strength of $n^* + \sigma^*$ becomes the lowest. The line profile clearly depicts the intensity change at the interface, see Figure 3.28d. At the interface between ZIF-7 and the polymer, C-N-C type of bonding (n^*) can be prominent in comparison to σ^* type of bonding.

3.5 Conclusions

A high-performance MOF-based MMM was prepared using a controlled thermal treatment which remarkably boosts the gas separation performance to the highest CO_2/CH_4 selectivities ever reported to date for MOF loaded MMMs. The polymer and the MOF become covalently bound, thus decreasing the risk for defects due to grain boundary formation. Advanced TEM imaging of the thin cross-sectional sample prepared via ultramicrotomy successfully provides insights into the cross-linking of the MOF with the membrane, which effectively sealed the grain boundary at the interface between the MOF particle and the polymer for the very first time. In addition, the MOF amorphises thanks to the protection of the surrounding polymer, while the polymer phase gets simultaneously cross-linked, resulting in superior separation performances, even under realistic process conditions for natural gas purification. More importantly, the selectivity and permeability of CO_2 could be simply tuned through thermal

treatment temperature and time, depending on the targeted applications. As demonstrated in this work using a readily available commercial polymer and ZIF-8 filler, the amorphous MMMs have a great potential as stable and highly selective materials for other gas or liquid membrane separations, adsorption, chromatography or catalysis.

3.6 Acknowledgements

A.K. acknowledges financial support from the Erasmus-Mundus Doctorate in Membrane Engineering (EUDIME) Programme. L.H.W. thanks the FWO-Vlaanderen for a postdoctoral research fellowship (12M1415N). M.P. acknowledges financial support by the FP7 European project SUNFLOWER (FP7 #287594). S.B. acknowledges financial support from European Research Council (ERC Starting Grant #335078-COLOURATOMS). J.A.M. gratefully acknowledges financial supports from the Flemish Government for long-term Methusalem funding and the Belgian Government for IAP-PAI networking. A.K. would also like to thank Frank Mathijs for the mechanical tests, Roy Bernstein for the XPS analysis and Lien Telen and Bart Goderis for the DSC measurements.

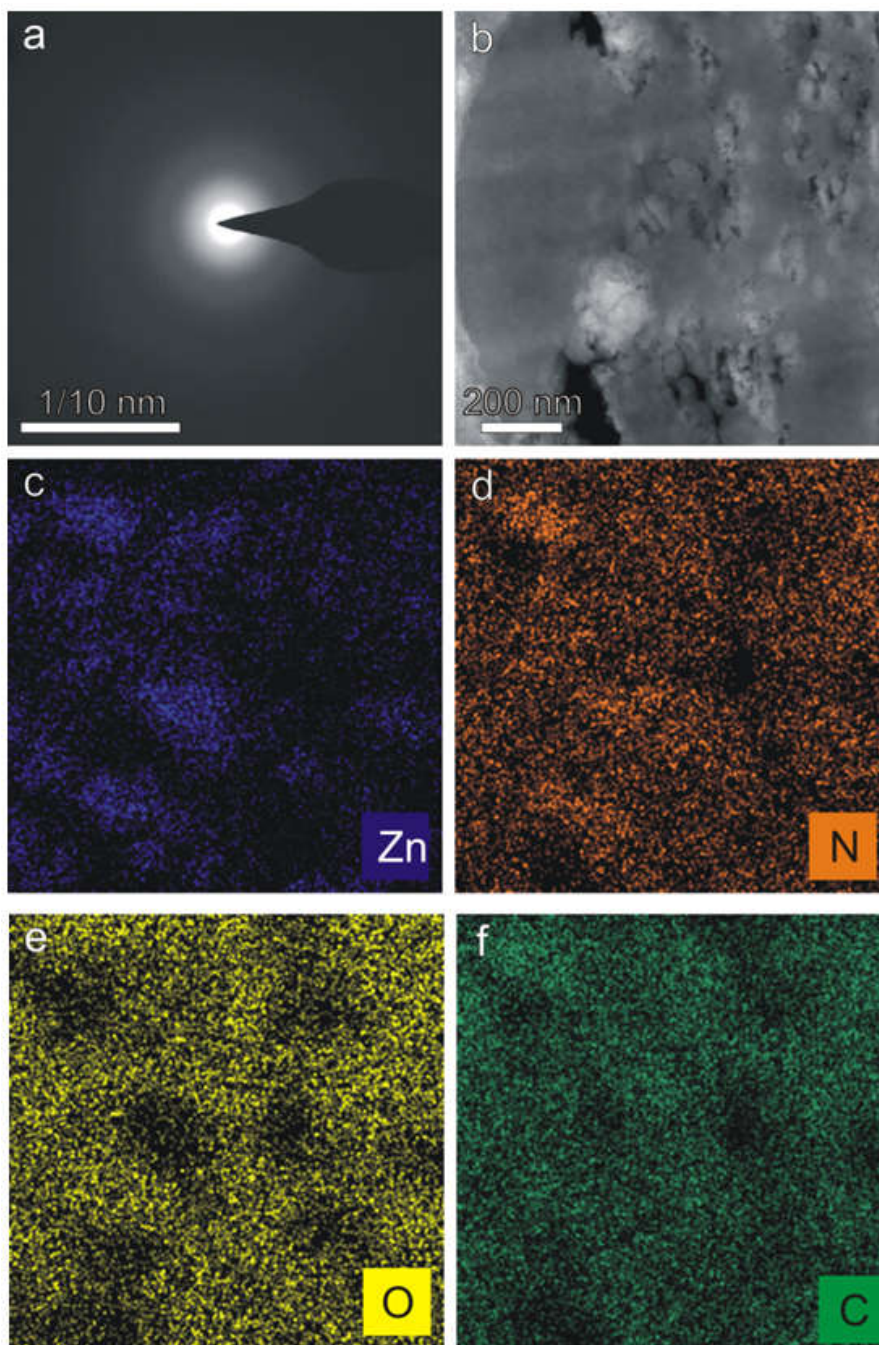


Figure 3.26: TEM characterisation of MMMs with 40 wt.% ZIF 7 loading. (a) Selected area electron diffraction pattern recorded from the MMM. (b) HAADF-STEM image displaying the distribution of ZIF-7 particles embedded in the MMM. The elemental maps for (c) Zn, (d) N, (e) O, (f) C.

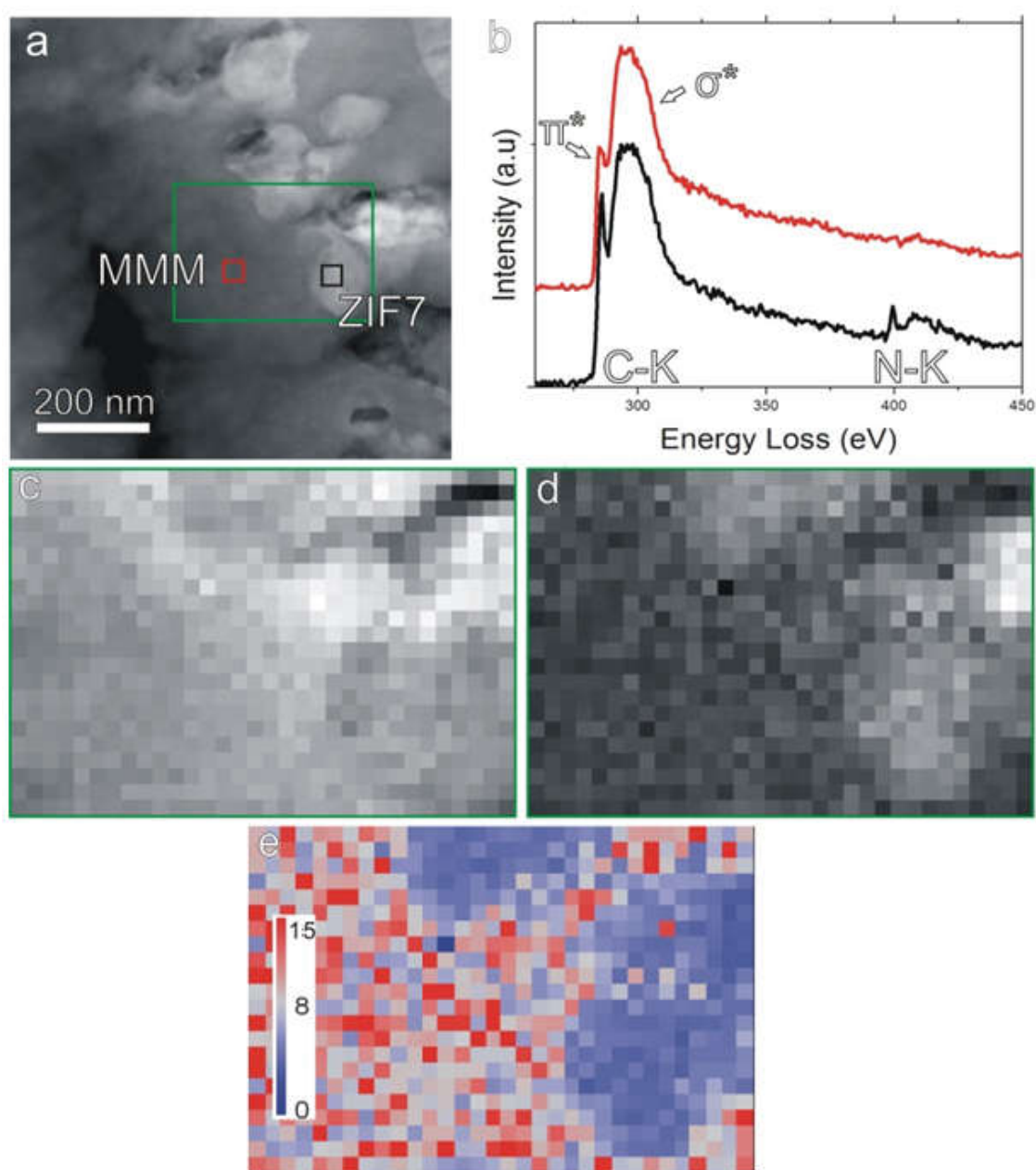


Figure 3.27: (a) HAADF-STEM image from the 40% ZIF-7 loaded MMM. (b) Background-subtracted EEL spectra from the indicated regions in (a). (c) Carbon K-edge peak strength map (d) Nitrogen K-edge peak strength map (e) C-to-N ratio map.

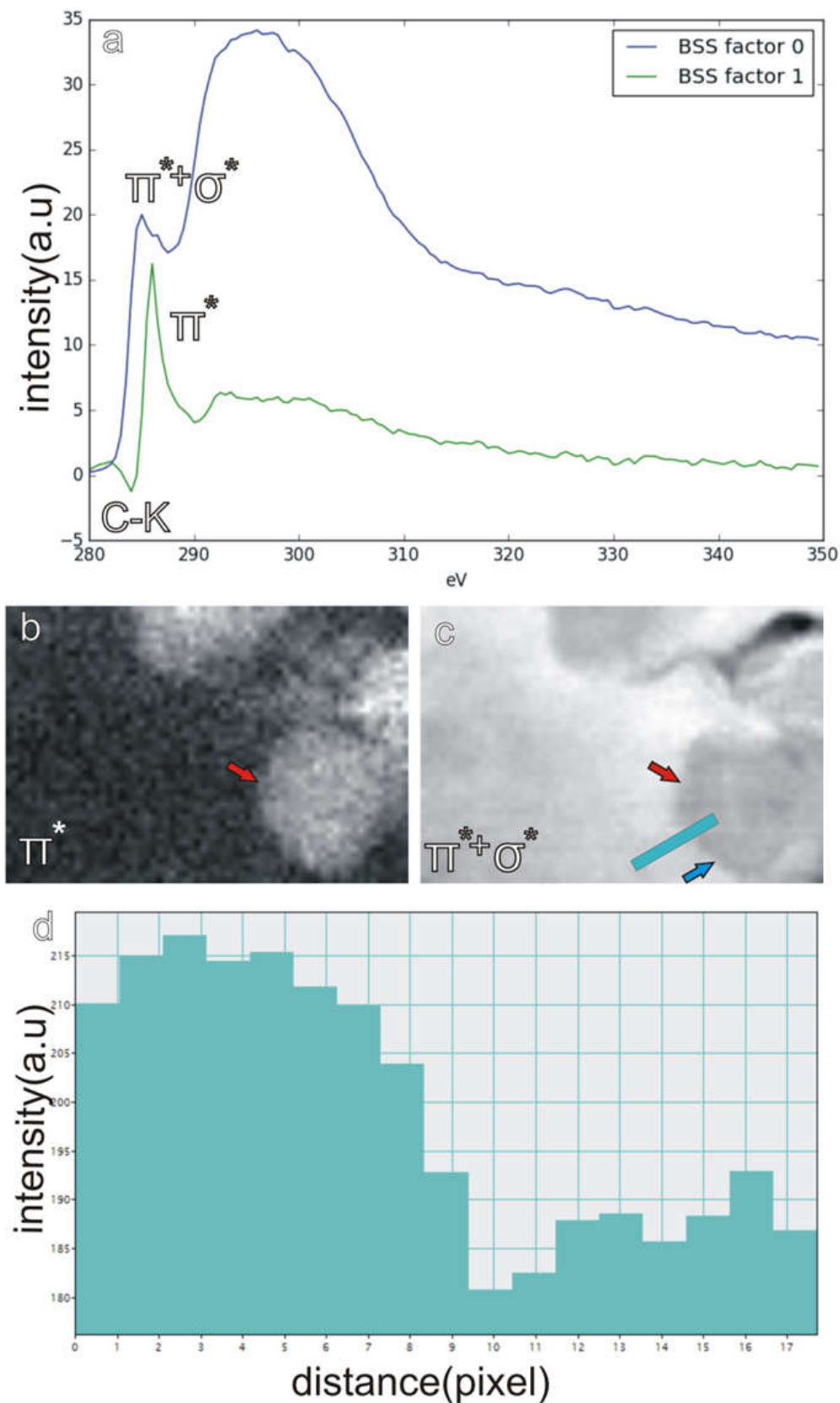


Figure 3.28: (a) The components of C-K edge obtained from the ZIF-7 loaded membrane, the n^* excitation component is plotted in green, the $n^* + \sigma^*$ excitation component is plotted in blue. (b) The intensity distribution of the n^* bond excitations. (c) The intensity distribution of the $n^* + \sigma^*$ bond excitations. (d) The line profile taken from green line depicted in (c).

Table 3.3: The gas separation data of MMMs and polymeric membranes from this work and literature.

Polymer	MOF	Loading, wt. %	Treatment	Measurement conditions	CO ₂ permeability, Barrer	CO ₂ /CH ₄ selectivity	Ref.
Matrimid®	none	0	100 °C, 24 h, in air	10 bar, 35 °C, 50 vol% CO ₂ /50 vol% CH ₄	5.6±0.7 ¹	22.3±0.2	This work
			160 °C, 24 h, in air	8.2±0.2	31.6±1	This work	
			250 °C, 24 h, in air	5.3±0.2	40.4±3.5	This work	
			350 °C, 24 h, in air	7.4±0.7	76.3±0.8	This work	
Matrimid	ZIF-8	20	350 °C, 24 h, in air	40 bar, 35 °C, 50 vol% CO ₂ /50 vol% CH ₄	2.6±0.02	90.8±4.2	This work
			100 °C, 24 h, in air	10 bar, 35 °C, 50 vol% CO ₂ /50 vol% CH ₄	19.3±3.6	22.4±3.2	This work
			160 °C, 24 h, in air	20.8±6	44.3±4.5	This work	
			250 °C, 24 h, in air	4.5±0.5	60.0±3.4	This work	
Matrimid	ZIF-8	30	350 °C, 24 h, in air	2.8±0.1	91.3±11.7	This work	
			100 °C, 24 h, in air	19.6±4.9	18.6±4	This work	
			160 °C, 24 h, in air	46.2±9.6	24.3±2	This work	
			250 °C, 24 h, in air	3.4±0.2	111.4±18.1	This work	
Matrimid	pre- amorphised ZIF-8 ²	30	350 °C, 24 h, in air	4.5±0.6	162.0±6.6	This work	
			350 °C, 24 h, in air	47.9±0.48	0.83±0.001	This work	
			100 °C, 24 h, in air	6.5±0.4	18.4±2.4	This work	
			160 °C, 24 h, in air	56.6±4.7	20.0±1.8	This work	
Matrimid	ZIF-8	40	250 °C, 24 h, in air	11.8±1.3	52.6±1.9	This work	
			350 °C, 24 h, in air	4.9±1.2	91.5±12	This work	
			350 °C, 24 h, in air	1.9±0.01	134±7.6	This work	

Continued on next page

¹1 Barrer = [10⁻¹⁰ cm³ (STP) cm/(cm² s cmHg)]²Obtained via ball-milling

Table 3.3 – continued from previous page

Polymer	MOF	Loading, wt. %	Treatment	Measurement conditions	CO ₂ permeability, Barrer	CO ₂ /CH ₄ selectivity	Ref.
Matrimid®	ZIF-7	20	100 °C, 24 h, in air	10 bar, 35 °C, 50 vol% CO ₂ /50 vol% CH ₄	6.1±1.4	25.4±1.4	This work
			160 °C, 24 h, in air		6.1±0.7	32.8±3.9	This work
			250 °C, 24 h, in air		5.4±0.5	56.1±1	This work
			350 °C, 24 h, in air		5.4±1.1	112.0±8.4	This work
Matrimid	ZIF-7	30	100 °C, 24 h, in air	10 bar, 35 °C, 50 vol% CO ₂ /50 vol% CH ₄	6.1±0.4	26.8±3.4	This work
			160 °C, 24 h, in air		5.4±3.5	40.6±1.4	This work
			250 °C, 24 h, in air		5.0±1.2	91.5±12	This work
			350 °C, 24 h, in air		5.1±0.8	147.2±11.4	This work
Matrimid	ZIF-7	40	100 °C, 24 h, in air	10 bar, 35 °C, 50 vol% CO ₂ /50 vol% CH ₄	5.7±1.5	24.5±8	This work
			160 °C, 24 h, in air		11.8±1.3	52.6±1.9	This work
			250 °C, 24 h, in air		7.8±2	114.4±9.6	This work
			350 °C, 24 h, in air		4.5±1.7	155.8±11.5	This work
Matrimid	ZIF-7	40	350 °C, 24 h, in air	40 bar, 35 °C, 50 vol% CO ₂ /50 vol% CH ₄	1.9±0.05	140±11.5	This work
Matrimid®	ZIF-8	20	180 °C, 18 h, in vacuo	4 bar, 22 °C	12.96	41.5	[43]
Matrimid	ZIF-8	50 ⁴	240 °C, overnight, in vacuo	2 bar, 35 °C, 10 mol% CO ₂ /90 mol% CH ₄	n/a ⁵	89.15	[34]
Matrimid	CuBDC (nanosheet)	8.2	180 °C, 12 h, in vacuo	7.5 bar, 25 °C, equimolar CO ₂ /CH ₄	2.78	88.2	[57]
Matrimid	Ni ₂ (dodbc)	23	120 °C, 24 h, in vacuo	10 bar, 35 °C, equimolar CO ₂ /CH ₄	14.7	32.5	[43]
Matrimid	MIL-53	15	80 °C, 24 h, 150 °C, in vacuo	3 bar, 35 °C ⁶	12.43	51.8	[58]

Continued on next page

³For each reference, the best performance was listed.⁴Loading calculated as (wt. MOF)/(wt. polymer)⁵Not reported⁶If a gas mixture composition is not listed, the data represents pure gas measurements.

Table 3.3 – continued from previous page

Polymer	MOF	Loading, wt. %	Treatment	Measurement conditions	CO ₂ permeability, Barrer	CO ₂ /CH ₄ selectivity	Ref.
Matrimid	Cu-BTC	30	90 °C, 24 h	4 bar, 35 °C, 35 vol% CO ₂ /65 vol% CH ₄	176	23	[59]
Matrimid	MOF-5	10	240 °C, 24 h, in vacuo	2 atm, 35 °C	11.10	51	[60]
Matrimid	NH ₂ -MIL-53(Al)	25	180 °C, 10 h, in vacuo	3 bar, 0 °C, equimolar CO ₂ /CH ₄	107	3.9	[61]
Ultem	Cu-BTC	35	in vacuo	3.5 bar, 35 °C	4.1	34	[62]
PEI	Cubic-MOF-5	25	70 °C, 2 d, in vacuo	6 bar, 25 °C	5.39	23.43	[63]
PSf	NH ₂ -MIL-53(Al)	25	180 °C, 10 h, in vacuo	3 bar, 35 °C, equimolar CO ₂ /CH ₄	5.5	27.5	[61]
PSf	MIL-68(Al)	8	120 °C, 24 h, in vacuo	2 bar, 35 °C, equimolar CO ₂ /CH ₄	5.7	36.5	[64]
PMP	NH ₂ -MIL-53(Al)	30	50 °C, 12 h, in vacuo	30 °C	358.2	24.4	[55]
ODPA-TMPDA	Cu-BTC	40	200 °C, 24 h, in vacuo	2 atm, 35 °C	260.7	27.75	[62]
6FDA-ODA	UiO-66	25	230 °C, 15 h, in vacuo	10 bar, 35 °C	50.4	46.1	[65]
Pebax	ZIF-7	34	Room temperature, 24 h	3.75 bar (CO ₂), 7.5 bar (CH ₄), 20 °C	41	44	[46]
PVC-g-POEM	ZIF-8 (hollow sphere)	30	50 °C, 4 h, in vacuo, 24 h	1 bar, 35 °C	623	11.2	[66]
Poly(vinylidene fluoride)	Cu-BTC	10	120 °C, 24 h, in vacuo	5 bar, 25 °C	2.002	41.7	[67]
Poly(phenylene oxide)	Cu-BTC	40	200 °C, 24 h, in vacuo	30 °C	115	34	[68]
Ultem	none	0	120 °C, 24 h, in vacuo	3.5 bar, 35 °C	1.48	37	[69]
Poly(methyl methacrylate)	none	0	>Tg	5 atm, 35 °C	0.35	60	[70]
Matrimid	none	0	130 °C, overnight, in vacuo	1 atm, 35 °C	8.7	36.3	[71]
Poly(ether sulfone)	none	0	Compression molding, 300 °C	10 atm, 35 °C	2.8	28	[72]

Continued on next page

Table 3.3 – continued from previous page

Polymer	MOF	Loading, wt. %	Treatment	Measurement conditions	CO ₂ permeability, Barrer	CO ₂ /CH ₄ selectivity	Ref.
PEEK	none	0	Tg+5 °C	10 atm, 35 °C	0.963	31	[73]
Brominated Matrimid® 5218	none	0	250 °C, 48 h, in vacuo	10 atm, 35 °C	13.3	30.2	[74]
Cellulose acetate	none	0	150 °C, 48 h, in vacuo	10 atm, 35 °C	3.04	38	[75]
Poly(vinylidene fluoride)	none	0	120 °C, 24 h, in vacuo	5 bar, 25 °C	0.915	21.27	[67]
Poly(vinyl chloride)	none	0	Room temperature, 2 h, in vacuo	1 bar, 25 °C	0.54	22.5	[76]
PDMS	none	0	75 °C, 45 min, 25 °C, 3 d	4 bar, 35 °C	3970	4	[77]
Polysulfone	none	0	Tg+10 °C, 2 d, in vacuo	10 atm, 35 °C	5.6	22	[78]
Polycarbonate	none	0	Tg+10 °C, several days, in vacuo	10 atm, 35 °C	6.8	18.9	[79]
Polystyrene	none	0	85 °C, 24 h	4.4 atm, 23 °C	14.1	18.1	[80]
PPO	none	0	7	1 atm, 35 °C	82	12.8	[81]
Ethyl cellulose	none	0	25 °C, 20 h, 60% relative humidity	2 bar, 25 °C	67.7	11.1	[82]
Torlon	none	0	250 °C, overnight, in vacuo	10 atm, 35 °C	0.83	27.8	[83]

⁷Rate of permeation is reported as GPU, 1 GPU = $[10^{-6} \text{ cm}^3(\text{STP})/(\text{cm}^2 \text{ s cmHg})] = [3.35 \times 10^{-10} \text{ mol}/(\text{m}^2 \text{ s Pa})]$

References

- [1] A. Kertik, L. H. Wee, M. Pfannmoeller, S. Bals, J. Martens and I. F. Vankelecom. “Highly selective gas separation membrane using in-situ amorphised metal-organic frameworks”. *Energy Environ. Sci.* 10 (11 2017), pp. 2342–2351.
- [2] K. W. Chapman, G. J. Halder and P. J. Chupas. “Pressure-Induced Amorphization and Porosity Modification in a Metal-Organic Framework”. *Journal of the American Chemical Society* 131.48 (2009), pp. 17546–17547.
- [3] S. Li and F. Huo. “Metal-organic framework composites: from fundamentals to applications”. *Nanoscale* 7 (17 2015), pp. 7482–7501.
- [4] Q. Song, S. K. Nataraj, M. V. Roussanova, J. C. Tan, D. J. Hughes, W. Li, P. Bourgoïn, M. A. Alam, A. K. Cheetham, S. a. Al-Muhtaseb and E. Sivaniah. “Zeolitic imidazolate framework (ZIF-8) based polymer nanocomposite membranes for gas separation”. *Energy & Environmental Science* 5.8 (2012), pp. 8359–8369.
- [5] T. D. Bennett and A. K. Cheetham. “Amorphous Metal-Organic Frameworks”. *Accounts of Chemical Research* 47.5 (2014), pp. 1555–1562.
- [6] N. Rangnekar, N. Mittal, B. Elyassi, J. Caro and M. Tsapatsis. “Zeolite membranes-a review and comparison with MOFs”. *Chemical Society Reviews* 44.20 (2015), pp. 7128–7154.
- [7] L. M. Robeson. “Correlation of separation factor versus permeability for polymeric membranes”. *Journal of Membrane Science* 62.2 (1991), pp. 165–185.
- [8] L. M. Robeson. “The upper bound revisited”. *Journal of Membrane Science* 320.1-2 (2008), pp. 390–400.
- [9] M. Rezakazemi, A. E. Amooghin, M. M. Montazer-Rahmati, A. F. Ismail and T. Matsuura. “State-of-the-art membrane based CO₂ separation using mixed matrix membranes (MMMs): an overview on current status and future directions”. *Progress in Polymer Science* 39.5 (2014), pp. 817–861.
- [10] R. Mahajan and W. J. Koros. “Factors Controlling Successful Formation of Mixed-Matrix Membranes”. *Ind. Eng. Chem. Res.* 39 (2000), pp. 2692–2696.
- [11] H. Hayashi, A. P. Cote, H. Furukawa, M. O’Keeffe and O. M. Yaghi. “Zeolite A imidazolate frameworks”. *Nature materials* 6.7 (2007), p. 501.
- [12] M. C. McCarthy, V. Varela-Guerrero, G. V. Barnett and H.-K. Jeong. “Synthesis of zeolitic imidazolate framework films and membranes with controlled microstructures”. *Langmuir* 26.18 (2010), pp. 14636–14641.

- [13] S. R. Venna and M. A. Carreon. "Highly permeable zeolite imidazolate framework-8 membranes for CO₂/CH₄ separation". *Journal of the American Chemical Society* 132.1 (2009), pp. 76–78.
- [14] K. S. Park, Z. Ni, A. P. Coté, J. Y. Choi, R. Huang, F. J. Uribe-Romo, H. K. Chae, M. O'Keeffe and O. M. Yaghi. "Exceptional chemical and thermal stability of zeolitic imidazolate frameworks". *Proceedings of the National Academy of Sciences* 103.27 (2006), pp. 10186–10191.
- [15] H. Bux, A. Feldhoff, J. Cravillon, M. Wiebcke, Y.-S. Li and J. Caro. "Oriented zeolitic imidazolate framework-8 membrane with sharp H₂C₃H₈ molecular sieve separation". *Chemistry of Materials* 23.8 (2011), pp. 2262–2269.
- [16] T. Li, Y. Pan, K.-V. Peinemann and Z. Lai. "Carbon dioxide selective mixed matrix composite membrane containing ZIF-7 nano-fillers". *Journal of Membrane Science* 425-426 (2013), pp. 235–242.
- [17] J. Caro. "Hierarchy in inorganic membranes." *Chemical Society reviews* 45 12 (2016), pp. 3468–78.
- [18] Y.-S. Li, F.-Y. Liang, H. Bux, A. Feldhoff, W.-S. Yang and J. Caro. "Molecular sieve membrane: supported metal-organic framework with high hydrogen selectivity". *Angewandte Chemie* 122.3 (2010), pp. 558–561.
- [19] T. W. Pechar, S. Kim, B. Vaughan, E. Marand, M. Tsapatsis, H. K. Jeong and C. J. Cornelius. "Fabrication and characterization of polyimide-zeolite L mixed matrix membranes for gas separations". *Journal of Membrane Science* 277 (2006), pp. 195–202.
- [20] Y. Li, T. Chung, C. Cao and S. Kulprathipanja. "The effects of polymer chain rigidification, zeolite pore size and pore blockage on polyethersulfone (PES)-zeolite A mixed matrix membranes". *Journal of Membrane Science* 260.1-2 (2005), pp. 45–55.
- [21] Y. Li, T.-S. Chung, Z. Huang and S. Kulprathipanja. "Dual-layer polyethersulfone (PES)/BTDA-TDI/MDI co-polyimide (P84) hollow fiber membranes with a submicron PES-zeolite beta mixed matrix dense-selective layer for gas separation". *Journal of Membrane Science* 277 (2006), pp. 28–37.
- [22] T. M. Gur. "Permselectivity of zeolite filled polysulfone gas separation membranes". *Journal of Membrane Science* 93.3 (1994), pp. 283–289.
- [23] H. H. Yong, H. C. Park, Y. S. Kang, J. Won and W. N. Kim. "Zeolite-filled polyimide membrane containing 2,4,6-triaminopyrimidine". *Journal of Membrane Science* 188 (2001), pp. 151–163.

- [24] R. Mahajan, R. Burns, M. Schaeffer and W. J. Koros. “Challenges in forming successful mixed matrix membranes with rigid polymeric materials”. *Journal of Applied Polymer Science* 86.4 (2002), pp. 881–890.
- [25] Y.-R. Lee, M.-S. Jang, H.-Y. Cho, H.-J. Kwon, S. Kim and W.-S. Ahn. “ZIF-8: A comparison of synthesis methods”. *Chemical Engineering Journal* 271 (2015), pp. 276–280.
- [26] E. Perez, C. Karunaweera, I. Musselman, K. Balkus and J. Ferraris. “Origins and Evolution of Inorganic-Based and MOF-Based Mixed-Matrix Membranes for Gas Separations”. *Processes* 4.3 (2016), p. 32.
- [27] Z. Zhang, S. Xian, Q. Xia, H. Wang, Z. Li and J. Li. “Enhancement of CO₂ adsorption and CO₂/N₂ selectivity on ZIF-8 via postsynthetic modification”. *AIChE Journal* 59.6 (2013), pp. 2195–2206.
- [28] T. D. Bennett, A. L. Goodwin, M. T. Dove, D. A. Keen, M. G. Tucker, E. R. Barney, A. K. Soper, E. G. Bithell, J.-C. Tan and A. K. Cheetham. “Structure and properties of an amorphous metal-organic framework”. *Physical review letters* 104.11 (2010), p. 115503.
- [29] J. M. Thomas and L. A. Bursill. “Amorphous Zeolites”. *Angewandte Chemie International Edition* 19.9 (1980), pp. 745–746.
- [30] C. Orellana-Tavra, E. F. Baxter, T. Tian, T. D. Bennett, N. K. Slater, A. K. Cheetham and D. Fairen-Jimenez. “Amorphous metal-organic frameworks for drug delivery”. *Chemical Communications* 51.73 (2015), pp. 13878–13881.
- [31] P. Horcajada, C. Serre, M. Vallet-Regi, M. Sebban, F. Taulelle and G. Férey. “Metal-organic frameworks as efficient materials for drug delivery”. *Angewandte chemie* 118.36 (2006), pp. 6120–6124.
- [32] T. D. Bennett, P. J. Saines, D. A. Keen, J.-C. Tan and A. K. Cheetham. “Ball-Milling-Induced Amorphization of Zeolitic Imidazolate Frameworks (ZIFs) for the Irreversible Trapping of Iodine”. *Chemistry-A European Journal* 19.22 (2013), pp. 7049–7055.
- [33] K. W. Chapman, D. F. Sava, G. J. Halder, P. J. Chupas and T. M. Nenoff. “Trapping guests within a nanoporous metal-organic framework through pressure-induced amorphization”. *Journal of the American Chemical Society* 133.46 (2011), pp. 18583–18585.
- [34] M. J. C. Ordoñez, K. J. Balkus Jr., J. P. Ferraris and I. H. Musselman. “Molecular sieving realized with ZIF-8/Matrimid® mixed-matrix membranes”. *Journal of Membrane Science* 361.1-2 (2010), pp. 28–37.

- [35] S. Cao, T. D. Bennett, D. A. Keen, A. L. Goodwin and A. K. Cheetham. “Amorphization of the prototypical zeolitic imidazolate framework ZIF-8 by ball-milling”. *Chemical Communications* 48.63 (2012), pp. 7805–7807.
- [36] HyperSpy. <HyperSpy, <https://zenodo.org/record/28025>>. 2017.
- [37] S. Sridhar, R. Veerapur, M. Patil, K. Gudasi and T. Aminabhavi. “Matrimid polyimide membranes for the separation of carbon dioxide from methane”. *Journal of applied polymer science* 106.3 (2007), pp. 1585–1594.
- [38] S.-i. Kuroda and I. Mita. “Degradation of aromatic polymers—II. The crosslinking during thermal and thermo-oxidative degradation of a polyimide”. *European Polymer Journal* 25.6 (1989), pp. 611–620.
- [39] V. Kholodovych and W. J. Welsh. *Thermal-Oxidative stability and degradation of polymers*. Springer, 2007, pp. 927–938.
- [40] R. Jewell and G. Sykes. *Chemistry and Properties of Crosslinked Polymers*. 1977, p. 97.
- [41] G. Tillet, B. Boutevin and B. Ameduri. “Chemical reactions of polymer crosslinking and post-crosslinking at room and medium temperature”. *Progress in Polymer Science* 36.2 (2011), pp. 191–217.
- [42] P. S. Tin, T. S. Chung, Y. Liu, R. Wanc, S. L. Liu and K. P. Pramoda. “Effects of cross-linking modification on gas separation performance of Matrimid membranes”. *Journal of Membrane Science* 225 (2003), pp. 77–90.
- [43] J. E. Bachman and J. R. Long. “Plasticization-resistant Ni₂(dobdc)/polyimide composite membranes for the removal of CO₂ from natural gas”. *Energy Environ. Sci.* 9.6 (2016), pp. 2031–2036.
- [44] J. E. Bachman, Z. P. Smith, T. Li, T. Xu and J. R. Long. “Enhanced ethylene separation and plasticization resistance in polymer membranes incorporating metal-organic framework nanocrystals”. *Nature materials* 15.8 (2016), pp. 845–849.
- [45] T. Ishiwata, Y. Furukawa, K. Sugikawa, K. Kokado and K. Sada. “Transformation of Metal–Organic Framework to Polymer Gel by Cross-Linking the Organic Ligands Preorganized in Metal–Organic Framework”. *Journal of the American Chemical Society* 135.14 (2013), pp. 5427–5432.
- [46] T. Friscic, I. Halasz, P. J. Beldon, A. M. Belenguer, F. Adams, S. A. Kimber, V. Honkimaki and R. E. Dinnebier. “Real-time and in situ monitoring of mechanochemical milling reactions”. *Nature chemistry* 5.1 (2013), pp. 66–73.

- [47] A. D. Katsenis, A. Puskaric, V. Strukil, C. Mottillo, P. A. Julien, K. Uzarevic, M.-H. Pham, T.-O. Do, S. A. Kimber, P. Lazic et al. "In situ X-ray diffraction monitoring of a mechanochemical reaction reveals a unique topology metal-organic framework". *Nature communications* 6 (2015), p. 6662.
- [48] T. Lee, H. Kim, W. Cho, D.-Y. Han, M. Ridwan, C. W. Yoon, J. S. Lee, N. Choi, K.-S. Ha, A. C. Yip et al. "Thermosensitive structural changes and adsorption properties of zeolitic imidazolate framework-8 (ZIF-8)". *The Journal of Physical Chemistry C* 119.15 (2015), pp. 8226–8237.
- [49] A. Bos, I. Pünt, M. Wessling and H. Strathmann. "Plasticization-resistant glassy polyimide membranes for CO₂/CO₄ separations". *Separation and Purification Technology* 14.1 (1998), pp. 27–39.
- [50] Q. Song, S. Cao, R. H. Pritchard, B. Ghalei, S. A. Al-Muhtaseb, E. M. Terentjev, A. K. Cheetham and E. Sivaniah. "Controlled thermal oxidative crosslinking of polymers of intrinsic microporosity towards tunable molecular sieve membranes". *Nature communications* 5 (2014), p. 4813.
- [51] Y. Hu, Z. Liu, J. Xu, Y. Huang and Y. Song. "Evidence of pressure enhanced CO₂ storage in ZIF-8 probed by FTIR spectroscopy". *Journal of the American Chemical Society* 135.25 (2013), pp. 9287–9290.
- [52] A. B. Cairns and A. L. Goodwin. "Structural disorder in molecular framework materials". *Chemical Society Reviews* 42.12 (2013), pp. 4881–4893.
- [53] J. A. Thompson, N. A. Brunelli, R. P. Lively, J. Johnson, C. W. Jones and S. Nair. "Tunable CO₂ adsorbents by mixed-linker synthesis and postsynthetic modification of zeolitic imidazolate frameworks". *The Journal of Physical Chemistry C* 117.16 (2013), pp. 8198–8207.
- [54] J. A. Thompson, J. T. Vaughn, N. A. Brunelli, W. J. Koros, C. W. Jones and S. Nair. "Mixed-linker zeolitic imidazolate framework mixed-matrix membranes for aggressive CO₂ separation from natural gas". *Microporous and Mesoporous Materials* 192 (2014), pp. 43–51.
- [55] R. Abedini, M. Omidkhah and F. Dorosti. "Highly permeable poly(4-methyl-1-pentyne)/NH₂-MIL-53(Al) mixed matrix membrane for CO₂/CH₄ separation". en. *RSC Advances* 4.69 (2014), p. 36522.
- [56] J. Verbeeck and G. Bertoni. "Model-based quantification of EELS: is standardless quantification possible?" *Microchimica Acta* 161.3 (2008), pp. 439–443.

- [57] T. Rodenas, I. Luz, G. Prieto, B. Seoane, H. Miro, A. Corma, F. Kapteijn, F. X. Llabres i Xamena and J. Gascon. "Metal-organic framework nanosheets in polymer composite materials for gas separation." *Nature materials* 14.1 (2015), pp. 48–55.
- [58] F. Dorosti, M. Omidkhah and R. Abedini. "Fabrication and characterization of Matrimid/MIL-53 mixed matrix membrane for CO₂/CH₄ separation". *Chemical Engineering Research and Design* 92.11 (2014), pp. 2439–2448.
- [59] S. Basu, A. Cano-Odena and I. F. Vankelecom. "Asymmetric Matrimid®/[Cu₃(BTC)₂] mixed-matrix membranes for gas separations". *Journal of membrane science* 362.1 (2010), pp. 478–487.
- [60] E. V. Perez, K. J. Balkus Jr., J. P. Ferraris and I. H. Musselman. "Mixed-matrix membranes containing MOF-5 for gas separations". *Journal of Membrane Science* 328.1-2 (2009), pp. 165–173.
- [61] T. Rodenas, M. Van Dalen, P. Serra-Crespo, F. Kapteijn and J. Gascon. "Mixed matrix membranes based on NH₂-functionalized MIL-type MOFs: Influence of structural and operational parameters on the CO₂/CH₄ separation performance". *Microporous and Mesoporous Materials* 192 (2013), pp. 35–42.
- [62] C. Duan, X. Jie, D. Liu, Y. Cao and Q. Yuan. "Post-treatment effect on gas separation property of mixed matrix membranes containing metal organic frameworks". *Journal of Membrane Science* 466 (2014), pp. 92–102.
- [63] M. Arjmandi and M. Pakizeh. "Mixed matrix membranes incorporated with cubic-MOF-5 for improved polyetherimide gas separation membranes: Theory and experiment". *Journal of Industrial and Engineering Chemistry* 20.5 (2014), pp. 3857–3868.
- [64] B. Seoane, V. Sebastian, C. Téllez and J. Coronas. "Crystallization in THF: the possibility of one-pot synthesis of mixed matrix membranes containing MOF MIL-68(Al)". *CrystEngComm* 68.Table 1 (2013), pp. 1–5.
- [65] O. G. Nik, X. Y. Chen and S. Kaliaguine. "Functionalized metal organic framework-polyimide mixed matrix membranes for CO₂/CH₄ separation". *Journal of Membrane Science* 414 (2012), pp. 48–61.
- [66] S. Hwang, W. S. Chi, S. J. Lee, S. H. Im, J. H. Kim and J. Kim. "Hollow ZIF-8 nanoparticles improve the permeability of mixed matrix membranes for CO₂/CH₄ gas separation". *Journal of Membrane Science* 480 (2015), pp. 11–19.

- [67] E. A. Feijani, H. Mahdavi and A. Tavasoli. “Poly(vinylidene fluoride) based mixed matrix membranes comprising metal organic frameworks for gas separation applications”. *Chemical Engineering Research and Design* 96 (2015), pp. 87–102.
- [68] L. Ge, W. Zhou, V. Rudolph and Z. Zhu. “Mixed matrix membranes incorporated with size-reduced Cu-BTC for improved gas separation”. *Journal of Materials Chemistry A* 1.21 (2013), p. 6350.
- [69] L. Hao, P. Li and T.-S. Chung. “PIM-1 as an organic filler to enhance the gas separation performance of Ultem polyetherimide”. *Journal of Membrane Science* 453 (2014), pp. 614–623.
- [70] P. Raymond, W. Koros and D. Paul. “Comparison of mixed and pure gas permeation characteristics for CO₂ and CH₄ in copolymers and blends containing methyl methacrylate units”. *Journal of Membrane Science* 77.1 (1993), pp. 49–57.
- [71] M. D. Guiver, G. P. Robertson, Y. Dai, F. Bilodeau, Y. S. Kang, K. J. Lee, J. Y. Jho and J. Won. “Structural characterization and gas-transport properties of brominated Matrimid polyimide”. *Journal of Polymer Science Part A: Polymer Chemistry* 40.23 (2002), pp. 4193–4204.
- [72] J. S. Chiou, Y. Maeda and D. R. Paul. “Gas permeation in polyethersulfone”. *Journal of Applied Polymer Science* 33.5 (1987), pp. 1823–1828.
- [73] Y. P. Handa, J. Roovers and P. Moulini. “Gas transport properties of substituted PEEKs”. *Journal of Polymer Science Part B: Polymer Physics* 35.14 (1997), pp. 2355–2362.
- [74] Y. Xiao, Y. Dai, T.-S. Chung and M. D. Guiver. “Effects of brominating matrimid polyimide on the physical and gas transport properties of derived carbon membranes”. *Macromolecules* 38.24 (2005), pp. 10042–10049.
- [75] J. Li, K. Nagai, T. Nakagawa and S. Wang. “Preparation of polyethylene glycol (PEG) and cellulose acetate (CA) blend membranes and their gas permeabilities”. *Journal of Applied Polymer Science* 58.9 (1995), pp. 1455–1463.
- [76] P. Tiemblo, J. Guzman, E. Riande, C. Mijangos and H. Reinecke. “The gas transport properties of PVC functionalized with mercapto pyridine groups”. *Macromolecules* 35.2 (2002), pp. 420–424.
- [77] K. Berean, J. Z. Ou, M. Nour, K. Latham, C. McSweeney, D. Paull, A. Halim, S. Kentish, C. M. Doherty, A. J. Hill and K. Kalantar-zadeh. “The effect of crosslinking temperature on the permeability of PDMS membranes: Evidence of extraordinary CO₂ and CH₄ gas permeation”. *Separation and Purification Technology* 122 (2014), pp. 96–104.

- [78] J. McHattie, W. Koros and D. Paul. "Gas transport properties of polysulphones: 1. Role of symmetry of methyl group placement on bisphenol rings". *Polymer* 32.5 (1991), pp. 840–850.
- [79] M. Hellums, W. Koros, G. Husk and D. Paul. "Fluorinated polycarbonates for gas separation applications". *Journal of Membrane Science* 46.1 (1989), pp. 93–112.
- [80] W.-J. Chen and C. R. Martin. "Gas-transport properties of sulfonated polystyrenes". *Journal of Membrane Science* 95.1 (1994), pp. 51–61.
- [81] G. Perego, A. Roggero, R. Sisto and C. Valentini. "Membranes for gas separation based on silylated polyphenylene oxide". *Journal of Membrane Science* 55.3 (1991), pp. 325–331.
- [82] X.-G. Li, I. Kresse, Z.-K. Xu and J. Springer. "Effect of temperature and pressure on gas transport in ethyl cellulose membrane". *Polymer* 42.16 (2001), pp. 6801–6810.
- [83] S. S. Hosseini and T. S. Chung. "Carbon membranes from blends of PBI and polyimides for N₂/CH₄ and CO₂/CH₄ separation and hydrogen purification". *Journal of Membrane Science* 328.1-2 (2009), pp. 174–185.

Chapter 4

Controlling the topological pore channels of NH₂-MIL-53(Al) via cross-linking with polymer chains for selective natural gas purification

Adapted and largely based on:

Aylin Kertik, Lik H. Wee, Kadir Sentosun, Sara Bals, Johan A. Martens, and Ivo F.J. Vankelecom, *Controlling the topological pore channels of NH₂-MIL-53 via cross-linking with polymer chains for selective natural gas purification*, submitted to Joule.

A.K. contributed by the design and conduction of experiments, data analysis, and writing. *L. H. W.* helped with data interpretation and writing, revised the paper. *K.S.* and *S.B.* conducted the TEM experiments and analysed the results. *J.A.M.* revised the paper. *I.F.J.V.* helped with the data interpretation, and revised the paper.

4.1 Abstract

The implementation of commercial polymeric membranes is limited by their permeability and selectivity trade-off and the insufficient thermal and chemical stability. In the previous chapters, we have shown an efficient method to prepare highly loaded MMMs, and to improve their performance by applying a detailed thermal treatment. The amorphisation of the MOF and cross-linking due to the heat treatment lead to the highest selectivities reported for MMMs with commercial polymers. Herein, we demonstrate a method to control the thermochemical reactions *in-situ*, to delicately fine-tune the topological pore channels of a breathing metal-organic framework (MOF), NH₂-MIL-53(Al) within the polymer matrix and their molecular sieving properties in order to achieve a separation performance reaching the state-of-the-art Robeson upper-bound of 2008 in CO₂/CH₄ separations. NH₂-MIL-53(Al) crystals are embedded in a commercial polyimide matrix and the mixed-matrix membranes (MMMs) are treated at elevated temperatures (350 °C) in air under control thermal conditions in order to trigger concurrent polymer-polymer and polymer-MOF cross-linking and simultaneously provide thermal protection for the embedded MOF. As a result, the MOF undergoes a transition from its narrow-pore form to large-pore form, supposably allowing the polymer chains to penetrate the pores and cross-link with the amino functions of the one-dimensional pore wall of NH₂-MIL-53(Al). The cross-linked MMMs containing networks of NH₂-MIL-53 with narrower channels offer remarkably enhanced thermal and chemical stability, enabling the material to discriminate between CO₂ and CH₄ gases achieving outstanding CO₂/CH₄ selectivities, marking a new milestone as new molecular sieve MOF-containing MMMs for challenging natural gas purification applications.

4.2 Introduction

Natural gas is an energy source favoured for its significantly lower carbon emissions compared to other fossil-fuels. Purification of natural gas is the largest industrial separation that involves the removal of contaminants such as hydrocarbons, H₂O, N₂, H₂S and CO₂ from CH₄.^[1,2] Also known as natural gas enrichment or sweetening, this operation has been active since the 1980's.^[2,3] Many natural gas wells are majorly contaminated by CO₂, which has to be removed, typically down to <2% prior to delivery to pipelines to minimise corrosion and increase calorific value.^[1] In 2015, natural gas accounted for 23.8% of global energy consumption.^[4] Therefore, efficient next-generation CO₂/CH₄ separations are becoming increasingly important for clean gaseous

fuel production.^[5] In the past decades and pushed by the global conversion from fossil fuels to renewable energy sources, biogas gained importance.^[6,7] The biogas upgrading market is in a stage of development and potential growth. In Europe, the number of biogas upgrading plants is estimated to grow by an annual rate of 10-20%.^[6] Biogas upgrading is an ideal candidate for membrane-based separations, with usually low flow rates and CO₂ contents that exceed 40%.^[6] As the main competitor, membrane technologies offer viable solutions to the drawbacks of adsorption which is a well-accepted technology that suffers from heavy investment and maintenance costs.^[1] Processing conditions, such as gas flow rate and total gas composition, also play a role in the choice of the preferred separation process. For example, for a gas mixture with high CO₂ concentration and relatively low flow, membrane processes will generally be more favourable.^[1] New gas separation equipment constitutes a market of about \$5 billion annually, where CO₂ separation membranes currently amount to less than 5% of this market only.^[1]

Among the membranes developed for natural gas purification, only polymeric membranes have been commercialised thanks to their processibility and mechanical stability.^[8,9] However, membranes with higher selectivity without productivity loss are still needed for continued market growth.^[9] In the US, e.g. almost half of the natural gas reserves are not explored due to high treatment costs,^[9] but these resources could be made available with the help of appropriate membranes. Currently, the typical CO₂/CH₄ selectivity available in industrial separations is in the range of 10-20.^[1] There is a permeability-selectivity trade-off for polymeric membranes, as illustrated by the Robeson upper-bound.^[10,11] Usually, membranes that approach or surpass the upper-bound can be considered to have commercial potential. Another challenge relates to plasticisation where polymers lose separation power at high partial pressures. Where natural gas purification is concerned, CO₂ will swell the polymer and ease the permeation of CH₄ to reduce selectivities.^[8] Membrane cross-linking has been suggested to overcome this drawback.^[12-14]

Inorganic membranes offer excellent plastic stability and superior molecular sieving but severe problems with defect-free membrane formation currently impedes their application on a wider scale.^[15] Membranes based on carbon molecular sieves and thermally rearranged polymers show high separation properties, but are brittle and susceptible to defects.^[8,15] Mixed-matrix membranes (MMMs) are composite materials that consist of filler particles homogeneously dispersed in a polymeric matrix have been attractive alternatives since their discovery in the 1970s.^[16] MMMs have the aim of combining the processibility of polymers and the superior separation properties of porous fillers.

Metal-organic frameworks (MOFs) are hybrid inorganic-organic crystalline

porous materials which have attracted considerable attention owing to their tailorable functionality, well-defined pore size, pore tunability and breathing effects.^[17] MOFs emerged as promising filler alternatives to conventional inorganic porous solids thanks to their excellent filler-polymer compatibility.^[18] Breathing of MOFs refers to a double structural transition related to pore flexibility^[19]: it is the reversible opening or contraction of pores upon adsorption of guest molecules.^[19,20] MIL-53 is one of the best representatives of the “breathing” MOFs.^[21] It is constructed from MO₄(OH)₂ octahedra (M=Fe³⁺, Cr³⁺, Al³⁺ or Ga³⁺) and terephthalate linkers, exhibiting the unique transition of large-pore (*lp*) to narrow-pore (*np*) forms upon adsorption/desorption of several gases.^[21–33] The breathing MIL-53 framework is well known for its unusually high selectivity for CO₂ adsorption over CH₄ via the quadrupole moment interaction of CO₂ with the corner-sharing hydroxyl groups of the MIL-53 pore wall.^[22,34–37] A similar topology but with amine-functionalisation was made by simple replacement of terephthalic acid by 2-aminoterephthalic acid.^[38–40] NH₂-MIL-53(Al) (Figure 4.1) has 1-D diamond-shaped channels with a pore diameter of 7.5 Å and with amino groups that point inwards to the pore.^[39] Unlike many amino-functionalised materials, NH₂-MIL-53(Al) does not form a chemical bond between CO₂ molecules and the NH₂ groups. Instead, the amino functions regulate the breathing behaviour, resulting in excellent separation power for CO₂ and CH₄ under very mild conditions.^[22]

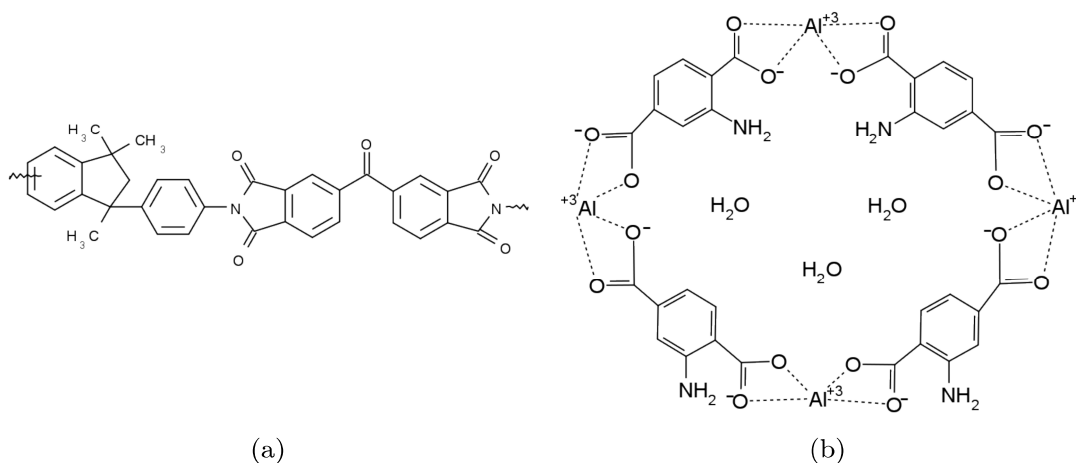


Figure 4.1: The chemical structure of (a) Matrimid® and (b) NH₂-MIL-53(Al).

Outstanding results have been recently reported using CuBDC nanosheets^[41] or Ni₂(dobdc) nanocrystals^[6] as MOF filler for CO₂/CH₄ membrane separations. Despite extensive effort, however, the obtained data sets representing the trade-off between permeability and selectivity obtained from hundreds of MOF-loaded MMMs for CO₂/CH₄ separations are restricted by the upper-bound trade-off

between CO₂ permeability and CO₂/CH₄ selectivity. It was reported that the separation of CO₂ from CH₄ over FDA-DAM MMMs containing NH₂-MIL-53(Al) nanoparticles could fall close to the Robeson limit of 2008 but only at relatively low pressure (3 bar).^[42] Bulk NH₂-MIL-53(Al) has shown to possess high selectivity in CO₂/CH₄ separation, but failed to reach the Robeson upper bound in MMM-based separation of CO₂/CH₄. This is mainly due to its open pore configuration upon solvent removal via uncurbed solvent evaporation during MMM preparation. These results highlight the challenge of translating MOF breathing properties to the field of MMMs.^[43]

In the previous chapter, we have reported in-situ, thermally induced amorphisation of ZIF-8 in the Matrimid® matrix which simultaneously triggers amorphous ZIF-8-polymer and polymer-polymer cross-linking. This new hybrid amorphous cross-linked composite membranes show outstanding performances in the selective separation of CO₂/CH₄ mixed gas.^[44] In this work, the MOF breathing effects are fully exploited by maintaining the large-pore structure via a controlled thermal treatment of the MMM at 350°C in air. In addition, simultaneous *in-situ* polymer cross-linking takes place in the membrane matrix at elevated temperatures. The MOF transforms into its *lp* form during this treatment and the thermally enhanced polymer mobility allows penetration of the polymer chains into these pores where they link covalently to the amino functions in the *lp* cages of NH₂-MIL-53(Al) for effective control over the breathing phenomenon. Despite its irreversibly opened pores, the rigid large pore structure of NH₂-MIL-53(Al) anchored with polymer chains inside the pore shows remarkable selectivity in CO₂/CH₄ separation over NH₂-MIL-53(Al)@polyimide membranes, while permeabilities hardly drop with polymer penetration.

4.3 Experimental procedure

4.3.1 Materials

Commercially available polyimide (PI, Matrimid®5218,4.1) was kindly provided by Huntsman and used after drying at 110 °C overnight. For NH₂-MIL-53(Al) synthesis, the linker source 2-aminoterephthalic acid (H₂BDC, H₂NC₆H₃-1,4-(CO₂H)₂, 99+%) and the Al source aluminum nitrate nonahydrate (Al(NO₃·9H₂O, 98.5+%) were obtained from ChemLab and Acros Organics, respectively, and used without further treatment. The solvents used in the solvent exchange and membrane preparation were dimethylformamide (99+%), chloroform (99.8%), and methanol (99.8%), purchased from Acros Organics.

4.3.2 Synthesis of NH₂-MIL-53(Al) nanoparticles

NH₂-MIL-53(Al) was synthesised by dissolving H₂BDC (2 g) and Al(NO₃)₃·9H₂O (2 g) in distilled water (400 mL). The solution was heated to 100 °C for 6 hours. Upon cooling, the MOF particles were centrifuged and washed with DMF, methanol and chloroform, respectively. The MOF sludge collected after the final centrifugation step was re-distributed in CHCl₃ and stored as such.

4.3.3 Fabrication of PI-NH₂-MIL-53(Al)- MMMs

MMMs of 20, 30 and 40 wt.% were prepared for this work. An amount of the MOF mixture with known MOF content was weighed, and the Matrimid® (dried overnight at 110 °C) was dissolved in this mixture. The polymer concentration was adjusted to 7 wt.% to obtain a reasonably viscous solution that can still be cast and will not suffer from MOF precipitation upon casting. The final mixture was given enough time for the polymer to fully dissolve. As proof of the effectiveness of our membrane fabrication method, extra mixing elements, such as ultrasonication, were not needed to obtain perfect MOF distribution. The MOF loading was calculated as given in Equation 4.1:

$$Loading(wt.%) = 100 * \frac{wt_{MOF}}{(wt_{MOF} + wt_{polymer})} \quad (4.1)$$

where wt_{MOF} and $wt_{polymer}$ are amounts of MOF and polymer, respectively. The membrane solution was cast into specially designed petri dishes that consist of glass rings attached to flat glass surfaces to ensure uniform membrane thickness. The cast solution was allowed to dry overnight at room temperature in N₂ atmosphere to prevent contact with the humidity of air. Upon vitrification, the membrane was carefully removed from the petri dish, and placed in an oven for annealing.

The dried membranes were placed between glass supports to prevent curving and placed in an oven. The oven was heated to 100 °C (above the boiling point of CHCl₃), 160 °C (slightly above the boiling point of DMF), 250 °C (above the boiling points of CHCl₃ and DMF and below the T_g of Matrimid) or 350 °C (above the T_g of Matrimid), and the process was carried out in air. The heating process was designed as heating at 1 °C/min from room temperature to the final annealing temperature with 50 °C increments. At each increment, the oven was kept isothermally for 2 hours. The membranes remained at the final temperature for 24 hours, and were removed after the oven cooled down to room temperature naturally. Immediate quenching is known to cause the

formation of voids between the polymer and the filler due to the difference in the thermal expansion coefficients of the two materials.^[45] By allowing the MMMs to cool down naturally, the attachment between the polymer chains and the MOFs was protected.

4.3.4 Characterisation of membranes

Attenuated total reflectance Fourier transform infrared spectroscopy (ATR-FTIR) was conducted in air using a Varian 620 FT-IR imaging microscope with a Germanium crystal. The samples were analysed over a wavelength range from 400 to 4000 cm^{-1} with a spectral resolution of 4 cm^{-1} and 64 scans.

The morphology of the membrane cross-sections was observed with a JEOL JSM-1060LV scanning electron microscope (SEM). The flexible membranes were freeze-fractured, and those that were already too brittle were broken in liquid N_2 . In order to prevent charge build-up due to the non-conductive nature of the polymers, the samples were sputtered with Au/Pd for three cycles of 20 seconds.

X-ray diffraction (XRD) patterns of MOF particles and membranes were obtained by using a Stoe-HT X-ray diffractometer, with $\text{CuK}\alpha$ radiation, $\lambda=1.54$ Å at room temperature. The mechanical strength tests were conducted at room temperature using a Universal Testsystem (UTS) with 0.0001 mm position resolution and load cells up to 200 N. Differential scanning calorimetry (DSC) measurements were carried out using a TA Instruments DSC Q2000 using Al hermetic closed pans and in N_2 atmosphere. The samples were first kept isothermally at 20 °C for 10 minutes, then heated to 370 °C for with a heating rate of 10 °C/minute. After 5 minutes, the samples were cooled down 20 °C at 10 °C/minute, and re-heated to 370 °C using the previously described method.

The thermogravimetric behaviour of the MOFs and membranes was analysed with TA Instruments TGA-Q500. The samples were heated from room temperature with a heating rate of 5 °C/min up to 100 °C, kept isothermally for 10 minutes, then with 2 °C/min up to 160 °C, and remained at 160 °C for 10 minutes, and finally with 10 °C/min to 500 °C under N_2 or O_2 .

TEM samples were prepared by gluing the sample on a support to fit the holder of the microtome. Since the matrix of the sample consists of polymeric membrane, embedding in an epoxy resin was not necessary. Next, slices with a thickness of 100 nm were cut using a Leica UC7 ultramicrotome equipped with a histo diamond knife. Selected area electron diffraction (SAED) patterns, high resolution TEM (HRTEM) and high angle annular dark field scanning TEM (HAADF-STEM) images were acquired using a FEI Osiris microscope, operated

at 200 kV. Acquisition of energy dispersive X-ray spectroscopy (EDX) maps was performed using a ChemiSTEM system, whereas the analysis was carried out using the Bruker ESPRIT software.

Gas separation measurements

The gas separation performance of membranes for binary gas mixtures was tested using a custom-built, high-throughput gas separation system (HTGS), described in detail in ref.^[46]. The membranes were tested with a 50-50 vol% CO₂/CH₄ mixture at 35°C and 10 bar cross-membrane pressure difference. The composition of the permeate side was measured by gas chromatography (GC). The membranes were first allowed to reach steady-state overnight while flushing with gas. Steady-state was confirmed when consecutive GC measurements gave the same result. Then three more measurements were taken and their average was reported. Each final data point reported is an average of two membranes, and two coupons from each membrane. The permeabilities were measured at steady-state using a constant-volume variable-pressure permeation system. The overall permeability (P_o) and the relative permeability of CO₂ (P_{CO_2}) was calculated using Equations 4.2 and 4.3, respectively.

$$P_o = \frac{\alpha V l}{A R T \Delta P} \quad (4.2)$$

where α is the rate of pressure increase in the downstream with respect to time, V is the downstream volume, l is the membrane thickness, A is the membrane surface area, R is the ideal gas constant, T is the permeation temperature, and ΔP is the cross-membrane pressure difference.

$$P_{CO_2} = P_o \frac{y_{CO_2}}{x_{CO_2}} \quad (4.3)$$

where P_o is the overall permeability, y_{CO_2} and x_{CO_2} denote the CO₂ content at the permeate and the feed side, respectively.

4.4 Results and discussion

The well-controlled thermal treatment at 350 °C induced a significant change in membrane colour, as shown in Figure 4.2. The PI membrane turned from yellow to dark-brown at 350 °C, whereas the MMMs started to darken at lower temperatures already. According to TGA (Figure 4.3), bulk NH₂-MIL-53(AL)

starts to decompose at 200 °C, whereas upon embedding in a Matrimid® matrix, the thermal stability of the NH₂-MIL-53(Al) is significantly improved.

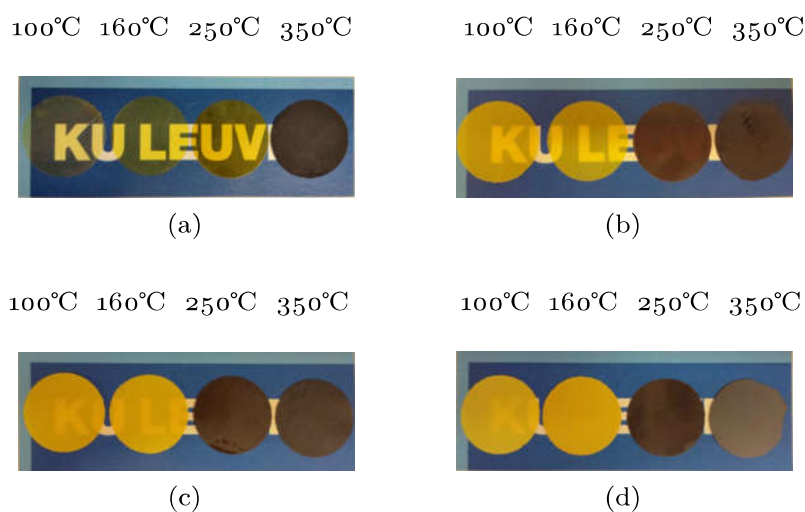


Figure 4.2: The change in colour of the (a) pure PI membranes and MMMs with (b) 20 wt.%, (c) 30 wt.% and (d) 40 wt.% MOF loading with increasing treatment temperature.

Solubility tests (Figure 4.4) showed that, after 2 days, the membranes treated at 160 °C were completely soluble in chloroform, while the MMMs treated at 250 or 350 °C were insoluble in chloroform, further confirming an important thermally-induced stability increase. The improved thermal and chemical stabilities indicate cross-linking of the polymer. In order to provide insight into the interactions between the polymer and the embedded MOF, the MMMs were characterised by ATR-FTIR (Figure 4.5).

Thermal cross-linking of Matrimid® in air involves free radical reactions. A loss in intensity of the characteristic bands corresponding to the aliphatic C-H stretching (2960 , 2927 and 2864 cm^{-1}) at elevated temperatures was observed (Figure 4.5). It was suggested that oxidative cross-linking of Matrimid® occurs through the C-H groups. A decrease at 823 cm^{-1} and increase at 1720 and 1606 cm^{-1} are now observed, which could be tentatively assigned to methyl and C=O oxidation, respectively, in line with increasing thermal treatment temperature (Figure 4.5).^[47] The methyl groups in the polyimide are oxidised to provide readily available $-\text{CH}_2$ radicals needed for oxidative cross-linking. The formation of hydroperoxide moieties involves a two-step reaction: (1) reaction of free radicals with O_2 to form peroxy radicals and (2) subsequent abstraction of a hydrogen from adjacent polymer chains. These unstable hydroperoxides will continue to propagate to initiate new free radical chain reactions until termination occurs. The thermally-induced oxidative cross-linking mechanism of the polymer due to the combination of radical sites on adjacent chains has

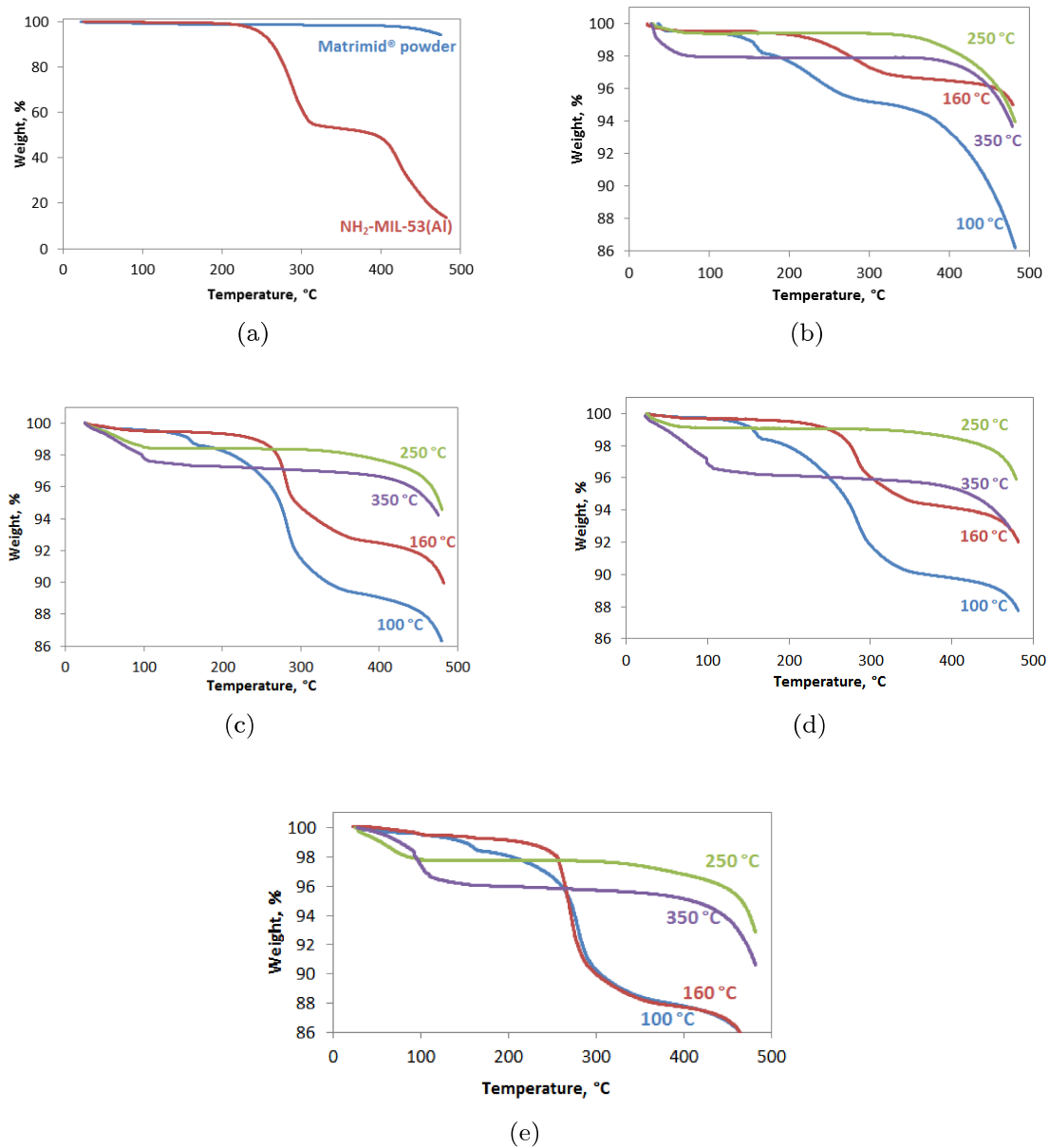


Figure 4.3: The TGA plots of (a) Matrimid® powder and Matrimid® -NH₂-MIL-53(Al), (b) Matrimid membranes, and MMMs with (c) 20 (d) 30 (e) 40 wt.% NH₂-MIL-53(Al) loading.

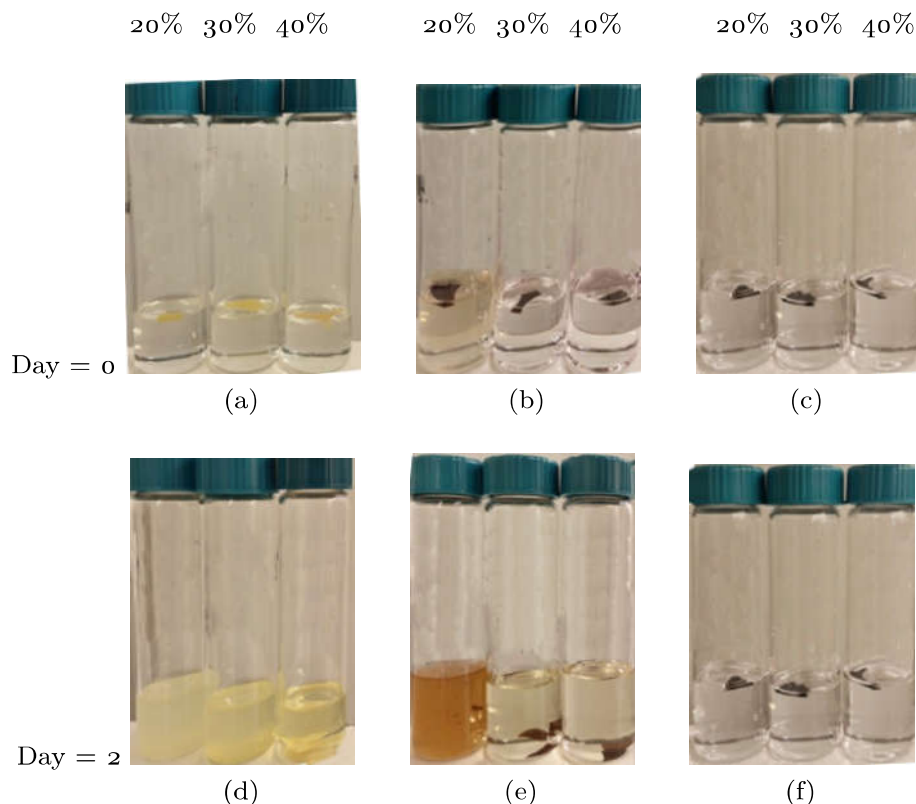


Figure 4.4: The solubility tests of MMMs treated at (a,d) 160 °C, (b,e) 250 °C, (c,f) 350 °C.

been previously described in detail.^[44] Interestingly, a chemical interaction between the polymer and the MOF crystal at the imide functionality was observed. The ATR-FTIR spectra of the MMMs are characterised by the imide group of Matrimid® (1720 cm^{-1}) attributed to symmetric stretching of C=O in the imide group as depicted in Figure 4.5.^[48,49] The intensity of this characteristic peak gradually decreased with increasing degree of cross-linking. An additional band at 1542 cm^{-1} , attributed to the aromatic N–H stretching band of the amide group, confirms the cross-linking of Matrimid® with the amino function grafted on the MOF pore walls. This was further supported by a gradual decrease of the primary amine groups characteristic adsorption bands at 3380 and 3494 cm^{-1} with increasing temperature. The cross-linking process is initiated by the attack of the imide functional groups of Matrimid® from the amino groups of the bridging terephthalates at the pore mouth and resulting in a cross-linked pore structure (Figure 4.6).

Cross-linking is known to restrict polymer chain mobility and increase rigidity. Reduced chain mobility was directly reflected in the Tg of the membranes.^[50] The Tg of the MMMs increased from 318 to 326, 328 and 337 °C with 20,

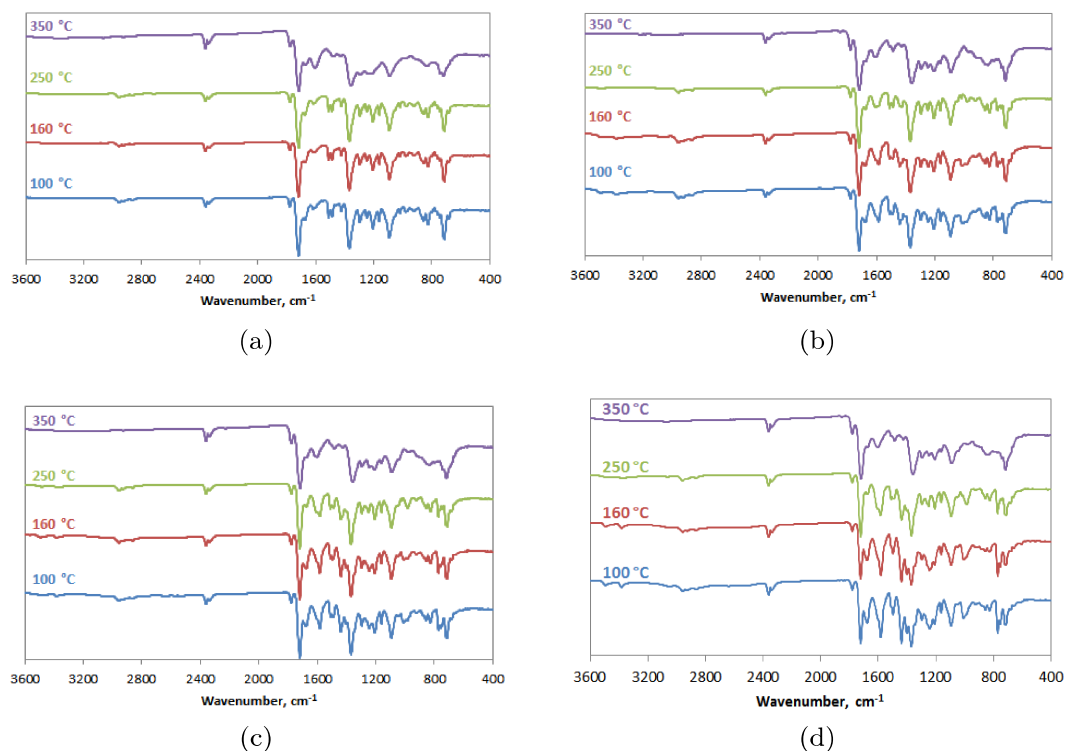


Figure 4.5: FTIR spectra of (a) Matrimid® and MMMs with (b) 20 wt.% (c) 30 wt.% (d) 40 wt.% NH₂-MIL-53(Al) loading.

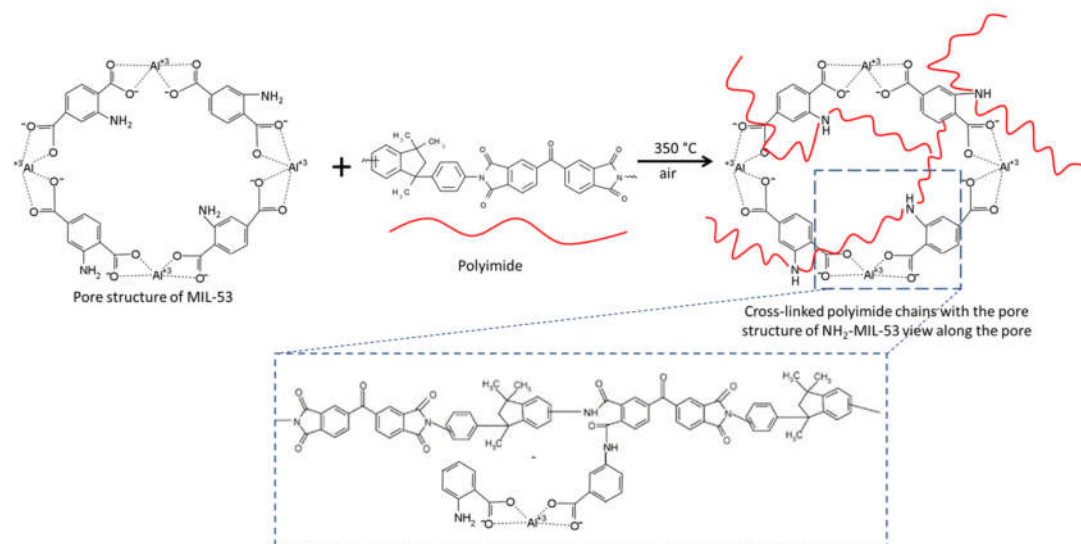


Figure 4.6: The proposed mechanism for cross-linking between the polymer and the NH₂-MIL-53(Al) upon annealing at 350 °C in air.

30 and 40 wt.% loading, respectively. Similarly, the tensile strength of the membranes evolved in line with cross-linking, as shown in the Table 4.1 and Figure 4.7.

Table 4.1: The tensile strength of unfilled Matrimid® and MMMs with 40 wt.% NH₂-MIL-53(Al).

Sample	Tensile strength (MPa)
Matrimid® treated at 100 °C (M100)	85.3
Matrimid® treated at 160 °C (M160)	101.8
Matrimid® treated at 250 °C (M250)	118.6
Matrimid® treated at 350 °C (M350)	135.2
MMM with 40 wt.% NH ₂ -MIL-53(Al), treated at 100 °C (MIL-40-100)	24.5
MMM with 40 wt.% NH ₂ -MIL-53(Al), treated at 160 °C (MIL-40-160)	27.5
MMM with 40 wt.% NH ₂ -MIL-53(Al), treated at 250 °C (MIL-40-250)	30.5
MMM with 40 wt.% NH ₂ -MIL-53(Al), treated at 350 °C (MIL-40-350)	32.7

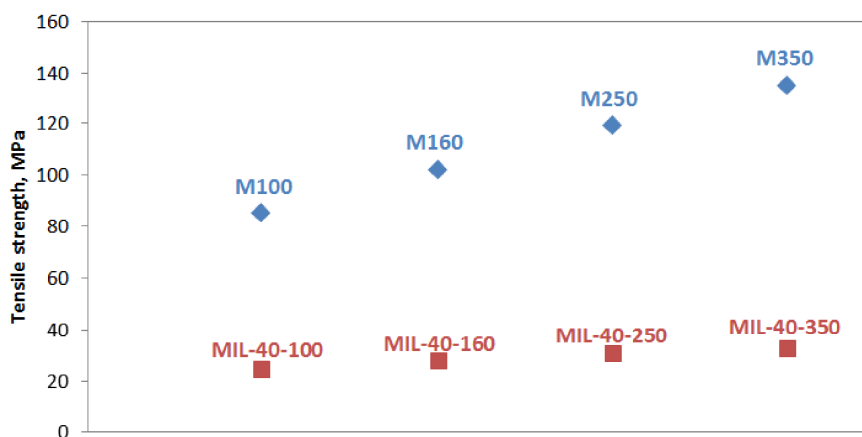


Figure 4.7: The evolution of the tensile strength of unfilled Matrimid® and MMMs with 40 wt.% NH₂-MIL-53(Al).

XRD diffractograms of the MMMs (Figure 4.8 and Figure 4.9,4.10,4.11) reveal that the structure of NH₂-MIL-53(Al) was preserved despite a sign of crystallinity loss observed at 350 °C. It was noted from the TG analyses that the MMMs treated at high temperatures (250 and 350 °C) exhibit an enhanced thermal stability up to 400 °C, whereas the MMMs annealed at lower temperatures (160 and 100 °C) start to decompose at 200 °C. Similar thermal behaviour was observed for bulk NH₂-MIL-53(Al). The results suggest that the thermal cross-linking significantly enhanced the thermal stability of the NH₂-MIL-53(Al) embedded in the polymer matrix. This observation was further confirmed by XRD, as shown in Figure 4.8, showing exclusively the *np* configuration for bulk NH₂-MIL-53(Al) and the MMMs treated at low temperature (100 and 160 °C). Interestingly, the embedded NH₂-MIL-53(Al)

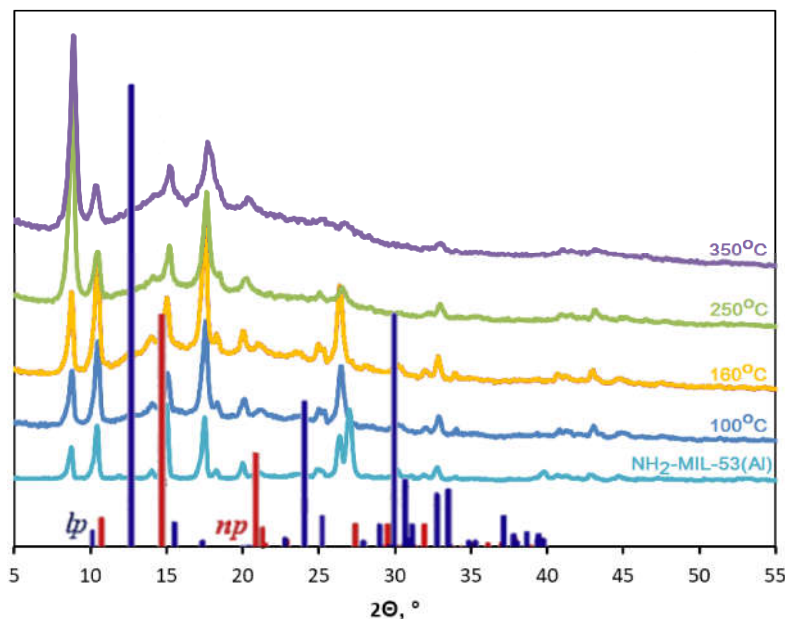


Figure 4.8: XRD diffractogram of MMMs with 40 wt.% NH₂-MIL-53(Al) loading. The dark blue and red lines refer to the simulated XRD diffractogram of the *lp* and *np* forms, respectively.^[55]

in the polymer matrix undergoes a transition from *np* form to *lp* form upon heating above 160 °C.^[51–53] Although this transition may normally occur due to the presence of penetrants, such as DMF^[53] or CO₂,^[54] in the MOF pores, the FTIR (Figure 4.5) and TGA results (Figure 4.3) however, confirm the absence of any adsorbed species: the lack of FTIR signals in the 1673–1690 cm⁻¹ range, assigned to the amide group of the DMF, indicates that the MOF was well-washed and solvent exchanged with methanol and chloroform. Moreover, the TGA plots do not exhibit any observable weight loss around the boiling point of DMF. The *np* form of NH₂-MIL-53(Al) is energetically preferred over the *lp* form. As the temperature increases to 250 and 350 °C, the expanded MOF framework configuration in the MMMs is retained as evidenced from the XRD diffractograms, mainly due to the partial penetration of polymer chains in the pore structure of the NH₂-MIL-53(Al), and cross-linking of the polymer with the amino functions on the pore walls, most probably occurs at the pore entrance only.

Interfacial voids in MMMs, created by polymer-filler detachment are detrimental to membrane selectivity.^[56] Figure 4.12 shows the cross-sectional SEM images of unfilled PI membranes and MMMs with 20, 30 and 40 wt.% loading. The unfilled PI membranes do not show observable change in morphology with increasing treatment temperature. With the present NH₂-MIL-53(Al)-Matrimid® system, the polymer and the MOF create a perfectly homogeneous

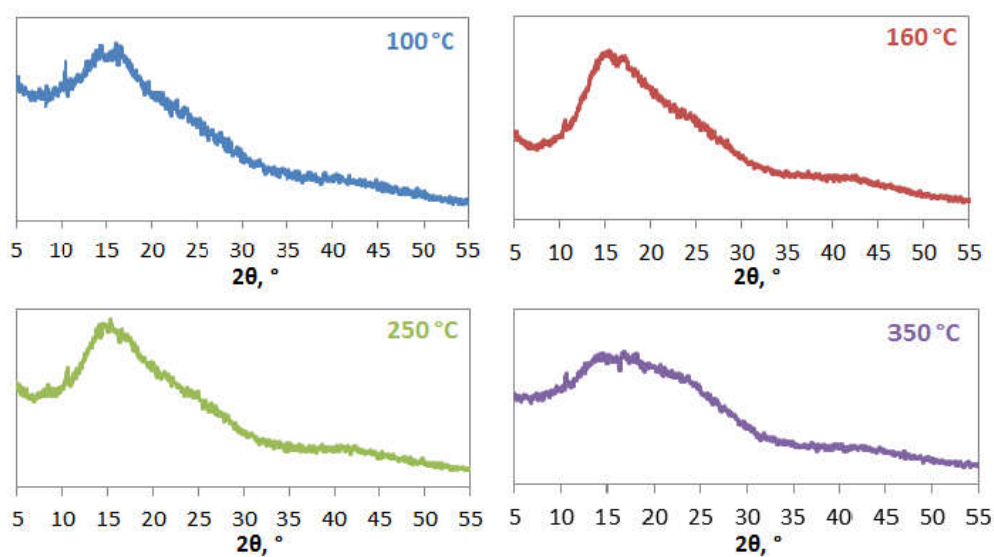


Figure 4.9: XRD diffractogram of Matrimid® membranes.

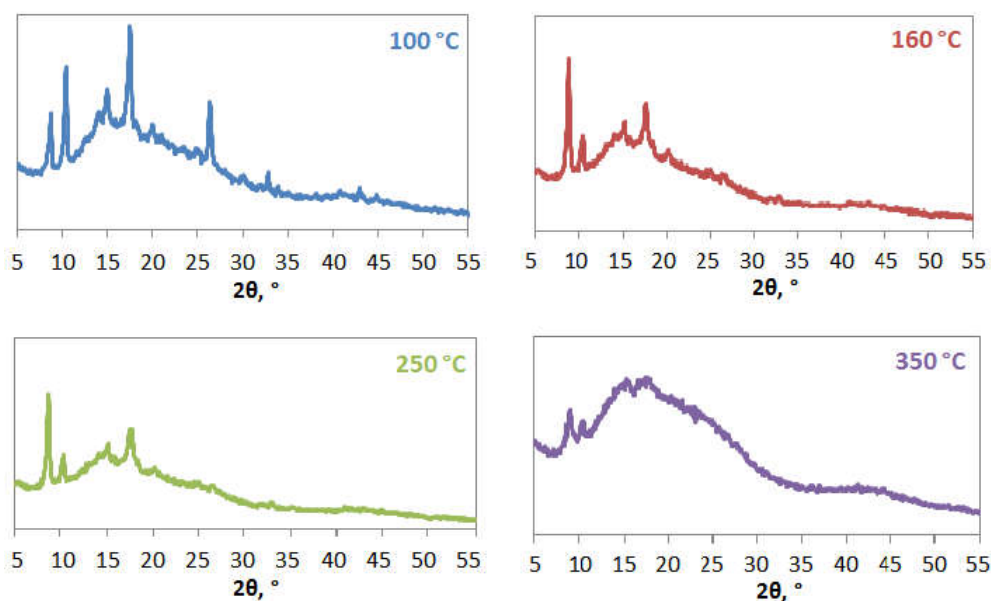


Figure 4.10: XRD diffractogram of MMMs with 20 wt.% $\text{NH}_2\text{-MIL-53(Al)}$ loading.

and defect-free morphology, even at high MOF loading. When the T_g of Matrimid® ($\approx 305^\circ\text{C}$) is surpassed,^[57] the polymer chains relax and become more mobile. Therefore, they interact and adhere to the surface of the MOF particles better, creating an increasingly homogeneous structure. By allowing the membranes to cool down naturally, this adhesion was protected.^[45]

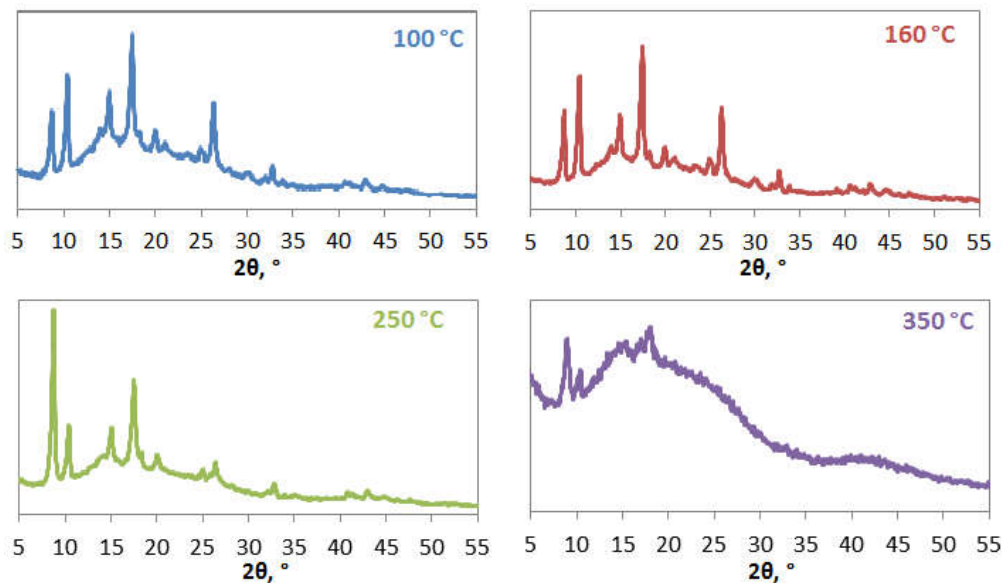


Figure 4.11: XRD diffractogram of MMMs with 30 wt.% NH₂-MIL-53(Al) loading.

A combination of high angle annular dark field scanning transmission electron microscopy (HAADF-STEM), selected area electron diffraction (SAED) and energy dispersive X-ray (EDX) analysis was performed to investigate the compatibility and crystallinity of embedded NH₂-MIL-53(Al) in the polymer matrix. The results reveal that the crystallinity of the incorporated NH₂-MIL-53(Al) is preserved as illustrated in Figure 4.13a. Since the structure and morphology of the nanoparticles change quickly under electron beam irradiation, a low dose electron beam was selected to record reliable diffraction data. Figure 4.13b displays an HRTEM micrograph acquired from a similar particle along the [001] zone axis. The measured d-values and diffraction angles from the SAED pattern are in strong agreement with the known orthorhombic (space group: Imma) structure model, as reported and in full agreement with the XRD results (Figure 4.8).^[58] An overview HAADF-STEM image depicting the morphology of the particles embedded inside the MMM is presented in Figure 4.13c which shows excellent compatibility at the interface between the NH₂-MIL-53(Al) particle and the polymer matrix. The blue arrows indicate a dark contrast at the interface between the particles and the MMM, mainly due to cutting artefacts during the sample preparation. The chemical distribution of the individual Al and O elements was visualised by EDX mapping (Figure 4.13d,e), confirming the presence of incorporated NH₂-MIL-53(Al) in the polymer matrix. The EDX map was acquired from the red highlighted region in Figure 4.13c.

Figure 4.14 and Table 4.2 show the mixed-gas permselectivity as a function

of the heat treatment temperature for unfilled Matrimid® and MMMs with different loadings. This work highlights the importance of the thermal treatment method in order to preserve the *np* form of $\text{NH}_2\text{-MIL-53(Al)}$ after membrane casting and thermal treatment at 100 and 160°C. Despite only a marginal gain in selectivity for MMMs with filler loadings from 20-40 wt.%, a relatively good selectivity ($\text{CO}_2/\text{CH}_4 = 40$) was achieved without sacrificing permeability at high filler loading (40 wt.%). It should be mentioned that the unfilled Matrimid® membranes only show a CO_2/CH_4 selectivity of about 22 under reported

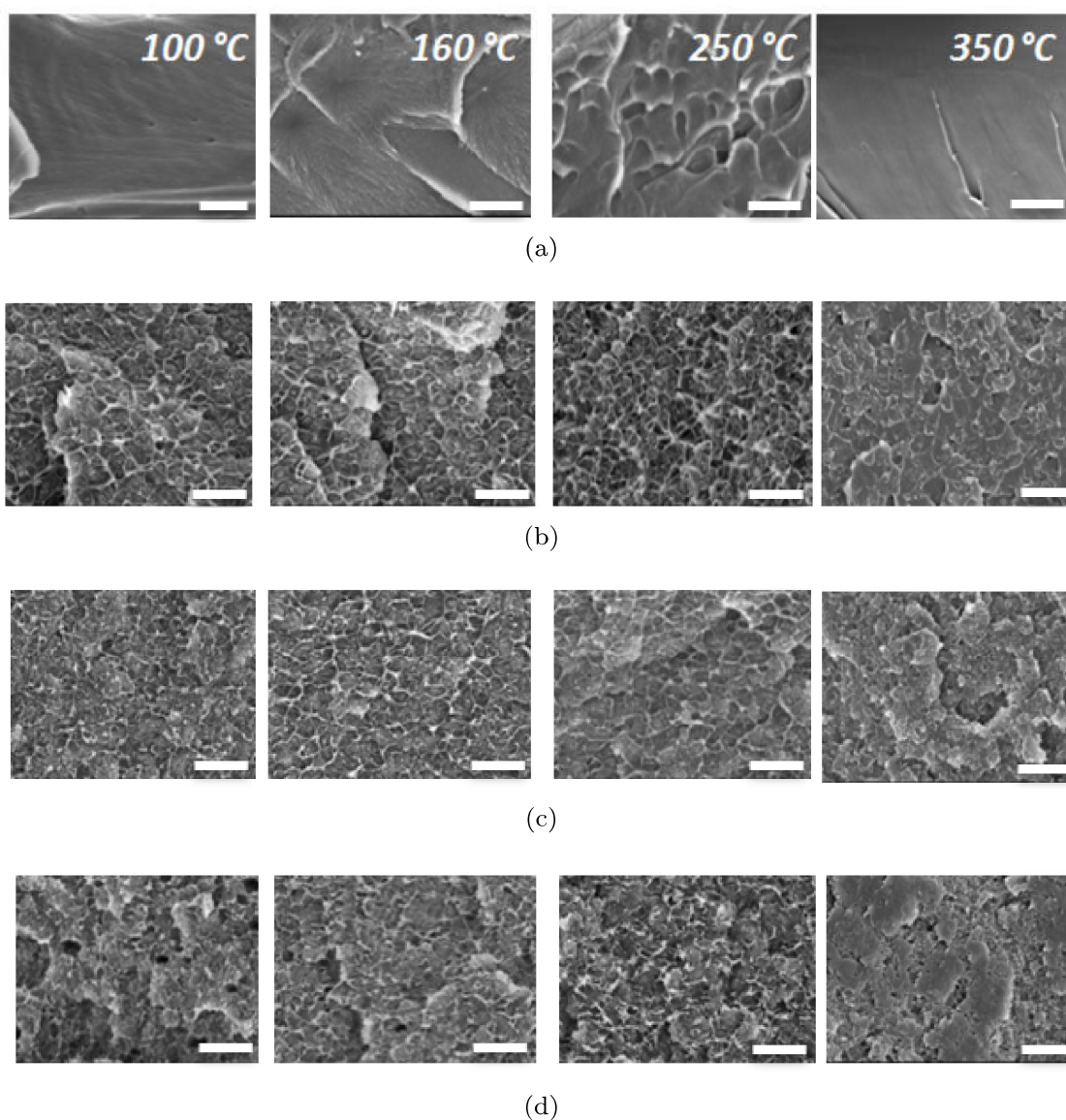


Figure 4.12: SEM images of (a) unfilled PI , and MMMs with (b) 20 wt.% , (c) 30 wt.% and 40 wt.% $\text{NH}_2\text{-MIL-53(Al)}$. Scale bars represent 5 μm.

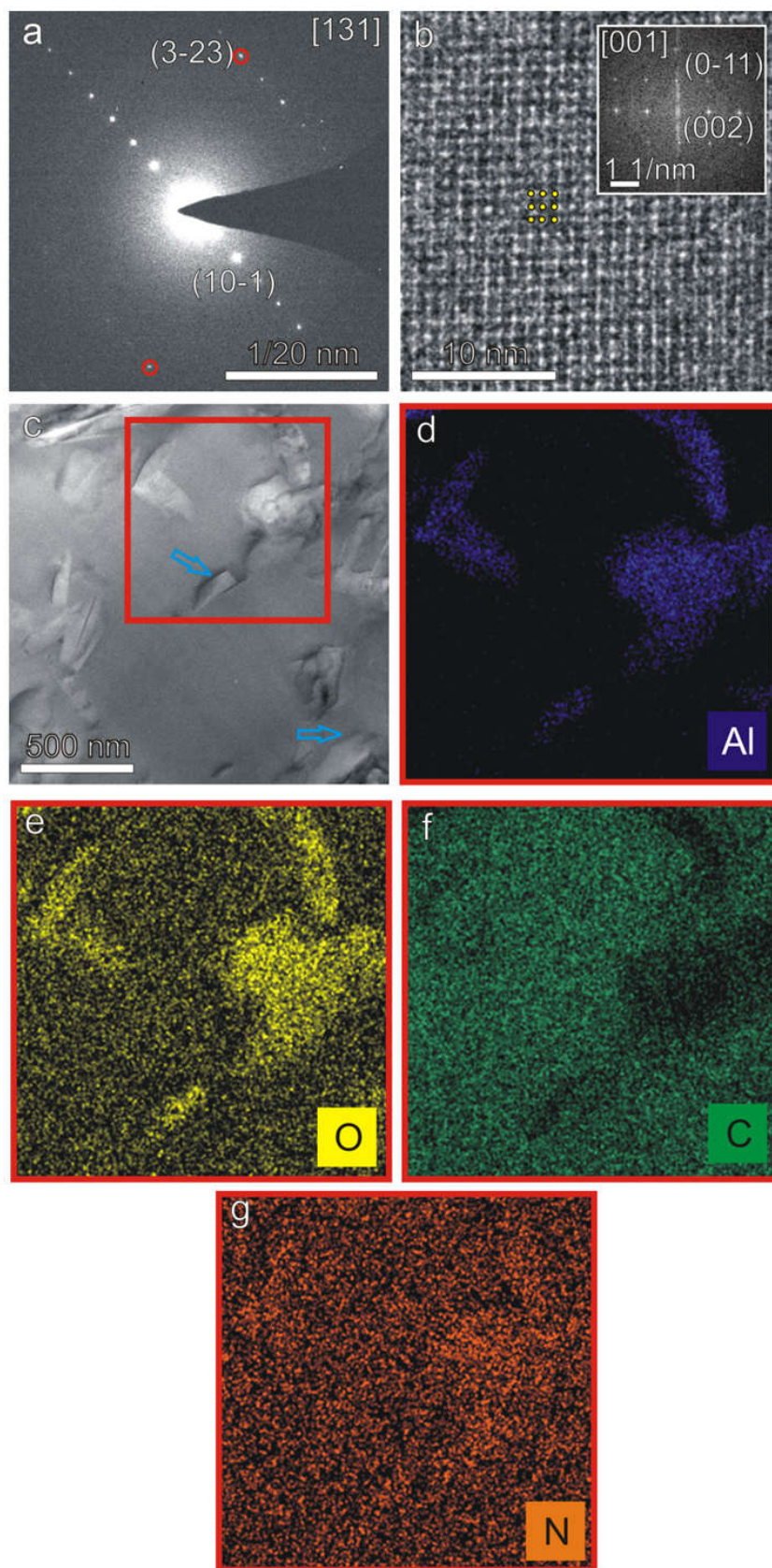


Figure 4.13: TEM characterisation of MMMs with 40 wt.% NH₂-MIL-53(Al) loading. (a) SAED pattern recorded along [131] zone axis from NH₂-MIL-53(Al) nanoparticle. (b) HRTEM micrograph and corresponding FFT pattern from a similar particle as in (a). (c) HAADF-STEM image displaying the morphology of NH₂-MIL-53(Al) particles embedded in a MMM. (d-e) EDX elemental maps of Al, O, C and N, respectively, obtained from the area shown in (c).

conditions (Table 4.2). The Matrimid® membranes showed an exponential increase in selectivity in line with increasing treatment temperature and filler loading (Figure 4.14a). A remarkable gain in selectivity ($\text{CO}_2/\text{CH}_4 = 154$) was observed for MMMs treated at $350\text{ }^\circ\text{C}$, while conserving high permeabilities (Figure 4.14d). The results suggest that a relatively high filler loading is required in order to gain the synergy effect from the incorporation of MOF crystals and cross-linking with the polymeric matrix. A major drawback for natural gas purification is the unpredictable loss in selectivity that is often encountered as a result of polymer swelling upon exposure to polarisable CO_2 gas at high pressures. The cross-linked MMMs with 40 wt.% MOF loading were therefore evaluated for their plasticisation resistance. The gas separation measurements performed at 40 bar feed pressure confirmed that the implemented post-synthesis treatment rendered the MMMs plasticisation resistant, with selectivities up to 139.

The pore diameter of $\text{NH}_2\text{-MIL-53(Al)}$ (7.5 \AA) is far larger than the kinetic diameters of CO_2 (3.3 \AA) and CH_4 (3.8 \AA),^[39] which is contradicting the outstanding selectivities achieved for the cross-linked MMMs with 40 wt.% filler loading. However, the selectivity increase can be ascribed to the partial pore blockage of the pores by the penetrated and cross-linked polymer chains.^[43,58] As indicated by the XRD diffractograms, the MOF undergoes an *np-to-lp* transition upon heating above $160\text{ }^\circ\text{C}$. When the polymer chains become more mobile at these high temperatures, they will penetrate the thermally-enlarged MOF pores and link to the amino functions on the *lp* pore walls, as to create effective molecular sieves by reducing the effective diameter of the pore entrance (Figure 4.6). Coupled with the simultaneous polymer-polymer cross-linking in the bulk of the membrane, a network that is sufficiently dense to hinder the permeation of CH_4 is thus formed, as illustrated by the small sacrifices in CO_2 permeability but exceptional improvement in selectivity. The limited reduction in CO_2 permeability is possibly realised thanks to the fact that only MOF pore entrances were made more selective, while the majority of the pores remained uncovered in the *lp* form. The Robeson upper-bound is a benchmark that states that membranes with high selectivity often exhibit low permeability and vice versa.^[10,11] It defines a performance limitation for traditional materials based on physical interaction and is often employed to characterise membrane performance.^[59] Figure 4.14e shows the CO_2/CH_4 selectivities and CO_2 permeabilities for the MMMs composed of $\text{NH}_2\text{-MIL-53(Al)}$ and also includes other MIL-53 loaded MMMs obtained from literature. A complete comparison of the separation performance of our MMMs, with all of reported MOF-loaded MMMs for CO_2/CH_4 separation is presented in Table 4.2. The MMM treated at $350\text{ }^\circ\text{C}$ with 40 wt.% loading achieved the highest mixed-gas selectivity (purple circles), and hit the 2008 upper-bound, clearly outperforming the unfilled Matrimid® membranes (blue diamonds) and $\text{NH}_2\text{-}$

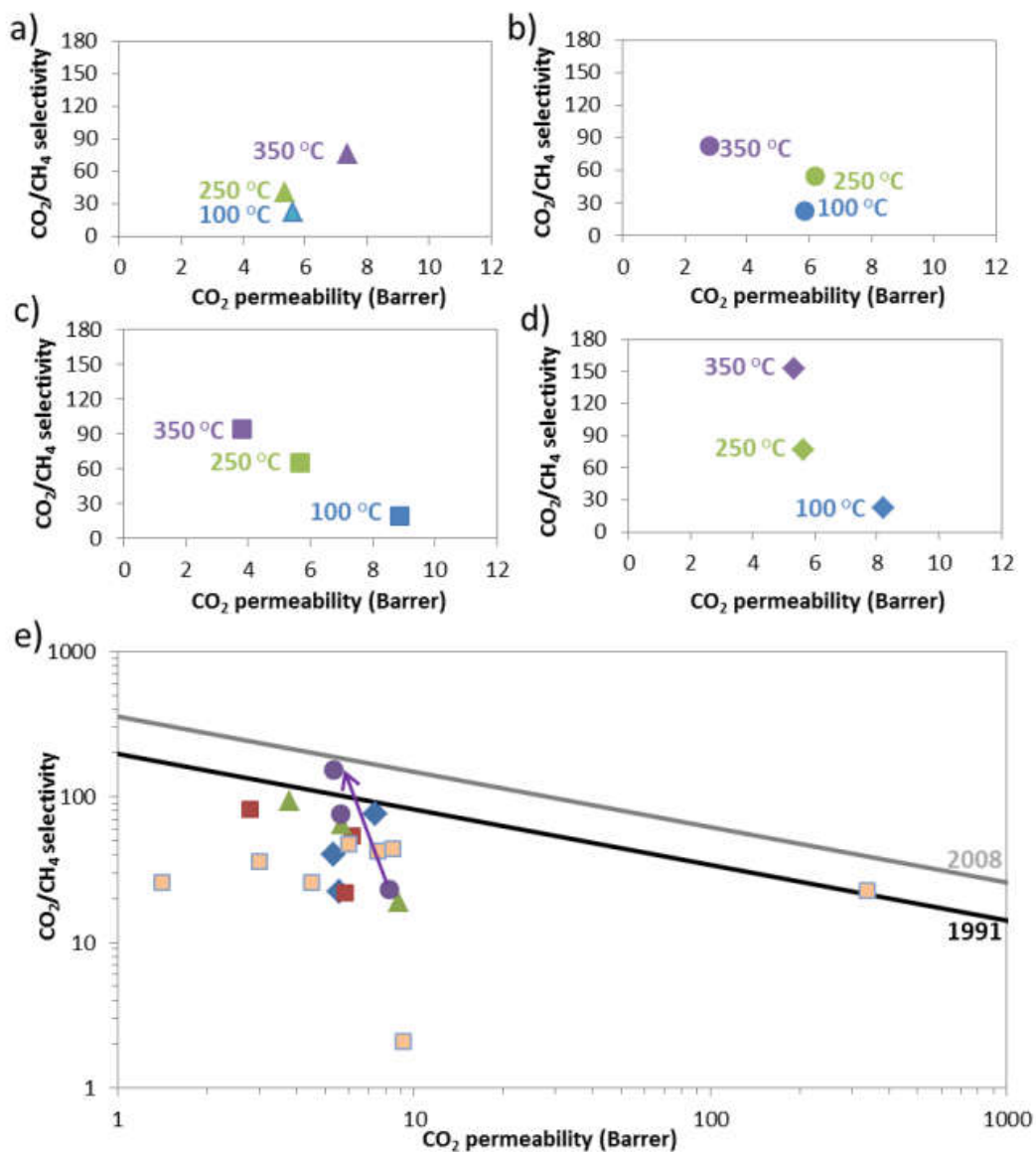


Figure 4.14: The evolution of the gas selectivity of the thermally treated membranes. (a) Matrimid® and (b-d) MMMs with 20, 30 and 40% NH₂-MIL-53(AL) loading with increasing annealing temperature. (e) The Robeson plot of 1991 and 2008 compared with the results from literature (orange squares), and results obtained from this work (blue diamonds: unfilled Matrimid, red squares: MMM with 20 wt.% loading, green triangle: MMM with 30 wt.% loading and purple circles: MMM with 40 wt.% loading). A fully detailed comparison of the performances of all MOF-loaded MMMs prepared for this work, with the measurement conditions is presented in Table 4.2.

MIL-53(Al)-loaded MMMs reported earlier (orange squares). These cross-linked MMMs also reached and surpassed the state-of-the-art separation performances of MOF-loaded MMMs with commercially available polymers for CO₂/CH₄ separations.

4.5 Conclusions

In summary, NH₂-MIL-53(Al) loaded MMMs with excellent MOF dispersion and polymer-MOF adhesion were prepared. Treatment at high temperatures created thermo-oxidative cross-linking of the Matrimid® matrix, as well as an interaction between the polymer and the -NH₂ groups on the MOF surface. The synergetic effect of polymeric thermal protection and cross-linking significantly improved the chemical and thermal stability of the embedded MOF as well as the MMMs. Upon thermal treatment, the MOF underwent configurational transition from its *np* to *lp* form, which allows the polymer chains to penetrate and cross-link to the amine groups at the entrance of the MOF pores to achieve the highest molecular sieving performance of CO₂ from CH₄, ever reported for MOF-loaded MMMs. Importantly, the cross-linked MMMs showed significant improvement in CO₂/CH₄ selectivity and resistance to plasticisation at high pressures of a binary feed mixture up to 40 bar. These cross-linked MMMs with enhanced plasticisation resistance show exciting potential for the purification of biogas and highly contaminated natural gas wells. This novel membrane type also potential for use in liquid and other gas phase petrochemical separations.

4.6 Acknowledgements

A. Kertik is grateful to the Erasmus Mundus Doctorate in Membrane Engineering (EUDIME) programme. L.H.W. thanks the FWO-Vlaanderen for a postdoctoral research fellowships under contract number 12M1415N. The authors would like to thank Methusalem and IAP-PAI for research funding. We are also grateful to Frank Mathijs (KU Leuven) for the mechanical tests, Bart Goderis and Olivier Verkinderen for the DSC measurements and Huntsman (Switzerland) for providing the Matrimid® polymer.

Table 4.2: Comparison of GS performance from this work with literature data from MMMs comprising commercial polymers.

Polymer	MOF	Loading, wt. %	Treatment	Measurement conditions	CO ₂ permeability, Barrer	CO ₂ /CH ₄ selectivity	Ref.
Poly(methyl methacrylate)	none	0	>T _g	5 atm, 35°C	0.35 ¹	60 ²	[60]
Matrimid	none	0	130°C, overnight, <i>in vacuo</i>	1 atm, 35°C	8.7	36.3	[61]
Poly(ether sulfone)	none	0	Compression molding, 300°C	10 atm, 35°C	2.8	28	[62]
PEEK	none	0	Tg+5	10 atm, 35°C	0.96 ³	31	[63]
Ultem	none	0	120 °C, 24 h, <i>in vacuo</i>	3.5 bar, 35 °C	1.48	37	[64]
Brominated Matrimid®	none	0	250°C, 48 h, <i>in vacuo</i>	10 atm, 35°C	13.3	30.2	[65]
5218 PI	none	0	150°C, 48 h, <i>in vacuo</i>	10 atm, 35°C	3.04	38	[66]
Cellulose acetate	none	0	120°C, 24 h, <i>in vacuo</i>	5 bar, 25°C	0.915	21.27	[67]
Poly(vinylidene fluoride)	none	0	Room temperature, 2 h, <i>in vacuo</i>	1 bar, 25°C	0.54	22.5	[68]
Poly(vinyl chloride)	none	0	75°C, 45 min, 25°C, 3 d	4 bar, 35°C	3970	4	[69]
PDMS	none	0	Tg+10, 2 d, <i>in vacuo</i>	10 atm, 35°C	5.6	22	[70]
Polysulfone	none	0	Tg+10, several days, <i>in vacuo</i>	10 atm, 35°C	6.8	18.9	[71]
Polycarbonate	none	0	85°C, 24 h	4.4 atm, 23°C	14.1	18.1	[72]
Polystyrene	none	0	3	1 atm, 35°C	82	12.8	[73]
PPO	none	0	25°C, 20 h, 60% relative humidity	2 bar, 25°C	67.7	11.1	[74]

Continued on next page

¹1 Barrer = [10⁻¹⁰ cm³ (STP) cm/(cm² s cmHg)]²For each reference, the best performance was listed.³Rate of permeation is reported as GPU, 1 GPU = [10⁻⁶ cm³ (STP)/(cm² scmHg)] = [3.35x10⁻¹⁰ mol/(m² sPa)]

Table 4.2 – continued from previous page

Polymer	MOF	Loading, wt. %	Treatment	Measurement conditions	CO ₂ permeability, Barrer	CO ₂ /CH ₄ selectivity	Ref.
Torlon	none	0	250 °C, overnight, <i>in vacuo</i>	10 atm, 35 °C	0.83	27.8	[75]
PSf (4.8 Barrer, 24) ⁴	NH ₂ -MIL-53(Al)	25	<i>in vacuo</i> , 383 K	1: 1 CO ₂ :CH ₄ , 308 K, ΔP= 3 bar	6	47	[76]
PVDF (0.9 Barrer, 21.3)	NH ₂ -MIL-53(Al)	10	<i>in vacuo</i> , 120 °C, 24 h	Pure gas, 298 K, 0.5 bar	1.406	26.03	[67]
PSf (5.3 Barrer, 23)	NH ₂ -MIL-53(Al)	20	<i>in vacuo</i> , 120 °C, 10 h	1:1 CO ₂ :CH ₄ , 35 °C(308 K), 3 bar	4.5	26	[55]
PI (9 Barrer, 37.5)	NH ₂ -MIL-53(Al)	20	<i>in vacuo</i> , 180 °C, 10 h	1:1 CO ₂ :CH ₄ , 35 °C(308 K), 3 bar	8.5	44	[55]
PMP (80 Barrer, 8.12)	NH ₂ -MIL-53(Al)	30	<i>in vacuo</i> , 50 °C, 12 h	10% CO ₂ , 30 °C, 8 bar	339.5	22.8	[77]
PI (6.2 Barrer, 28.5)	NH ₂ -MIL-53(Al)	15	<i>in vacuo</i> , 200 °C, 15 h	50:50 CO ₂ :CH ₄ , 35 °C, 150 psi	9.2	2.1	[78]
Ultem (1.46 Barrer, 31.6)	NH ₂ -MIL-53(Al)	15	<i>in vacuo</i> , 200 °C, 15 h	50:50 CO ₂ :CH ₄ , 35 °C, 150 psi	3	36.1	[78]
Matrimid® (8.2 Barrer, 37.5)	NH ₂ -MIL-53(Al)	16	<i>in vacuo</i> , 453 K, 24 h	50:50 CO ₂ :CH ₄ , 298 K, 3 bar	7.5	42	[42]
Matrimid® (9.55 Barrer, 34.5)	Ni ₂ (dobc)	23	<i>in vacuo</i> , 120 °C, 24 h	Pure gas, 308 K, 1 bar	9.31	29.5	[6]
Matrimid®	ZIF-8	20	180 °C, 18 h, <i>in vacuo</i>	4 bar, 22 °C	12.96	41.5	[79]
Matrimid®	ZIF-8	50 ⁵	240 °C, overnight, <i>in vacuo</i>	2 bar, 35 °C, 10 mol% CO ₂ /90 mol% CH ₄	6	89.15	[80]
Matrimid®	CuBDC (nanosheet)	8.2	180 °C, 12 h, <i>in vacuo</i>	7.5 bar, 25 °C, equimolar CO ₂ /CH ₄	2.78	88.2	[41]
Matrimid	Ni ₂ (dodbc)	23	120 °C, 24 h, <i>in vacuo</i>	10 bar, 35 °C, equimolar CO ₂ /CH ₄	14.7	32.5	[6]

Continued on next page

⁴The values next to polymer names correspond to the permeability/selectivity reported in the same reference.⁵Loading calculated as (wt. MOF)/(wt. polymer).⁶Not reported.

Table 4.2 – continued from previous page

Polymer	MOF	Loading, wt. %	Treatment	Measurement conditions	CO ₂ permeability, Barrer	CO ₂ /CH ₄ selectivity	Ref.
Matrimid®	MIL-53	15	80 °C, 24 h, 150°C, <i>in vacuo</i>	3 bar, 35 °C	12.43	51.8	[81]
Matrimid®	Cu-BTC	30	90 °C, 24 h	4 bar, 35 °C, 35 vol% CO ₂ /65 vol% CH ₄	176	23	[82]
Matrimid®	MOF-5	10	240 °C, 24 h, <i>in vacuo</i>	2 atm, 35 °C	11.10	51	[83]
Matrimid®	NH ₂ -MIL-53(Al)	25	180 °C, 10 h, <i>in vacuo</i>	3 bar, 0 °C, equimolar CO ₂ /CH ₄	107	3.9	[55]
Ultem	Cu-BTC	35	<i>in vacuo</i>	3.5 bar, 35 °C	4.1	34	[84]
PEI	Cubic-MOF-5	25	70 °C, 2 d, <i>in vacuo</i>	6 bar, 25 °C	5.39	23.43	[85]
PSf	NH ₂ -MIL-53(Al)	25	180 °C, 10 h, <i>in vacuo</i>	3 bar, 35 °C, equimolar CO ₂ /CH ₄	5.5	27.5	[55]
PSf	MIL-68(Al)	8	120 °C, 24 h, <i>in vacuo</i>	2 bar, 35 °C, equimolar CO ₂ /CH ₄	5.7	36.5	[86]
PMP	NH ₂ -MIL-53(Al)	30	50 °C, 12 h, <i>in vacuo</i>	30 °C	358.2	24.4	[77]
ODPA-TMPDA	Cu-BTC	40	200 °C, 24 h, <i>in vacuo</i>	2 atm, 35 °C	260.7	27.75	[84]
6FDA-ODA	UiO-66	25	230 °C, 15 h, <i>in vacuo</i>	10 bar, 35 °C	50.4	46.1	[87]
Pebax	ZIF-7	34	Room temperature, 24 h	3.75 bar (CO ₂), 7.5 bar (CH ₄), 20 °C	41	44	[88]
PVC-g-POEM	ZIF-8 (hollow sphere)	30	50 °C, 4 h, <i>in vacuo</i> , 24 h	1 bar, 35 °C	623	11.2	[89]
Poly(vinylidene fluoride)	Cu-BTC	10	120 °C, 24 h, <i>in vacuo</i>	5 bar, 25 °C	2.002	41.7	[67]
Poly(phenylene oxide)	Cu-BTC	40	200 °C, 24 h, <i>in vacuo</i>	30 °C	115	34	[90]
Matrimid®	n/a	0	in air, 100 °C	50-50 vol. CO ₂ /CH ₄ , 35 °C, 10 bar	5.6±0.7	22.3±0.2	This work
			in air, 160 °C	50-50 vol. CO ₂ /CH ₄ , 35 °C, 10 bar	8.2±0.2	31.6±1	This work
			in air, 250 °C	50-50 vol. CO ₂ /CH ₄ , 35 °C, 10 bar	5.3±0.2	40.4± 3.5	This work
			in air, 350 °C	50-50 vol. CO ₂ /CH ₄ , 35 °C, 10 bar	7.4±0.7	76.3±0.8	This work

Continued on next page

Table 4.2 – continued from previous page

Polymer	MOF	Loading, wt. %	Treatment	Measurement conditions	CO ₂ /CH ₄ , 35	CO ₂ permeability, Barrer	CO ₂ /CH ₄ selectivity	Ref.
Matrimid®	NH ₂ -MIL-53(Al)	20	in air, 100 °C	50-50 vol. °C, 10 bar	CO ₂ /CH ₄ , 35	5.84±1.4	21.9±1.3	This work
			in air, 160 °C	50-50 vol. °C, 10 bar	CO ₂ /CH ₄ , 35	5.09±0.3	29±3.4	This work
			in air, 250 °C	50-50 vol. °C, 10 bar	CO ₂ /CH ₄ , 35	6.18±0.7	53.9±8.3	This work
			in air, 350 °C	50-50 vol. °C, 10 bar	CO ₂ /CH ₄ , 35	2.8±0.5	82.2±9.6	This work
Matrimid®	NH ₂ -MIL-53(Al)	30	in air, 100 °C	50-50 vol. °C, 10 bar	CO ₂ /CH ₄ , 35	8.89±1.8	18.9±4.9	This work
			in air, 160 °C	50-50 vol. °C, 10 bar	CO ₂ /CH ₄ , 35	6.33±0.8	24.5±6.1	This work
			in air, 250 °C	50-50 vol. °C, 10 bar	CO ₂ /CH ₄ , 35	5.68±0.7	65.1±9.8	This work
			in air, 350 °C	50-50 vol. °C, 10 bar	CO ₂ /CH ₄ , 35	3.81±1.5	94±13.3	This work
Matrimid®	NH ₂ -MIL-53(Al)	40	in air, 100 °C	50-50 vol. °C, 10 bar	CO ₂ /CH ₄ , 35	8.22±1.3	22.9±1.2	This work
			in air, 160 °C	50-50 vol. °C, 10 bar	CO ₂ /CH ₄ , 35	10±1.2	40.7±3.4	This work
			in air, 250 °C	50-50 vol. °C, 10 bar	CO ₂ /CH ₄ , 35	5.64±0.7	76.8±7.8	This work
			in air, 350 °C	50-50 vol. °C, 10 bar	CO ₂ /CH ₄ , 35	5.34±1.3	152.6±11.5	This work
			in air, 350 °C	50-50 vol. °C, 40 bar	CO ₂ /CH ₄ , 35	1.71±0.1	139±3.1	This work

References

- [1] R. W. Baker and K. Lokhandwala. "Natural gas processing with membranes: An overview". *Industrial & Engineering Chemistry Research* 47.7 (2008), pp. 2109–2121.
- [2] R. W. Baker. *Membrane Technology and Applications*. Chichester, UK: John Wiley & Sons, Ltd, 2012.
- [3] Y. Yampolskii, I. Pinnau and B. Freeman, eds. *Materials Science of Membranes for Gas and Vapor Separation*. Chichester, UK: John Wiley & Sons, Ltd, 2006.
- [4] B. Global. *Natural gas - 2015 in review*. 2016.
- [5] W. J. Koros and R. Mahajan. "Pushing the limits on possibilities for large scale gas separation: which strategies?" *Journal of Membrane Science* 175.2 (2000), pp. 181–196.
- [6] J. E. Bachman and J. R. Long. "Plasticization-resistant Ni₂(dobdc)/polyimide composite membranes for the removal of CO₂ from natural gas". *Energy Environ. Sci.* 9.6 (2016), pp. 2031–2036.
- [7] A. W. Thornton, D. Dubbeldam, M. S. Liu, B. P. Ladewig, A. J. Hill and M. R. Hill. "Feasibility of zeolitic imidazolate framework membranes for clean energy applications". *Energy & Environmental Science* 5.6 (2012), p. 7637.
- [8] A. Makaruk, M. Miltner and M. Harasek. "Membrane biogas upgrading processes for the production of natural gas substitute". *Separation and Purification Technology* 74.1 (2010), pp. 83–92.
- [9] M. Scholz, T. Melin and M. Wessling. "Transforming biogas into biomethane using membrane technology". *Renewable and Sustainable Energy Reviews* 17 (2013), pp. 199–212.
- [10] L. M. Robeson. "Correlation of separation factor versus permeability for polymeric membranes". *Journal of Membrane Science* 62.2 (1991), pp. 165–185.
- [11] L. M. Robeson. "The upper bound revisited". *Journal of Membrane Science* 320.1-2 (2008), pp. 390–400.
- [12] A. M. Hillock, S. J. Miller and W. J. Koros. "Crosslinked mixed matrix membranes for the purification of natural gas: Effects of sieve surface modification". *Journal of Membrane Science* 314.1-2 (2008), pp. 193–199.
- [13] J. Wind. "Natural gas permeation in polyimide membranes". *Journal of Membrane Science* 228.2 (2004), pp. 227–236.

- [14] C. Cao. “Chemical cross-linking modification of 6FDA-2,6-DAT hollow fiber membranes for natural gas separation”. *Journal of Membrane Science* 216.1-2 (2003), pp. 257–268.
- [15] T.-S. Chung, L. Y. Jiang, Y. Li and S. Kulprathipanja. “Mixed Matrix Membranes (MMMs) comprising organic polymers with dispersed inorganic fillers for gas separation”. *Prog. Poly. Sci.* 32 (2007), pp. 483–507.
- [16] R. Mahajan and W. J. Koros. “Factors Controlling Successful Formation of Mixed-Matrix Membranes”. *Ind. Eng. Chem. Res.* 39 (2000), pp. 2692–2696.
- [17] J.-R. Li, R. J. Kuppler and H.-C. Zhou. “Selective gas adsorption and separation in metal–organic frameworks”. *Chemical Society Reviews* 38.5 (2009), p. 1477.
- [18] B. Seoane, J. Coronas, I. Gascon, M. E. Benavides, O. Karvan, J. Caro, F. Kapteijn and J. Gascon. “Metal–organic framework based mixed matrix membranes: a solution for highly efficient CO₂ capture?” *Chem. Soc. Rev.* 44.8 (2015), pp. 2421–2454.
- [19] G. Férey. “Hybrid porous solids: past, present, future”. *Chem. Soc. Rev.* 37.1 (2008), pp. 191–214.
- [20] G. Férey and C. Serre. “Large breathing effects in three-dimensional porous hybrid matter: facts, analyses, rules and consequences”. *Chemical Society Reviews* 38.5 (2009), p. 1380.
- [21] M. Alhamami, H. Doan and C.-H. Cheng. “A review on breathing behaviors of metal-organic-frameworks (MOFs) for gas adsorption”. en. *Materials* 7.4 (2014), pp. 3198–3250.
- [22] E. Stavitski, E. A. Pidko, S. Couck, T. Remy, E. J. M. Hensen, B. M. Weckhuysen, J. Denayer, J. Gascon and F. Kapteijn. “Complexity behind CO₂ capture on NH₂-MIL-53(Al)”. *Langmuir* 27.7 (2011), pp. 3970–3976.
- [23] Y. Liu, J.-H. Her, A. Dailly, A. J. Ramirez-Cuesta, D. A. Neumann and C. M. Brown. “Reversible Structural Transition in MIL-53 with Large Temperature Hysteresis”. *Journal of the American Chemical Society* 130.35 (2008), pp. 11813–11818.
- [24] F. Salles, A. Ghoufi, G. Maurin, R. G. Bell, C. Mellot-Draznieks and G. Férey. “Molecular Dynamics Simulations of Breathing MOFs: Structural Transformations of MIL-53(Cr) upon Thermal Activation and CO₂ Adsorption”. *Angewandte Chemie* 120.44 (2008), pp. 8615–8619.

- [25] N. Rosenbach, H. Jobic, A. Ghoufi, F. Salles, G. Maurin, S. Bourrelly, P. L. Llewellyn, T. Devic, C. Serre and G. Férey. “Quasi-Elastic Neutron Scattering and Molecular Dynamics Study of Methane Diffusion in Metal Organic Frameworks MIL-47(V) and MIL-53(Cr)”. *Angewandte Chemie International Edition* 47.35 (2008), pp. 6611–6615.
- [26] L. Hamon, C. Serre, T. Devic, T. Loiseau, F. Millange, G. Férey and G. D. Weireld. “Comparative Study of Hydrogen Sulfide Adsorption in the MIL-53(Al, Cr, Fe), MIL-47(V), MIL-100(Cr), and MIL-101(Cr) Metal-Organic Frameworks at Room Temperature”. *Journal of the American Chemical Society* 131.25 (2009), pp. 8775–8777.
- [27] A. Boutin, M.-A. Springuel-Huet, A. Nossov, A. Gedeon, T. Loiseau, C. Volkringer, G. Férey, F.-X. Coudert and A. H. Fuchs. “Breathing Transitions in MIL-53(Al) Metal-Organic Framework Upon Xenon Adsorption”. *Angewandte Chemie International Edition* 48.44 (2009), pp. 8314–8317.
- [28] G. Férey, M. Latroche, C. Serre, F. Millange, T. Loiseau and A. Percheron-Guegan. “Hydrogen adsorption in the nanoporous metal-benzenedicarboxylate M(OH)(O₂ C–C₆H₄–CO₂) (M=Al³⁺, Cr³⁺), MIL-53”. *Chem. Commun.* 24 (2003), pp. 2976–2977.
- [29] S. Bourrelly, P. L. Llewellyn, C. Serre, F. Millange, T. Loiseau and G. Férey. “Different Adsorption Behaviors of Methane and Carbon Dioxide in the Isotypic Nanoporous Metal Terephthalates MIL-53 and MIL-47”. *Journal of the American Chemical Society* 127.39 (2005), pp. 13519–13521.
- [30] T. K. Trung, P. Trens, N. Tanchoux, S. Bourrelly, P. L. Llewellyn, S. Loera-Serna, C. Serre, T. Loiseau, F. Fajula and G. Férey. “Hydrocarbon Adsorption in the Flexible Metal Organic Frameworks MIL-53(Al,Cr)”. *Journal of the American Chemical Society* 130.50 (2008), pp. 16926–16932.
- [31] P. L. Llewellyn, P. Horcajada, G. Maurin, T. Devic, N. Rosenbach, S. Bourrelly, C. Serre, D. Vincent, S. Loera-Serna, Y. Filinchuk and G. Férey. “Complex Adsorption of Short Linear Alkanes in the Flexible Metal-Organic-Framework MIL-53(Fe)”. *Journal of the American Chemical Society* 131.36 (2009), pp. 13002–13008.
- [32] D. I. Kolokolov, H. Jobic, A. G. Stepanov, V. Guillerm, T. Devic, C. Serre and G. Férey. “Dynamics of Benzene Rings in MIL-53(Cr) and MIL-47(V) Frameworks Studied by ²H NMR Spectroscopy”. *Angewandte Chemie International Edition* 49.28 (2010), pp. 4791–4794.

- [33] V. Finsy, C. E. A. Kirschhock, G. Vedts, M. Maes, L. Alaerts, D. E. De Vos, G. V. Baron and J. F. M. Denayer. "Framework Breathing in the Vapour-Phase Adsorption and Separation of Xylene Isomers with the Metal-Organic Framework MIL-53". *Chemistry - A European Journal* 15.31 (2009), pp. 7724–7731.
- [34] P. L. Llewellyn, S. Bourrelly, C. Serre, Y. Filinchuk and G. Férey. "How Hydration Drastically Improves Adsorption Selectivity for CO₂ over CH₄ in the Flexible Chromium Terephthalate MIL-53". *Angewandte Chemie* 118.46 (2006), pp. 7915–7918.
- [35] L. Hamon, P. L. Llewellyn, T. Devic, A. Ghoufi, G. Clet, V. Guillerm, G. D. Pirngruber, G. Maurin, C. Serre, G. Driver, W. van Beek, E. Jolimaitre, A. Vimont, M. Daturi and G. Férey. "Co-adsorption and Separation of CO₂-CH₄ Mixtures in the Highly Flexible MIL-53(Cr) MOF". *Journal of the American Chemical Society* 131.47 (2009), pp. 17490–17499.
- [36] A. Boutin, F.-X. Coudert, M.-A. Springuel-Huet, A. V. Neimark, G. Férey and A. H. Fuchs. "The Behavior of Flexible MIL-53(Al) upon CH₄ and CO₂ Adsorption". *The Journal of Physical Chemistry C* 114.50 (2010), pp. 22237–22244.
- [37] S. Couck, J. F. M. Denayer, G. V. Baron, T. Remy, J. Gascon and F. Kapteijn. "An Amine-Functionalized MIL-53 Metal-Organic Framework with Large Separation Power for CO₂ and CH₄". *Journal of the American Chemical Society* 131.18 (2009), pp. 6326–6327.
- [38] F. Zhang, X. Zou, X. Gao, S. Fan, F. Sun, H. Ren and G. Zhu. "Hydrogen selective NH₂-MIL-53(Al) MOF membranes with high permeability". *Advanced Functional Materials* 22.17 (2012), pp. 3583–3590.
- [39] S. Couck, T. Remy, G. V. Baron, J. Gascon, F. Kapteijn and J. F. M. Denayer. "A pulse chromatographic study of the adsorption properties of the amino-MIL-53 (Al) metal-organic framework". *Physical Chemistry Chemical Physics* 12.32 (2010), p. 9413.
- [40] A. Boutin, S. Couck, F. X. Coudert, P. Serra-Crespo, J. Gascon, F. Kapteijn, A. H. Fuchs and J. F. M. Denayer. "Thermodynamic analysis of the breathing of amino-functionalized MIL-53(Al) upon CO₂ adsorption". *Microporous and Mesoporous Materials* 140.1-3 (2011), pp. 108–113.
- [41] T. Rodenas, I. Luz, G. Prieto, B. Seoane, H. Miro, A. Corma, F. Kapteijn, F. X. Llabres i Xamena and J. Gascon. "Metal-organic framework nanosheets in polymer composite materials for gas separation." *Nature materials* 14.1 (2015), pp. 48–55.

- [42] A. Sabetghadam, B. Seoane, D. Keskin, N. Duim, T. Rodenas, S. Shahid, S. Sorribas, C. L. Guillouzer, G. Clet, C. Téllez, M. Daturi, J. Coronas, F. Kapteijn and J. Gascon. “Metal Organic Framework Crystals in Mixed-Matrix Membranes: Impact of the Filler Morphology on the Gas Separation Performance”. *Advanced Functional Materials* 26.18 (2016), pp. 3154–3163.
- [43] T. Rodenas, M. van Dalen, E. Garcia-Perez, P. Serra-Crespo, B. Zornoza, F. Kapteijn and J. Gascon. “Visualizing MOF mixed matrix membranes at the nanoscale: Towards structure-performance relationships in CO₂/CH₄ separation over NH₂-MIL-53(Al)@PI”. *Advanced Functional Materials* 24.2 (2014), pp. 249–256.
- [44] A. Kertik, L. H. Wee, M. Pfannmoeller, S. Bals, J. Martens and I. F. Vankelecom. “Highly selective gas separation membrane using in-situ amorphised metal-organic frameworks”. *Energy Environ. Sci.* 10 (11 2017), pp. 2342–2351.
- [45] Y. Li, T. Chung, C. Cao and S. Kulprathipanja. “The effects of polymer chain rigidification, zeolite pore size and pore blockage on polyethersulfone (PES)-zeolite A mixed matrix membranes”. *Journal of Membrane Science* 260.1-2 (2005), pp. 45–55.
- [46] A. L. Khan, S. Basu, A. Cano-Odena and I. F. Vankelecom. “Novel high throughput equipment for membrane-based gas separations”. *Journal of Membrane Science* 354.1-2 (2010), pp. 32–39.
- [47] S.-i. Kuroda and I. Mita. “Degradation of aromatic polymers—II. The crosslinking during thermal and thermo-oxidative degradation of a polyimide”. *European Polymer Journal* 25.6 (1989), pp. 611–620.
- [48] P. S. Tin, T. S. Chung, Y. Liu, R. Wanc, S. L. Liu and K. P. Pramoda. “Effects of cross-linking modification on gas separation performance of Matrimid membranes”. *Journal of Membrane Science* 225 (2003), pp. 77–90.
- [49] M. W. Anjum, F. Vermoortele, A. L. Khan, B. Bueken, D. E. De Vos and I. F. J. Vankelecom. “Modulated UiO-66-Based Mixed-Matrix Membranes for CO₂ Separation”. *ACS Applied Materials & Interfaces* 7.45 (2015), pp. 25193–25201.
- [50] L. E. Nielsen. “Cross-linking—effect on physical properties of polymers”. *Journal of Macromolecular Science, Part C: Polymer Reviews* 3.1 (1969), pp. 69–103.
- [51] M. G. Goesten, K. B. Sai Sankar Gupta, E. V. Ramos-Fernandez, H. Khajavi, J. Gascon and F. Kapteijn. “Chloromethylation as a functionalisation pathway for metal–organic frameworks”. *CrystEngComm* 14.12 (2012), p. 4109.

- [52] X. Cheng, A. Zhang, K. Hou, M. Liu, Y. Wang, C. Song, G. Zhang and X. Guo. "Size- and morphology-controlled NH₂-MIL-53(Al) prepared in DMF-water mixed solvents". *Dalton Transactions* 42.37 (2013), p. 13698.
- [53] P. Serra-Crespo, E. Gobechiya, E. V. Ramos-Fernandez, J. Juan-Alcaniz, A. Martinez-Joaristi, E. Stavitski, C. E. A. Kirschhock, J. A. Martens, F. Kapteijn and J. Gascon. "Interplay of metal node and amine functionality in NH₂-MIL-53: Modulating breathing behavior through intra-framework interactions". *Langmuir* 28.35 (2012), pp. 12916–12922.
- [54] B. Seoane, C. Téllez, J. Coronas and C. Staudt. "NH₂-MIL-53(Al) and NH₂-MIL-101(Al) in sulfur-containing copolyimide mixed matrix membranes for gas separation". *Separation and Purification Technology* 111 (2013), pp. 72–81.
- [55] T. Rodenas, M. Van Dalen, P. Serra-Crespo, F. Kapteijn and J. Gascon. "Mixed matrix membranes based on NH₂-functionalized MIL-type MOFs: Influence of structural and operational parameters on the CO₂/CH₄ separation performance". *Microporous and Mesoporous Materials* 192 (2013), pp. 35–42.
- [56] G. Dong, H. Li and V. Chen. "Challenges and opportunities for mixed-matrix membranes for gas separation". *Journal of Materials Chemistry A* 1.15 (2013), p. 4610.
- [57] R. Mahajan, R. Burns, M. Schaeffer and W. J. Koros. "Challenges in forming successful mixed matrix membranes with rigid polymeric materials". *Journal of Applied Polymer Science* 86.4 (2002), pp. 881–890.
- [58] T. Loiseau, C. Serre, C. Huguenard, G. Fink, F. Taulelle, M. Henry, T. Bataille and G. Férey. "A rationale for the large breathing of the porous aluminum terephthalate (MIL-53) upon hydration." *Chemistry (Weinheim an der Bergstrasse, Germany)* 10.6 (2004), pp. 1373–1382.
- [59] Z. Tian, T. Saito and D.-e. Jiang. "Ab initio screening of CO₂-philic groups". *The Journal of Physical Chemistry A* 119.16 (2015), pp. 3848–3852.
- [60] P. Raymond, W. Koros and D. Paul. "Comparison of mixed and pure gas permeation characteristics for CO₂ and CH₄ in copolymers and blends containing methyl methacrylate units". *Journal of Membrane Science* 77.1 (1993), pp. 49–57.
- [61] M. D. Guiver, G. P. Robertson, Y. Dai, F. Bilodeau, Y. S. Kang, K. J. Lee, J. Y. Jho and J. Won. "Structural characterization and gas-transport properties of brominated Matrimid polyimide". *Journal of Polymer Science Part A: Polymer Chemistry* 40.23 (2002), pp. 4193–4204.

- [62] J. S. Chiou, Y. Maeda and D. R. Paul. "Gas permeation in polyethersulfone". *Journal of Applied Polymer Science* 33.5 (1987), pp. 1823–1828.
- [63] Y. P. Handa, J. Roovers and P. Moulini. "Gas transport properties of substituted PEEKs". *Journal of Polymer Science Part B: Polymer Physics* 35.14 (1997), pp. 2355–2362.
- [64] L. Hao, P. Li and T.-S. Chung. "PIM-1 as an organic filler to enhance the gas separation performance of Ultem polyetherimide". *Journal of Membrane Science* 453 (2014), pp. 614–623.
- [65] Y. Xiao, Y. Dai, T.-S. Chung and M. D. Guiver. "Effects of brominating matrimid polyimide on the physical and gas transport properties of derived carbon membranes". *Macromolecules* 38.24 (2005), pp. 10042–10049.
- [66] J. Li, K. Nagai, T. Nakagawa and S. Wang. "Preparation of polyethylene glycol (PEG) and cellulose acetate (CA) blend membranes and their gas permeabilities". *Journal of Applied Polymer Science* 58.9 (1995), pp. 1455–1463.
- [67] E. A. Feijani, H. Mahdavi and A. Tavasoli. "Poly(vinylidene fluoride) based mixed matrix membranes comprising metal organic frameworks for gas separation applications". *Chemical Engineering Research and Design* 96 (2015), pp. 87–102.
- [68] P. Tiemblo, J. Guzman, E. Riande, C. Mijangos and H. Reinecke. "The gas transport properties of PVC functionalized with mercapto pyridine groups". *Macromolecules* 35.2 (2002), pp. 420–424.
- [69] K. Berean, J. Z. Ou, M. Nour, K. Latham, C. McSweeney, D. Paull, A. Halim, S. Kentish, C. M. Doherty, A. J. Hill and K. Kalantar-zadeh. "The effect of crosslinking temperature on the permeability of PDMS membranes: Evidence of extraordinary CO₂ and CH₄ gas permeation". *Separation and Purification Technology* 122 (2014), pp. 96–104.
- [70] J. McHattie, W. Koros and D. Paul. "Gas transport properties of polysulphones: 1. Role of symmetry of methyl group placement on bisphenol rings". *Polymer* 32.5 (1991), pp. 840–850.
- [71] M. Hellums, W. Koros, G. Husk and D. Paul. "Fluorinated polycarbonates for gas separation applications". *Journal of Membrane Science* 46.1 (1989), pp. 93–112.
- [72] W.-J. Chen and C. R. Martin. "Gas-transport properties of sulfonated polystyrenes". *Journal of Membrane Science* 95.1 (1994), pp. 51–61.
- [73] G. Perego, A. Roggero, R. Sisto and C. Valentini. "Membranes for gas separation based on silylated polyphenylene oxide". *Journal of Membrane Science* 55.3 (1991), pp. 325–331.

- [74] X.-G. Li, I. Kresse, Z.-K. Xu and J. Springer. “Effect of temperature and pressure on gas transport in ethyl cellulose membrane”. *Polymer* 42.16 (2001), pp. 6801–6810.
- [75] S. S. Hosseini and T. S. Chung. “Carbon membranes from blends of PBI and polyimides for N₂/CH₄ and CO₂/CH₄ separation and hydrogen purification”. *Journal of Membrane Science* 328.1-2 (2009), pp. 174–185.
- [76] B. Zornoza, A. Martinez-Joaristi, P. Serra-Crespo, C. Téllez, J. Coronas, J. Gascon and F. Kapteijn. “Functionalized flexible MOF as filler in mixed matrix membranes for highly selective separation of CO₂ from CH₄ at elevated pressures”. *Chemical communications (Cambridge, England)* 47.33 (2011), pp. 9522–9524.
- [77] R. Abedini, M. Omidkhah and F. Dorosti. “Highly permeable poly(4-methyl-1-pentyne)/NH₂ -MIL-53(Al) mixed matrix membrane for CO₂/CH₄ separation”. en. *RSC Advances* 4.69 (2014), p. 36522.
- [78] X. Y. Chen, V.-T. Hoang, D. Rodrigue and S. Kaliaguine. “Optimization of continuous phase in amino-functionalized metal–organic framework (MIL-53) based co-polyimide mixed matrix membranes for CO₂/CH₄ separation”. *RSC Advances* 3.46 (2013), p. 24266.
- [79] Q. Song, S. K. Nataraj, M. V. Roussenova, J. C. Tan, D. J. Hughes, W. Li, P. Bourgoïn, M. A. Alam, A. K. Cheetham, S. a. Al-Muhtaseb and E. Sivaniah. “Zeolitic imidazolate framework (ZIF-8) based polymer nanocomposite membranes for gas separation”. *Energy & Environmental Science* 5.8 (2012), pp. 8359–8369.
- [80] M. J. C. Ordoñez, K. J. Balkus Jr., J. P. Ferraris and I. H. Musselman. “Molecular sieving realized with ZIF-8/Matrimid® mixed-matrix membranes”. *Journal of Membrane Science* 361.1-2 (2010), pp. 28–37.
- [81] F. Dorosti, M. Omidkhah and R. Abedini. “Fabrication and characterization of Matrimid/MIL-53 mixed matrix membrane for CO₂/CH₄ separation”. *Chemical Engineering Research and Design* 92.11 (2014), pp. 2439–2448.
- [82] S. Basu, A. Cano-Odena and I. F. Vankelecom. “Asymmetric Matrimid®/[Cu₃(BTC)₂] mixed-matrix membranes for gas separations”. *Journal of membrane science* 362.1 (2010), pp. 478–487.
- [83] E. V. Perez, K. J. Balkus Jr., J. P. Ferraris and I. H. Musselman. “Mixed-matrix membranes containing MOF-5 for gas separations”. *Journal of Membrane Science* 328.1-2 (2009), pp. 165–173.

- [84] C. Duan, X. Jie, D. Liu, Y. Cao and Q. Yuan. “Post-treatment effect on gas separation property of mixed matrix membranes containing metal organic frameworks”. *Journal of Membrane Science* 466 (2014), pp. 92–102.
- [85] M. Arjmandi and M. Pakizeh. “Mixed matrix membranes incorporated with cubic-MOF-5 for improved polyetherimide gas separation membranes: Theory and experiment”. *Journal of Industrial and Engineering Chemistry* 20.5 (2014), pp. 3857–3868.
- [86] B. Seoane, V. Sebastian, C. Téllez and J. Coronas. “Crystallization in THF: the possibility of one-pot synthesis of mixed matrix membranes containing MOF MIL-68(Al)”. *CrystEngComm* 68.Table 1 (2013), pp. 1–5.
- [87] O. G. Nik, X. Y. Chen and S. Kaliaguine. “Functionalized metal organic framework-polyimide mixed matrix membranes for CO₂/CH₄ separation”. *Journal of Membrane Science* 414 (2012), pp. 48–61.
- [88] T. Li, Y. Pan, K.-V. Peinemann and Z. Lai. “Carbon dioxide selective mixed matrix composite membrane containing ZIF-7 nano-fillers”. *Journal of Membrane Science* 425-426 (2013), pp. 235–242.
- [89] S. Hwang, W. S. Chi, S. J. Lee, S. H. Im, J. H. Kim and J. Kim. “Hollow ZIF-8 nanoparticles improve the permeability of mixed matrix membranes for CO₂/CH₄ gas separation”. *Journal of Membrane Science* 480 (2015), pp. 11–19.
- [90] L. Ge, W. Zhou, V. Rudolph and Z. Zhu. “Mixed matrix membranes incorporated with size-reduced Cu-BTC for improved gas separation”. *Journal of Materials Chemistry A* 1.21 (2013), p. 6350.

Chapter 5

General conclusions

This dissertation focused on the development of mixed-matrix membranes (MMMs) comprising metal-organic frameworks (MOFs) for CO₂/CH₄ separation applications. The effect of membrane preparation factors were investigated to improve the gas separation performance of the resulting MMMs. The gas separation results were supported by structural characterisations, in order to uncover the underlying chemical processes that lead to the obtained performances.

Chapter 1 started with an overall introduction to the concept and fundamentals of the gas separation market. It continued with a deeper focus on membrane-based separations, the mechanisms thereof and the market for membrane-based gas separations. A literature background on the materials research for gas separation, as well as their limitations, followed. The motivation for this work was defined. The chapter was concluded with an overview of the chapters of this dissertation.

The goal of the work in Chapter 2 was to exploit the relative ease of synthesising MOFs to produce MMMs *in-situ*, namely by synthesising them *inside* the polymer solution. Directly mixing the MOF precursors in a dilute polymer solution did not give the desired loading (>20 wt.%). Increasing the precursor concentration did not increase the MOF synthesis yield, moreover the membranes became plasticised by the unreacted precursors. Upon re-modifying the process to synthesise MOFs in pure solvent, but not drying them after the synthesis proved to be an efficient method to control the MMM loading. Membranes with 30 and 50 wt.% MOF loading were fabricated with a homogeneous distribution of the particles. Compared to control samples prepared with dried MOFs, these membranes showed superior separation properties.

In order to improve the separation performance of the membranes, Chapter 3 focused on applying a detailed heat treatment in air. The membranes treated up to 350°C showed outstanding selectivities, that are marked as the highest reported for MMMs with commercial polymers. Upon further analysis, it was revealed that the thermal treatment induces the amorphisation of ZIF-8, resulting in a loss of crystallinity, but also a denser structure that maintains its building units to achieve molecular sieving. Moreover, thermo-oxidative cross-linking between the polymer chains, as well as between the polymer chains and the MOF contributed to the overall separation performance. Owing to the extensive cross-linking, the membranes proved to be highly resistant to CO₂-induced plasticisation at pressures as high as 40 bar, marking their stability in industrial separation conditions. The method was shown to be generic, as similar behaviour was observed when ZIF-8 was replaced by ZIF-7.

Chapter 4 details the application of the same method to a MOF that shows breathing behaviour: NH₂-MIL-53(Al). The MOF did not undergo amorphisation upon heat treatment, but showed evidence that it retained its large-pore form after cooling down to room temperature. It should be noted that the large-pore form is reached at higher temperatures, and normally the MOF will revert to its narrow-pore form upon cooling. It was speculated that the polymer partially penetrates and cross-links at the mouth of the pore, preventing the MOF from reverting to the narrow-pore form. Thanks to this modified pore structure, and in combination with the polymer-polymer and polymer-MOF cross-linking, selectivities that even surpass the previous studies reported here were achieved. Moreover, the membranes were still resistant to plasticisation owing to their high level of cross-linking.

Chapter 6

Future prospects

6.1 Future prospects

For this work, a very effective membrane separation method has been devised and optimised. The possible steps forward are as follows:

6.1.1 Improvement of membrane fluxes

The membranes reported in Chapters 3 and 4 exhibit outstanding selectivities. Select membranes from these studies have even been able to surpass the Robeson upper-bounds of both 1991 and 2008. The Robeson upper-bound is a well-known indicator of the commercial relevance of the performance of a membrane. Although the selectivities reported were extraordinary, they were coupled with a decrease in the permeability. High productivity (in terms of separations) can only be achieved by increasing the permeability without sacrificing the current selectivities. For this purpose, preparing thin film composite variants of the membranes reported here would be a viable starting point. An important practical point of concern would be to find a support material that could withstand the high-temperature treatment, which is necessary to obtain the unique synergy of MOF amorphisation and polymer cross-linking.

6.1.2 Investigation of other polymer-MOF pairs

The choice of material plays a fundamental role in the performance of MMMs: the polymer determines the starting point, and the properties of the MOF determine the maximum possible improvement. This study has used a well-known commercial polymer, Matrimid®, which is a soluble thermoplastic polyimide used in high-temperature adhesives, composites, and gas separation. Regarding MOFs, ZIF-8, ZIF-7, and NH₂-MIL-53(Al) were used. Especially in the rapidly-growing MOF literature, state-of-the-art MOF structures are reported frequently. A suggested path for future work is to try different polymer-MOF combinations, and search for further possible synergies. For example, polymers with high thermal stability such as Ultem®1000, polybenzimidazole, Kapton® and P84, and MOFs with promising CO₂/CH₄ separation performance in MMMs such as HKUST-1, CuBDC nanosheets and MOF-5 can be used. For further studies on the *in-situ* synthesis of MOF particles in polymer solutions, solvents such as water, methanol, and tetrahydrofuran can be used with the respectively soluble polymers mentioned above.

6.1.3 Investigation of other applications

Within the scope of this work, the membranes were tested for the separation of CO₂/CH₄ mixtures. However, this work is only the pioneer for composite materials comprising *in-situ* amorphised or gate-opening MOFs; and the synergy between MOF characteristics and polymer cross-linking is certain to produce more interesting results in other applications. First and foremost, it is suggested that these membranes be tested with actual industrial gas mixtures at industrial conditions, especially to assess the effect of contaminants such as H₂S, H₂O, etc. Moreover, it is needed to pursue other fields of application for these unique materials, e.g. other gas membrane separations, gas storage, adsorption or catalysis. Membranes of MOFs such as ZIF-8,^[1] ZIF-7,^[2] ZIF-69,^[3] MOF-5,^[4] and HKUST-1^[5] have exhibited promising performances for separations of e.g. CO₂/CH₄,^[1] CO₂/N₂,^[3] and H₂/CO₂.^[4,5] Some MOFs have shown interesting abilities, such as reversible amorphisation upon application of pressure.^[6] There are no reports of membranes with amorphous MOFs in literature. Our *in-situ* amorphisation approach can offer a starting point for the use of amorphous MOFs as gas separation membranes with outstanding properties. MOFs used in sensing harmful guest species are prone to stress-induced collapse and guest immobilisation.^[6] For such applications, mixed-matrix membranes combined with MOF amorphisation, can offer a method to control structural collapse: the side groups of polymer chains penetrating the pores can act to protect the MOF structure from total collapse. The same principle can be applied for

adsorption applications: selective adsorption is determined by the pore size and shape, as well as adsorbate-surface interactions.^[7] By controlling the pore openings through penetration of polymer side groups, the selective adsorption properties of amorphous MOFs can be tailored. Hughes et al.^[8] have shown that the reusability of amorphous MOFs in reversible gas storage is hindered by their instability in acidic environments. In our work, we have observed a strong increase in the chemical stability of MMMs, as the polymer phase cross-linked at high temperatures. A similar method can enable the use of amorphous MOFs for reversible gas storage. For catalysis, MOFs offer great flexibility and variety in synthesis of new structures, compared to zeolites.^[9] The controllable porosity, pore size and shape, and presence of metal sites in MOFs promises a great potential for catalytic applications. Only a few examples have been reported to date.^[10] In our study, we have seen that amorphisation of MOFs can create unsaturated metal sites i.e. Zn^{2+} , which is suggested to increase the quadrupolar interactions with CO_2 . Such a property can be useful for the fixation of CO_2 into cyclic carbonates. Moreover, amorphisation can help in controlling the pore size and shape, opening new doors for very interesting research in the field of shape-selective catalysis.

References

- [1] S. R. Venna and M. A. Carreon. “Highly permeable zeolite imidazolate framework-8 membranes for CO₂/CH₄ separation”. *Journal of the American Chemical Society* 132.1 (2009), pp. 76–78.
- [2] M. C. McCarthy, V. Varela-Guerrero, G. V. Barnett and H.-K. Jeong. “Synthesis of zeolitic imidazolate framework films and membranes with controlled microstructures”. *Langmuir* 26.18 (2010), pp. 14636–14641.
- [3] Y. Liu, G. Zeng, Y. Pan and Z. Lai. “Synthesis of highly c-oriented ZIF-69 membranes by secondary growth and their gas permeation properties”. *Journal of membrane science* 379.1 (2011), pp. 46–51.
- [4] Y. Liu, Z. Ng, E. A. Khan, H.-K. Jeong, C.-b. Ching and Z. Lai. “Synthesis of continuous MOF-5 membranes on porous α -alumina substrates”. *Microporous and Mesoporous Materials* 118.1 (2009), pp. 296–301.
- [5] Y. Mao, H. Huang, W. Cao, J. Li, L. Sun, X. Jin, X. Peng et al. “Room temperature synthesis of free-standing HKUST-1 membranes from copper hydroxide nanostrands for gas separation”. *Chemical Communications* 49.50 (2013), pp. 5666–5668.
- [6] T. D. Bennett and A. K. Cheetham. “Amorphous Metal-Organic Frameworks”. *Accounts of Chemical Research* 47.5 (2014), pp. 1555–1562.
- [7] J.-R. Li, R. J. Kuppler and H.-C. Zhou. “Selective gas adsorption and separation in metal–organic frameworks”. *Chemical Society Reviews* 38.5 (2009), pp. 1477–1504.
- [8] J. T. Hughes, T. D. Bennett, A. K. Cheetham and A. Navrotsky. “Thermochemistry of zeolitic imidazolate frameworks of varying porosity”. *Journal of the American Chemical Society* 135.2 (2012), pp. 598–601.
- [9] J. Lee, O. K. Farha, J. Roberts, K. A. Scheidt, S. T. Nguyen and J. T. Hupp. “Metal–organic framework materials as catalysts”. *Chemical Society Reviews* 38.5 (2009), pp. 1450–1459.
- [10] R. J. Kuppler, D. J. Timmons, Q.-R. Fang, J.-R. Li, T. A. Makal, M. D. Young, D. Yuan, D. Zhao, W. Zhuang and H.-C. Zhou. “Potential applications of metal-organic frameworks”. *Coordination Chemistry Reviews* 253.23 (2009), pp. 3042–3066.

Curriculum vitae



Personal

Name Aylin Kertik
Date of birth: November 3rd, 1985
Place of birth: Bursa, Turkey

Professional

2016-Present Materialise (BE)

Education

2011-2018 PhD, Faculty of Bioscience Engineering, Katholieke Universiteit Leuven (BE)
PhD, Faculty of Science and Technology, Universiteit Twente (NL)
2007-2010 MSc, Polymer Science and Technology, Istanbul Technical University (TR)
2003-2007 BSc, Chemical Engineering, Yildiz Technical University (TR)
1996-2003 Middle and high school, Bursa Anatolian High School (TR)

Other

Languages Turkish, English, Dutch, German, French, Japanese
Hobbies Reading, travelling, sports, video games, cooking, handcraft

List of publications

Publications

Kertik, A., Wee, L. H., Pfannmoeller, M., Bals, S., Martens, J., & Vankelecom, I. F. (2017). Highly selective gas separation membrane using in-situ amorphised metal-organic frameworks. *Energy & Environmental Science*.

Kertik, A., Khan, A. L., & Vankelecom, I. F. (2016). Mixed matrix membranes prepared from non-dried MOFs for CO₂/CH₄ separations. *RSC Advances*.

(In resubmission) Kertik, A., Wee, L. H., Sentosun, K., Bals, S., Martens, J., & Vankelecom, I. F. (2017). High-performance CO₂-selective mixed matrix membranes by exploiting MOF-breathing effects, *Joule*.

Conferences

International Congress on Membranes and Membrane Processes, ICOM 2014 (Suzhou, China), *Alternative methods for preparation of mixed matrix membranes comprising metal organic frameworks*, oral presentation.

Euromembrane 2012 (London, UK). *Metal organic framework-containing mixed matrix membranes for gas separation: A different approach to MMM preparation methods*, oral presentation.

Workshops

Alternative preparation methods for metal organic framework-based mixed matrix membranes, International EUDIME&EM3E Joint Workshop on Membrane Engineering, Montpellier, France, September 2014.

Mixed matrix membranes containing metal organic frameworks for gas separation, EUDIME Workshop in Leuven, Belgium, September 2013.

Gas separation with polymer/MOF mixed matrix membranes, EUDIME Workshop in Calabria, Italy, February 2012.

